

SISSA

Scuola
Internazionale
Superiore di
Studi Avanzati

Physics Area

Ph.D. course in Theoretical Particle Physics

**dS QNMs and PBHs
beyond the Gaussian limit**

Candidate:
Flavio Ricciardi

Supervisors:
Mehrdad Mirbabayi
Alfredo Urbano

Academic Year 2022-23



ACKNOWLEDGEMENTS

During my PhD, I received support and assistance from various people, who were able to direct and instruct me where necessary.

First of all, my thanks go to my supervisor Mehrdad Mirbabayi. His quick, brilliant mind and rich physical intuition make him one of the best scientists I have had the pleasure of knowing. His patience in explaining and repeating concepts to me makes him a professor from whom one can glean a wealth of knowledge.

At the beginning of this journey, I was fortunate to be able to collaborate with Alfredo Urbano, co-signer of this thesis, that is also based on our work together. From Alfredo I had the opportunity to learn an extremely precise and rigorous working method, combined with a crystal clarity of exposition.

Alongside these people, with whom I have actively collaborated scientifically, there are others who have guided me, sometimes in a personal and inspirational way, in my growth. Most of all, I have to thank Paolo Creminelli, from whom I had the opportunity to learn by working alongside him as a tutor and who has guided me greatly in my path. I thank Oliver Janssen, whose energy, passion and style of studying physics I admire.

I thank the ICTP, which has hosted me for the past three years and from which I have been able to experience a modern, cutting-edge and extremely rich environment from a cultural and intercultural point of view. I thank the professors at SISSA for their lectures that completed my training as a physicist, in particular Marco Serone and Roberto Percacci.

I cannot miss to thank my PhD fellows. Physics is not a job that can be done alone, at least for me. In particular, I shared a lot of knowledge and help (and nights doing QFT exercises) with Davide Dal Cin, Mehmet Asim Gumus, Vicharit Yingcharoenrat and Giovanni Galati.

Last but not least, I would like to thank Guido Martinelli, who despite no longer being my teacher, continues to follow me and give me the right advice at the right time.

ABSTRACT

In this thesis we propose two (non standard) mathematical methods to deal with different aspects of theoretical cosmology.

The first problem we face is the computation of Quasinormal Modes (QNMs) of oscillation of a scalar field on a pure de Sitter (dS) background with an S-matrix like approach. In a QFT on de Sitter background, one can study correlators between fields pushed to the future and past horizons of a comoving observer. This is a neat probe of the physics in the observer's causal diamond (known as the static patch). We use this observable to give a generalization of the quasinormal spectrum in interacting theories, and to connect it to the spectral density that appears in the Källén-Lehmann expansion of dS correlators. We also introduce a finite-temperature effective field theory consisting of free bulk fields coupled to a boundary. In matching it to the low frequency expansion of correlators, we find positivity constraints on the EFT parameters following from unitarity. This first part is based on reference [1].

The second problem is the computation of the Primordial Black Holes (PBHs) abundance in a mathematical framework called Peak Theory. The method is independent on the specific inflationary model that one considers and therefore is general. We compute the probability density distribution of maxima for a scalar random field in the presence of local non-gaussianities. The physics outcome of this analysis is the following. If we focus on maxima whose curvature is larger than a certain threshold for gravitational collapse, our calculations illustrate how the fraction of the Universe's mass in the form of PBHs changes in the presence of local non-gaussianities. This second part is based on reference [2].

PUBLICATIONS

The content of this thesis is based on the following publications:

- M. Mirbabayi and F. Ricciardi, “Probing de Sitter from the horizon,” JHEP **04** (2023), 053
arXiv:2211.11672 [hep-th]
- F. Ricciardi, M. Taoso and A. Urbano, “Solving peak theory in the presence of local non-gaussianities,” JCAP **08** (2021), 060
arXiv:2102.04084 [astro-ph.CO]

CONTENTS

1	INTRODUCTION	1
I	DE SITTER QUASINORMAL MODES	3
2	QUASINORMAL MODES FROM ANALYTICAL PROPERTIES	5
2.1	In-out correlators	6
2.2	The free case	7
2.3	Spectrum of interacting theories	9
2.4	A continuous spectrum	10
2.5	Discrete spectrum in Rindler space	11
3	BOUNDARY EFFECTIVE FIELD THEORY	13
3.1	Free theory	13
3.2	Interacting theory	15
4	CONCLUSIONS OF PART I	19
II	PRIMORDIAL BLACK HOLES	21
5	PRIMORDIAL BLACK HOLES	23
5.1	Physical motivation	23
5.2	Problem setup and solution strategy	25
6	RESULTS AND DISCUSSION	29
6.1	The abundance of PBHs in the presence of primordial local non-gaussianities	29
6.2	Comparison with the literature	37
7	CONCLUSIONS OF PART II	45
III	APPENDIX	47
A	DE SITTER QUASINORMAL MODES	49
A.1	Free commutator	49
A.2	Closure of the contour	50
A.3	SK perturbation theory for the 2-point function	52
B	SCALAR PERTURBATIONS DURING INFLATION IN THE PRESENCE OF ULTRA SLOW-ROLL	55
C	CLIFFSNOTES ON GAUSSIAN PEAK THEORY	61
D	PEAK STATISTICS WITH LOCAL NON-GAUSSIANITIES	75
D.1	Number density of peaks	75
D.2	From the number density to the abundance	78
E	PEAK THEORY WITH LOCAL NON-GAUSSIANITIES: A PERTURBATIVE APPROACH IN 2D	81
F	TOWARDS AN EXACT COMPUTATION	107
F.1	Cancellation of the contributes up to $\mathcal{O}(\alpha^{n-2})$	107

F.2	Computation of the $\mathcal{O}(\alpha^{n-2})$	110
F.3	Computation of the $\mathcal{O}(\alpha^{n-1})$	111
F.4	Computation of the $\mathcal{O}(\alpha^n)$	111
F.5	Computation of the generic cumulant	112

BIBLIOGRAPHY	
--------------	--

113

INTRODUCTION

Sometimes in physics, the use of a different mathematical method to solve a problem of which the solution is already known leads to extensions and generalizations.

Some remarkable examples are Lagrangian and Hamiltonian formulations of classical mechanics. They could appear as very sophisticated versions of the simple mechanics already explained by Galilei and Newton's *Principia Mathematica*. However the Hamiltonian and the Poisson Brackets become basic tools of non relativistic quantum mechanics, or the Lagrangian in a relativistic theory.

Similarly, Quantum Mechanics made with these (now basic) instruments can be entirely reformulated via the sophisticated Feynman's path integral, that instead become a basic tool in Quantum Field Theory.

Therefore to rewatch a solved problem from an higher perspective is not an unrewarded effort.

It is often heard that the only system that can always be solved in physics is the harmonic oscillator. Everything else is found in perturbation theory around the quadratic potential, first approximation of each point of minimum of a generic potential. This statement is ubiquitous in physics: from classical mechanics to quantum mechanics, the harmonic oscillator is always an integrable problem. In quantum field theory, the study of free fields passes through an infinity of decoupled harmonic oscillators. And the term *free theory* goes hand in hand with another term: *Gaussianity*. These two terms, distant at first sight, find their union in the path integral, where the free Lagrangian, that is quadratic, is exponentiated. Schematically, the action for a free field Φ can be written using a differential operator \mathcal{O} :

$$\mathcal{Z} = \int \mathcal{D}\Phi e^{i \int d^4x \Phi \mathcal{O} \Phi} \quad (1.0.1)$$

This integral is a well known Gaussian integral and it is analitically computable.

Deviations from Gaussianity are difficult to deal with, as are problems other than the harmonic oscillator. In this thesis, using non-standard mathematical approaches, an attempt is made to go beyond Gaussianity in two different cosmologically inspired physical problems.

DE SITTER QUASINORMAL MODES In the first part of the thesis we will apply the study of complex analitic properties of correlation functions to rederive the QNMs of oscillation of a free scalar field on dS. This provides a straightforward generalization for interacting theories, where instead there is not a standard definition of QNMs.

The usual approach to the problem is to consider the classical free field equations of motion on the de Sitter background and to solve it with specific boundary conditions. If we work in spherical symmetry this means to impose that the field is purely outgoing at the cosmological horizon and regular at the origin. These conditions constraint the QNM spectrum to be discrete and complex.

The alternative approach we follow, based on the study of analytic properties of the 2-point correlation function, allows us to recover the same result that one finds with the usual approach based on the solution of differential equations for the free theory. On the other side it makes possible to generalize the concept of QNMs for interacting theories, where instead the standard approach does not give a clear definition of modes of oscillation, being the interactive equations of motion non linear.

PRIMORDIAL BLACK HOLES In the second part of the thesis, we solve the (abstract) problem of peak theory of a random field in presence of a local Non-Gaussianity.

In our context, this mathematical model will be useful to describe the density perturbation field of the early universe as a random field with a generic statistics (so not necessarily Gaussian) and, when the fluctuations overcome a certain threshold, a Black Hole is formed.

Despite the clear inspiration from inflationary physics, this mathematical problem is independent on the specific model and switching from one model to another only changes the form and the size of the Non-Gaussianity.

Part I

DE SITTER QUASINORMAL MODES

QUASINORMAL MODES FROM ANALYTICAL PROPERTIES

An important characteristic of a spacetime with an horizon is the spectrum of exponents that control the relaxation of perturbations. At linear level, these exponents coincide with the (generically complex) frequencies of the *quasinormal* modes [3]. But they can also be thought of as the poles of the retarded Green's function.

De Sitter spacetime has observer-dependent horizons, and is described within these horizons by the metric

$$ds^2 = -(1 - r^2) dt^2 + \frac{dr^2}{1 - r^2} + r^2 d\Omega^2. \quad (2.0.1)$$

It is therefore natural to explore the quasinormal-mode (QNM) spectrum of fields on dS [4]. One motivation is that we believe there has been a long period of inflation in our past. This is a geometry that is locally close to dS, and the above-mentioned exponents control the power-law decay of cosmological correlators. For instance, the infrared dynamics of light scalar fields in de Sitter provides a rare example of a Markovian process whose decay exponents can be explicitly computed in terms of the UV couplings [5].

An interesting feature of free field theories on dS background is the fact that the poles associated to the quasinormal modes are the only singularities of the retarded Green's function, while in asymptotically flat black hole spacetimes there are additional singularities (branch-points) corresponding to the power-law tails [6]. One goal of this work is to explore the analytic structure of the retarded function at the interacting level.

To this end, we find it convenient to consider in-out correlators obtained by pushing the operator insertions to the future and past horizons (see figure 1). Operationally, this can be thought of as a scattering experiment in the static patch, where the scattering states are prepared by a family of accelerating observers at fixed r , in the limit $r \rightarrow 1$. We will show in section 2.2 that the poles of the retarded in-out correlators coincide with the well-known spectrum of quasinormal modes for free scalar fields.

At the interacting level, we use the Källén-Lehmann representation for the 2-point correlators in dS. That is, expand the interacting 2-point correlator in terms of correlators of free fields associated to the unitary representations of dS isometry group [7]. Schematically

$$\langle \phi(X)\phi(Y) \rangle = \sum_{\Delta} \rho(\Delta) G_f(X, Y; \Delta). \quad (2.0.2)$$

We will see how the singularity structure of the retarded function (in ω) is inherited from that of the spectral density $\rho(\Delta)$. Explicit examples and perturbative arguments given in [8, 9] suggest that $\rho(\Delta)$ is *generically* a meromorphic function. This implies that the static patch retarded function too will generically have a set of isolated poles as its singularities.

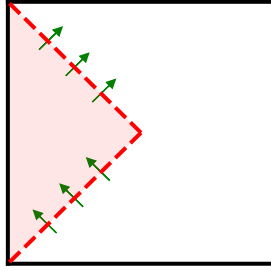


Figure 1: The Penrose diagram of dS . We study in and out states in one static patch (shaded).

A priori, this sounds surprising.¹ Correlators of interacting theories typically have a more intricate singularity structure (e.g. loops usually introduce branch-cuts). The finiteness of volume in the static patch does not seem to be a good explanation for the simplicity of its correlators. In fact, the static patch Hamiltonian ($i\partial_t$) has a continuous spectrum, and one can find (rare) examples with a continuous spectrum of decay exponents. We present one in section 2.4.

In section 2.5, we present an analogy that might be helpful in understanding why the spectrum is generically discrete. There we see that the Rindler-space correlator is a meromorphic function of Rindler frequency for a generic interacting theory on 2d Minkowski spacetime.

Apart from the simple analytic structure, the spectral density $\rho(\Delta)$ was shown in [8, 9] to be non-negative as a consequence of unitarity. It is often the case that the unitarity of the UV completion constrains the low energy observables and the effective field theory that governs them [10]. In section 3, we will find a similar application. Indeed, the small ω expansion of in-out correlators of a free theory can be reproduced by a *boundary effective field theory* (BEFT). As we will see, the emergence of this BEFT is quite natural when using the tortoise coordinate $\chi = \text{arctanh } r$, with $0 \leq \chi < \infty$. Spherical modes of the field are effectively free 2d fields except in the vicinity of $0 < \chi \sim 1$ (see figure 2). For small ω this region can be collapsed to a one-dimensional boundary on which composite operators are localized.

In section 3.2, we will discuss the condition under which a similar BEFT description is applicable to interacting theories. Naturally, this BEFT has to be formulated at finite temperature, and in matching it with (2.0.2) it is necessary to include dissipative terms. We will see that unitarity leads to positivity constraints on the EFT coefficients. We will give a summary in section 4.

2.1 IN-OUT CORRELATORS

When it is possible to define the scattering matrix, it is often a more convenient observable to work with than the local correlation functions. It depends on fewer variables, for a fixed number of

¹ We thank Victor Gorbenko for bringing this curious feature to our attention.

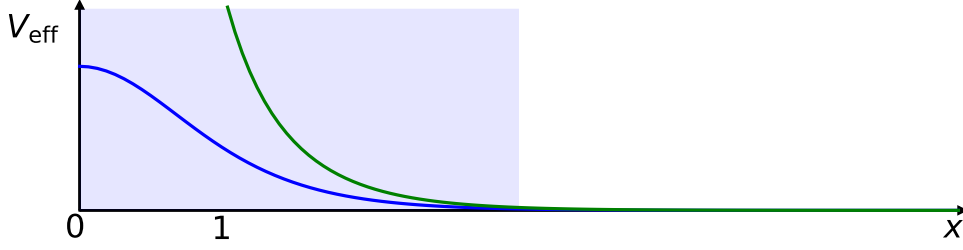


Figure 2: The effective potential for the spherical harmonics of a free field consists of a mass term (blue) and a centrifugal barrier (green). They decay exponentially toward the horizon $x \rightarrow \infty$. When $\omega \ll 1$, the interaction region (shaded) can be collapsed to a boundary with localized interactions.

external legs, and is invariant under field redefinition. For similar reasons, we consider static patch correlators for operators that are pushed to its null boundaries, namely the past and future horizons. In tortoise coordinate

$$x = \operatorname{arctanh} r, \quad (2.1.1)$$

the horizon is at $x \rightarrow \infty$, and the in and out fields are defined as

$$\phi_{\text{out}}(u, \hat{r}) = \lim_{\substack{t, x \rightarrow \infty \\ u = t - x}} \phi(t, x, \hat{r}), \quad (2.1.2)$$

$$\phi_{\text{in}}(v, \hat{r}) = \lim_{\substack{-t, x \rightarrow \infty \\ v = t + x}} \phi(t, x, \hat{r}). \quad (2.1.3)$$

Some earlier works that motivate working with such in-out observables in the static patch include [11–13].

To discuss quasinormal spectrum, we will focus on

$$\hat{C}(\omega, \theta) \equiv \int_{-\infty}^{\infty} du e^{i\omega u} \langle [\phi_{\text{out}}(u, \hat{r}), \phi_{\text{in}}(0, \hat{z})] \rangle, \quad (2.1.4)$$

where θ is the angle between the two versors \hat{r} and \hat{z} . In a free theory (2.1.4) is the Fourier transform of the retarded Green's function between two points approaching the past and future horizons. Note that there is no translation symmetry $x \rightarrow x + \epsilon$. Therefore, even the two-point correlator is nontrivial. In a free theory, the above commutator is independent of the choice of state, but encodes the information about propagation of waves on the curved background. In an interacting theory, $\hat{C}(\omega, \theta)$ depends on the state. For instance, the Hartle-Hawking state is a thermal state in the static patch, and $\hat{C}(\omega, \theta)$ carries information about the interactions with the thermal excitations.

2.2 THE FREE CASE

The exact dS_{d+1} correlation function of a free scalar field is [14]

$$G_f(\xi, \Delta) \equiv \langle \phi(X)\phi(Y) \rangle = \frac{\Gamma(\Delta)\Gamma(d-\Delta)}{(4\pi)^{\frac{d+1}{2}}\Gamma(\frac{d+1}{2})} {}_2F_1\left(\Delta, d-\Delta; \frac{d+1}{2}; 1 - \frac{1}{\xi}\right) \quad (2.2.1)$$

where $\Delta = \frac{d}{2} + i\sqrt{m^2 - \frac{d^2}{4}}$, and X and Y are the coordinates of a $d + 2$ -Minkowski spacetime that embeds dS_{d+1} as the hyperboloid with $X \cdot X = Y \cdot Y = 1$. In terms of this Minkowski inner product

$$\xi = \frac{2}{1 - X \cdot Y}. \quad (2.2.2)$$

When X and Y are timelike separated $\xi < 0$, and we are on the branch-cut of G_f . The two choices of the branch correspond to the two different ordering of the fields. The commutator is the discontinuity across this cut:

$$[\phi(X), \phi(Y)] = -\Theta(-\xi) \frac{2\pi i}{(4\pi)^{\frac{d+1}{2}} \Gamma(\frac{3-d}{2})} (-\xi)^{\frac{d-1}{2}} \left(1 - \frac{1}{\xi}\right)^{\frac{1-d}{2}} {}_2F_1\left(1 - \Delta, 1 - d + \Delta; \frac{3-d}{2}; \frac{1}{\xi}\right). \quad (2.2.3)$$

For the particular in-out configuration of the last section,

$$\xi = \frac{2}{1 - \cos\theta - 2e^u}, \quad (2.2.4)$$

and hence $\xi < 0$ corresponds to $2e^u > 1 - \cos\theta$. After changing the integration variable in (2.1.4) to $U = e^u - \frac{1 - \cos\theta}{2}$, we find

$$\hat{C}(\omega, \theta) = \frac{-2\pi i}{(4\pi)^{\frac{d+1}{2}} \Gamma(\frac{3-d}{2})} \int_0^\infty dU \left(U + \frac{1 - \cos\theta}{2}\right)^{i\omega - 1} U^{\frac{1-d}{2}} (1 + U)^{\frac{1-d}{2}} {}_2F_1\left(1 - \Delta, 1 - d + \Delta; \frac{3-d}{2}; -U\right). \quad (2.2.5)$$

As a function of ω , this integral is analytic in the upper half complex ω plane unless $\theta = 0$. Its singularities arise from the $U \rightarrow \infty$ limit of the integral. Indeed, the asymptotic expansion of the hypergeometric function is:

$${}_2F_1(a, b; c; -x) \sim \frac{\Gamma(b-a)\Gamma(c)}{\Gamma(b)\Gamma(c-a)} x^{-a} + \frac{\Gamma(a-b)\Gamma(c)}{\Gamma(a)\Gamma(c-b)} x^{-b} \quad \text{as } x \rightarrow +\infty \quad (2.2.6)$$

Therefore the poles are located at

$$\begin{aligned} i\omega &= \Delta + n, \\ i\omega &= d - \Delta + n, \quad n \in \mathbb{N}. \end{aligned} \quad (2.2.7)$$

The explicit answer for (2.2.5) is given in appendix A.1.

The frequencies (2.2.7) are precisely the quasinormal mode spectrum of a scalar field on de Sitter [4]. In dS, the quasinormal modes are defined as eigensolutions of the linear field equations with outgoing boundary condition at the cosmological horizon and regularity at the origin. They are called *quasinormal* because with these boundary conditions the linear differential operator is not Hermitian. Quasinormal modes characterize the decay of perturbations since their frequencies appear as the poles (in the lower half-plane) of the retarded Green's function. By the Cauchy theorem the response to a source J at $t = 0$ is [3]

$$\phi(t, \vec{x}) = \int d^3x' \int_{-\infty}^{+\infty} \frac{d\omega}{2\pi} e^{-i\omega t} G_R(\omega, \vec{x}; \vec{x}') J(\vec{x}') = \sum_{\text{QNMs}} a_n e^{-i\omega_n t} + \text{tail}. \quad (2.2.8)$$

The “tail” corresponds to non-exponential contributions (often power-law decays that eventually dominate) and comes from additional singularities of the Green’s function. dS Green’s function is special in that there are no other singularities except for the QNM poles, and hence there is no tail. We see that $\hat{C}(\omega, \theta)$ has the same analytic structure.

2.3 SPECTRUM OF INTERACTING THEORIES

The description of the quasinormal modes as the eigensolutions of the wave equation with particular boundary conditions is specific to free fields. However, we can still wonder about the analytic structure of the Green’s function, or $\hat{C}(\omega, \theta)$, in an interacting theory. The poles would still describe the exponential decay of perturbations and hence they are the most natural generalization of the quasinormal spectrum to the interacting case. However, one might expect a more complicated singularity structure (such as branch-points) to appear at the interacting level. We can use the Källén-Lehmann representation for the 2-point correlators [8, 9]

$$\langle \phi(X)\phi(Y) \rangle = \int_{\frac{d}{2}-i\infty}^{\frac{d}{2}+i\infty} \frac{d\Delta}{2\pi i} \rho(\Delta) G_f(\xi; \Delta) + \dots, \quad (2.3.1)$$

to evaluate $\hat{C}(\omega, \theta)$. In the above expression, the integral runs over the unitary representations of dS called the principal series. This is a redundant (but useful) presentation, since $\Delta \sim d - \Delta$ and $\rho(\Delta) = \rho(d - \Delta)$. By analytic continuation to $d + 1$ sphere, one can show that $\rho^*(\Delta) = \rho(\Delta^*)$. Perturbative computations suggest that $\rho(\Delta)$ is generically meromorphic even in an interacting theory. Dots account for other unitary representations, such as the complementary series. In perturbative examples, those will form a discrete sum of $G_f(\xi; \Delta)$ with real Δ .

We would like to connect the analytic structure of $\rho(\Delta)$ to that of $\hat{C}(\omega, \theta)$, by a contour deformation from the path $\Delta \in \frac{d}{2} + i\mathbb{R}$ closing it to the right half plane in (2.3.1). For this purpose it is useful to use the identity

$$G_f(\xi; \Delta) = \frac{g(\Delta)\psi_\Delta(\xi) + (\Delta \rightarrow d - \Delta)}{2} \quad (2.3.2)$$

where

$$g(\Delta) = \frac{\Gamma(\frac{d}{2} - \Delta)\Gamma(\Delta)}{2^{2\Delta+1}\pi^{d/2+1}}, \quad \psi_\Delta(\xi) = \xi^\Delta {}_2F_1\left(\Delta, \Delta - \frac{d-1}{2}; 2\Delta - d + 1; \xi\right). \quad (2.3.3)$$

Using the symmetry $\rho(\Delta) = \rho(d - \Delta)$, we can write (2.3.1) as

$$\langle \phi(X)\phi(Y) \rangle = \int_{\frac{d}{2}-i\infty}^{\frac{d}{2}+i\infty} \frac{d\Delta}{2\pi i} \tilde{\rho}(\Delta)\psi_\Delta(\xi), \quad (2.3.4)$$

where

$$\tilde{\rho}(\Delta) \equiv \rho(\Delta)g(\Delta). \quad (2.3.5)$$

In appendix A.2, we show that the contour in (2.3.4) can be deformed to the right if ρ decays faster than a d -dependent power of Δ .² Assuming also that $\tilde{\rho}(\Delta)$ is meromorphic, we find

$$\langle \phi(X)\phi(Y) \rangle = - \sum_i \text{Res}_{\Delta_i}(\tilde{\rho})\psi_{\Delta_i}(\xi). \quad (2.3.6)$$

Now the discontinuity of ψ_Δ in the timelike region comes entirely from the factor ξ^Δ in (2.3.3). The anti-symmetrized correlator $C(\xi, \theta) = \langle [\phi(X), \phi(Y)] \rangle$ has support only in this region:

$$C(\xi, \theta) = -\Theta(-\xi) \sum_i 2i \sin(\pi\Delta) \text{Res}_{\Delta_i}(\tilde{\rho})(-\xi)^{\Delta_i} {}_2F_1\left(\Delta_i, \Delta_i - \frac{d-1}{2}; 2\Delta_i - d + 1; \xi\right), \quad (2.3.7)$$

where Θ is the Heaviside function. As an example, we fix $\theta = \pi$ in (2.2.4) and Fourier transform with respect to u to find $\hat{C}(\omega, \pi)$ (except for $\theta = 0$, at which ϕ_{out} is in the future lightcone of ϕ_{in} , the singularity structure of $\hat{C}(\omega, \theta)$ is the same as $\hat{C}(\omega, \pi)$). A single term in the sum (2.3.6), after the change of variable $V = -\xi = 1/(e^u - 1)$, gives

$$\int_0^\infty dV (1+V)^{i\omega-1} V^{\Delta_i-i\omega-1} {}_2F_1\left(\Delta_i, \Delta_i - \frac{d-1}{2}; 2\Delta_i - d + 1; -V\right). \quad (2.3.8)$$

As a function of ω , the singularities of $\hat{C}(\omega, \pi)$ arise from the $V \rightarrow 0$ region of integration. These are poles located at

QNM spectrum of interacting theories

$$i\omega_n = \Delta_i + n, \quad n \in \mathbb{N}. \quad (2.3.9)$$

Given that $\text{Re}(\Delta_i) \geq d/2$, these poles are all in the lower half-plane as expected from causality. Hence, if $\tilde{\rho}$ is meromorphic, for every pole Δ_i , we have the full family of the poles corresponding to the QNMs spectrum of a fictitious field with dimension Δ_i (thought not $d - \Delta_i$). The real analyticity of $\tilde{\rho}$ implies the existence of another family with associated to Δ_i^* . The overtones (frequencies with $n \geq 1$) can be thought of as arising from the descendants of a conformal primary operator with dimension Δ_i . Similarly, for every complementary series representations that appears in (2.3.1), there will be the full set of associated QNMs.

2.4 A CONTINUOUS SPECTRUM

In [9], the in-in perturbation theory was analytically continued to one in Euclidean AdS. This automatically results in a meromorphic $\rho(\Delta)$, and a discrete sum over complementary series representations. Hence, if there is a counter-example, it must be non-perturbative. It is well known that for light interacting scalar fields in dS, perturbation theory fails. Originally, this problem was solved by

² This is the same contour deformation performed in [8], but instead of $\xi \rightarrow 0^+$ we are interested in the timelike configuration $\xi < 0$, where there is no obvious exponential decay coming from $\psi_\Delta(\xi)$.

switching to a stochastic description [15, 16]. This allows a reliable non-perturbative computation of the relaxation exponents as the eigenvalues of the Fokker-Planck equation

$$\partial_t p(t, \varphi) = \frac{1}{8\pi} \partial_\varphi^2 p(t, \varphi) + \frac{1}{3} \partial_\varphi (V'(\varphi) p(t, \varphi)) + \dots \quad (2.4.1)$$

where $V(\varphi)$ is the scalar potential and dots include corrections that can be computed perturbatively (in slow-roll parameters such as $V'^2/H^2V, V''/H^2$) [5, 17, 18]. The eigenvalue problem can be mapped to a Schrödinger equation with an effective potential [16]

$$V_{\text{eff}}(\varphi) = \frac{1}{2}(v'^2(\varphi) - v''(\varphi)), \quad v(\varphi) \equiv \frac{4\pi^2}{3} V(\varphi). \quad (2.4.2)$$

If we take $v(\varphi) \propto \varphi \tanh \varphi$, the effective potential approaches a constant as $\varphi \rightarrow \pm\infty$ and hence the spectrum of decay exponents will have a continuum above a gap. It follows that the corresponding $\rho(\Delta)$ is not meromorphic in this example. For an application of this model see [19].

2.5 DISCRETE SPECTRUM IN RINDLER SPACE

As a simpler example, we consider the retarded function in the Rindler wedge of 2d Minkowski spacetime. We will see that generic interacting theories will have a discrete spectrum of singularities in terms of the Rindler frequency. As before, we define the in and out fields by taking the fields to the past and future Rindler horizons. The metric in the left Rindler wedge can be written as

$$ds^2 = 4e^{-2x}(-dt^2 + dx^2). \quad (2.5.1)$$

The Minkowski coordinates are related to these by

$$X^0 = 2e^{-x} \sinh t, \quad X^1 = -2e^{-x} \cosh t. \quad (2.5.2)$$

The past and future horizons correspond to $x \rightarrow \infty$ and $t \rightarrow \mp\infty$:

$$\begin{aligned} X^0 = -X^1 = e^{t-x} &\equiv e^u, & \text{future} \\ X^0 = X^1 = -e^{-t-x} &\equiv e^{-v}. & \text{past.} \end{aligned} \quad (2.5.3)$$

We define $\phi_{\text{in}}(v)$ and $\phi_{\text{out}}(u)$ as the fields pushed to the horizons and study

$$C(u) \equiv \langle [\phi_{\text{out}}(u), \phi_{\text{in}}(0)] \rangle \quad (2.5.4)$$

Note that the expectation values in (2.5.4) could be thought of as being computed in the thermal state obtained after tracing out the complement of the Rindler wedge, or as Minkowski correlators. We are interested in the analytic structure of the Fourier transform of $C(u)$:³

$$\hat{C}(\omega) = \int_{-\infty}^{+\infty} du e^{i\omega u} C(u). \quad (2.5.5)$$

³ From the perspective of Minkowski coordinates, this transform is similar to going to rapidity space and $\hat{C}(\omega)$ resembles the celestial amplitudes. For two recent works on the analytic properties of such amplitudes see [Duary_2022, Kapec_2023].

Let us compute this in a theory with mass gap m and a density of states $\rho(s) \geq 0$. The Källén-Lehmann representation of the Minkowski Feynman correlator is

$$\langle T\{\phi(X)\phi(0)\} \rangle = \int_{\mathbb{R}^2} d^2k \int_0^\infty \frac{ds}{2\pi} \frac{\rho(s)}{k^2 + s + i\epsilon} e^{ik \cdot X}. \quad (2.5.6)$$

The commutator (2.5.4) is the difference between the time-ordered and anti-time-ordered correlators, which implies (after switching to $k_\pm = k^0 \pm k^1$)

$$\hat{C}(\omega) = \frac{1}{2} \int_{-\infty}^\infty du \int dk_+ dk_- \int_0^\infty ds \rho(s) \delta(k_+ k_- - s) e^{i\omega u - ik_- e^u - ik_+}. \quad (2.5.7)$$

It is straightforward to perform k_+ , then u and then k_- integrals. For instance, the u integral can be rewritten in terms of $U \equiv e^u$ as

$$\int_0^\infty dU U^{i\omega-1} e^{-ik_- U} = \Gamma(i\omega) (ik_-)^{-i\omega}. \quad (2.5.8)$$

The final result is

$$\hat{C}(\omega) = \frac{1}{2\pi} \sinh(\pi\omega) \Gamma^2(i\omega) \int_0^\infty ds \rho(s) s^{-i\omega}. \quad (2.5.9)$$

In a free theory $\rho(s) = \delta(s - m^2)$ and we see that $\hat{C}(\omega)$ is meromorphic. In this case it has poles in the upper half plane. Given that the fields are always timelike separated for any u , there is no reason for the Fourier transform to be analytic in the upper-half-plane.⁴

In the interacting case, one expects additional singularities to arise in (2.5.9). Now $\rho(s)$ is in general a continuous function. For instance, it accounts for the multi-particle states that mix with the single particle states via interactions. However, if the theory is gapped, i.e. $\rho(s < m^2) = 0$, then the additional singularities in (2.5.9) can only arise from the $s \rightarrow \infty$ limit of the integral. Generically, $\rho(s)$ behaves as a power (or a combination of powers) of s . This would again lead to a discrete set of poles in ω .

In general the same thing does not apply to dS : if the spectral function is not meromorphic, then in the deformation of the contour in the integral (2.3.1) one must take into account the contribution coming from branchcuts, that result in integral of some discontinuities. Generically, this cannot be represented as a discrete sum over pure exponentials.

⁴ In fact, the function decays fast enough in the upper-half ω plane that the inverse Fourier transform for both signs of u can be computed by closing the integration contour on that side.

A useful setup for studying low-frequency perturbations in a black hole geometry is the worldline EFT [20]. The idea is that for long wavelength perturbations the neighborhood of a black hole can be replaced by a worldline on a weakly curved geometry and with interactions localized on it. This is an open system because waves can fall through the horizon. The effect can be taken into account by introducing additional operators on the worldline that represent near horizon degrees of freedom and are short-lived [20, 21]. One might expect a local dissipative EFT, formulated on the Schwinger-Keldysh (SK) contour, to arise after integrating out these operators [22].

In this section, we ask if a similar idea can be applied to the low-frequency in-out observables in dS static patch. The analog of the black hole region is now the region $0 < x \sim 1$. Since the size of S^{d-1} factor reaches an $\mathcal{O}(1)$ constant as $x \rightarrow \infty$, the appropriate EFT would be a collection of KK modes propagating on a half-line, and with interactions localized at the boundary. The EFT is dissipative because we are interested in a description of modes with $\omega \ll 1$ in a system at finite temperature $T = \frac{1}{2\pi}$.

3.1 FREE THEORY

To motivate the idea, consider a massive free field and decompose it in terms of spherical harmonics

$$\phi(t, \vec{r}) = \sum_{l,m} \phi_{lm}(t, x) Y_{lm}(\hat{r}). \quad (3.1.1)$$

In a free theory, different ϕ_{lm} decouple. The action for the s-wave perturbations is

$$S_{00} = \frac{1}{2} \int dt \int_0^\infty dx \tanh^2 x \left[\dot{\phi}_{00}^2 - \phi_{00}'^2 - \frac{m^2}{\cosh^2 x} \phi_{00}^2 \right]. \quad (3.1.2)$$

We expand ϕ_{00} in radial eigenmodes

$$\phi_{00}(t, x) = \int_0^\infty \frac{d\omega}{2\pi} \phi_\omega(t) f_\omega(x), \quad (3.1.3)$$

where asymptotically

$$f_\omega(x) \sim e^{i\omega x + i\alpha(\omega)} + e^{-i\omega x - i\alpha(\omega)}, \quad \text{for } x \rightarrow \infty, \quad (3.1.4)$$

and the phase shift is given by¹

$$e^{2i\alpha(\omega)} = \frac{2^{-2i\omega}\Gamma(i\omega)\Gamma(\frac{1}{2}(\Delta_+ - i\omega))\Gamma(\frac{1}{2}(\Delta_- - i\omega))}{\Gamma(-i\omega)\Gamma(\frac{1}{2}(\Delta_+ + i\omega))\Gamma(\frac{1}{2}(\Delta_- + i\omega))}. \quad (3.1.6)$$

Now every $\phi_\omega(t)$ is a harmonic oscillator with frequency ω and the Hartle-Hawking state corresponds to a thermal state with $T = 1/2\pi$. The ladder operators, defined via:

$$\phi_\omega(t) = \frac{1}{\sqrt{2\omega}} (a_\omega e^{-i\omega t} + a_\omega^\dagger e^{i\omega t}), \quad (3.1.7)$$

satisfy

$$\langle a_\omega^\dagger a_{\omega'} \rangle = 2\pi\delta(\omega - \omega') \frac{1}{e^{2\pi\omega} - 1}. \quad (3.1.8)$$

The in-out correlator is given by

$$\langle \phi_{00}^{\text{out}}(u)\phi_{00}^{\text{in}}(0) \rangle = \oint \frac{d\omega}{2\pi} e^{-i\omega u} \frac{e^{2i\alpha}}{2\omega(1 - e^{-2\pi\omega})}, \quad (3.1.9)$$

where the integration contour runs from $-\infty$ to $+\infty$ and below the double pole at 0. Naively, one gets a singular integral that goes through 0. This singularity is an artifact of the exchange of the limit $\chi \rightarrow \infty$ and the integral. The contour deformation is the one that reproduces the correct result.

What suggests the possibility of an effective worldline theory that matches this result at low ω is that at large χ the action (3.1.2) reduces to that of a massless 2d field on a half-line. We can couple this to a boundary by writing (we drop the 00 index to avoid clutter)

$$S_{\text{BEFT}} = \int dt \int_0^\infty dx \left[\frac{1}{2} (\dot{\phi}^2 - \phi'^2) - \delta(x) \sum_n c_n (\partial_t^n \phi)^2 \right]. \quad (3.1.10)$$

We now show that with an appropriate choice of c_n this BEFT matches the expansion around $\omega = 0$ of the full result. It is enough to match the low- ω expansion of the phase-shifts on the two sides. The equation for the mode functions in the EFT reads

$$f_\omega''(x) + \omega^2 f_\omega(x) = \delta(x) f_\omega(0) \sum_{n=0}^\infty c_n \omega^{2n}. \quad (3.1.11)$$

The correctly normalized solution is $f_\omega(x) = 2 \cos(\omega x + \alpha)$ where

$$\omega \tan \alpha = i\omega \frac{1 - e^{2i\alpha}}{1 + e^{2i\alpha}} = - \sum_{n=0}^\infty c_n \omega^{2n}. \quad (3.1.12)$$

A unique choice of $\{c_n\}$ exists because the phase shift given in (3.1.6) is real for real ω and satisfies

$$e^{2i\alpha(0)} = -1, \quad e^{2i\alpha(-\omega)} = e^{-2i\alpha(\omega)}. \quad (3.1.13)$$

¹ For generic l the mode function is

$$\phi_{\omega l}(t, x) \propto e^{-i\omega t} \tanh^l x (\cosh x)^{-i\omega} {}_2F_1\left(\frac{l + \Delta_+ + i\omega}{2}, \frac{l + \Delta_- + i\omega}{2}; \frac{d}{2} + l; \tanh^2 x\right), \quad (3.1.5)$$

being $\Delta_\pm = \frac{d}{2} \pm i\sqrt{m^2 - (\frac{d}{2})^2}$.

For an application of the dS phase shift and its analogs on black hole backgrounds to the computation of the free field partition function see [11, 13].

3.2 INTERACTING THEORY

It is natural to ask if the in-out correlators of an interacting theory can also be matched to a BEFT, and what constraints unitarity imposes on the EFT parameters. Intuitively, this would be the case if interactions turn off fast enough for $\chi \gg 1$. Then for the low-frequency observables the interaction region $\chi \sim 1$ can be collapsed into a point at $\chi = 0$.

It would be interesting to find a classification of theories for which this is possible. We did not succeed so far, but we do not expect the set to be empty either. It plausibly includes super-renormalizable theories because of the large blue-shift toward the horizon. The example of last section supports this expectation: We can think of the mass term as an interaction added to the free massless theory. As we showed explicitly, the correlators of this theory match with a massless free theory coupled to a boundary.

Given $\rho(\Delta)$, a way to check the rapid fall-off of interactions is to inspect the projection of (2.3.1) into the space of spherical harmonics

$$\langle [\phi_{lm}^{\text{out}}(u), \phi_{lm}^{\text{in}}(0)] \rangle = \int_{\frac{d}{2}-i\infty}^{\frac{d}{2}+i\infty} \frac{d\Delta}{2\pi i} \rho(\Delta) C_f(u, l; \Delta). \quad (3.2.1)$$

If the interactions turn off at large χ , we would expect the LHS to be universal for $u \ll -1$ because an in-state that travels all the way to $\chi \sim 1$ region and reflects back arrives to the future horizon at u not much less than -1 . We note that regardless of Δ , all free commutators $C_f(u, l; \Delta)$ approach a universal form in the limit $u \rightarrow -\infty$:

$$C_f(u, l; \Delta) \sim -\frac{i}{2} + \mathcal{O}(e^u), \quad u \ll -\log |\Delta|. \quad (3.2.2)$$

Therefore, if the integration over Δ converges with a negative power of $|\Delta|$, the interacting commutator will approach the same universal behavior exponentially in u .² Since nontrivial interactions would ultimately leave their imprint in this observable, if the latter is universal for $u \ll -1$, we expect a boundary description to emerge at low frequency. Assuming this, we proceed to show that unitarity (i.e. $\rho(\Delta) > 0$) constrains this BEFT.

First, we write (3.2.1) as

$$\langle [\phi_{lm}^{\text{out}}(u), \phi_{lm}^{\text{in}}(0)] \rangle = \oint \frac{d\omega}{4\pi\omega} e^{-i\omega u} \mathcal{S}(\omega), \quad (3.2.3)$$

where the contour is the same as in (3.1.9) and

$$\mathcal{S}(\omega) \equiv \int_{\frac{d}{2}-i\infty}^{\frac{d}{2}+i\infty} \frac{d\Delta}{2\pi i} \rho(\Delta) e^{2i\alpha_\Delta(\omega, l)}. \quad (3.2.4)$$

Above, to exchange the order of the ω and Δ integrals, we assumed a sufficiently fast convergence of the integral over Δ . More generally, one might need to perform a number of subtractions before

² One advantage of S-matrix is its invariance under field redefinitions. This does not hold for static-patch in-out correlators since, from a global perspective, they are just a particular configuration of local correlators. For instance, changing $\phi \rightarrow \phi + \phi^2$ in a free theory results in $\rho(\Delta) = \rho_\phi(\Delta) + \rho_{\phi^2}(\Delta)$ that given $\rho_{\phi^2}(\Delta)$ (see [8, 23]) does not satisfy the above convergence requirement.

being able to do so. Depending on l , the free phase shifts $e^{2i\alpha_\Delta(\omega,l)}$ approach 1 or -1 as $\omega \rightarrow 0$. In an interacting theory, $\rho(\Delta)$ is supported on more than one Δ . Therefore, there has to be nonzero absorption:

$$|\mathcal{S}(\omega)| < |\mathcal{S}(0)|, \quad \text{interacting theory.} \quad (3.2.5)$$

Let us focus on the $l = 0$, $d = 3$ case and try to match the low ω behavior of $\mathcal{S}(\omega)$ with a BEFT. In an interacting theory, the boundary action will include interactions and not just quadratic operators. Moreover, this effective theory includes the novel features of a finite temperature EFT, namely dissipative terms that have to be formulated on the SK contour. Absorption is caused not only by the production of the low-energy effective degrees of freedom, but also via interaction with the thermal bath.

It is believed that when the environment degrees of freedom have a short correlation time τ , the long wavelength ‘‘hydro description’’ admits a local expansion controlled by τ [22]. For us τ is related to the quasinormal decay time. We have seen that the spectrum is typically discrete and $\tau \sim H^{-1} (= 1)$. This implies the existence of a local expansion for $\omega \ll 1$

$$\mathcal{S}(\omega) = - \sum_{n=0}^{\infty} \frac{1}{n!} s_n (-i\omega)^n \quad (3.2.6)$$

(the overall minus is for later convenience). Since this is a 2-point correlator, the coefficients s_n could be matched with a quadratic action. However, in addition to (3.1.10), we have to include the dissipative terms to the action (dropping as before the 00 index of the s -wave)

$$S_{\text{diss.}}^{(2)} = - \int dt \int_0^\infty dx \delta(x) \sum_{n=0}^{\infty} b_n \partial_t^n \phi_- \partial_t^{n+1} \phi_+, \quad (3.2.7)$$

where in terms of the fields on the forward and backward part of the SK contour (respectively ϕ_R and ϕ_L)

$$\phi_+ = \frac{\phi_L + \phi_R}{2}, \quad \phi_- = \phi_R - \phi_L. \quad (3.2.8)$$

Following the SK perturbation theory (see Appendix A.3), we compute the leading dissipative correction

$$\mathcal{S}^{\text{EFT}}(\omega) = e^{2i\alpha} \left[1 - \frac{2b_0}{c_0^2} \omega^2 + \mathcal{O}(\omega^3) \right], \quad (3.2.9)$$

where α is fixed by the conservative coefficients as in (3.1.12). Note that $\mathcal{S}^{\text{EFT}}(0) = -1$. This means that matching is possible only if

$$\int_{\frac{d}{2}-i\infty}^{\frac{d}{2}+i\infty} \frac{d\Delta}{2\pi i} \rho(\Delta) = 1. \quad (3.2.10)$$

Furthermore, in the presence of interactions (3.2.5) implies a positive friction term

$$b_0 > 0. \quad (3.2.11)$$

It is of course natural to have a friction rather than an anti-friction in an open system.

There is an alternative way to find this bound and new ones on the higher derivative conservative terms using the moments constraints. First, we expand the free phase shifts (3.1.6):

$$e^{2i\alpha_\Delta(\omega, l=0)} = - \sum_{n=0}^{\infty} \frac{1}{n!} s_n(\Delta) (-i\omega)^n. \quad (3.2.12)$$

For $m^2 > 2$ (i.e. above the conformal mass), we have

$$s_n(\Delta) > 0, \quad s_1(\Delta) = [s_0(\Delta)]^2, \quad s_2(\Delta) \geq \frac{2}{3} [s_0(\Delta)]^3. \quad (3.2.13)$$

Substituting the expansion in (3.2.4),

$$\mathcal{S}(\omega) = - \sum_{n=0}^{\infty} \left[\int_{\frac{d}{2}-i\infty}^{\frac{d}{2}+i\infty} \frac{d\Delta}{2\pi i} \rho(\Delta) s_n(\Delta) \right] (-i\omega)^n, \quad (3.2.14)$$

we can write the coefficients as averages of over the following distribution:

$$\int_{\frac{d}{2}-i\infty}^{\frac{d}{2}+i\infty} \frac{d\Delta}{2\pi i} \rho(\Delta) s_n(\Delta) = \int_0^\infty ds_0 \underbrace{\frac{ds_0}{ds_0} \frac{\rho(\Delta(\alpha_n))}{2\pi i}}_{\equiv \hat{\rho}(s_0) > 0} s_n(s_0) \equiv \langle s_n \rangle. \quad (3.2.15)$$

On the other hand, these coefficients must match the EFT result (see Appendix A.3):

$$-S^{\text{EFT}}(\omega) = 1 + \frac{2}{-c_0} (-i\omega) + \frac{2(b_0 + 1)}{c_0^2} (-i\omega)^2 + \frac{2(1 + 2b_0 + b_0^2 + c_0 c_1)}{-c_0^3} (-i\omega)^3 + \mathcal{O}(\omega^4), \quad (3.2.16)$$

where $c_0 < 0$ if ρ has support only for $m^2 > 2$. The second relation in (3.2.13) and the fact that $\langle s_0^2 \rangle \geq \langle s_0 \rangle^2$ implies

$$\frac{1 + b_0}{c_0^2} \geq \frac{1}{c_0^2} \quad (3.2.17)$$

therefore:

$$b_0 \geq 0. \quad (3.2.18)$$

The third relation in (3.2.13) and $\langle s_0 \rangle \langle s_0^3 \rangle \geq \langle s_0^2 \rangle^2$ implies

$$c_1 \leq \frac{(1 + b_0)^2}{-3c_0} \quad (3.2.19)$$

So far we did not include boundary interactions. Loops from those would lead to additional analytic contributions to (3.2.16) starting from $\mathcal{O}(\omega)$. Therefore, they are degenerate with the b_n and c_n parameters, and our bounds should be interpreted as unambiguous constraints on the expansion coefficients of $\mathcal{S}(\omega)$ rather than coefficients in the Lagrangian. The scheme dependence of the Lagrangian is, of course, a general fact.

CONCLUSIONS OF PART I

In this work, we used in-out correlators in dS static patch to give a generalization of the quasinormal spectrum in interacting theories. We related this spectrum to the spectrum of dimensions that appear in the Kälén-Lehmann spectral density $\rho(\Delta)$ of the 2-point correlators. We have seen that the quasinormal spectrum is generically (though not always) discrete, and the analytic structure of the correlators is similar to the celestial amplitudes.

The downside of our approach is that the horizon correlators are not well-defined when gravity is dynamical. In that context, it seems more natural to define the operator insertions with respect to the worldline of a dS observer. On the other hand, the generalization of the quasinormal spectrum to the interacting case might be relevant in computing the corrections to de Sitter entropy as thoroughly discussed in [11].

We have also showed that at low frequencies, the in-out correlators can, under certain conditions, be matched to a finite temperature boundary EFT. This BEFT can be thought of as the hydrodynamic limit of the problem. It might be useful in understanding the structure of thermal EFTs and dissipative hydrodynamics. In particular, it would be interesting to find similar positivity bounds in them.

Finally, it would be interesting to explore the consequences of unitarity for the cosmological correlation functions, and to find potentially observable consistency conditions. See [24] for an earlier work in this direction.

Part II

PRIMORDIAL BLACK HOLES

5.1 PHYSICAL MOTIVATION

The possibility that the totality of dark matter in the Universe consists of primordial black holes (PBHs) still holds the stage even though almost half-a-century has passed after the pioneering proposal of Hawking and Carr [25, 26]. This is especially true in the mass range $10^{18} \lesssim M_{\text{PBH}} [\text{g}] \lesssim 10^{21}$ in which black holes are neither too light (otherwise they would have evaporated in the past through Hawking radiation [27]) or too heavy (otherwise they would distort space-time in a way that contradicts present bounds from lensing experiments [28, 29]).

PBHs could have formed in the very early Universe during the radiation dominated era.¹ The key ingredient that triggers the formation of a PBH is the presence of an over-fluctuation in the density of the Universe which, if large enough, gravitationally collapses dragging down any matter within its horizon, that is the parcel of space around any point reachable at the speed of light.

The theory of inflation provides an elegant mechanism that explains the origin of density perturbations in the Universe. In the inflationary picture, space-time fluctuates quantum mechanically around a background that is expanding exponentially fast. After the end of inflation, these curvature fluctuations are transferred to the radiation field, creating slightly overdense and under-dense regions. It is, therefore, fascinating to ask whether the formation of PBHs fits in the inflationary picture of structure formation.² To answer this question, two (related) aspects need to be addressed.

- i)* The inflaton dynamics should give rise to a peak in the power spectrum of curvature perturbations.³ This translates into a large variance for density perturbations that, in turn, enhances the chance to create overdense regions above the threshold for gravitational collapse.
- ii)* The abundance of such collapsing regions should be large enough to explain the totality of dark matter.

Here we focus on simple single-field inflationary models. It is known that in order to fulfil point *i)* slow-roll conditions must be violated. The simplest option is to introduce, few e -folds before the end of inflation, an approximate stationary inflection point in the inflaton potential (see refs. [35–37] for the earliest proposal in this direction). When the inflaton, during its classical dynamics, crosses this region (during the so-called “ultra slow-roll phase”), curvature perturbations, due to the presence of

¹ It is also possible to have PBH formation during matter domination [30].

² This is not the only option. The formation of PBHs may have been independent of inflationary physics; PBHs may have been originated from topological defects formed during symmetry breaking phase transition, for instance from the collapse of string loops [31–33].

³ An exception, where no amplification of the power spectrum is needed, are models where PBHs form from the collapse of domain walls created during inflation [34].

negative friction, get exponentially enhanced [38–42].⁴ Point *ii*) is more subtle. Due of their intrinsic quantum-mechanical origin, the way in which quantum fluctuations lead to a classical pattern of perturbations can be described only in a probabilistic sense. Consequently, the computation of the abundance of collapsing regions requires informations about the statistical distribution of density perturbations. Most of the time, for simplicity, the gaussian approximation is assumed. However, the very same fact that slow-roll conditions are violated as a consequence of point *i*) suggests that non-gaussianities may play a relevant role. Refs. [45, 46] indeed find that during an ultra slow-roll phase sizable non-gaussianities of local type are generated. In the rest of this paper we will dub these non-gaussianities “primordial” to distinguish them from non-gaussianities that arise from the non-linear relation between curvature and density perturbations.

What is the impact of primordial non-gaussianities on the gaussian approximation when computing the PBH abundance? Ref. [47] addressed this question in the context of threshold statistics. The main result of ref. [47] is that the abundance of PBHs is exponentially sensitive to primordial non-gaussianities⁵. Based on this result, ref. [45] claims that, in the context of single-field inflationary models which feature an approximate stationary inflection point, the gaussian approximation is hardly trustable when computing the PBH abundance.

The goal of this work is to address the same question using a different computational strategy inspired by peak theory [48]. More precisely, we associate regions where the overdensity field takes values above the threshold for gravitational collapse with spiky local maxima of the curvature perturbation field, and compute the number density of the latter using peak theory that we extend to include local non-gaussianities.

Our main conclusion is that the impact of local non-gaussianities on the PBH abundance is far less important compared to what previously thought. We confirm that in models for PBH production (at least the class of models that we are going to consider), local non-gaussianities are sizeable enough to invalid the use of the the gaussian approximation to estimate their abundance. However we find that their impact is modest when translated in terms of the amplitude of curvature power spectrum, namely it is enough to change it by a factor $\simeq 2$ or smaller to obtain the same PBH abundance predicted by the gaussian calculation. This shift can be obtained by a small change of the parameters of the inflationary model.

En route, we discuss the difference between threshold statistics and peak theory, and we explain under which conditions (and why) peak theory gives a PBH abundance which is larger than the one computed by means of threshold statistics.

The structure of this part is as follows.

⁴ Alternatively, a parametric amplification of curvature perturbations could be caused by resonance with oscillations in the sound speed of their propagation [43]. Another possibility is that, after the inflationary phase, the inflaton begins to oscillate near the minimum of the potential and fragments into oscillons which, in turn, lead to copious production of PBHs [44].

⁵ More precisely this means that in the context of threshold statistics the PBH abundance is given by eq. (6.2.14), where C_n are the n^{th} normalized cumulants of the non-gaussian distribution.

- * In section 5.2 we introduce the problem and present our solution strategy. This section is paired with appendix B where we explain in more detail the cosmological interpretation of all quantities involved.
- * In chapter 6 we discuss our main results and we explain the discrepancy with the previous literature. This section is paired with appendix C-F where we collect all relevant technical details.
- * We conclude in chapter 7.

5.2 PROBLEM SETUP AND SOLUTION STRATEGY

Consider in position space

$$h(\vec{x}) = \mathcal{R}(\vec{x}) + \alpha \mathcal{R}(\vec{x})^2, \quad (5.2.1)$$

where α is a constant, $\mathcal{R}(\vec{x})$ is a gaussian scalar random field while $h(\vec{x})$ is non-gaussian because of the presence of the non-linear term on the right-hand side. In this case, non-gaussianities are called of local type because for a given \vec{x} at which we evaluate h the amount of non-gaussianity is localized at the same position. We briefly discuss in appendix B the physical interpretation of eq. (5.2.1) and the limitations of this parametrization of non-gaussianities.

The first observation is that

$$\partial_i h(\vec{x}) = [\partial_i \mathcal{R}(\vec{x})][1 + 2\alpha \mathcal{R}(\vec{x})], \quad (5.2.2)$$

meaning that stationary points of \mathcal{R} are also stationary points of h ($\partial_i \mathcal{R} = 0$ implies $\partial_i h = 0$).

What is crucial, however, is that the nature (saddle points, maxima or minima) of these “shared” stationary points depends on the sign of the factor $1 + 2\alpha \mathcal{R}$. Consider the matrix of second derivatives evaluated at a stationary point \vec{x}_{st} (we will further indicate a minimum with \vec{x}_m and a maximum with \vec{x}_M). One finds the Hessian matrix $h_{ij}(\vec{x}_{st}) = [\mathcal{R}_{ij}(\vec{x}_{st})](1 + 2\alpha \mathcal{R}_{st})$.⁶

To fix ideas, consider the simple case of two spatial dimensions $\vec{x} = (x, y)^T$ and the case in which the stationary point \vec{x}_m is a minimum of \mathcal{R} .

Minima of \mathcal{R} are identified by two conditions. The first one, $\mathcal{R}_{xx}(\vec{x}_m)\mathcal{R}_{yy}(\vec{x}_m) - \mathcal{R}_{xy}(\vec{x}_m)^2 > 0$ separates extrema from saddle points. The second one, $\mathcal{R}_{xx}(\vec{x}_m) > 0$ and $\mathcal{R}_{yy}(\vec{x}_m) > 0$, separates minima from maxima. Since we have $h_{xx}(\vec{x}_m)h_{yy}(\vec{x}_m) - h_{xy}(\vec{x}_m)^2 = (1 + 2\alpha \mathcal{R}_m)^2 [\mathcal{R}_{xx}(\vec{x}_m)\mathcal{R}_{yy}(\vec{x}_m) - \mathcal{R}_{xy}(\vec{x}_m)^2]$ it is obvious that the condition $\mathcal{R}_{xx}(\vec{x}_m)\mathcal{R}_{yy}(\vec{x}_m) - \mathcal{R}_{xy}(\vec{x}_m)^2 > 0$ is also satisfied by h .

On the contrary, since $h_{xx}(\vec{x}_m) = (1 + 2\alpha \mathcal{R}_m)\mathcal{R}_{xx}(\vec{x}_m)$ and $h_{yy}(\vec{x}_m) = (1 + 2\alpha \mathcal{R}_m)\mathcal{R}_{yy}(\vec{x}_m)$, it is possible that a minimum of \mathcal{R} becomes a maximum of h if $1 + 2\alpha \mathcal{R}_m < 0$. Viceversa, a maximum of \mathcal{R} can become a minimum of h .

The argument trivially generalizes to the more realistic case of three spatial dimensions.

⁶ We use the short-hand notation $f_k \equiv f(\vec{x}_k)$, $f_i(\vec{x}_k) \equiv \partial_i f(\vec{x})$ evaluated at \vec{x}_k and $f_{ij}(\vec{x}_k) \equiv \partial_{ij} f(\vec{x})$ evaluated at \vec{x}_k for some generic function f . The flat spatial Laplacian is $\nabla^2 f(\vec{x}) \equiv \sum_i f_{ii}(\vec{x})$.

In peak theory, one computes the number density of maxima [48]. We are interested in the number density of maxima of the non-gaussian variable h . As argued before, identifying this quantity with the number density of maxima of \mathcal{R} (based on the observation that h and \mathcal{R} have the same stationary points) is not correct. Let us give a quantitative argument to support this claim. From the previous discussion, it is clear that counting the maxima of \mathcal{R} might be not enough. On the contrary, a simple modification could be the following. One should

- i)* Count the maxima of \mathcal{R} ;
- ii)* Add the minima of \mathcal{R} that, depending on the value of $(1 + 2\alpha\mathcal{R}_m)$, become maxima of h ;
- iii)* Subtract the maxima of \mathcal{R} that, depending on the value of $(1 + 2\alpha\mathcal{R}_M)$, become minima of h .

Ref. [49] assumes *i)*. However, the two operations *ii)* and *iii)* do not balance between each others, and a sizable correction to *i)* will be introduced if α is large enough. In fig. 3 we show how the number density of maxima of the gaussian variable \mathcal{R} changes (in percentage) as a function of α when *ii)* and *iii)* are implemented. Schematically, we compute

$$\Delta n_{\max} = \frac{(\# \text{minima of } \mathcal{R} \rightarrow \text{maxima of } h) - (\# \text{maxima of } \mathcal{R} \rightarrow \text{minima of } h)}{\# \text{maxima of } \mathcal{R}}. \quad (5.2.3)$$

We obtain fig. 3 using gaussian peak theory (implementing the results of ref. [48], see appendix C). If we take $\alpha \ll 1$, *ii)* and *iii)* do not alter the estimate of *i)*. However, for sizable $\alpha \gtrsim 0.2$ the change in the number density of maxima of \mathcal{R} becomes evident.

In situations of cosmological interest, the issue is further complicated by the fact that we are not really interested in *all* maxima of h but only in those which are “spiky enough.” The reason is that the quantity which is relevant is the density contrast $\delta(\vec{x}, t)$ (also dubbed overdensity field in the following) whose relation with $h(\vec{x})$ (assuming radiation dominated epoch) reads [50]

$$\delta(\vec{x}, t) = -\frac{4}{9} \left(\frac{1}{aH} \right)^2 e^{-2h(\vec{x})} \left[\nabla^2 h(\vec{x}) + \frac{1}{2} h_i(\vec{x}) h_i(\vec{x}) \right], \quad (5.2.4)$$

where the time dependence comes from the scale factor $a = a(t)$ and the Hubble rate $H = H(t)$ while h does not depend on time because eq. (5.2.4) assumes perturbations to be on super-horizon scales. Eq. (5.2.4) can be thought as a Poisson equation in which h plays the role of gravitational potential while the density contrast can be written more precisely as $\delta(\vec{x}, t) \equiv \delta\rho(\vec{x}, t)/\rho_b(t)$ where $\rho_b(t)$ is the average background radiation energy density and $\delta\rho(\vec{x}, t) = \rho(\vec{x}, t) - \rho_b(t)$ its perturbation. The physics-case that is relevant for the present study is the one in which the density contrast has a peak localized in some region of space that is high enough to trigger the gravitational collapse into a black hole. If the number of these peaks above threshold is large enough, these black holes can be part of dark matter. In the range $10^{18} \lesssim M_{\text{PBH}} [\text{g}] \lesssim 10^{21}$, a population of PBHs may account for the totality of dark matter observed in the Universe today.

Consider a peak of the overdensity field, located at some spatial point \vec{y}_{pk} .

$$\delta(\vec{y}_{\text{pk}}, t) = -\frac{4}{9} \left(\frac{1}{aH} \right)^2 e^{-2h(\vec{y}_{\text{pk}})} \left[\nabla^2 h(\vec{y}_{\text{pk}}) + \frac{1}{2} h_i(\vec{y}_{\text{pk}}) h_i(\vec{y}_{\text{pk}}) \right] \approx -\frac{4}{9} \left(\frac{1}{aH} \right)^2 \nabla^2 h(\vec{y}_{\text{pk}}), \quad (5.2.5)$$

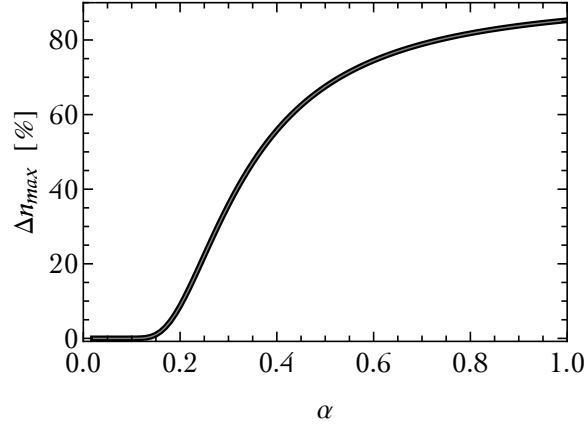


Figure 3: Percentage increase in the number density of maxima of \mathcal{R} when we ii) add the minima of \mathcal{R} that become maxima of h and iii) subtract the maxima of \mathcal{R} that become minima of h (see eq.(5.2.3)). To make this (illustrative) plot we set $\sigma_0 = 1$ and $\gamma = 3/4$ (see appendix C for definitions).

where in the second step we linearized in h . We follow here the approach of refs. [51, 52] in which the linear approximation was adopted. Since the peak amplitude of the overdensity must be larger than some critical value δ_c , we deduce the condition

$$-\nabla^2 h(\vec{y}_{pk}) \gtrsim \frac{9}{4} (aH)^2 \delta_c, \quad (5.2.6)$$

on the curvature of h at the peak of δ .

If we assume that local maxima of h coincide with peaks of δ (that is $\vec{y}_{pk} \simeq \vec{x}_M$), then the condition in eq. (5.2.6) tells that only maxima of h which are “spiky enough” contribute to the formation of black holes. Of course, the assumption that local maxima of h coincide with peaks of δ requires some care. Ref. [53] argues, both analytically and numerically, that this assumption is well justified. However, ref. [53] only considers the case in which h is gaussian, that is, $h = \mathcal{R}$ with $\alpha = 0$ in our case (but they include the presence of the non-linearities in eq. (5.2.5)). Since stationary points of \mathcal{R} are also stationary points of h , we tend to believe that the same conclusion holds true in the case with $\alpha \neq 0$ but of course this is an important point that has to be checked explicitly.

All in all, the strategy we shall follow in the course of this work is the following.

First, we will compute the number density of maxima of the non-gaussian random field h that are “spiky enough” according to the condition in eq. (5.2.6). This requires a generalization of the work in ref. [48] such as to implement local non-gaussianities. Second, we will check that these maxima are also peaks of the overdensity field. If this last point will turn out to be true, our computation of the number density of “spiky enough” maxima of h will provide the abundance of peaks of the overdensity field that are large enough to form black holes.

RESULTS AND DISCUSSION

We present in this section the main results of our analysis. In section 6.1 we discuss how primordial non-gaussianities of local type alter the abundance of PBHs. In section 6.2 we compare with the existing literature.

All technical details are collected in appendix B (where we discuss the origin of eq. (5.2.1) from a cosmological viewpoint), appendix C (where we discuss the gaussian limit), appendixes D and E (where we discuss how to construct the non-gaussian part and the approximations that are involved) and appendix F (where we give formulas for computing cumulants of generic order).

6.1 THE ABUNDANCE OF PBHS IN THE PRESENCE OF PRIMORDIAL LOCAL NON-GAUSSIANITIES

The quantity of central interest is the fraction of the Universe's mass in the form of PBHs at the time of their formation. As customary in the literature, we indicate this quantity with β . The present-day fractional abundance of dark matter in the form of PBHs is given by (for a review, see ref. [54])

$$\frac{\Omega_{\text{PBH}}}{\Omega_{\text{DM}}} = \mathcal{O}(1) \times \left(\frac{\beta}{10^{-16}} \right) \left[\frac{g_*(t_f)}{106.75} \right]^{-1/4} \left(\frac{M_{\text{PBH}}}{10^{18} \text{ g}} \right)^{-1/2}, \quad (6.1.1)$$

where $g_*(t_f)$ is the number of relativistic degrees of freedom at the time of black hole formation (that we normalize and set to its standard model value). Eq. (6.1.1) is defined modulo an overall $\mathcal{O}(1)$ factor whose precise value depends on the detail of the gravitational collapse that leads to black hole formation. In this paper we consider $M_{\text{PBH}} \simeq 10^{18} \text{ g}$; consequently, as an order-of-magnitude estimate, $\beta \gtrsim 10^{-16}$ is excluded since it would imply overclosure of the present-day Universe, $\Omega_{\text{PBH}} > \Omega_{\text{DM}}$.

We find the following formula

fraction of the Universe's mass in PBH in the presence of primordial local non-gaussianities

$$\beta \approx \frac{1}{4\sqrt{2\pi(1-\gamma^2)}} \left[\int_{-\frac{1}{2\alpha\sigma_0}}^{\infty} d\tilde{\nu} \int_{x_\delta(\tilde{\nu})}^{\infty} dx e^{-\tilde{\nu}^2/2} f(x) e^{-\frac{(x-x_*)^2}{2(1-\gamma^2)}} + \int_{-\infty}^{-\frac{1}{2\alpha\sigma_0}} d\tilde{\nu} \int_{-\infty}^{x_\delta(\tilde{\nu})} dx e^{-\tilde{\nu}^2/2} f(x) e^{-\frac{(x-x_*)^2}{2(1-\gamma^2)}} \right] \quad (6.1.2)$$

that we derive in detail in appendix C (as far as the gaussian limit is concerned) and appendix D (where we discuss how to construct the non-gaussian part and the approximations that are involved).

In short:

- * The parameter α , already defined in eq. (5.2.1), indicates the presence of local non-gaussianities (of quadratic type). The limit $\alpha \rightarrow 0$ reproduces the gaussian result. A more physical interpretation of this parameter is given in appendix B. In concrete models of inflation which generate a sizable abundance of dark matter in the form of PBHs (see, for instance, ref. [55]), we expect $\alpha \in [0.24, 0.61]$ [45, 46].

We derive our result based on peak theory. More precisely, we associate regions where the overdensity field takes large values with spiky local maxima of the comoving curvature perturbation, and compute the number density of the latter using peak theory that we extend to include local non-gaussianities. Within this approach, eq. (6.1.2) represents an original result.

- * The spectral moments σ_j^2 are defined by (see eq. (C.0.9) and discussion in appendix C)

$$\sigma_j^2 \equiv \int \frac{dk}{k} \mathcal{P}_{\mathcal{R}}(k) k^{2j}, \quad (6.1.3)$$

where $\mathcal{P}_{\mathcal{R}}(k)$ is the dimensionless power spectrum of the gaussian random field \mathcal{R} . The a -dimensional parameter γ is defined as $\gamma = \sigma_1^2 / \sigma_2 \sigma_0$ and takes values $0 < \gamma < 1$. In this paper we analyze two possible cases. In order to elucidate some intermediate results of our computational strategy, we use in appendix C a simple toy-model for the power spectrum given by the log-normal function (see eq. (C.0.24) and related discussion)

$$\mathcal{P}_{\mathcal{R}}(k) = \frac{A_g}{\sqrt{2\pi v}} \exp\left[-\frac{\log^2(k/k_*)}{2v^2}\right], \quad (6.1.4)$$

since in this case the spectral moments can be computed analytically and they are given by $\sigma_j^2 = A_g k_*^{2j} e^{2j^2 v^2}$. The three parameters $\{k_*, A_g, v\}$ in eq. (6.1.4) control, respectively, the position of the peak of the power spectrum, the peak amplitude of the power spectrum and its width. However, we remark that in single-field inflationary models the value of α that defines the amount of local non-gaussianities and the shape of the power spectrum are intimately related, and in general one can not take α as a free parameter and fix the power spectrum to a specific functional form like the one introduced in eq. (6.1.4). A more realistic example is the following. Consider the power spectrum defined by the piecewise function

$$\text{realistic power spectrum : } \mathcal{P}_{\mathcal{R}}(k) = \mathcal{P}_{\mathcal{R}}(k_*) \times \begin{cases} \left(\frac{k}{k_1}\right)^{n_1} \exp\left[-\frac{\log^2(k_1/k_*)}{2v^2}\right] & \text{for } k < k_1 \\ \exp\left[-\frac{\log^2(k/k_*)}{2v^2}\right] & \text{for } k_1 \leq k \leq k_2 \\ \left(\frac{k}{k_2}\right)^{n_2} \exp\left[-\frac{\log^2(k_2/k_*)}{2v^2}\right] & \text{for } k > k_2 \end{cases} \quad (6.1.5)$$

with two power-law behaviors for $k \ll k_*$ and $k \gg k_*$ that, for $k \approx k_*$, are connected by the log-normal function in eq. (6.1.4). In this case, it is possible to show that the spectral index of the fall-off of the power spectrum after the peak at $k = k_*$ is related to α by the relation $n_2 \approx -4\alpha$ that is twice the value of the Hubble parameter η after the end of the ultra slow-roll

phase.¹ In our numerical analysis, therefore, we use the realistic power spectrum in eq. (6.1.5) with the condition $n_2 = -4\alpha$ for fixed α . This provides the above-mentioned relation between the amount of local non-gaussianities and the shape of the power spectrum. We remark that this point is often overlooked in the literature. As a numerical check, we show in fig. 4 (left

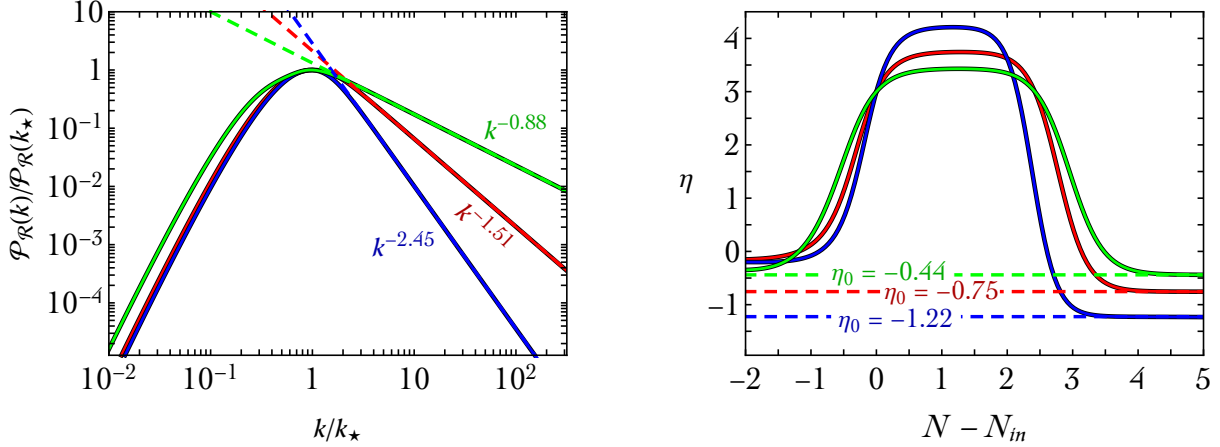


Figure 4: Power spectra for the model in ref. [55] (red, with label $k^{-1.51}$), ref. [56] (blue, with label $k^{-2.45}$) and ref. [57] (green, with label $k^{-0.88}$) computed numerically by solving the Mukhanov-Sasaki equation (left panel). The slope of the power-law falloff after the peak is $k^{2\eta_0}$ where η_0 is the value of the Hubble parameter η (whose evolution, as function of the e -fold time N with N_{in} the beginning of the ultra slow-roll phase, is shown in the right panel) after the end of the ultra slow-roll phase; η_0 , in turn, is related to the parameter α that controls the size of local non-gaussianities via $\alpha = -\eta_0/2$ (see appendix B).

panel) the power spectra of comoving curvature perturbations computed numerically for three inflationary models in which a ultra slow-roll phase takes place. All power spectra are well described by the analytical ansatz in eq. (6.1.5). The slope of the power spectra after the peak is related to the value of the Hubble parameter η (shown in the right panel of the same figure) after the end of the ultra slow-roll phase which, in turn, controls the size of local non-gaussianities (see caption and appendix B for more details).

As far as the values of the other parameters in eq. (6.1.5) are concerned, we use $k_* = 1.5 \times 10^{14} \text{ Mpc}^{-1}$, $n_1 = 3.4$, $k_1 = k_*/5$, $k_2 = 3k_*/2$ and $\nu = 0.7$; the values of $k_{1,2}$, ν and n_1 are motivated by a fit of eq. (6.1.5) done with respect to the numerical power spectrum obtained in the context of

¹ This can be understood as follows. The modes that constitute the fall-off of the power spectrum after the peak are those for which the horizon-crossing condition $k = aH$ happens after the end of the ultra slow-roll phase [55]; during this part of the dynamics the power spectrum can be approximated by means of the conventional slow-roll relation $\mathcal{P}_{\mathcal{R}}(k) = H^2/8\pi^2\epsilon$ where the Hubble parameter ϵ evolves in time according to $\epsilon(N) \propto e^{-2\eta_0 N}$ where η_0 (which is a negative number, $\eta_0 < 0$, see appendix B) is the value of the Hubble parameter η after the end of the ultra slow-roll phase. We neglect the contribution coming from the time-evolution of H , which is sub-leading. This means that we have $\mathcal{P}_{\mathcal{R}}(k) \propto e^{2\eta_0 N}$. From $k = aH$ we have $dk/k = dN$, and we can convert the e -fold time-dependence into a k -dependence, $\mathcal{P}_{\mathcal{R}}(k) \propto k^{2\eta_0} = k^{-4\alpha}$ where we used that $\alpha = -\eta_0/2$ (see appendix B).

the explicit models studied in ref. [55]. In particular, notice that the spectral index n_1 describes the growth of the power spectrum that leads to the formation of the peak; its value is related to the value of the Hubble parameter η during the ultra slow-roll phase and the duration of the latter. Semi-analytical arguments (see ref. [58]) suggest that $n_1 < 4$.² The value $k_* = 1.5 \times 10^{14} \text{ Mpc}^{-1}$ is chosen because it implies $M_{\text{PBH}} \simeq 10^{18} \text{ g}$ (for which $\Omega_{\text{PBH}} \simeq \Omega_{\text{DM}}$ is possible, see ref. [46]). We consider the peak amplitude of the power spectrum $\mathcal{P}_{\mathcal{R}}(k_*)$ as a free parameter. The power spectra that we consider lead to a narrow PBHs mass function.

- * The function $f(x)$ is given in eq. (D.1.17) and the quantity χ_* in eq. (D.1.12). The function $\chi_\delta(\bar{v})$ is defined by the relation (see eq. (D.1.14))

$$(1 + 2\alpha\sigma_0\bar{v})\chi_\delta(\bar{v}) = \frac{9(a_m H_m)^2}{4\sigma_2} \delta_c, \quad (6.1.6)$$

where $\delta_c = \mathcal{O}(1)$ is a threshold value above which a peak of the overdensity field collapses to form a black hole. The left hand side of eq. (6.1.6) corresponds to the critical curvature of h in eq. (5.2.6), see section D. Formally, eq. (6.1.6) depends on time via the comoving Hubble radius $1/aH$. We evaluate eq. (6.1.6) at the time t_m when curvature perturbations re-enter the horizon and become causally connected (see refs. [51, 52] and appendix F of ref. [2])³. In eq. (6.1.6) we use the short-hand notation $a_m H_m \equiv a(t_m)H(t_m)$.

- * An important comment concerns the so-called smoothing procedure. Consider the case in which one takes a very narrow power spectrum, like the toy-model introduced in eq. (6.1.4) with a small value of ν , say $\nu = 0.1$. In this case it is not strictly necessary to introduce a smoothing procedure because the power spectrum is characterized by a well-defined scale in momentum space, $k = k_*$. The realistic case introduced in eq. (6.1.5), on the contrary, requires more care. Although the power spectrum peaks at $k = k_*$, the peak is broadened by the relatively large value of ν , and it also possesses a pronounced power-law tail at large $k \gg k_*$. In this situation we can not blindly apply eq. (6.1.2) to compute the PBH abundance because the spectral moment σ_2^2 is formally ultraviolet-divergent unless the power spectrum decays fast enough, which is however not the case in the realistic model.⁴ The solution to this issue (discussed in appendix F of ref. [2]) is to smooth-out small scales by introducing an appropriate cut-off. At the operative level, we use, instead of eq. (6.1.5), the power spectrum $\mathcal{P}_{\mathcal{R}}^{\text{cut}}(k) \equiv \mathcal{P}_{\mathcal{R}}(k) \exp(-k^2/k_{\text{cut}}^2)$ and we choose k_{cut} such as to minimize the threshold value in the right-hand side of eq. (6.1.6). Notice that this smoothing procedure is relevant for the determination both of the threshold value and the spectral moments in eq. (6.1.3).

² However, see ref. [59] for a special case (derived in the context of non-attractor inflation) in which the growth of the power spectrum can be steeper, although for a limited range of k . A steeper growth can also be attained in multi-field inflationary scenarios [60].

³ Notice however that eq. (5.2.4) is valid on super-horizon scales. This means that at horizon-crossing additional non linear effects are present. Recently, these corrections have been considered in ref. [61].

⁴ Of course, any power spectrum generated by the inflationary dynamics has an intrinsic cut-off set by the smallest scale (largest k) that exits the Hubble horizon before inflation ends. More precisely, therefore, with the words ‘‘ultraviolet-divergent integral’’ we mean that σ_2^2 is dominated by small scales.

Physically, the fact that the power spectrum in eq. (6.1.5) does not possess a well-defined scale means that the PBHs it generates will be characterized by a relatively broad mass distribution (rather than sharply peaked at the value associated to k_*). The cut-off procedure described before selects the scale (and, therefore, the value of the mass M_{PBH}) at which the abundance of PBH will be the largest.

* We use the linear approximation in eq. (5.2.4).

We now discuss the implications of eq. (6.1.2). In the left panel of fig. 5 we show the fraction of

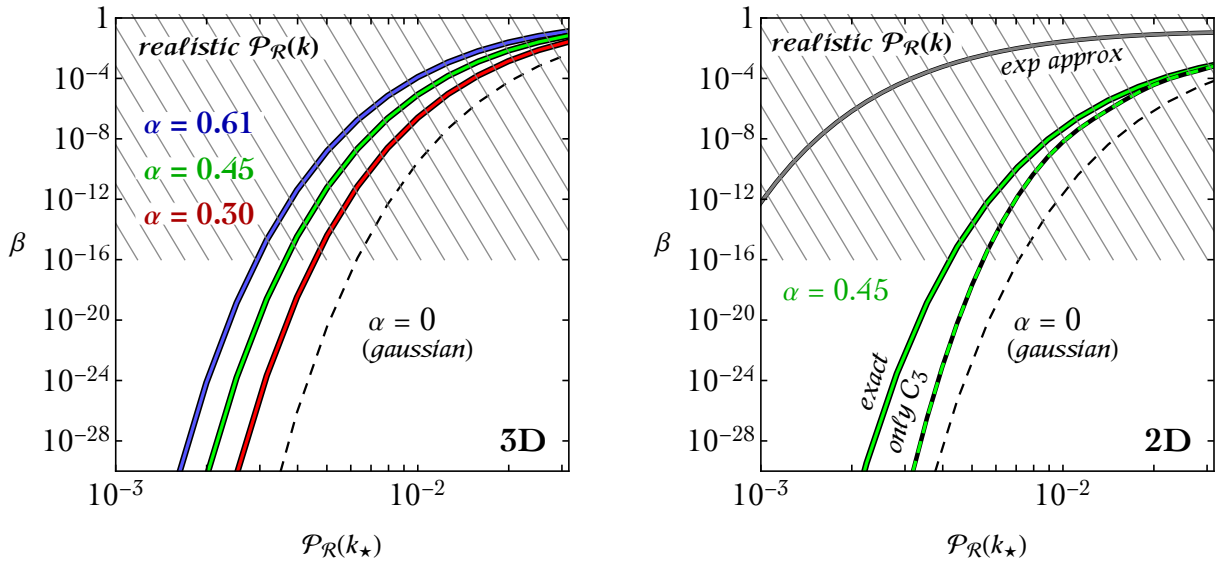


Figure 5: Left panel: Fraction of the Universe’s mass in PBHs at the time of their formation computed with (solid lines with colors) and without (dashed black line) non-gaussianities as a function of the peak amplitude of the power spectrum $\mathcal{P}_{\mathcal{R}}(k_*)$. We adopt the realistic model for the power spectrum introduced in eq. (6.1.5) and the abundance is computed using eq. (6.1.2). We show the impact of non-gaussianities for different benchmark values of α . In the hatched region we have $\beta > 10^{-16}$ and the Universe is overclosed (see eq. (6.1.1) and related discussion). Right panel: we consider two spatial dimensions, and compare the exact computation of β with the approximation obtained including only the third-order cumulants. We also show the value of β obtained by means of the exponential approximation in eq. (E.0.104); the latter gives an estimate of the abundance off by many orders of magnitude compared with the actual result.

Universe’s mass in the form of PBH computed according to eq. (6.1.2) for increasing values of the parameter α starting from the gaussian case with $\alpha = 0$. What values of α are expected in concrete models? In popular single-field models of inflation that generate a sizable abundance of dark matter in the form of PBHs, we find $\alpha \simeq 0.38$ (ref. [55]), $\alpha \simeq 0.37$ (ref. [62]), $\alpha \simeq 0.30$ (ref. [63]), $\alpha \simeq 0.22$ (ref. [57]), $\alpha \simeq 0.61$ (ref. [56]). The plot shows that including local non-gaussianities of primordial origin makes the formation of PBHs easier, and the value of $\mathcal{P}_{\mathcal{R}}(k_*)$ required to reproduce the benchmark abundance $\beta = 10^{-16}$ turns out to be smaller than the gaussian one. We find that the rescaling of the peak amplitude implied by the presence of local non-gaussianities is modest, a

factor a few in realistic models. Moreover, let us mention that it can be obtained at a price of an even smaller retuning of the parameters of the inflationary models. Similar results have been obtained in [46] for the calculation of the PBH abundance with threshold statistics.

In addition to the exact result presented in eq. (6.1.2), we also consider a “perturbative” approach based on a power-series α -expansion around the gaussian distribution. To this end, we work in two (instead of three) spatial dimensions. This simplifying assumption allows to perform most of the computations in appendix C and appendix E analytically, and makes possible to visualize and check numerically a number of intermediate results by means of simple two-dimensional plots.

Let us first clarify the exact meaning of the word “perturbative.” From a statistical viewpoint, the α -expansion corresponds to an expansion in cumulants of the joint non-gaussian probability distribution according to the schematic summarized in table 1 (see appendix C, appendix E and appendix F for details). In the gaussian approximation, all cumulants $C_{n \geq 3}$ vanish and the second-

	Gaussian $\alpha = 0$	$\mathcal{O}(\alpha)$	$\mathcal{O}(\alpha^2)$	$\mathcal{O}(\alpha^3)$	$\mathcal{O}(\alpha^4)$	$\mathcal{O}(\alpha^5)$...
second-order cumulants C_2	✓	✗	✓	✗	✗	✗	...
third-order cumulants C_3	✗	✓	✗	✓	✗	✗	...
fourth-order cumulants C_4	✗	✗	✓	✗	✓	✗	...
fifth-order cumulants C_5	✗	✗	✗	✓	✗	✓	...
...

Table 1: We organize the cumulants C_n of the joint six-dimensional probability distribution $P(h, h_x, h_y, h_{xx}, h_{xy}, h_{yy})$ as a series expansion in α . In the case $\alpha = 0$, only second-order cumulants are non-vanishing (eqs. (E.0.77-E.0.80) with $\alpha = 0$), and we reconstruct the gaussian limit. At order $\mathcal{O}(\alpha)$, the leading correction is given by third-order cumulants (eqs. (E.0.85-E.0.92)). At order $\mathcal{O}(\alpha^2)$, we include corrections to the second-order cumulants (eqs. (E.0.77-E.0.80)) and the leading pieces in the expression of fourth-order cumulants (eqs. (E.0.105-E.0.120)).

order ones correspond to the entries of the covariance matrix of the distribution. This result is valid in the limit $\alpha \rightarrow 0$. If $\alpha \neq 0$, all cumulants $C_{n \geq 3}$ are generated. However, the non-zero cumulants

can be organized in terms of an α -expansion as shown in table 1 (see caption, and appendix E and appendix F for details). Crudely speaking, we have

$$C_{n \geq 2} \sim \mathcal{O}(\alpha^{n-2}) + \mathcal{O}(\alpha^n). \quad (6.1.7)$$

At order $\mathcal{O}(\alpha)$, only the leading part of the third-order cumulants C_3 appears.⁵ We can, therefore, consider an expansion around the gaussian distribution including only the leading part of the third-order cumulants C_3 . The rationale for this approximation is twofold.


- i)* If we compare the perturbative approach with the exact computation (downgraded in two spatial dimensions) we can estimate the validity of the approximation in which only the leading part of the third-order cumulant C_3 is included.

This exercise is useful for the following reason. In the approach based on threshold statistics, one usually computes, using the tools of cosmological perturbation theory, the cumulants in the form of (the connected part of) correlators of the density perturbation field. In the presence of ultra slow-roll, however, this computation is not simple (see refs. [45, 46]), and one typically includes only the leading term in the so-called bispectrum (that is the three-point correlator). This approximation precisely corresponds to the one in which only the leading part of the third-order cumulant C_3 is included (that is the one proportional to α in eq. (6.1.7)). In the right panel of fig. 5 we show the comparison between the exact computation of β and the approximation in which only the leading part of C_3 is included; as mentioned before, we work in two spatial dimensions and we fix $\alpha = 0.45$. The comparison shows that truncating the expansion at the first order in the non-gaussian corrections does not fully capture the impact of non-gaussianities on β .

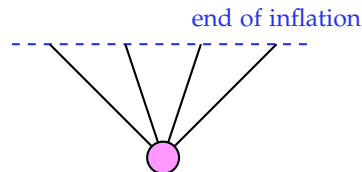
Based on this result, we pose the attention on the fact that a similar conclusion is likely to be valid also when computing correlators in cosmological perturbation theory. The local non-gaussianity which is present at the level of the three-point correlator (computed, for instance, in refs. [45, 46] and used in ref. [45] to estimate the impact of non-gaussianities on β) induces

⁵ More precisely, for each cumulant the expansion is controlled—considering for simplicity the log-normal power spectrum in eq. (6.1.4)—by the dimensionless parameter $\alpha A_g \ll 1$.

corrections also at higher orders. In terms of (cosmological) Feynman diagrams, the situation can be sketched as follows



third-order cumulant
fourth-order cumulant from (cubic interactions)²
(6.1.8)



pure fourth-order cumulant
(6.1.9)

where the square of the third-order local interaction enters at the fourth-order (as well as at higher ones).⁶ The comparison shown in the right panel of fig. 5 suggests that, without including the contributions that third-order local interactions induce in higher-order cumulants, a precise computation of β cannot be claimed.

In addition to this observation there is a second, and by far more problematic, issue that we shall discuss next.

- ii)* When computing non-gaussian corrections in the form of a series expansion around the gaussian distribution, some care must be taken. Seemingly harmless approximations, indeed, may lead to erroneous conclusions. Consider the simplified case discussed before in which only the leading part of the third-order cumulants C_3 is included. A wrong approximation in the evaluation of the non-gaussian probability distribution leads to the expression of the abundance that we report in eq. (E.0.104). In this compact expression, the non-gaussian correction exponentiates and alters the argument of the exponential function in the gaussian distribution. If this approximation were true, the effect of non-gaussianities would be exponentially large. For illustration, we add in the right panel of fig. 5 the value of β that one gets by means of eq. (E.0.104). Clearly, eq. (E.0.104) overestimates the actual value of β by many orders of magnitude. In appendix E we explain why this approximation is wrong and what is the correct procedure to follow.

The reader may wonder why we are wasting time discussing a wrong result. The reason is that it rings a bell. Previous studies on the impact of primordial non-gaussianities found, although in a slightly different statistical context, that non-gaussian corrections alter exponentially the gaussian value of β , analogously to what happens with eq. (E.0.104), an expression that we

⁶ Of course, higher-order correlators generated by pure higher-order interactions—for instance, a pure quartic interaction in the violet vertex of the example above—could also be present but, as discussed in appendix B, we do not consider them explicitly in this paper.

just branded inaccurate. A closer look at this literature, therefore, is mandatory. This will be the subject of the next section.

6.2 COMPARISON WITH THE LITERATURE

The impact of primordial non-gaussianities on the computation of PBH abundance was discussed in ref. [47] in the context of the so-called threshold statistics. Ref. [47] finds that primordial non-gaussianities may play a very relevant role because they alter the argument of the exponential function that sets the value of the PBH abundance in the gaussian case. Ref. [45] applies the results of ref. [47] to the case of single-field inflationary models which feature the presence of an approximate stationary inflection point, and concludes that the gaussian approximation does not give the correct estimate of the PBHs abundance precisely because the non-gaussian correction exponentiates and drastically changes the gaussian result.

However, this conclusion clashes with our result. In fact, as we are going to show, the impact of non-gaussianities on the PBH abundance is much smaller than what found in ref. [47]. To explain the discrepancy, let us first re-derive the main result of ref. [47] in a simplified way.

In a nutshell, in the context of threshold statistics one computes, assuming a gaussian distribution, the probability to find regions where the overdensity field δ takes values above a given threshold. It is known that threshold statistics gives a smaller PBH abundance if compared with peak theory. Let us briefly explain the origin of this difference even if this point is not crucial to understand the discrepancy between our conclusions and ref. [47]. In this section we work directly with the density contrast δ . Furthermore, we start considering the gaussian limit. The gaussian probability density distribution of δ with variance σ_δ and spectral moments $\bar{\sigma}_j$ (where $\bar{\sigma}_0 = \sigma_\delta$) is given in the two cases by the expressions

$$P_{\text{threshold}}(\delta) = \frac{1}{\sqrt{2\pi}\sigma_\delta} e^{-\delta^2/2\sigma_\delta^2}, \quad (6.2.1)$$

$$P_{\text{peak}}(\delta) = \frac{1}{(2\pi)^2\sigma_\delta R_*^3} \left\{ \underbrace{\int_0^\infty dx \frac{f(x)}{\sqrt{2\pi(1-\gamma^2)}} \exp\left[-\frac{(x-\delta\gamma/\sigma_\delta)^2}{2(1-\gamma^2)}\right]}_{\equiv G(\gamma,\delta)} \right\} e^{-\delta^2/2\sigma_\delta^2} \equiv \quad (6.2.2)$$

$$\equiv \frac{1}{(2\pi)^2\sigma_\delta R_*^3} \int_0^\infty dx P_{\text{peak}}(x, \delta), \quad (6.2.3)$$

where the function $f(x)$ is given explicitly in eq. (D.1.17). The two quantities $0 \leq \gamma \equiv \bar{\sigma}_1^2/\bar{\sigma}_2\sigma_\delta < 1$ and $R_* \equiv \sqrt{3}\bar{\sigma}_1/\bar{\sigma}_2$ are factors depending on the power spectrum of δ (notice in particular that γ is the same defined below eq. (6.1.3) but now written in terms of the spectral moments of δ instead of \mathcal{R}). The variable x is defined by $x \equiv -\nabla^2\delta/\bar{\sigma}_2$. The two expressions are similar but there are two differences. First, $P_{\text{peak}}(\delta)$ has dimension of inverse spatial volume (because of the factor $1/R_*^3$). This is because $P_{\text{peak}}(\delta)$ is defined in peak theory as a number density of maxima. This implies that the true comparison is between the a -dimensional quantities $P_{\text{threshold}}(\delta)$ and $R_*^3 P_{\text{peak}}(\delta)$. Second, $P_{\text{peak}}(\delta)$ contains an extra factor (the one in curly brackets) with respect to $P_{\text{threshold}}(\delta)$. This factor

arises because in peak theory one starts from the ten-dimensional gaussian joint probability density distribution $P(\delta, \delta_i, \delta_{ij})$ of δ and its first (δ_i) and second (δ_{ij}) spatial derivatives and imposes a number of conditions that select among the stationary points those that are maxima [48]. In threshold statistics, on the contrary, one simply integrates out all spatial informations by reducing $P(\delta, \delta_i, \delta_{ij})$ to the one-dimensional gaussian distribution in eq. (6.2.1). The crucial aspect is that the function $G(\gamma, \delta)$ in eq. (6.2.3) depends on δ in a way which is proportional to the parameter γ . The latter controls the degree of correlation between δ and χ . When $\gamma = 0$, the two variables are completely uncorrelated, and we find that $G(0, \delta) = (29 - 6\sqrt{6})/10\sqrt{10\pi}$. In this case, $G(0, \delta)$ does not depend on δ : peak theory and threshold statistics give the same qualitative answer (in the sense that the only δ -dependence is encoded in the gaussian exponential which is in common between the two). When $\gamma \rightarrow 1$, δ and χ are strongly correlated. This fact deforms the shape of the probability density distri-

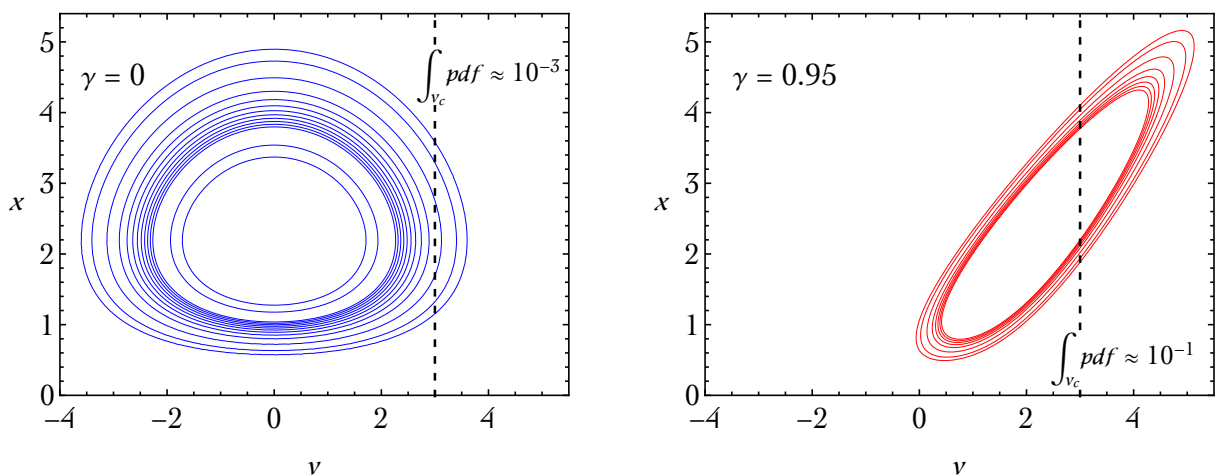


Figure 6: Isocontours of constant probability density distribution $P_{\text{peak}}(x, \delta)$ defined in eq. (6.2.3). We use $\nu \equiv \delta/\sigma_\delta$ and we set (for illustrative purposes only) the threshold at $\nu_c = 3$. The probability above the threshold is obtained integrating $P_{\text{peak}}(x, \delta)$ for $x \in [0, \infty)$ and $\nu \in [\nu_c, \infty)$. We show the case with $\gamma = 0$ (no correlation between x and δ , left panel) and $\gamma = 0.95$ (strong correlation between x and δ , right panel).

bution of x and δ and gives more weight to the region in which δ crosses the threshold for collapse. This is illustrated schematically in fig. 6 (using $\nu \equiv \delta/\sigma_\delta$). In the case of strong correlation between δ and x , therefore, it is well expected that after integrating above the threshold $\nu > \nu_c$ peak theory gives a result which is larger than threshold statistics.⁷ In threshold statistics, this information about the correlation between δ and x is completely lost since δ is treated independently from the spatial configuration. We remark that the difference between threshold statistics and peak theory is more and more relevant as we approach the limit $\gamma \rightarrow 1$. As already pointed out, the value of γ is dictated by the properties of the power spectrum (in this case, strictly speaking, the power spectrum of δ

⁷ Notice that, for the sake of simplicity, we are implicitly assuming in this example the same threshold value ν_c in the case of peak theory and threshold statistics in order to highlight the main difference between the two statistical approaches.

which is however related to the power spectrum of comoving curvature perturbations) with a very peaked power spectrum that corresponds to the limit $\gamma \rightarrow 1$.

After this digression, we can back to the main point of this section. In the context of threshold statistics, non-gaussianities are included in the form of a Gram–Charlier A series around the gaussian ansatz [64]

$$\begin{aligned} P_{\text{NG}}(\delta) &= P_{\text{G}}(\delta) \left[1 + \sum_{n=3}^{\infty} \frac{1}{n!2^{n/2}} B_n(0,0,\mathcal{C}_3,\dots,\mathcal{C}_n) H_n\left(\frac{\nu}{\sqrt{2}}\right) \right] \\ &= P_{\text{G}}(\delta) \left[1 + \frac{\mathcal{C}_3}{3!2^{3/2}} H_3\left(\frac{\nu}{\sqrt{2}}\right) + \frac{\mathcal{C}_4}{4!2^{4/2}} H_4\left(\frac{\nu}{\sqrt{2}}\right) + \frac{\mathcal{C}_5}{5!2^{5/2}} H_5\left(\frac{\nu}{\sqrt{2}}\right) + \frac{(10\mathcal{C}_3^2 + \mathcal{C}_6)}{6!2^{6/2}} H_6\left(\frac{\nu}{\sqrt{2}}\right) + \dots \right], \end{aligned} \quad (6.2.4)$$

where $P_{\text{G}}(\delta) = (1/\sqrt{2\pi}\sigma_\delta) \exp(-\delta^2/2\sigma_\delta^2)$ is the gaussian probability density distribution of δ with variance σ_δ (that is $P_{\text{threshold}}(\delta)$ introduced in eq. (6.2.1)) and H_n are the physicists' Hermite polynomials.⁸ We define $\nu \equiv \delta/\sigma_\delta$ and we introduce the n -th complete exponential Bell polynomial $B_n(x_1, \dots, x_n) = \sum_{k=1}^n B_{n,k}(x_1, \dots, x_{n-k+1})$ with $B_{n,k}$ the partial exponential Bell polynomials. We indicate with \mathcal{C}_n the n -th normalized cumulant defined as the connected part of the n -point correlator (evaluated at the same point) of the overdensity field normalized by the n -th power of the standard deviation

$$\mathcal{C}_n \equiv \frac{\overbrace{\langle \delta(\vec{x}) \dots \delta(\vec{x}) \rangle_{\text{conn}}}^{n \text{ times}}}{\sigma_\delta^n}. \quad (6.2.6)$$

The explicit computation of eq. (6.2.6) in the presence of an ultra-slow roll phase is discussed, in the context of cosmological perturbation theory, in ref. [46] (see also ref. [45]). Notice that the quantity $\langle \delta(\vec{x}) \dots \delta(\vec{x}) \rangle$ is dimensionless, and so is \mathcal{C}_n . We now integrate $P_{\text{NG}}(\delta)$ over some threshold $\delta_c = \nu_c \sigma_\delta$. We define the abundance $\beta(\nu_c) = \int_{\delta_c}^{\infty} d\delta P_{\text{NG}}(\delta)$. We find⁹

$$\beta(\nu_c) = \frac{1}{2} \text{Erfc}\left(\frac{\nu_c}{\sqrt{2}}\right) + \frac{1}{\sqrt{2\pi\nu_c}} e^{-\nu_c^2/2} \sum_{n=3}^{\infty} \frac{\sqrt{2}\nu_c}{n!2^{n/2}} B_n(0,0,\mathcal{C}_3,\dots,\mathcal{C}_n) H_{n-1}\left(\frac{\nu_c}{\sqrt{2}}\right) \approx \quad (6.2.8)$$

$$\approx \underbrace{\frac{1}{\sqrt{2\pi\nu_c}} e^{-\nu_c^2/2}}_{\text{gaussian approx } \beta_{\text{G}}(\nu_c)} \underbrace{\left[1 + \sum_{n=3}^{\infty} \frac{\sqrt{2}\nu_c}{n!2^{n/2}} B_n(0,0,\mathcal{C}_3,\dots,\mathcal{C}_n) H_{n-1}\left(\frac{\nu_c}{\sqrt{2}}\right) \right]}_{\text{non gaussian correction}}, \quad (6.2.9)$$

where in the last step we use $(1/2)\text{Erfc}(x/\sqrt{2}) \approx (1/\sqrt{2\pi}x)e^{-x^2/2}$ for $x \gg 1$.

⁸ We remind that

$$\frac{d^n}{dx^n} e^{-x^2/2\sigma^2} = \frac{(-1)^n}{2^n/2\sigma^n} e^{-x^2/2\sigma^2} H_n\left(\frac{x}{\sqrt{2}\sigma}\right), \quad \text{with } H_n(x) = (-1)^n e^{x^2} \frac{d^n}{dx^n} e^{-x^2}, \quad (6.2.5)$$

so that the reader can immediately recognize in eq. (6.2.4) the structure of a derivative expansion.

⁹ We use the property

$$\frac{1}{\sqrt{2\pi}\sigma} \int_{\delta_c}^{\infty} d\delta e^{-\delta^2/2\sigma^2} H_n\left(\frac{\delta}{\sqrt{2}\sigma}\right) = \frac{1}{\sqrt{\pi}} e^{-\nu_c^2/2} H_{n-1}\left(\frac{\nu_c}{\sqrt{2}}\right). \quad (6.2.7)$$

We now adopt the approach suggested in ref. [47] and approximate

$$H_n\left(\frac{\nu_c}{\sqrt{2}}\right) = 2^{n/2}\nu_c^n + \mathcal{O}(\nu_c^{n-2}), \quad (6.2.10)$$

which seems justified since $\nu_c \gg 1$. In this case eq. (6.2.9) becomes¹⁰

$$\beta(\nu_c) \approx \frac{1}{\sqrt{2\pi\nu_c}} \exp\left(-\frac{\nu_c^2}{2} + \sum_{n=3}^{\infty} \frac{C_n \nu_c^n}{n!}\right). \quad (6.2.14)$$

We find, therefore, the main result of ref. [47]: The non-gaussian correction exponentiates, and changes the argument of the exponential in the gaussian distribution.

¹⁰ The complete exponential Bell polynomial is defined by the exponential generating function [65]

$$\exp\left(\sum_{j=1}^{\infty} \frac{x_j t^j}{j!}\right) = \sum_{n=0}^{\infty} B_n(x_1, \dots, x_n) \frac{t^n}{n!}, \quad (6.2.11)$$

and the first few complete Bell polynomials are $B_0 = 1$, $B_1(x_1) = x_1$, $B_2(x_1, x_2) = x_1^2 + x_2$, $B_3(x_1, x_2, x_3) = x_1^3 + 3x_1 x_2 + x_3$. In our case we have $x_1 = x_2 = 0$ and the previous definition takes the form

$$\exp\left(\sum_{j=3}^{\infty} \frac{x_j t^j}{j!}\right) = 1 + \sum_{n=3}^{\infty} B_n(0, 0, x_3, \dots, x_n) \frac{t^n}{n!}, \quad (6.2.12)$$

which applies to our case with $t = \nu_c$ and $x_{i \geq 3} = C_{i \geq 3}$ since the application of eq. (6.2.10) to eq. (6.2.9) gives

$$\beta(\nu_c) \simeq \frac{1}{\sqrt{2\pi\nu_c}} e^{-\nu_c^2/2} \left[1 + \sum_{n=3}^{\infty} B_n(0, 0, C_3, \dots, C_n) \frac{\nu_c^n}{n!} \right]. \quad (6.2.13)$$

Notice that, compared to our result, ref. [47] finds an additional factor $(-1)^n$ in eq. (6.2.14) which, however, does not appear in our computation.

Consider the simplified case in which only the third-order normalized cumulant (a.k.a. skewness) is non-vanishing, $\mathcal{C}_3 \neq 0$ and $\mathcal{C}_{n>3} = 0$. This is the approximation studied in ref. [45] in which the third-order cumulant is computed in the case of local non-gaussianities.¹¹ We find

$$\beta(\nu_c) \approx \frac{1}{\sqrt{2\pi\nu_c}} \exp\left(-\frac{\nu_c^2}{2} + \frac{\mathcal{C}_3\nu_c^3}{6}\right), \quad \text{with } \mathcal{C}_3 \neq 0 \text{ and } \mathcal{C}_{n>3} = 0. \quad (6.2.16)$$

Ref. [47] and ref. [45] used the above equations to conclude that the gaussian estimate of the PBH abundance is hardly trustable. This result is based on the approximation in eq. (6.2.10). However, as we shall now discuss, the applicability of this approximation is not as straightforward as one may think. Let us critically inspect the issue.

We define, for ease of reading, the quantity $b_n(\nu_c) \equiv (\sqrt{2}\nu_c/n!2^{n/2})B_n(0,0,\mathcal{C}_3,\dots,\mathcal{C}_n)H_{n-1}(\nu_c/\sqrt{2})$ which enters in the non-gaussian correction in eq. (6.2.9). As a consequence of eq. (6.2.10), we have (slashed terms are neglected if we apply the approximation in eq. (6.2.10))

$$b_3 = \frac{\mathcal{C}_3\nu_c^3}{6} \left(1 - \frac{1}{\nu_c^2}\right), \quad (6.2.17)$$

$$b_6 = \frac{\mathcal{C}_3^2\nu_c^6}{72} \left(1 - \frac{10}{\nu_c^2} + \frac{15}{\nu_c^4}\right), \quad (6.2.18)$$

$$b_9 = \frac{\mathcal{C}_3^3\nu_c^9}{1296} \left(1 - \frac{28}{\nu_c^2} + \frac{210}{\nu_c^4} - \frac{420}{\nu_c^6} + \frac{105}{\nu_c^8}\right), \quad (6.2.19)$$

$$b_{12} = \dots \quad (6.2.20)$$

and so on. We see, for instance, that we neglected the term $-7\mathcal{C}_3^3\nu_c^7/324$ in eq. (6.2.19) but we kept the term $\mathcal{C}_3\nu_c^3/6$ in eq. (6.2.17). This is hardly justifiable given that $\nu_c \gg 1$ and we expect $\mathcal{C}_3 \sim \mathcal{O}(1)$

¹¹ Notice, however, that assuming $\mathcal{C}_3 \neq 0$ and $\mathcal{C}_{n>3} = 0$ is not fully consistent with the local non-gaussianities computed in ref. [45]. Indeed, local non-gaussianities automatically generate non-vanishing cumulants of any order. This is evident in our approach, in which $\alpha \neq 0$ generates a whole tower of non-zero cumulants. From a more mathematical viewpoint, consider the following theorem. *The sequence $\{\mu_n, n = 0, 1, 2, \dots\}$ corresponds to moments of a non-negative probability density function if and only if the determinants*

$$D_{n+1} \equiv \det \begin{pmatrix} \mu_0 & \mu_1 & \mu_2 & \dots & \mu_n \\ \mu_1 & \mu_2 & \mu_3 & \dots & \mu_{n+1} \\ \mu_2 & \mu_3 & \mu_4 & \dots & \mu_{n+2} \\ \vdots & \vdots & \vdots & \ddots & \vdots \\ \mu_n & \mu_{n+1} & \mu_{n+2} & \dots & \mu_{2n} \end{pmatrix}, \quad n = 0, 1, 2, \dots, \quad (6.2.15)$$

are all non-negative [66]. Consider the illustrative case with $\mathcal{C}_n = 0$ for $n \geq 4$. We have $\mu_0 = 1$, $\mu_1 = 0$, $\mu_2 = \sigma_8^2$, $\mu_3 = \langle \delta^3 \rangle$ and $\mu_n = \sigma_8^n (n-1)!!$ for $n \geq 4$ even ($\mu_n = 0$ for $n \geq 4$ odd). The last condition simply means that cumulants of order higher than three vanish (and the corresponding moments purely gaussian). The first determinant $D_3 > 0$ already sets a non-trivial condition on the skewness, that is $-\sqrt{2} < \mathcal{C}_3 < \sqrt{2}$. However, there is more than this. It is indeed trivial to see that higher-order conditions $D_n > 0$ for $n > 3$ impose increasingly strong bound on \mathcal{C}_3 so that only $\mathcal{C}_3 = 0$ is allowed if all the infinite number of constraints are implemented. In other words, the theorem above implies that *skewness alone can not consistently parameterize a non-gaussian probability density function*. This result resonates with what we discussed at point ii) in section 6.1. Computing only the three-point correlator of the overdensity field does not fully describe non-gaussianities but one should at least include the contributions that the three-point function generates at higher orders.

(see ref. [46] for a careful computation of C_3). This is enough to question the validity of the result based on eq. (6.2.10). Furthermore, from this simple comparison, we also see that the approximation in eq. (6.2.10)—contrary to what naïvely expected—gets worse for larger ν_c .

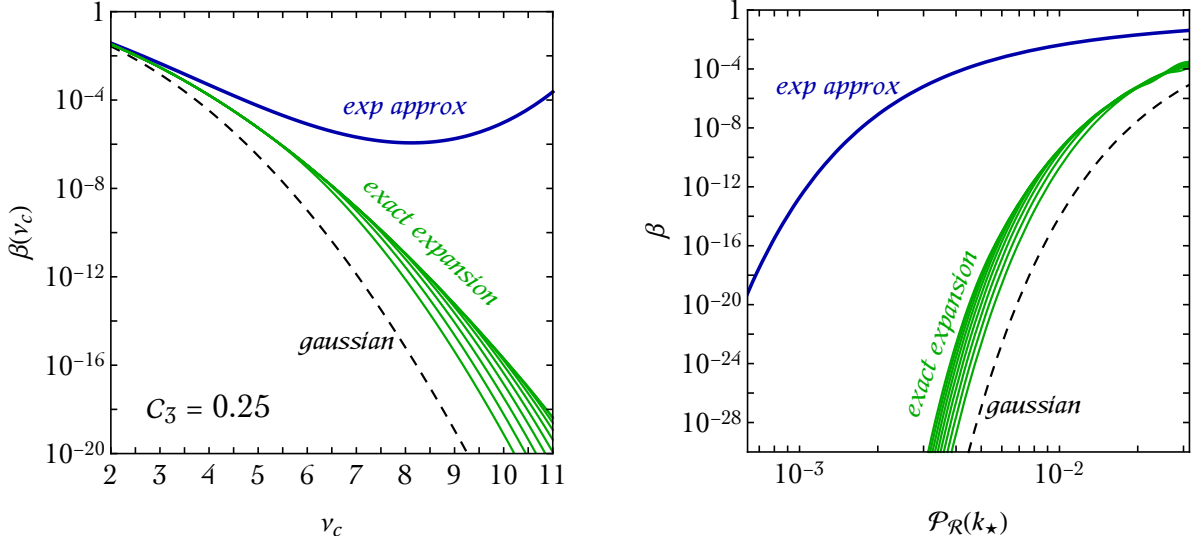


Figure 7: Left panel. Numerical comparison between i) the gaussian result $\beta_G(\nu_c)$ defined in eq. (6.2.9), ii) the exponential approximation in eq. (6.2.16) and iii) the exact expansion of $\beta(\nu_c) = \beta_G(\nu_c)[1 + \sum_{n=3}^{\nu_{\max}} b_n(\nu_c)]$ for increasing values of ν_{\max} . We take $C_3 = 0.25$ and we show our results as function of ν_c . Right panel. Same as in the left panel but using the scaling in eq. (6.2.25) to draw β as function of $\mathcal{P}_{\mathcal{R}}(k_*)$. We take $\delta_c = 1.2$.

In particular, in this specific case, we can rewrite the sum (6.2.8) by using the recurrence property of the Bell polynomials:

$$B_{n+1}(x_1, \dots, x_{n+1}) = \sum_{k=0}^n \binom{n}{k} B_{n-k}(x_1, \dots, x_{n-k}) x_{k+1}. \quad (6.2.21)$$

In our particular case $x_{k+1} = C_3 \delta_{k+1,3}$, therefore

$$B_{3(k+1)}(0, 0, C_3, 0, \dots, 0) = \frac{1}{2} (3k+1)(3k+2) C_3 B_{3k}(0, 0, C_3, 0, \dots, 0). \quad (6.2.22)$$

This can be easily recasted in the form:

$$B_n(0, 0, C_3, 0, \dots, 0) = \begin{cases} 3 \left(\frac{C_3}{6}\right)^k \frac{(3k-1)!}{(k-1)!}, & \text{if } n = 3k, \\ 0, & \text{if } n \neq 3k. \end{cases} \quad (6.2.23)$$

Using this identity inside the eq. (6.2.8) we get:

$$\beta(\nu_c) = \frac{1}{2} \text{Erfc}\left(\frac{\nu_c}{\sqrt{2}}\right) + \frac{1}{\sqrt{\pi}} e^{-\nu_c^2/2} \sum_{k=1}^{\infty} \frac{1}{k!} \left(\frac{C_3}{12\sqrt{2}}\right)^k H_{3k-1}\left(\frac{\nu_c}{\sqrt{2}}\right). \quad (6.2.24)$$

To show more explicitly the error that one makes by taking the exponential approximation in eq. (6.2.16) we plot in the left panel of fig. 7 the comparison between *i*) the gaussian result $\beta_G(\nu_c)$ defined in eq. (6.2.9), *ii*) the exponential approximation in eq. (6.2.16) and *iii*) the exact expansion of $\beta(\nu_c) = \beta_G(\nu_c)[1 + \sum_{n=3}^{n_{\max}} b_n(\nu_c)]$ for increasing values of n_{\max} ¹². We take $\mathcal{C}_3 = 0.25$ and we set $\mathcal{C}_{n>3} = 0$. The approximation gives a wrong estimate of the actual magnitude of the non-gaussianities. As expected, the exponential approximation diverges from the actual result for larger values of ν_c .

There is another point that is worth emphasizing. Taking \mathcal{C}_3 fixed and changing only ν_c , as done in the left panel of fig. 7 is not fully consistent since both \mathcal{C}_3 and ν_c are functions of the power spectrum $\mathcal{P}_{\mathcal{R}}$. More explicitly, we have the scaling $\nu_c \propto \mathcal{P}_{\mathcal{R}}(k_*)^{-1/2}$ and $\mathcal{C}_3 \propto \mathcal{P}_{\mathcal{R}}(k_*)^{1/2}$ (see appendix B). This means that reducing $\mathcal{P}_{\mathcal{R}}(k_*)$ to decrease \mathcal{C}_3 does not improve on the applicability of the exponential approximation since ν_c , in turn, increases. To better visualize this point let us consider the following benchmark scalings

$$\sigma_\delta = 0.35 \left[\frac{\mathcal{P}_{\mathcal{R}}(k_*)}{0.05} \right]^{1/2}, \quad \mathcal{C}_3 = 0.8 \left[\frac{\mathcal{P}_{\mathcal{R}}(k_*)}{0.05} \right]^{1/2}, \quad (6.2.25)$$

and take $\delta_c = 1.2$. We can now redo the comparison we did before but now as function of $\mathcal{P}_{\mathcal{R}}(k_*)$. The result is shown in the right panel of fig. 7. We conclude again that the exponential approximation overestimates the impact of local non-gaussianities on the PBH abundance by many orders of magnitude compared with the actual result. Using the exponential approximation, one would wrongly conclude that, in order to fit the reference value $\beta \simeq 10^{-16}$, an order-of-magnitude decrease in the peak amplitude of the power spectrum is needed compared to the gaussian result.

¹² One can argue that the power series $\sum_{k=1}^{\infty} \frac{z^k}{k!} H_{3k-1}(x)$ contained in eq. (6.2.24) is not convergent. Nevertheless it should be regarded as an asymptotic series that gives a trustable value after an optimal truncation. Moreover it is Borel summable, and its value can be computed numerically evaluating the Borel sum $\int_0^\infty e^{-t} \left[\sum_{k=1}^{\infty} \frac{(tz)^k}{(k!)^2} H_{3k-1}(x) \right] dt$. This check has been done and the value obtained agrees with the one got by the optimal truncation.

CONCLUSIONS OF PART II

We conclude summarizing the main results and novelties of our work.

- We have studied the impact of primordial non-gaussianities of local type on the abundance of PBHs. For this purpose we have focused on the maxima of the the comoving curvature perturbations. We have shown that those peaks “spiky enough”, i.e. with a curvature larger than a certain threshold, are good proxies for the maxima of the density field which undergo gravitational collapse, and produce PBHs. Exploiting this observation, we have obtained that the cosmological abundance of PBHs can be computed using eq. (6.1.2). Our calculations extend the gaussian peak theory formalism [48] to include the effect of local non-gaussianities.

We have examined the consequences of our results for models of single-field inflation with an ultra slow-roll phase. These scenarios have been investigated for the production of PBHs. In this context, the impact of primordial non-gaussianities is not dramatic. In fact, the desired PBH abundance can be obtained with an amplitude of the power spectrum of curvature perturbations which is only a factor $\lesssim 2$ smaller from the value inferred with the gaussian approximation.

- In parallel to the exact result presented in eq. (6.1.2), we have developed a computational strategy that approximates the effect of primordial non-gaussianities in the form of an expansion in cumulants around the gaussian result. In order to have full analytical control, we worked out this part in two (instead of three) spatial dimensions. The presence of local non-gaussianities affect cumulants at any order, and we have shown what is their structure. Furthermore, we have shown that the only inclusion of third-order cumulants is not sufficient to fully capture the effect of local non-gaussianities.
- Previous works have studied primordial non-gaussianities in the context of threshold statistics, finding that non-gaussianities exponentially affect the PBH abundance as given by eq. (6.2.14). We have found that that result is not correct and largely overestimate the PBH abundance.
- En route, we discuss the difference between threshold statistics and peak theory, and we explain under which conditions (and why) peak theory gives a PBH abundance which is larger than the one computed by means of threshold statistics.

Part III

APPENDIX

DE SITTER QUASINORMAL MODES

A.1 FREE COMMUTATOR

Starting from eq. (2.2.5) and setting $\Delta = \frac{d}{2} + i\nu$:

$$\begin{aligned} \hat{C}(\omega, \theta) &= \frac{2\pi i}{(4\pi)^{\frac{d+1}{2}} \Gamma\left(\frac{3-d}{2}\right)} \times \\ &\times \mathcal{M}\left[\nu \mapsto \left(\nu + \frac{1 - \cos \theta}{2}\right)^{i\omega-1} {}_2F_1\left(\frac{1}{2} - i\nu, \frac{1}{2} + i\nu; \frac{3-d}{2}; -\nu\right)\right]\left(\frac{3-d}{2}\right), \end{aligned} \quad (\text{A.1.1})$$

where $\mathcal{M}[f](s) = \int_0^\infty x^{s-1} f(x) dx$ is the Mellin transform that can be analytically computed.

$$\begin{aligned} \hat{C}(\omega, \theta) &= \frac{i\Gamma\left(\frac{d+1}{2} - i\omega\right) \Gamma\left(\frac{1-d}{2} + i\omega\right)}{2^d \pi^{\frac{d+1}{2}} \Gamma(1 - i\omega)} \times \\ &\times \left[\frac{\Gamma\left(\frac{d}{2} + i\nu - i\omega\right) \Gamma\left(\frac{d}{2} - i\nu - i\omega\right)}{\Gamma\left(\frac{1}{2} + i\nu\right) \Gamma\left(\frac{1}{2} - i\nu\right)} {}_2\tilde{F}_1\left(\frac{d}{2} + i\nu - i\omega, \frac{d}{2} - i\nu - i\omega, \frac{d+1}{2} - i\omega, \sin^2 \frac{\theta}{2}\right) + \right. \\ &\left. - \left(\sin^2 \frac{\theta}{2}\right)^{i\omega + \frac{1-d}{2}} {}_2\tilde{F}_1\left(\frac{1}{2} + i\nu, \frac{1}{2} - i\nu, \frac{3-d}{2} + i\omega, \sin^2 \frac{\theta}{2}\right) \right], \end{aligned} \quad (\text{A.1.2})$$

where ${}_2\tilde{F}_1$ is the regularized hypergeometric function that has no singularities. From the expression (A.1.2) it is straightforward the evaluation for $\theta = 0, \frac{\pi}{2}, \pi$, where we can use that:

$${}_2\tilde{F}_1(a, b; c; 0) = \frac{1}{\Gamma(c)}, \quad (\text{A.1.3})$$

$${}_2\tilde{F}_1\left(a, 1-a; c; \frac{1}{2}\right) = \frac{\Gamma\left(\frac{c}{2}\right) \Gamma\left(\frac{c+1}{2}\right)}{\Gamma(c) \Gamma\left(\frac{c+a}{2}\right) \Gamma\left(\frac{c-a+1}{2}\right)}, \quad (\text{A.1.4})$$

$${}_2\tilde{F}_1(a, b; c; 1) = \frac{\Gamma(c-a-b)}{\Gamma(c-a) \Gamma(c-b)}, \quad (\text{A.1.5})$$

to show that:

$$\hat{C}(\omega, 0) = \frac{i\Gamma\left(\frac{1-d}{2} + i\omega\right) \Gamma\left(\frac{d}{2} + i\nu - i\omega\right) \Gamma\left(\frac{d}{2} - i\nu - i\omega\right)}{2^d \pi^{\frac{d+1}{2}} \Gamma(1 - i\omega) \Gamma\left(\frac{1}{2} + i\nu\right) \Gamma\left(\frac{1}{2} - i\nu\right)}, \quad (\text{A.1.6})$$

$$\hat{C}\left(\omega, \frac{\pi}{2}\right) = \frac{i\Gamma\left[\frac{1}{2}\left(\frac{d}{2} + i\nu - i\omega\right)\right] \Gamma\left[\frac{1}{2}\left(\frac{d}{2} - i\nu - i\omega\right)\right]}{2^{2(1+i\omega)} \pi^{\frac{d}{2}} \Gamma(1 - i\omega)}, \quad (\text{A.1.7})$$

$$\hat{C}(\omega, \pi) = \frac{i\Gamma\left(\frac{d}{2} + i\nu - i\omega\right) \Gamma\left(\frac{d}{2} - i\nu - i\omega\right)}{2^d \pi^{\frac{d+1}{2}} \Gamma(1 - i\omega) \Gamma\left(\frac{d+1}{2} - i\omega\right)}. \quad (\text{A.1.8})$$

The poles are those in eq. (2.2.7). For $\theta = 0$ there is an additional set of poles that extends to the upper half plane:

$$\omega = i \left(n + \frac{1-d}{2} \right), \quad n \in \mathbb{N}. \quad (\text{A.1.9})$$

For $\theta \neq 0$ microcausality condition ensure the analyticity in the upper half plane. Indeed the condition $[\phi(X), \phi(Y)] = 0$ when $(X - Y)^2 > 0$ means that the in-out commutator vanishes for $u < u_0(\theta) = \log(\sin^2 \frac{\theta}{2})$. If we anti-Fourier transform $\hat{C}(\omega, \theta)$ to have the commutator in the real space:

$$C(u, \theta) = \int_{-\infty}^{+\infty} \frac{d\omega}{2\pi} e^{-i\omega u} \hat{C}(\omega, \theta), \quad (\text{A.1.10})$$

for $\theta = \pi$, $u_0(\pi) = 0$, then:

$$C(u, \pi) = \int_{-\infty}^{+\infty} \frac{d\omega}{2\pi} e^{-i\omega u} \hat{C}(\omega, \pi) = 0 \text{ for } u < 0. \quad (\text{A.1.11})$$

If $u < 0$ we close the contour upwards and this means that $\hat{C}(\omega, \pi)$ has to be analytic in the upper half plane because of the residue theorem.

If $\theta \in (0, \pi)$:

$$C(u, \theta) = \int_{\mathbb{R}} \frac{d\omega}{2\pi} e^{-i\omega(u-u_0(\theta))} e^{-i\omega u_0(\theta)} \hat{C}(\omega, \theta) = 0 \text{ for } u < u_0(\theta). \quad (\text{A.1.12})$$

Again, for $u < u_0(\theta)$ we close the contour upwards and then the function $\omega \mapsto e^{-i\omega u_0(\theta)} \hat{C}(\omega, \theta)$ has to be analytic in the upper-half plane, but since $\omega \mapsto e^{-i\omega u_0(\theta)}$ is an entire function, therefore $\omega \mapsto \hat{C}(\omega, \theta)$ has to be analytic.

The only failure of this argument is for $\theta \rightarrow 0$, because $u_0(\theta) \rightarrow -\infty$ and so the microcausality condition is not applicable, since the commutator can be non-vanishing $\forall u \in \mathbb{R}$, that is why its Fourier transform $\hat{C}(\omega, \theta)$ can have poles in the upper-half plane, as indeed happens e.g. in the free case in eq. (A.1.6).

The analytic structures of $\hat{C}(\omega, 0)$ and $\hat{C}(\omega, \pi)$ for the free theory are reported in figure 8.

A.2 CLOSURE OF THE CONTOUR

We want to show under which conditions the integral in eq. (2.3.4) can be computed via contour deformation to use the residue theorem. It is sufficient to prove that the integral on the arc at infinity vanishes. In terms of ν defined via $\Delta = \frac{d}{2} - i\nu$, the condition is

$$\left| \lim_{R \rightarrow \infty} R \int_0^\pi d\theta \rho \left(\frac{d}{2} - i\nu \right) g \left(\frac{d}{2} - i\nu \right) \psi_{\frac{d}{2} - i\nu}(\xi) \right|_{\nu = R e^{i\theta}} = 0. \quad (\text{A.2.1})$$

We make a technical hypothesis on ρ that is:

$$\left| \nu \rho \left(\frac{d}{2} - i\nu \right) \right| \lesssim \left| \frac{\Gamma \left(\frac{3}{2} - i\nu \right)}{\Gamma \left(\frac{d}{2} - i\nu \right)} \right| \quad \text{as } |\nu| \rightarrow \infty, \quad (\text{A.2.2})$$

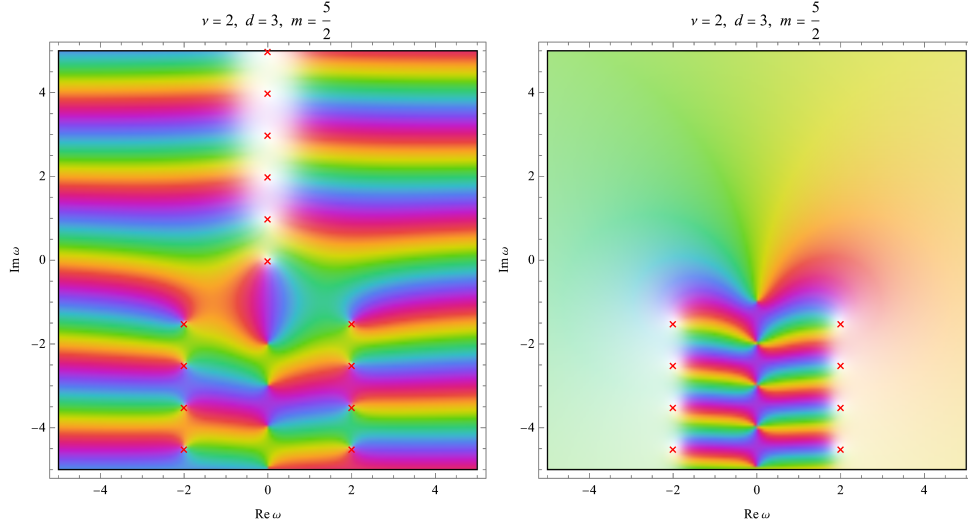


Figure 8: Complex plot of $\text{Arg}[\hat{C}(\omega, \theta)]$ vs ω . Left $\theta = 0$ and right $\theta = \pi$. The red crosses highlight the poles.

otherwise one can see that the (A.2.1) is not zero. This condition imposes d -dependent power-like decay on ρ . The perturbative examples in $d = 2, 3$ satisfy this requirement.

The hypergeometric function can be approximated via the saddle point approximation of its integral representation:

$$\left| {}_2F_1\left(\frac{d}{2} - i\nu, \frac{1}{2} - i\nu; 1 - 2i\nu; \xi\right) \right| = \quad (\text{A.2.3})$$

$$= \left| \frac{\Gamma(1 - 2i\nu)}{\Gamma^2\left(\frac{1}{2} - i\nu\right)} \int_0^1 dx [x(1-x)]^{-\frac{1}{2}} (1 - \xi x)^{-\frac{d}{2}} \exp\left[-i\nu \log \frac{x(1-x)}{1 - \xi x}\right] \right| \sim \quad (\text{A.2.4})$$

$$\sim \left| \alpha(\xi) \frac{\Gamma(1 - 2i\nu)}{\Gamma^2\left(\frac{1}{2} - i\nu\right)} \frac{1}{\sqrt{\nu}} \frac{1}{(2 - \xi + 2\sqrt{1 - \xi})^{-i\nu}} \right| \quad (\text{A.2.5})$$

One finds that, for $|\nu| \rightarrow \infty$:

$$\left| g\left(\frac{d}{2} - i\nu\right) \psi_{\frac{d}{2} - i\nu}(\xi) \right| \sim A(\xi) \left| \frac{\Gamma\left(\frac{d}{2} - i\nu\right)}{\Gamma\left(\frac{1}{2} - i\nu\right) \sin(i\pi\nu)} \right| |\nu|^{-\frac{1}{2}} e^{\pi \text{Re}\nu} [c(\xi)]^{\text{Im}\nu} \quad (\text{A.2.6})$$

where $A(\xi)$ is a constant and:

$$c(\xi) = \frac{-\xi}{2 - \xi + 2\sqrt{1 - \xi}} \in (0, 1), \quad \text{for } \xi \in (-\infty, 0) \quad (\text{A.2.7})$$

We can observe that:

$$|\sin(i\pi\nu)| = |\sinh(\pi\nu)| = \sqrt{\frac{\cosh(2\pi \text{Re}\nu) - \cos(2\pi \text{Im}\nu)}{2}} \geq \quad (\text{A.2.8})$$

$$\geq \frac{1}{\sqrt{2}} \sqrt{\frac{1}{2} e^{2\pi \text{Re}\nu} - 1} \sim \frac{1}{2} e^{\pi \text{Re}\nu} \quad (\text{A.2.9})$$

Now we use the hypothesis (A.2.2) so that:

$$\left| \nu \rho \left(\frac{d}{2} - i\nu \right) g \left(\frac{d}{2} - i\nu \right) \psi_{\frac{d}{2} - i\nu}(\xi) \right| \lesssim \mathcal{A}(\xi) |\nu|^{1/2} [c(\xi)]^{\text{Im}\nu} \quad (\text{A.2.10})$$

where $\mathcal{A}(\xi)$ is another constant. Therefore:

$$\mathbb{R} \int_0^\pi d\theta \left| \rho \left(\frac{d}{2} - i\mathbb{R}e^{i\theta} \right) g \left(\frac{d}{2} - i\mathbb{R}e^{i\theta} \right) \psi_{\frac{d}{2} - i\mathbb{R}e^{i\theta}}(\xi) \right| \lesssim \tilde{\mathcal{A}}(\xi) \sqrt{\mathbb{R}} \int_0^\pi d\theta [c(\xi)]^{\mathbb{R} \sin \theta} = \quad (\text{A.2.11})$$

$$= \pi \tilde{\mathcal{A}}(\xi) \sqrt{\mathbb{R}} [I_0(\mathbb{R} \log c(\xi)) + L_0(\mathbb{R} \log c(\xi))] \xrightarrow{\mathbb{R} \rightarrow \infty} 0 \quad (\text{A.2.12})$$

where I_n and L_n are respectively the modified Bessel function of the first kind and the modified Struve function and $\tilde{\mathcal{A}}(\xi)$ is again a constant.

A.3 SK PERTURBATION THEORY FOR THE 2-POINT FUNCTION

In the BEFT one can treat perturbatively both the conservative and non conservative interactions with the SK formalism [67]. The exception is the ϕ^2 operator which is relevant and must be treated non-perturbatively. So as the free action we take

$$S_0 = \int_{-\infty}^{+\infty} dt \int_0^\infty dx \left[\frac{1}{2} (\dot{\phi}^2 - \phi'^2) - \delta(x) c_0 \phi^2 \right]. \quad (\text{A.3.1})$$

The presence of the “mass” produces the phase shift:

$$e^{2i\alpha(\omega)} = \frac{\omega - ic_0}{\omega + ic_0} \quad (\text{A.3.2})$$

Differently from the non perturbative approach followed in section (3), one can treat perturbatively with the SK formalism also the conservative term. Indeed one can define the SK action starting from the action (3.1.10) as:

$$S_{\text{SK}}[\phi_{\text{R}}, \phi_{\text{L}}] = S_{\text{BEFT}}[\phi_{\text{R}}] - S_{\text{BEFT}}[\phi_{\text{L}}] \quad (\text{A.3.3})$$

The conservative term in SK language are all of the form $\partial_t^n \phi_+ \partial_t^n \phi_-$.

The insertion of a generic derivative operator inside the action of the form:

$$S_g[\phi_+, \phi_-] = -g \int_{-\infty}^{+\infty} dt \partial_t^n \phi_+(t, 0) \partial_t^m \phi_-(t, 0) \quad (\text{A.3.4})$$

gives, at $\mathcal{O}(g)$, the following deformation of the commutator:¹

$$\delta_g \langle [\phi(X), \phi(Y)] \rangle \equiv \delta_g \langle \phi_+(X) \phi_-(Y) \rangle = \quad (\text{A.3.5})$$

$$= -ig \int_{\mathbb{R}} dt \partial_t^n \langle \phi_+(t, 0) \phi_-(Y) \rangle_0 \partial_t^m \langle \phi_-(t, 0) \phi_+(X) \rangle_0, \quad (\text{A.3.6})$$

¹ In what follows $\langle \cdot \rangle$ means expected value in the SK formalism.

where the subscript 0 means that those are computed in the free theory. The SK correlator are connected with usual correlators as:

$$\langle\langle\phi_+(t_X, x)\phi_-(t_Y, y)\rangle\rangle_0 = \Theta(t_X - t_Y) [\phi(t_X, x), \phi(t_Y, y)]_0; \quad (\text{A.3.7})$$

$$\langle\langle\phi_-(t_X, x)\phi_-(t_Y, y)\rangle\rangle_0 = 0; \quad (\text{A.3.8})$$

$$\langle\langle\phi_+(t_X, x)\phi_+(t_Y, y)\rangle\rangle_0 = \frac{1}{2} \langle\{\phi(t_X, x), \phi(t_Y, y)\}\rangle_0; \quad (\text{A.3.9})$$

$$[\phi(t_X, x), \phi(t_Y, y)]_0 = -\frac{i}{\pi} \int_{-\infty}^{+\infty} \frac{d\omega}{\omega} \cos(\omega x + \alpha(\omega)) \cos(\omega y + \alpha(\omega)) \sin[\omega(t_X - t_Y)]; \quad (\text{A.3.10})$$

$$\langle\{\phi(t_X, x), \phi(t_Y, y)\}\rangle_0 = \frac{2}{\pi} \int_{-\infty}^{+\infty} \frac{d\omega}{\omega(e^{2\pi\omega} - 1)} \cos(\omega x + \alpha(\omega)) \cos(\omega y + \alpha(\omega)) \cos[\omega(t_X - t_Y)]. \quad (\text{A.3.11})$$

The non-conservative terms inside the BEFT action appear as in eq. (3.2.7). With these tools we can compute the effect at linear level in the coupling of both the conservative and non-conservative terms:

$$\delta_c \langle[\phi_{\text{out}}(u), \phi_{\text{in}}(0)]\rangle = -i \sum_{n=1}^{\infty} c_n \int_{-\infty}^{+\infty} \frac{d\omega}{2\pi} \omega^{2(n-1)} \cos^2 \alpha(\omega) e^{2i\alpha(\omega) - i\omega u} \quad (\text{A.3.12})$$

$$\delta_{nc} \langle[\phi_{\text{out}}(u), \phi_{\text{in}}(0)]\rangle = - \sum_{n=0}^{\infty} b_n \int_{-\infty}^{+\infty} \frac{d\omega}{2\pi} \omega^{2n-1} \cos^2 \alpha(\omega) e^{2i\alpha(\omega) - i\omega u} \quad (\text{A.3.13})$$

This means, if we expand in powers of ω the EFT version of the function that appears in (3.2.3):

$$\mathcal{S}^{\text{EFT}}(\omega) = -1 - \frac{2i}{c_0} \omega + \frac{2(b_0 + 1)}{c_0^2} \omega^2 + \mathcal{O}(\omega^3). \quad (\text{A.3.14})$$

To achieve the $\mathcal{O}(\omega^3)$ term in the above expansion we need to include not only the conservative interaction at linear order $-c_1 \dot{\phi}^2(t, 0)$, but also the dissipative interaction $-b_0 (\phi_- \dot{\phi}_+)(t, 0)$ at quadratic level $\mathcal{O}(b_0^2)$.

From the path integral formulation one can see that:

$$\langle[\phi(X), \phi(Y)]\rangle = \langle\langle\phi_+(X)\phi_-(Y)\rangle\rangle = \quad (\text{A.3.15})$$

$$= \langle\langle\phi_+(X)\phi_-(Y)\rangle\rangle_0 + i \underbrace{(\langle\langle\phi_+(X)\phi_-(Y)S_{\text{int}}\rangle\rangle_0 - \langle\langle\phi_+(X)\phi_-(Y)\rangle\rangle_0 \langle\langle S_{\text{int}}\rangle\rangle_0)}_{\mathcal{O}(b_0)} + \quad (\text{A.3.16})$$

$$\left. \begin{aligned} & -\frac{1}{2} \langle\langle\phi_+(X)\phi_-(Y)S_{\text{int}}^2\rangle\rangle_0 + \langle\langle\phi_+(X)\phi_-(Y)S_{\text{int}}\rangle\rangle_0 \langle\langle S_{\text{int}}\rangle\rangle_0 + \\ & + \langle\langle\phi_+(X)\phi_-(Y)\rangle\rangle_0 \left(\frac{1}{2} \langle\langle S_{\text{int}}^2\rangle\rangle_0 - \langle\langle S_{\text{int}}\rangle\rangle_0^2 \right) + \end{aligned} \right\} \mathcal{O}(b_0^2) \quad (\text{A.3.17})$$

$$+ \mathcal{O}(b_0^3). \quad (\text{A.3.18})$$

For the specific case of $S_{\text{int}} = -b_0 \int_{\mathbb{R}} dt \dot{\phi}_+(t, 0) \phi_-(t, 0)$, after the Wick's contraction, we have that the $\mathcal{O}(b_0^2)$ term is:

$$\delta_{b_0^2} \langle[\phi(X), \phi(Y)]\rangle = -b_0^2 \int_{\mathbb{R}^2} dt dt' \langle\langle\phi_+(X)\phi_-(t, 0)\rangle\rangle_0 \langle\langle\dot{\phi}_+(t, 0)\phi_-(t', 0)\rangle\rangle_0 \langle\langle\phi_+(t', 0)\phi_-(Y)\rangle\rangle_0. \quad (\text{A.3.19})$$

So eventually we have that:

$$\delta_{b_0^2} \langle [\phi_{\text{out}}(\mathbf{u}), \phi_{\text{in}}(0)] \rangle = \int_{-\infty}^{+\infty} \frac{d\omega}{2\pi} e^{-i\omega u} \left[\frac{i b_0^2}{c_0^3} \omega^2 + \mathcal{O}(\omega^3) \right], \quad (\text{A.3.20})$$

from which:

$$\mathcal{S}^{\text{EFT}}(\omega) = -1 - \frac{2i}{c_0} \omega + \frac{2(b_0 + 1)}{c_0^2} \omega^2 + \frac{2i(1 + 2b_0 + b_0^2 + c_0 c_1)}{c_0^3} \omega^3 + \mathcal{O}(\omega^4). \quad (\text{A.3.21})$$

As a consistency check, setting $b_0 = 0$ gives the expansion of the exact phase shift (3.1.12) up to order ω^3 .

One might go beyond the quadratic action including a ϕ^3 interaction. The leading contribution in (A.3.21) is at $\mathcal{O}(\omega)$, that is the same order at which dependence on c_0 shows up.

B

SCALAR PERTURBATIONS DURING INFLATION IN THE PRESENCE OF ULTRA SLOW-ROLL

In this work we focus on single-field models of inflation. We indicate with ϕ the canonically normalized inflaton field and with $U = U(\phi)$ its potential. The dynamics of ϕ can be obtained solving the equation of motion

$$\frac{d^2\phi}{dN^2} + 3\frac{d\phi}{dN} - \frac{1}{2}\left(\frac{d\phi}{dN}\right)^2 + \left[3 - \frac{1}{2}\left(\frac{d\phi}{dN}\right)^2\right]\frac{d\log U}{d\phi} = 0, \quad (\text{B.0.1})$$

with slow-roll initial conditions; N indicates the number of e -folds defined by $dN = Hdt$, where $H \equiv \dot{a}/a$ is the Hubble rate, a the scale factor of the Friedmann-Lemaître-Robertson-Walker metric, and t the cosmic time (with $\dot{} \equiv d/dt$). We will also use in the following the conformal time τ defined by means of $dt/d\tau = a$ or, equivalently, $dN/d\tau = aH$ (notice that, in the limit in which H is constant, we have the relation $\tau = -1/aH$; the conformal time, therefore, is negative, and late times towards the end of inflation can be formally identify with the limit $\tau \rightarrow 0^-$).

Scalar fluctuations can be efficiently described in terms of the Mukhanov-Sasaki field variable $u(\tau, \vec{x})$ which is a gauge-invariant combination of both fluctuations of the inflaton field and scalar fluctuations of the background Friedmann-Lemaître-Robertson-Walker geometry. The Mukhanov-Sasaki field variable solves the differential equation (for a review, see ref. [68])

$$\frac{d^2u}{d\tau^2} = \left(\nabla^2 + \frac{1}{z}\frac{d^2z}{d\tau^2}\right)u, \quad (\text{B.0.2})$$

$$\frac{1}{z}\frac{d^2z}{d\tau^2} = \alpha^2 H^2 \left[(1 + \epsilon - \eta)(2 - \eta) + \frac{1}{\alpha H} \left(\frac{d\epsilon}{d\tau} - \frac{d\eta}{d\tau} \right) \right], \quad (\text{B.0.3})$$

with $z \equiv (1/H)(d\phi/d\tau)$ and ∇^2 the laplacian acting on spatial coordinates. The Hubble parameters are defined by $\epsilon \equiv -\dot{H}/H^2$ and $\eta \equiv -\ddot{H}/2H\dot{H}$.

The field u can be quantized by defining the operator

$$\hat{u}(\tau, \vec{x}) = \int \frac{d^3k}{(2\pi)^3} \left[u_k(\tau) a_{\vec{k}} e^{+i\vec{k}\cdot\vec{x}} + u_k^*(\tau) a_{\vec{k}}^\dagger e^{-i\vec{k}\cdot\vec{x}} \right], \quad (\text{B.0.4})$$

with the annihilation and creation operators that satisfy the commutation relations of bosonic fields

$$[a_{\vec{k}}, a_{\vec{k}'}] = [a_{\vec{k}}^\dagger, a_{\vec{k}'}^\dagger] = 0, \quad [a_{\vec{k}}, a_{\vec{k}'}^\dagger] = (2\pi)^3 \delta^{(3)}(\vec{k} - \vec{k}'), \quad a_{\vec{k}}|0\rangle = 0, \quad (\text{B.0.5})$$

where the last condition defines the vacuum. The equation of motion for each mode $u_k(\tau)$ takes the form of a Schrödinger equation

$$\frac{d^2u_k}{d\tau^2} + \left(k^2 - \frac{1}{z}\frac{d^2z}{d\tau^2} \right) u_k = 0, \quad (\text{B.0.6})$$

which can be solved imposing Bunch-Davies initial conditions at some initial time when $k \gg aH$. This choice defines the initial vacuum state as the minimum energy eigenstate for an harmonic oscillator with time-independent frequency in a space-time which is locally flat (because we are at length scales much smaller than the de Sitter curvature radius). Quantization of scalar perturbations is easier in terms of the Mukhanov-Sasaki field variable $u(\tau, \vec{x})$ since the quadratic action corresponding to the equation of motion in eq. (B.0.2) is the action describing a canonically normalized free field with an effective time-dependent mass. However, the dynamics of the modes u_k in Fourier space is more transparent if we introduce the so-called comoving curvature perturbation $\mathcal{R} = u/z$; in analogy with eq. (B.0.4), \mathcal{R} can be promoted to a quantum operator

$$\hat{\mathcal{R}}(\tau, \vec{x}) = \int \frac{d^3k}{(2\pi)^3} \left[\mathcal{R}_k(\tau) a_{\vec{k}} e^{+i\vec{k}\cdot\vec{x}} + \mathcal{R}_k^*(\tau) a_{\vec{k}}^\dagger e^{-i\vec{k}\cdot\vec{x}} \right], \quad (\text{B.0.7})$$

with $\mathcal{R}_k = u_k/z$ that satisfies the time-evolution equation

$$\frac{d^2\mathcal{R}_k}{dN^2} + (3 + \epsilon - 2\eta) \frac{d\mathcal{R}_k}{dN} + \frac{k^2}{a^2 H^2} \mathcal{R}_k = 0, \quad (\text{B.0.8})$$

which is the differential equation of a damped harmonic oscillator.

In the canonical picture of slow-roll inflation (that is for small Hubble parameters $\epsilon, \eta \ll 1$), eq. (B.0.8) can be solved in two complementary regimes divided by the so-called horizon-crossing condition $k = aH$. At early times, when $k \gg aH$ (in such case the modes are called sub-horizon), the last term dominates over the friction one, and the solution oscillates. As time passes by during inflation, the comoving Hubble radius $1/aH$ shrinks, the horizon-crossing condition is met, and one eventually enters in the regime characterized by $k \ll aH$ (in such case the modes are called super-horizon); the last term in eq. (B.0.8) can be neglected and the latter admits the constant solution $d\mathcal{R}_k/dN = 0$. In other words, after horizon crossing the mode \mathcal{R}_k freezes to a constant value that it maintains in time until the end of inflation (more precisely, until the mode re-enters the conformal Hubble horizon after the end of inflation).

In the canonical picture of slow-roll inflation, after horizon crossing quantum fluctuations can be regarded as classical, which motivates the description of cosmological perturbations in terms of classical random fields [69]. We will give a more precise definition of random fields in appendix C. At the conceptual level, the previous statement implies that one has the schematic relation $\lim_{k/aH \ll 1} \hat{\mathcal{R}}(\tau, \vec{x}) = \mathcal{R}(\vec{x})$ meaning that for super-horizon modes the quantum operator $\hat{\mathcal{R}}$ can be interpreted as a classical random field $\mathcal{R}(\vec{x})$; notice that the latter is time-independent because the modes \mathcal{R}_k are frozen in time. The previous relation can be formulated in a more precise form by saying that vacuum expectation values on the quantum side are interpreted as statistical averages on the classical side. Formally, in the classical picture we still have the Fourier decomposition

$$\mathcal{R}(\vec{x}) = \int \frac{d^3k}{(2\pi)^3} \left(\mathcal{R}_k a_{\vec{k}} e^{+i\vec{k}\cdot\vec{x}} + \mathcal{R}_k^* a_{\vec{k}}^\dagger e^{-i\vec{k}\cdot\vec{x}} \right), \quad (\text{B.0.9})$$

but now creation and annihilation operators are no longer q-numbers but stochastic c-numbers which are defined by the statistical averages

$$\langle a_{\vec{k}} a_{\vec{k}'}^\dagger \rangle = \frac{1}{2} (2\pi)^3 \delta^{(3)}(\vec{k} - \vec{k}') = \langle a_{\vec{k}'}^\dagger a_{\vec{k}} \rangle, \quad \langle a_{\vec{k}} a_{\vec{k}'} \rangle = \langle a_{\vec{k}}^\dagger a_{\vec{k}'}^\dagger \rangle = 0. \quad (\text{B.0.10})$$

Notice that $\langle a_{\vec{k}} a_{\vec{k}'}^\dagger \rangle = \langle a_{\vec{k}'}^\dagger a_{\vec{k}} \rangle$ is only valid for classical fluctuations, since it implies that the stochastic parameters commute. Furthermore, the stochastic parameters $a_{\vec{k}}$, $a_{\vec{k}}^\dagger$ have zero mean value (consequently, $\langle \mathcal{R}(\vec{x}) \rangle = 0$) in order to match the fact that the quantum operator $\hat{\mathcal{R}}(\tau, \vec{x})$ in eq. (B.0.7) has zero vacuum expectation value.

The random field $\mathcal{R}(\vec{x})$ is fully specified by the entire hierarchy of its correlation functions. The simplest one is the two-point correlation function. The latter can be defined by introducing the idea of power spectrum. The power spectrum $\Delta_{\mathcal{R}}(k)$ is defined by the Fourier transform of the two-point correlation function

$$\langle \mathcal{R}(\vec{x}) \mathcal{R}(\vec{x} + \vec{r}) \rangle = \int \frac{d^3k}{(2\pi)^3} e^{i\vec{k} \cdot \vec{r}} \Delta_{\mathcal{R}}(k) = \int_0^\infty dk \frac{\sin(kr)}{kr} \frac{k^2}{2\pi^2} \Delta_{\mathcal{R}}(k). \quad (\text{B.0.11})$$

The fact that $\Delta_{\mathcal{R}}(k)$ depends only on $k \equiv |\vec{k}|$ and the explicit angular integrations that we performed in eq. (B.0.11) are consequences of the assumptions of spatial homogeneity and isotropy (equivalently, spatial homogeneity and isotropy imply that $\langle \mathcal{R}(\vec{x}) \mathcal{R}(\vec{x} + \vec{r}) \rangle$ only depends on the relative distance $r \equiv |\vec{r}|$). The limit $r \rightarrow 0$ in eq. (B.0.11) defines the variance σ_0^2 of the comoving curvature perturbation

$$\sigma_0^2 \equiv \langle \mathcal{R}(\vec{x}) \mathcal{R}(\vec{x}) \rangle = \lim_{r \rightarrow 0} \langle \mathcal{R}(\vec{x}) \mathcal{R}(\vec{x} + \vec{r}) \rangle = \int_0^\infty \frac{dk}{k} \frac{k^3}{2\pi^2} \Delta_{\mathcal{R}}(k) \equiv \int_0^\infty \frac{dk}{k} \mathcal{P}_{\mathcal{R}}(k), \quad (\text{B.0.12})$$

where we defined the dimensionless power spectrum $\mathcal{P}_{\mathcal{R}}(k) \equiv (k^3/2\pi^2) \Delta_{\mathcal{R}}(k)$. This equation gives to the power spectrum an intuitive statistical meaning; $\mathcal{P}_{\mathcal{R}}(k)$ represents the contribution to the variance of the field per unit logarithmic bin around the comoving wavenumber k . As stated above, we can also compute eq. (B.0.12) by taking the vacuum expectation value of the quantum operator $\hat{\mathcal{R}}(\tau, \vec{x})$. We have (using eq. (B.0.5))

$$\lim_{k/aH \ll 1} \langle \hat{\mathcal{R}}(\tau, \vec{x}) \hat{\mathcal{R}}(\tau, \vec{x}) \rangle = \lim_{k/aH \ll 1} \int_0^\infty \frac{dk}{k} \frac{k^3}{2\pi^2} |\mathcal{R}_k(\tau)|^2 = \int_0^\infty \frac{dk}{k} \frac{k^3}{2\pi^2} |\mathcal{R}_k|^2, \quad (\text{B.0.13})$$

where the last step means that we are considering a sufficiently late time (the limit $\lim_{k/aH \ll 1}$, for fixed k , represents a time-limit since aH depends on time) such that the mode with comoving wavenumber k is frozen to its constant value after horizon crossing (and the time-dependence drops in the last equality). Eq. (B.0.13) gives an operative definition of the power spectrum. For a given model of inflation, we can solve eq. (B.0.8) (equivalently, eq. (B.0.6)) for each k and take a ‘‘late-time limit’’ in the sense specified above (that is we evaluate \mathcal{R}_k at some late time after it freezes to a constant value). The power spectrum is given by $\mathcal{P}_{\mathcal{R}}(k) \equiv (k^3/2\pi^2) |\mathcal{R}_k|^2$ and fully specifies the two-point correlator of the random field $\mathcal{R}(\vec{x})$. Equivalently, eq. (B.0.13) can be derived from the computation of $\langle \mathcal{R}(\vec{x}) \mathcal{R}(\vec{x}) \rangle$ by means of the decomposition given in eq. (B.0.9).

To proceed further, we need to specify the structure of higher-order correlators. Under the assumption that the random field $\mathcal{R}(\bar{x})$ is gaussian, however, the power spectrum is enough to fully reconstruct higher-order correlators. This is because the N-point correlation function either vanishes (for odd N) or can be expressed in terms of the power spectrum as a consequence of the Isserlis' theorem (for even N). The assumption that the statistics of the random field $\mathcal{R}(\bar{x})$ is gaussian is well-motivated in the context of the canonical picture of slow-roll inflation. This is because if one tries to compute, on the quantum-side, the three-point correlator $\lim_{k/aH \ll 1} \langle \hat{\mathcal{R}}(\tau, \bar{x}) \hat{\mathcal{R}}(\tau, \bar{x}) \hat{\mathcal{R}}(\tau, \bar{x}) \rangle$ the resulting expression turns out to be suppressed—compared to the two-point correlator—by additional powers of the Hubble parameters ϵ and η [70]. This means that non-gaussianities are not relevant during conventional slow-roll dynamics during which the Hubble parameters take $\mathcal{O}(\ll 1)$ values (said differently, this means that any detection of sizable non-gaussianities at CMB scales will rule out all single field slow-roll models of inflation).

However, we are interested in a situation which deviates from standard slow-roll dynamics. We refer to ref. [55] for a detailed (both analytical and numerical) study, and we summarize here the main points.

Standard slow-roll dynamics takes place at large field values. However, few e -folds before the end of inflation (which ends at the absolute minimum of the potential located at the origin) the inflaton field crosses an approximate stationary inflection point. The inflaton field almost stops but it possesses just enough inertia to overcome the approximate stationary inflection point. During this part of the dynamics the Hubble parameter η transits from $\eta \simeq 0$ (that is typical of slow-roll) to a large positive value that is maintained for few e -folds until the field crosses the approximate stationary inflection point. If $\eta \gtrsim 3/2$ (typically one has $\eta \gtrsim 3$), the friction term in eq. (B.o.8) becomes negative. This part of the dynamics characterized by the presence of negative friction is dubbed ultra slow-roll. During the negative friction phase, the modes \mathcal{R}_k —more precisely, their modulus $|\mathcal{R}_k|$ —change exponentially fast, and can be either enhanced or suppressed depending on the specific value of k .

After the end of ultra slow-roll, η transits to a phase during which it takes negative $\mathcal{O}(1)$ values. The friction term in eq. (B.o.8) turns positive, and the modes \mathcal{R}_k —after being enhanced or suppressed by the negative friction phase—are now free to freeze to their final constant value. Since $\mathcal{P}_{\mathcal{R}}(k) \equiv (k^3/2\pi^2)|\mathcal{R}_k|^2$, the negative friction phase that modifies exponentially $|\mathcal{R}_k|$ produces a distinctive peak in the power spectrum of curvature perturbations.

This peculiar dynamics has important consequences as far as non-gaussianities are concerned. Because of the presence of the negative friction phase, classicalization of the modes do not happens after their horizon crossing but is delayed after the end of ultra slow-roll [71]. This means that the three-point correlator $\langle \hat{\mathcal{R}}(\tau, \bar{x}) \hat{\mathcal{R}}(\tau, \bar{x}) \hat{\mathcal{R}}(\tau, \bar{x}) \rangle$ has to be evaluated after the end of ultra slow-roll. Crucially, after the end of ultra slow-roll η takes sizable negative $\mathcal{O}(1)$ values (while we expect $\epsilon \ll 1$). Let us indicate this value with η_0 (which is a negative number). This implies that non-gaussianities are no longer negligible since the expected slow-roll suppression is not valid anymore.

The explicit computation of the three-point correlator in Fourier space gives, for a triad of comoving wavenumbers k_1, k_2, k_3 , the so-called local bispectrum [45]

$$B_{\mathcal{R}}(k_1, k_2, k_3) \approx -\eta_0 [\Delta_{\mathcal{R}}(k_1)\Delta_{\mathcal{R}}(k_2) + \Delta_{\mathcal{R}}(k_1)\Delta_{\mathcal{R}}(k_3) + \Delta_{\mathcal{R}}(k_2)\Delta_{\mathcal{R}}(k_3)], \quad (\text{B.0.14})$$

where the three-point correlator is given by the Fourier transform

$$\lim_{\text{end of USR}} \langle \hat{\mathcal{R}}(\tau, \vec{x}) \hat{\mathcal{R}}(\tau, \vec{x}) \hat{\mathcal{R}}(\tau, \vec{x}) \rangle = \int \frac{d^3 k_1}{(2\pi)^3} \frac{d^3 k_2}{(2\pi)^3} \frac{d^3 k_3}{(2\pi)^3} (2\pi)^3 \delta^{(3)}(\vec{k}_1 + \vec{k}_2 + \vec{k}_3) B_{\mathcal{R}}(k_1, k_2, k_3), \quad (\text{B.0.15})$$

and where $\lim_{\text{end of USR}}$ indicates explicitly that the three-point correlator has to be evaluated at some late time after the end of ultra slow-roll, when the modes \mathcal{R}_k finally set to their final constant value (so that the right-hand side of eq. (B.0.15) does not depend on time).

The analysis carried out in refs. [45] shows that non-gaussianities in the presence of ultra slow-roll are expected to be non-negligible. Eqs. (B.0.14, B.0.15) represent the quantum side of the story, and eq. (B.0.14) can be obtained by means of the so-called “*in-in*” formalism [70]. It is important to understand the implications from the point of view of the random field $\mathcal{R}(\vec{x})$. Consider the non-gaussian random field $\mathcal{R}_{\text{NG}}(\vec{x})$ defined by

$$\mathcal{R}_{\text{NG}}(\vec{x}) \equiv \mathcal{R}_{\text{G}}(\vec{x}) + \frac{(-\eta_0)}{2} [\mathcal{R}_{\text{G}}(\vec{x})^2 - \langle \mathcal{R}_{\text{G}}(\vec{x})^2 \rangle], \quad (\text{B.0.16})$$

where $\mathcal{R}_{\text{G}}(\vec{x})$ is a gaussian random field—with variance σ_0^2 (see eq. (B.0.12))—which admits the decomposition given in eq. (B.0.9); it is a simple exercise to show that the three-point correlator $\langle \mathcal{R}_{\text{NG}}(\vec{x}) \mathcal{R}_{\text{NG}}(\vec{x}) \mathcal{R}_{\text{NG}}(\vec{x}) \rangle$ has precisely the form given in eq. (B.0.15). Notice that in eq. (B.0.16) the presence of the constant piece $\langle \mathcal{R}_{\text{G}}(\vec{x})^2 \rangle$ guarantees that the non-gaussian random field $\mathcal{R}_{\text{NG}}(\vec{x})$ has zero mean. This property is physically motivated by the fact that the background solution is stable.

The physics-case sketched in this appendix motivates the non-gaussianities studied in this paper which are of the form given in eq. (B.0.16). To avoid cluttering the notation, in the main part of this work we indicate simply with \mathcal{R} the gaussian random field \mathcal{R}_{G} in eq. (B.0.16) and with h the non-gaussian one \mathcal{R}_{NG} . Furthermore, we set $\alpha \equiv (-\eta_0)/2$.

Before proceeding, an important comment is in order. As we have discussed, the structure of the non-gaussian random field given in eq. (B.0.16) is motivated by the explicit computation of the three-point correlator in eqs. (B.0.14, B.0.15) in the presence of ultra slow-roll. This computation is based on the “*in-in*” formalism in which one expands the interaction Hamiltonian up to the cubic order.

However, computing only the bispectrum is not the end of the story. In principle, one should compute also the trispectrum (that is the connected part of the four-point correlator) and check that its contribution does not alter the form of non-gaussianities derived including only cubic interactions. Needless to say, the computation of the trispectrum is anything but simple, and we are not aware of explicit results in the context of ultra slow-roll. From a more pragmatic phenomenological

perspective, one possible way to proceed—widely used for the analysis of CMB non-Gaussianity, see ref. [72]—is the following. Instead of eq. (B.0.16), one takes the more general ansatz

$$\mathcal{R}_{\text{NG}}(\vec{x}) \equiv \mathcal{R}_{\text{G}}(\vec{x}) + f_2 [\mathcal{R}_{\text{G}}(\vec{x})^2 - \langle \mathcal{R}_{\text{G}}(\vec{x})^2 \rangle] + f_3 \mathcal{R}_{\text{G}}(\vec{x})^3, \quad (\text{B.0.17})$$

where $f_{2,3}$ are free coefficients that parametrize quadratic and cubic deviations from the gaussian limit. Notice that eq. (B.0.17) generalizes eq. (B.0.16) in the sense that it introduces cubic corrections but it preserves locality (in the sense that deviations from exact gaussianity at \vec{x} are located at the same spatial position). As discussed before, in the absence of an explicit computation there is no guarantee that ultra slow-roll generates deviations from eq. (B.0.16) that have the form given in eq. (B.0.17). Nevertheless, eq. (B.0.17) can be considered as a phenomenological parametrization to study deviations from from eq. (B.0.16), as done for instance in ref. [73]. For this reason, in our analysis we will try to set the formalism considering a generic deviation from gaussianity (but always assuming locality) even though we will present our results for the motivated case of quadratic non-gaussianities given in eq. (B.0.16).

Finally, let us mention that a resummation of local non-gaussianities at all orders has been presented in ref. [74, 75]. The analysis is based on an expansion of the inflaton potential around a local maximum. It would be interesting to go beyond such approximation and extend this analysis for the potentials studied here. Moreover it is also worth investigating the role of higher order contributions leading to non-local non-gaussianities.

As a warm-up, consider the case of a n -dimensional scalar gaussian random field $\mathcal{R}(\vec{x})$ that we identify with the random field associated to curvature perturbations. Peak theory in the case of a scalar gaussian random field is well-known [48]. However, in this appendix we will give a detailed discussion. The reason is that in our approach there is an important conceptual difference compared to the standard results of ref. [48]. Ref. [48] computes the number density of peaks of the overdensity field working directly with $\delta(\vec{x}, t)$, and without any reference to curvature perturbations. In this paper, on the contrary, we aim to compute the same quantity but starting from the distribution of local maxima of the curvature perturbation. Following this alternative route, we will be able to find (see appendix E) a generalization that accounts for the case in which local non-gaussianities in the definition of $\mathcal{R}(\vec{x})$ are present.

Let us start from basics. A n -dimensional scalar random field $\mathcal{R}(\vec{x})$ is a set of random variables, one for each point \vec{x} in the n -dimensional real space, equipped with a probability distribution $p[\mathcal{R}(\vec{x}_1), \dots, \mathcal{R}(\vec{x}_m)] d\mathcal{R}(\vec{x}_1) \dots d\mathcal{R}(\vec{x}_m)$ which measures the probability that the function \mathcal{R} has values in the range $\mathcal{R}(\vec{x}_j)$ to $\mathcal{R}(\vec{x}_j) + d\mathcal{R}(\vec{x}_j)$ for each of the $j = 1, \dots, m$, with m an arbitrary integer and $\vec{x}_1, \dots, \vec{x}_m$ arbitrary points.¹

We are interested in the behavior of the random field for a point in space that is stationary, and we consider $m = 1$ with $\vec{x}_1 = \vec{x}_{st}$. We can expand around this point according to

$$\mathcal{R}(\vec{x}) = \mathcal{R}(\vec{x}_{st}) + \frac{1}{2} \sum_{i,j=1}^n \mathcal{R}_{ij}(\vec{x}_{st}) (\vec{x} - \vec{x}_{st})_i (\vec{x} - \vec{x}_{st})_j, \quad (\text{C.0.1})$$

from which we have

$$\mathcal{R}_i(\vec{x}) = \sum_{j=1}^n \mathcal{R}_{ij}(\vec{x}_{st}) (\vec{x} - \vec{x}_{st})_j. \quad (\text{C.0.2})$$

The goal is to obtain the number density of these stationary points in the n -dimensional space. Not to violate the cosmological principle, we only want to consider random fields which are statistically homogeneous and isotropic. Consequently, the specific value of \vec{x}_{st} is irrelevant, and we can always shift to $\vec{x}_{st} = \vec{0}$. Let us, therefore, drop the explicit dependence on \vec{x}_{st} .

The quantity of central interest for the computation of the number density of stationary points of \mathcal{R} is the joint probability density distribution of the field \mathcal{R} , its first and second derivatives. This is intuitively obvious, since identifying maxima (or minima) implies a set of conditions on field derivatives, and it is thus mandatory to know what is their probability distribution (derivatives of a random field are also random variables themselves).

¹ Notice that, as in ref. [48], all spatial separations and length scales are described in comoving coordinates in the cosmological background. This means that the number density that we shall compute at the end of this section in eq. (C.0.33) must be understood as a comoving number density.

Consider the realistic case with $n = 3$. We indicate with $P(\mathcal{R}, \mathcal{R}_i, \mathcal{R}_{ij})d\mathcal{R}d^3\mathcal{R}_i d^6\mathcal{R}_{ij}$ the joint probability distribution for the field being in the range \mathcal{R} to $\mathcal{R} + d\mathcal{R}$, the field gradient being in the range \mathcal{R}_i to $\mathcal{R}_i + d\mathcal{R}_i$ and the second derivative matrix elements being in the range \mathcal{R}_{ij} to $\mathcal{R}_{ij} + d\mathcal{R}_{ij}$, all at the same point in space. $P(\mathcal{R}, \mathcal{R}_i, \mathcal{R}_{ij})$ is the joint ten-dimensional probability density distribution.

If the point is stationary, we can write the joint probability distribution as

$$P(\mathcal{R}, \mathcal{R}_i = 0, \mathcal{R}_{ij}) |\det(\mathcal{R}_{ij})| d\mathcal{R} d^3\bar{x} d^6\mathcal{R}_{ij}. \quad (\text{C.0.3})$$

We set $\mathcal{R}_i = 0$ since the point is stationary, and we used eq. (C.0.1) to change variables in the gradient volume element. We can, therefore, write the probability distribution to have a stationary point in a volume $d^3\bar{x}$ with the field being in the range \mathcal{R} to $\mathcal{R} + d\mathcal{R}$ as

$$n_{\text{st}}(\mathcal{R})d\mathcal{R}d^3\bar{x} \equiv d\mathcal{R}d^3\bar{x} \underbrace{\int P(\mathcal{R}, \mathcal{R}_i = 0, \mathcal{R}_{ij}) |\det(\mathcal{R}_{ij})| d^6\mathcal{R}_{ij}}_{\equiv n_{\text{st}}(\mathcal{R})}, \quad (\text{C.0.4})$$

where the integral is extended to the whole range of variability of the second derivatives since we are considering generic stationary points. The probability distribution to have a maximum in a volume $d^3\bar{x}$ with the field being in the range \mathcal{R} to $\mathcal{R} + d\mathcal{R}$ is

$$n_{\text{max}}(\mathcal{R})d\mathcal{R}d^3\bar{x} \equiv d\mathcal{R}d^3\bar{x} \underbrace{\int_{\text{max}} P(\mathcal{R}, \mathcal{R}_i = 0, \mathcal{R}_{ij}) |\det(\mathcal{R}_{ij})| d^6\mathcal{R}_{ij}}_{\equiv n_{\text{max}}(\mathcal{R})}, \quad (\text{C.0.5})$$

where now the integral is subject to the conditions on the Hessian matrix that define a maximum. An equivalent definition holds in the case of a minimum. The probability density distribution $n_{\text{max}}(\mathcal{R})$ represents the number density of local maxima (where ‘‘number density’’ is defined in a probabilistic sense) with field value in the range \mathcal{R} to $\mathcal{R} + d\mathcal{R}$.

In order to extract quantitative informations, we need to compute $P(\mathcal{R}, \mathcal{R}_i, \mathcal{R}_{ij})$, set $\mathcal{R}_i = 0$, and integrate. This strategy does not depend on the specific statistics of the random field.

The computation of $P(\mathcal{R}, \mathcal{R}_i, \mathcal{R}_{ij})$ drastically simplifies in the gaussian case. This is because the joint probability distribution of a gaussian field and its derivatives is a multivariate normal distribution. Consider the simplified case with $n = 2$ in which we have more control on analytical formulas;² we have six random variables that we collect in the column vector $\mathbf{R} \equiv (\mathcal{R}, \mathcal{R}_x, \mathcal{R}_y, \mathcal{R}_{xx}, \mathcal{R}_{xy}, \mathcal{R}_{yy})^T$. We have

$$P(\mathcal{R}, \mathcal{R}_i, \mathcal{R}_{ij}) = \frac{1}{(2\pi)^{k/2} \sqrt{\det C}} \exp \left[-\frac{1}{2} (\mathbf{R} - \langle \mathbf{R} \rangle)^T (C^{-1}) (\mathbf{R} - \langle \mathbf{R} \rangle) \right], \quad (\text{C.0.6})$$

where $k = 6$ is the dimension of \mathbf{R} , $\langle \mathbf{R} \rangle$ is the column vector of the expectation values of \mathbf{R} and C is the covariance matrix defined by $C \equiv \langle (\mathbf{R} - \langle \mathbf{R} \rangle) (\mathbf{R} - \langle \mathbf{R} \rangle)^T \rangle$ with elements

$$C_{ij} = \langle (\mathbf{R} - \langle \mathbf{R} \rangle)_i (\mathbf{R} - \langle \mathbf{R} \rangle)_j \rangle = \langle \mathbf{R}_i \mathbf{R}_j \rangle - \langle \mathbf{R}_i \rangle \langle \mathbf{R}_j \rangle. \quad (\text{C.0.7})$$

² The simplest possibility would be $n = 1$. However, the case $n = 2$ is the simplest setup in which a non-trivial discussion about spatial isotropy is possible.

From the computation of the covariance matrix one can fully reconstruct the joint probability distribution.

We restrict the analysis to zero-mean random fields since this assumption is physically motivated (see discussion in appendix B). From the explicit computation of the two-point correlators $\langle \mathcal{R}_i \mathcal{R}_j \rangle$, one finds that the covariance matrix takes the form

$$\mathbf{C} = \begin{matrix} & \mathcal{R} & \mathcal{R}_x & \mathcal{R}_y & \mathcal{R}_{xx} & \mathcal{R}_{xy} & \mathcal{R}_{yy} \\ \begin{matrix} \mathcal{R} \\ \mathcal{R}_x \\ \mathcal{R}_y \\ \mathcal{R}_{xx} \\ \mathcal{R}_{xy} \\ \mathcal{R}_{yy} \end{matrix} & \begin{pmatrix} \sigma_0^2 & 0 & 0 & -\sigma_1^2/2 & 0 & -\sigma_1^2/2 \\ 0 & \sigma_1^2/2 & 0 & 0 & 0 & 0 \\ 0 & 0 & \sigma_1^2/2 & 0 & 0 & 0 \\ -\sigma_1^2/2 & 0 & 0 & 3\sigma_2^2/8 & 0 & \sigma_2^2/8 \\ 0 & 0 & 0 & 0 & \sigma_2^2/8 & 0 \\ -\sigma_1^2/2 & 0 & 0 & \sigma_2^2/8 & 0 & 3\sigma_2^2/8 \end{pmatrix} \end{matrix}, \quad (\text{C.o.8})$$

and we find that \mathcal{R}_x , \mathcal{R}_y and \mathcal{R}_{xy} are completely uncorrelated while \mathcal{R} , \mathcal{R}_{xx} and \mathcal{R}_{yy} are correlated. We introduce the spectral moments

$$\sigma_j^2 \equiv \int \frac{dk}{k} \mathcal{P}_{\mathcal{R}}(k) k^{2j}, \quad (\text{C.o.9})$$

where $\mathcal{P}_{\mathcal{R}}(k)$ is the dimensionless power spectrum of \mathcal{R} . Notice that in two spatial dimensions the dimensionless power spectrum of \mathcal{R} is related to the power spectrum by means of $\mathcal{P}_{\mathcal{R}}(k) = (k^2/2\pi)\Delta_{\mathcal{R}}(k)$ with $\Delta_{\mathcal{R}}(k) = |\mathcal{R}_k|^2$.

Consider, as an illustrative example, the computation of $\langle \mathcal{R}_{xx} \mathcal{R}_{yy} \rangle$. We use the explicit form of \mathcal{R} given in eq. (B.o.9). We find

$$\begin{aligned} \langle \mathcal{R}_{xx} \mathcal{R}_{yy} \rangle &= \\ &= \int \frac{d^2k_1}{(2\pi)^2} \frac{d^2k_2}{(2\pi)^2} \left\langle \left(-k_{1,x}^2 \mathcal{R}_{k_1} a_{\vec{k}_1} e^{i\vec{k}_1 \cdot \vec{x}} - k_{1,x}^2 \mathcal{R}_{k_1}^* a_{\vec{k}_1}^{\dagger} e^{-i\vec{k}_1 \cdot \vec{x}} \right) \left(-k_{2,y}^2 \mathcal{R}_{k_2} a_{\vec{k}_2} e^{i\vec{k}_2 \cdot \vec{x}} - k_{2,y}^2 \mathcal{R}_{k_2}^* a_{\vec{k}_2}^{\dagger} e^{-i\vec{k}_2 \cdot \vec{x}} \right) \right\rangle \\ &= \int \frac{d^2k_1}{(2\pi)^2} \frac{d^2k_2}{(2\pi)^2} k_{1,x}^2 k_{2,y}^2 \left[e^{i(\vec{k}_1 - \vec{k}_2) \cdot \vec{x}} \mathcal{R}_{k_1} \mathcal{R}_{k_2}^* \langle a_{\vec{k}_1} a_{\vec{k}_2}^{\dagger} \rangle + e^{-i(\vec{k}_1 - \vec{k}_2) \cdot \vec{x}} \mathcal{R}_{k_2} \mathcal{R}_{k_1}^* \langle a_{\vec{k}_1}^{\dagger} a_{\vec{k}_2} \rangle \right] \\ &= \int \frac{d^2k}{(2\pi)^2} k_x^2 k_y^2 |\mathcal{R}_k|^2 = \frac{1}{4\pi^2} \int dk d\varphi k^5 \cos^2 \varphi \sin^2 \varphi \Delta_{\mathcal{R}}(k) = \frac{1}{8} \int \frac{dk}{k} k^4 \mathcal{P}_{\mathcal{R}}(k), \end{aligned}$$

where in the last line we just introduced polar coordinates. All the entries in eq. (C.o.8) can be computed in a similar way.

Interestingly, the pattern of zeros in eq. (C.o.8) and the relations among different non-zero entries—obtained before by means of a direct computation—can be understood as a consequence of homogeneity and isotropy.

Homogeneity, that is translational invariance, implies that correlators do not depend on the specific spatial position at which they are computed. For instance, this means that the spatial derivative of $\langle \mathcal{R} \mathcal{R} \rangle$ should vanish (this must be true for a generic correlator evaluated at a given spatial point); from this condition, one finds $\partial_i \langle \mathcal{R} \mathcal{R} \rangle = 0 \Rightarrow \langle \mathcal{R} \mathcal{R}_i \rangle = 0$ so that \mathcal{R} , \mathcal{R}_x and \mathcal{R}_y are uncorrelated.

Similarly, from $\partial_x(\langle \mathcal{R}_x \mathcal{R}_x \rangle) = 0$ one gets $\langle \mathcal{R}_x \mathcal{R}_{xx} \rangle = 0$ (with similar relations along other directions) so that first and second derivatives are uncorrelated. On the contrary, from $\partial_x(\langle \mathcal{R} \mathcal{R}_x \rangle) = 0$ it follows that $\langle \mathcal{R} \mathcal{R}_{xx} \rangle = -\langle \mathcal{R}_x \mathcal{R}_x \rangle$ as indeed obtained in eq. (C.0.8). Similarly, $\langle \mathcal{R} \mathcal{R}_{yy} \rangle = -\langle \mathcal{R}_y \mathcal{R}_y \rangle$.

Isotropy, that is rotational invariance, implies that correlators do not depend on a particular direction in space. The simplest consequence of isotropy is that $\langle \mathcal{R}_x \mathcal{R}_x \rangle = \langle \mathcal{R}_y \mathcal{R}_y \rangle$ and $\langle \mathcal{R}_x \mathcal{R}_y \rangle = 0$. In order to derive these two conditions, a very useful trick (that we shall use also in the non-gaussian computation) is to introduce—instead of the two components x and y of the two-dimensional vector \vec{x} —the complex conjugated variables $z \equiv x + iy$ and $z^* = x - iy$ from which we have $\partial_z = (\partial_x - i\partial_y)/2$ and $\partial_{z^*} = (\partial_x + i\partial_y)/2$. If we now rotate the two-dimensional vector \vec{x} (without changing its length) the complex number z changes by a phase factor $e^{i\tau}$, that is $z \rightarrow e^{i\tau}z$ (and $z^* \rightarrow e^{-i\tau}z^*$). Consequently, the derivatives with respect to z and z^* change according to $\partial_z \rightarrow e^{-i\tau}\partial_z$ and $\partial_{z^*} \rightarrow e^{i\tau}\partial_{z^*}$. If we now consider the correlators $\langle \mathcal{R}_z \mathcal{R}_z \rangle$ and $\langle \mathcal{R}_{z^*} \mathcal{R}_{z^*} \rangle$ they rotate according to $\langle \mathcal{R}_z \mathcal{R}_z \rangle \rightarrow e^{-2i\tau}\langle \mathcal{R}_z \mathcal{R}_z \rangle$ and $\langle \mathcal{R}_{z^*} \mathcal{R}_{z^*} \rangle \rightarrow e^{2i\tau}\langle \mathcal{R}_{z^*} \mathcal{R}_{z^*} \rangle$. Because of isotropy of the two-dimensional space, $\langle \mathcal{R}_z \mathcal{R}_z \rangle$ and $\langle \mathcal{R}_{z^*} \mathcal{R}_{z^*} \rangle$ can not depend on τ and, therefore, they must vanish. Consequently, the system of equations

$$\langle \mathcal{R}_z \mathcal{R}_z \rangle = \frac{1}{4} (\langle \mathcal{R}_x \mathcal{R}_x \rangle - 2i\langle \mathcal{R}_x \mathcal{R}_y \rangle - \langle \mathcal{R}_y \mathcal{R}_y \rangle) = 0, \quad (\text{C.0.10})$$

$$\langle \mathcal{R}_{z^*} \mathcal{R}_{z^*} \rangle = \frac{1}{4} (\langle \mathcal{R}_x \mathcal{R}_x \rangle + 2i\langle \mathcal{R}_x \mathcal{R}_y \rangle - \langle \mathcal{R}_y \mathcal{R}_y \rangle) = 0, \quad (\text{C.0.11})$$

admits the solution $\langle \mathcal{R}_x \mathcal{R}_x \rangle = \langle \mathcal{R}_y \mathcal{R}_y \rangle$ and $\langle \mathcal{R}_x \mathcal{R}_y \rangle = 0$ which are precisely the relations we were looking for. More in general, if we consider the rotation $\partial_z \rightarrow e^{-i\tau}\partial_z$ and $\partial_{z^*} \rightarrow e^{i\tau}\partial_{z^*}$ a generic correlator will take a phase factor $e^{i\kappa\tau}$ where $\kappa \equiv (\#z^* \text{ derivatives}) - (\#z \text{ derivatives})$. If $\kappa \neq 0$, then the correlator must be equal to zero as a consequence of isotropy. For instance, we have $\langle \mathcal{R}_{zz} \mathcal{R}_{z^*} \rangle = 0$ (because $\kappa = -1$) but $\langle \mathcal{R}_z \mathcal{R}_{z^*} \rangle \neq 0$ (because $\kappa = 0$).

Combining homogeneity and isotropy validates the remaining entries in eq. (C.0.8). For instance, from $\partial_y(\langle \mathcal{R} \mathcal{R}_x \rangle) = \langle \mathcal{R}_x \mathcal{R}_y \rangle + \langle \mathcal{R} \mathcal{R}_{xy} \rangle = 0$ (homogeneity) we find $\langle \mathcal{R} \mathcal{R}_{xy} \rangle = 0$ since isotropy implies $\langle \mathcal{R}_x \mathcal{R}_y \rangle = 0$. As a final check, we consider the block of the second derivatives in eq. (C.0.8). From the previous argument, isotropy implies that $\langle \mathcal{R}_{zz} \mathcal{R}_{zz} \rangle = 0$ and $\langle \mathcal{R}_{zz^*} \mathcal{R}_{zz} \rangle = 0$ (together with their complex conjugated $\langle \mathcal{R}_{z^*z^*} \mathcal{R}_{z^*z^*} \rangle = 0$ and $\langle \mathcal{R}_{zz^*} \mathcal{R}_{z^*z^*} \rangle = 0$). These two relations imply $\langle \mathcal{R}_{xx} \mathcal{R}_{xy} \rangle = \langle \mathcal{R}_{yy} \mathcal{R}_{xy} \rangle = 0$ and $\langle \mathcal{R}_{xx} \mathcal{R}_{xx} \rangle = \langle \mathcal{R}_{xx} \mathcal{R}_{yy} \rangle + 2\langle \mathcal{R}_{xy} \mathcal{R}_{xy} \rangle$. Both these relations are verified by the entries in eq. (C.0.8). We can actually do more since it is possible to show that $\langle \mathcal{R}_{xx} \mathcal{R}_{yy} \rangle = \langle \mathcal{R}_{xy} \mathcal{R}_{xy} \rangle$. Let us write

$$\begin{aligned} \langle \mathcal{R}_{xx} \mathcal{R}_{yy} \rangle &= \langle \partial_{xx} \mathcal{R}(\vec{x}) \partial_{yy} \mathcal{R}(\vec{x}) \rangle = \langle \partial_{x_1 x_1} \mathcal{R}(\vec{x}_1) \partial_{y_2 y_2} \mathcal{R}(\vec{x}_2) \rangle \Big|_{\vec{x}_1 = \vec{x}_2 = \vec{x}} \\ &= \partial_{x_1 x_1} \partial_{y_2 y_2} \langle \mathcal{R}(\vec{x}_1) \mathcal{R}(\vec{x}_2) \rangle \Big|_{\vec{x}_1 = \vec{x}_2 = \vec{x}} = \partial_{x_1} \partial_{y_2} \langle \mathcal{R}_{x_1}(\vec{x}_1) \mathcal{R}_{y_2}(\vec{x}_2) \rangle \Big|_{\vec{x}_1 = \vec{x}_2 = \vec{x}}. \end{aligned} \quad (\text{C.0.12})$$

where the first step is just a more explicit definition of $\langle \mathcal{R}_{xx} \mathcal{R}_{yy} \rangle$ while in the following ones we consider two distinct point $\vec{x}_1 = (x_1, y_1)$ and $\vec{x}_2 = (x_2, y_2)$ that we later set equal again. Now the point is that because of homogeneity of space the correlator $\langle \mathcal{R}_{x_1}(\vec{x}_1) \mathcal{R}_{y_2}(\vec{x}_2) \rangle$ depends only on the distance $|\vec{x}_1 - \vec{x}_2|$; we can, therefore, exchange $1 \leftrightarrow 2$ obtaining $\langle \mathcal{R}_{x_2}(\vec{x}_2) \mathcal{R}_{y_1}(\vec{x}_1) \rangle$ without altering the result. From eq. (C.0.12) this means that we have $\langle \mathcal{R}_{xx} \mathcal{R}_{yy} \rangle = \langle \mathcal{R}_{xy} \mathcal{R}_{xy} \rangle$ as indeed verified in

eq. (C.0.8). If we combine this result with the previous relation $\langle \mathcal{R}_{xx} \mathcal{R}_{xx} \rangle = \langle \mathcal{R}_{xx} \mathcal{R}_{yy} \rangle + 2\langle \mathcal{R}_{xy} \mathcal{R}_{xy} \rangle$ we find $\langle \mathcal{R}_{xx} \mathcal{R}_{xx} \rangle = 3\langle \mathcal{R}_{xy} \mathcal{R}_{xy} \rangle$ which is again verified in eq. (C.0.8). Finally, we also note that the condition $\langle \mathcal{R}_{xx} \mathcal{R}_{yy} \rangle = \langle \mathcal{R}_{xy} \mathcal{R}_{xy} \rangle$ implies that $\langle \mathcal{R}_{zz^*} \mathcal{R}_{zz^*} \rangle = \langle \mathcal{R}_{zz} \mathcal{R}_{z^*z^*} \rangle$. These kind of relations based on homogeneity and isotropy will be useful later in the non-gaussian case.

Using the properties of the exponential function, eq. (C.0.6) takes the form

$$P(\mathcal{R}, \mathcal{R}_i, \mathcal{R}_{ij}) = P(\mathcal{R}_x)P(\mathcal{R}_y)P(\mathcal{R}_{xy})P(\mathcal{R}, \mathcal{R}_{xx}, \mathcal{R}_{yy}), \quad (\text{C.0.13})$$

where

$$P(\mathcal{R}_x) = \frac{1}{\sqrt{\pi\sigma_1^2}} \exp\left(-\frac{\mathcal{R}_x^2}{\sigma_1^2}\right), \quad P(\mathcal{R}_y) = \frac{1}{\sqrt{\pi\sigma_1^2}} \exp\left(-\frac{\mathcal{R}_y^2}{\sigma_1^2}\right), \quad P(\mathcal{R}_{xy}) = \frac{2}{\sqrt{\pi\sigma_2^2}} \exp\left(-\frac{4\mathcal{R}_{xy}^2}{\sigma_2^2}\right), \quad (\text{C.0.14})$$

and

$$P(\mathcal{R}, \mathcal{R}_{xx}, \mathcal{R}_{yy}) = \frac{1}{(2\pi)^{3/2} \sqrt{\det \tilde{\mathbf{C}}}} \exp\left(-\frac{1}{2} \tilde{\mathbf{R}}^T \tilde{\mathbf{C}}^{-1} \tilde{\mathbf{R}}\right), \quad \tilde{\mathbf{C}} \equiv \begin{matrix} & \mathcal{R} & \mathcal{R}_{xx} & \mathcal{R}_{yy} \\ \mathcal{R} & \begin{pmatrix} \sigma_0^2 & -\sigma_1^2/2 & -\sigma_1^2/2 \\ -\sigma_1^2/2 & 3\sigma_2^2/8 & \sigma_2^2/8 \\ -\sigma_1^2/2 & \sigma_2^2/8 & 3\sigma_2^2/8 \end{pmatrix} \end{matrix}, \quad (\text{C.0.15})$$

with $\tilde{\mathbf{R}} \equiv (\mathcal{R}, \mathcal{R}_{xx}, \mathcal{R}_{yy})^T$. As customary in the gaussian case, from the knowledge of the power spectrum it is possible to fully reconstruct the statistics of the random field. From eq. (C.0.5) we get the number density of maxima

$$n_{\max}(\mathcal{R}) = \frac{1}{\pi\sigma_1^2} \int_{\max} d\mathcal{R}_{xx} d\mathcal{R}_{xy} d\mathcal{R}_{yy} |\mathcal{R}_{xx} \mathcal{R}_{yy} - \mathcal{R}_{xy}^2| P(\mathcal{R}_{xy}) P(\mathcal{R}, \mathcal{R}_{xx}, \mathcal{R}_{yy}), \quad (\text{C.0.16})$$

where we used $P(\mathcal{R}_x = 0) = P(\mathcal{R}_y = 0) = 1/\sqrt{\pi\sigma_1^2}$. The integration region is defined by the conditions $\max = \{\mathcal{R}_{xx} \mathcal{R}_{yy} - \mathcal{R}_{xy}^2 > 0 \wedge \mathcal{R}_{xx} < 0 \wedge \mathcal{R}_{yy} < 0\}$.

The change of variables $\{\mathcal{R}_{xx}, \mathcal{R}_{yy}, \mathcal{R}_{xy}\} \rightarrow \{r, s, \theta\}$ defined by

$$r \cos \theta \equiv \frac{1}{2} (\mathcal{R}_{xx} - \mathcal{R}_{yy}), \quad r \sin \theta \equiv \mathcal{R}_{xy}, \quad s \equiv -\frac{1}{2} (\mathcal{R}_{xx} + \mathcal{R}_{yy}), \quad (\text{C.0.17})$$

turns out to be useful. The Jacobian of the transformation is $J = 2r$, and we have $\mathcal{R}_{xx} \mathcal{R}_{yy} - \mathcal{R}_{xy}^2 = s^2 - r^2$. The condition $s^2 - r^2 > 0$ becomes $-s < r < s$ with $s > 0$ since $\mathcal{R}_{xx} < 0$ and $\mathcal{R}_{yy} < 0$. Furthermore, we restrict to $r > 0$ if $0 < \theta < 2\pi$. All in all, we have $\max = \{0 < \theta < 2\pi \wedge s > 0 \wedge 0 < r < s\}$.

The parametrization in terms of $\{r, s, \theta\}$ is useful because we have

$$2s = -(\mathcal{R}_{xx} + \mathcal{R}_{yy}) = -\nabla^2 \mathcal{R}. \quad (\text{C.0.18})$$

This implies that any condition that restricts the value of the curvature $-\nabla^2\mathcal{R}$ can be implemented through s by imposing $s > s_{\min}$ instead of $s > 0$. This is the case of eq. (5.2.6) with $\alpha = 0$ (thus $h = \mathcal{R}$), which reads

$$\frac{s_{\min}}{\sigma_2} = \frac{9}{8} \frac{(a_m H_m)^2}{\sigma_2} \delta_c, \quad (\text{C.0.19})$$

Eq. (C.0.16) becomes

$$n_{\max}(\mathcal{R}, s_{\min}) = \frac{8}{\pi^2 \sigma_1^2 \sigma_2^2 \sqrt{\sigma_2^2 \sigma_0^2 - \sigma_1^4}} \int_{s_{\min}}^{\infty} ds \int_0^s dr r (s^2 - r^2) \exp \left[-\frac{(\mathcal{R}^2 \sigma_2^2 + 4s^2 \sigma_0^2 - 4s \mathcal{R} \sigma_1^2)}{2(\sigma_0^2 \sigma_2^2 - \sigma_1^4)} - \frac{4r^2}{\sigma_2^2} \right], \quad (\text{C.0.20})$$

where, according to the previous argument, we set to s_{\min} the lower limit of integration over s and define $n_{\max}(\mathcal{R}, s_{\min})$ such that $n_{\max}(\mathcal{R}, s_{\min} = 0) = n_{\max}(\mathcal{R})$. The integration over r gives

$$\begin{aligned} n_{\max}(\mathcal{R}, s_{\min}) &= \quad (\text{C.0.21}) \\ &= \underbrace{\frac{\sigma_2^2}{4\pi^2 \sigma_1^2 \sqrt{\sigma_2^2 \sigma_0^2 - \sigma_1^4}} \int_{s_{\min}}^{\infty} ds \left(\frac{4s^2}{\sigma_2^2} + e^{-\frac{4s^2}{\sigma_2^2}} - 1 \right) \exp \left\{ -\frac{\sigma_0^2 \sigma_2^2}{2(\sigma_0^2 \sigma_2^2 - \sigma_1^4)} \left[\frac{4s^2}{\sigma_2^2} - \frac{4s}{\sigma_2} \left(\frac{\sigma_1^2}{\sigma_2 \sigma_0} \right) \frac{\mathcal{R}}{\sigma_0} + \frac{\mathcal{R}^2}{\sigma_0^2} \right] \right\}}_{\equiv \int_{s_{\min}}^{\infty} ds \bar{n}_{\max}(\mathcal{R}, s)}, \end{aligned}$$

where

$$\bar{n}_{\max}(\mathcal{R}, s) \equiv \frac{\sigma_2^2}{4\pi^2 \sigma_1^2 \sqrt{\sigma_2^2 \sigma_0^2 - \sigma_1^4}} \left(\frac{4s^2}{\sigma_2^2} + e^{-\frac{4s^2}{\sigma_2^2}} - 1 \right) \exp \left\{ -\frac{\sigma_0^2 \sigma_2^2}{2(\sigma_0^2 \sigma_2^2 - \sigma_1^4)} \left[\frac{4s^2}{\sigma_2^2} - \frac{4s}{\sigma_2} \left(\frac{\sigma_1^2}{\sigma_2 \sigma_0} \right) \frac{\mathcal{R}}{\sigma_0} + \frac{\mathcal{R}^2}{\sigma_0^2} \right] \right\}, \quad (\text{C.0.22})$$

can be interpreted as the number density of maxima with field value in the range \mathcal{R} to $\mathcal{R} + d\mathcal{R}$ and curvature $-\nabla^2\mathcal{R}$ in the range $2s$ to $2(s + ds)$. We note that the argument of the exponential function in $\bar{n}_{\max}(\mathcal{R}, s)$ is invariant under the exchange $\mathcal{R}/\sigma_0 \leftrightarrow 2s/\sigma_2$.

From the structure of the argument of the exponential function in $\bar{n}_{\max}(\mathcal{R}, s)$, it is natural to introduce the dimensionless parameter $\gamma \equiv \sigma_1^2/\sigma_2 \sigma_0$ which is completely determined, as we shall explain in a moment, by the properties of the power spectrum. Furthermore, it is easy to see that we have $0 < \gamma < 1$. In turn, this condition implies $\sigma_2^2 \sigma_0^2 - \sigma_1^4 > 0$ so that the square root in eq. (C.0.22) is always real valued. Let us verify the non-trivial condition $\sigma_2^2 \sigma_0^2 - \sigma_1^4 > 0$; from the definition in eq. (C.0.9), we have

$$\begin{aligned} \sigma_0^2 \sigma_2^2 - \sigma_1^4 &= \left[\int \frac{dk}{k} \mathcal{P}_{\mathcal{R}}(k) \right] \left[\int \frac{dk'}{k'} \mathcal{P}_{\mathcal{R}}(k') k'^4 \right] - \left[\int \frac{dk}{k} \mathcal{P}_{\mathcal{R}}(k) k^2 \right]^2 = \quad (\text{C.0.23}) \\ &= \int \frac{dk}{k} \frac{dk'}{k'} \mathcal{P}_{\mathcal{R}}(k) \mathcal{P}_{\mathcal{R}}(k') (k'^4 - k'^2 k^2). \end{aligned}$$

To conclude that $\sigma_0^2 \sigma_2^2 - \sigma_1^4 > 0$, we only need to show that $(k'^4 - k'^2 k^2) > 0$ since the power spectrum is positive definite and the integrals over k cover the positive real axis. In the first double-integral,

we can change $k \leftrightarrow k'$ without altering the result, and this means that we can also substitute $k'^4 \rightarrow (k^4 + k'^4)/2$; if we do this transformation, the factor $(k'^4 - k'^2 k^2)$ becomes $(k'^2 - k^2)^2/2$ which is always positive. This concludes the proof.

From eq. (C.0.22) we see that the value of γ controls the amount of correlation between \mathcal{R} and s . If we take $\gamma = 0$, the two variables are completely uncorrelated (because $\sigma_1^2 = 0$). On the contrary, $\gamma = 1$ corresponds to the case in which they are maximally correlated.

To proceed further, we assume the following analytical expression for the power spectrum

$$\mathcal{P}_{\mathcal{R}}(k) = \frac{A_g}{\sqrt{2\pi\nu}} \exp\left[-\frac{\log^2(k/k_*)}{2\nu^2}\right]. \quad (\text{C.0.24})$$

As far as the spectral moments in eq. (C.0.9) are concerned, we find the analytical result

$$\sigma_j^2 = A_g k_*^{2j} e^{2j^2\nu^2}, \quad (\text{C.0.25})$$

which implies $\sigma_0^2 = A_g$ and $\gamma = e^{-2\nu^2}$, where we see that $0 < \gamma < 1$ as expected. The three parameters $\{A_g, \nu, k_*\}$ fully specify our problem. The physical picture is the following.

- The scale k_* represents the comoving wavenumber at which the power spectrum peaks. This quantity is related to the mass of the black holes produced after the collapse of the regions where the overdensity field is above threshold. We take $k_* = \mathcal{O}(10^{14}) \text{ Mpc}^{-1}$ corresponding to $M_{\text{PBH}} = \mathcal{O}(10^{18}) \text{ g}$.
- The parameter ν controls the broadness of the power spectrum and, in turn, the broadness of the mass distribution of the black holes. The case $\nu = 0.1$, for instance, corresponds to a very narrow power spectrum. This, in turn, will generate a very narrow mass distribution of black holes.
- The amplitude of the power spectrum A_g is related to the abundance of dark matter in the present-day Universe in the form of black holes, and typical values are of order $A_g/\sqrt{2\pi\nu} = \mathcal{O}(10^{-2})$. To fix ideas, to get $\mathcal{P}_{\mathcal{R}}(k_*) = 10^{-2}$ one needs $A_g = 2.5 \times 10^{-3}$ for $\nu = 0.1$.

Let us now pause for a moment to clarify the rationale of the computation that we are doing. We are interested in regions of space where the field \mathcal{R} has large curvature $-\nabla^2\mathcal{R}$ since in this case the overdensity field (which is proportional to $-\nabla^2\mathcal{R}$) takes large values. In eq. (C.0.22) we can select regions with large curvature by implementing (as done in eq. (C.0.21)) a lower limit of integration over s . However, eq. (C.0.22) always associates, by construction, regions with large curvature (consequently, peaks of the overdensity field) with local maxima of \mathcal{R} . This association can be analytically justified as follows. Consider the Taylor expansion in eq. (C.0.1) which we rewrite in two spatial dimensions taking a local maximum as stationary point of \mathcal{R}

$$\mathcal{R}(\vec{x}) = \mathcal{R}_M + \frac{1}{2} \sum_{i,j=1}^2 \mathcal{R}_{ij}(\vec{x}_M) (\vec{x} - \vec{x}_M)_i (\vec{x} - \vec{x}_M)_j. \quad (\text{C.0.26})$$

This quadratic equation can be written in a canonical form (that is without cross terms) if we do a coordinate transformation $\bar{x} \rightarrow \bar{x}' \equiv (x', y')$ such that the new axes are aligned along the eigenvectors of the matrix $\mathcal{R}_{ij}(\bar{x}_M)$. We are free to do this rotation because of isotropy. In such case, eq. (C.0.26) takes the form

$$\mathcal{R}(\bar{x}') = \mathcal{R}_M - \frac{1}{2}(\lambda_1 x'^2 + \lambda_2 y'^2), \quad (\text{C.0.27})$$

where $\lambda_{i=1,2} > 0$ are the (minus) eigenvalues of $\mathcal{R}_{ij}(\bar{x}_M)$. Notice that in eq. (C.0.27) we used homogeneity to shift the position of the maximum \bar{x}_M to the origin of the new coordinate system. From eq. (C.0.27) we see that an iso-density surface with constant $\mathcal{R}_{\bar{x}'} \equiv \mathcal{R}(\bar{x}')$ is an ellipse with canonical equation

$$\frac{\lambda_1}{2(\mathcal{R}_M - \mathcal{R}_{\bar{x}'})} x'^2 + \frac{\lambda_2}{2(\mathcal{R}_M - \mathcal{R}_{\bar{x}'})} y'^2 = 1, \quad \alpha_i \equiv \left[\frac{2(\mathcal{R}_M - \mathcal{R}_{\bar{x}'})}{\lambda_i} \right]^{1/2}, \quad (\text{C.0.28})$$

and semi-axes $\alpha_{i=1,2}$. The key point is that the actual magnitude of the eigenvalues λ_i depends on the steepness of the field \mathcal{R} around the position of its maximum. This follows from eq. (C.0.27) if we apply the Laplacian with respect to the coordinates \bar{x}' since we find

$$\lambda_1 + \lambda_2 = -\nabla^2 \mathcal{R}(\bar{x}'). \quad (\text{C.0.29})$$

Suppose now that the point \bar{x}' coincides with a peak of the overdensity field, \bar{y}_{pk} . Using eq. (5.2.6), we find

$$\lambda_1 + \lambda_2 = -\nabla^2 \mathcal{R}(\bar{y}_{pk}) \gtrsim \frac{9}{4} (\text{aH})^2 \delta_c = 2\sigma_2 \underbrace{\frac{9}{8} \frac{(\text{aH})^2}{\sigma_2}}_{\gg 1} \delta_c \implies \frac{\lambda_i}{\sigma_2} \gg 1. \quad (\text{C.0.30})$$

In eq. (C.0.30) we used the fact that we typically expect $(\text{aH})^2/\sigma_2 \gg 1$; we will comment in more detail about this estimate at the end of this section. Notice that in eq. (C.0.30) we assumed that the two eigenvalues λ_i have the same magnitude. This is because we have separately $\lambda_1 = -\mathcal{R}_{xx}(\bar{y}_{pk})$ and $\lambda_2 = -\mathcal{R}_{yy}(\bar{y}_{pk})$, and the second derivatives \mathcal{R}_{xx} and \mathcal{R}_{yy} have the same covariance (see eq. (C.0.8)). We can now do the same expansion in eq. (C.0.26) but with respect to the first derivatives of \mathcal{R} at \bar{x}_M . The stationary condition $\mathcal{R}_i(\bar{x}_M) = 0$ reads

$$\mathcal{R}_i(\bar{x}) - \sum_{j=1}^2 \mathcal{R}_{ij}(\bar{x}_M)(\bar{x} - \bar{x}_M)_j = 0 \implies \begin{cases} \mathcal{R}_x(\bar{x}') + \lambda_1 x' = 0 \\ \mathcal{R}_y(\bar{x}') + \lambda_2 y' = 0 \end{cases} \quad (\text{C.0.31})$$

where in the last line we introduced, as done before, the eigenvalues $\lambda_{i=1,2}$. We identify again the point \bar{x}' with a peak of the overdensity field so that we can use the estimate in eq. (C.0.30). Furthermore, \bar{x}' represents now, by construction, the distance between the local maximum of \mathcal{R} and the peak of the overdensity field. We can estimate this distance by means of eq. (C.0.30) and eq. (C.0.31). In eq. (C.0.31), $\mathcal{R}_x(\bar{x}')$ and $\mathcal{R}_y(\bar{x}')$ are not equal to zero (since we moved away from the

local maximum of \mathcal{R}) and their magnitude can be estimated (in a probabilistic sense) by means of the covariance matrix. We have $\mathcal{R}_x(\bar{x}') \approx \mathcal{R}_y(\bar{x}') \approx \langle \mathcal{R}_x \mathcal{R}_x \rangle^{1/2} \approx \sigma_1$. We find

$$|\bar{x}'| \approx \frac{\sigma_1}{\sigma_2} \left(\frac{1}{\lambda_i/\sigma_2} \right) \ll \frac{\sigma_1}{\sigma_2} = \frac{e^{-3\nu^2}}{k_*}. \quad (\text{C.o.32})$$

As we will see in a moment, we have that $1/k_*$ is typically of the order of the comoving horizon length $1/aH$ at the time when the perturbations re-enter the horizon and become causally connected. Therefore, we find $|\bar{x}'| \ll 1/aH$. This means that high peaks of the overdensity field lie “close” (that is within an Hubble radius) to local maxima of the curvature perturbation. We can validate the

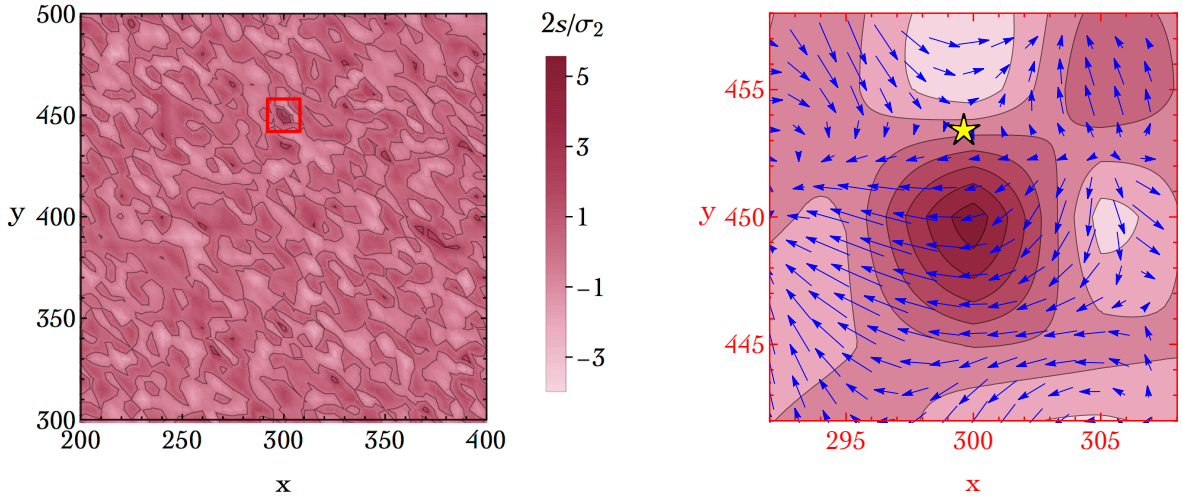


Figure 9: Numerical simulation of the random field \mathcal{R} together with its first and second derivatives. At each point in space (discretized in steps $\Delta x = 5$ and $\Delta y = 5$) we associate a vector of values $\{\mathcal{R}, \mathcal{R}_x, \mathcal{R}_y, \mathcal{R}_{xx}, \mathcal{R}_{xy}, \mathcal{R}_{yy}\}$ randomly generated from eq. (C.o.6). We use the power spectrum in eq. (C.o.24) to compute the correlation matrix. We set $\nu = 0.7$, $k_* = 1.5 \times 10^{14} \text{ Mpc}^{-1}$ and $A_g = 2.5 \times 10^{-3}$. Left panel. We show the density plot of the random variable $2s/\sigma_2 = -\nabla^2 \mathcal{R}/\sigma_2$ which is related to the overdensity field. Right panel. Same as in the left panel but zoomed in the region where the random variable $-\nabla^2 \mathcal{R}/\sigma_2$ has a pronounced peak. We superimpose (blue arrows) a vector plot that keeps track of the gradient field $\{\mathcal{R}_x, \mathcal{R}_y\}$. The yellow star marks the position of the local maximum of \mathcal{R} that lies close to the peak of $-\nabla^2 \mathcal{R}/\sigma_2$.

analytical approximation by means of a numerical check. To this end, we use the full joint probability density distribution in eq. (C.o.6) to generate a sample of random values that we distribute on a two-dimensional grid (see caption of fig. 9). In other words, at each point on the spatial grid corresponds a value of $\mathbf{R} = (\mathcal{R}, \mathcal{R}_x, \mathcal{R}_y, \mathcal{R}_{xx}, \mathcal{R}_{xy}, \mathcal{R}_{yy})^T$ randomly generated from eq. (C.o.6). In the left panel of fig. 9 we show the spatial distribution of the random variable $2s/\sigma_2 = -\nabla^2 \mathcal{R}/\sigma_2$. We focus on a region in which $-\nabla^2 \mathcal{R}$ takes a large value (in units of σ_2). In the left panel of fig. 9, we indicate this region with a red contour. We zoom in this part of the plot in the right panel of fig. 9. The analytical

argument explained before suggests that we should find a maximum close to the point where the curvature field peaks. We look for this maximum numerically by looking at the behavior of the gradient field $\{\mathcal{R}_x, \mathcal{R}_y\}$ that we plot using blue arrows. We indeed find a local maximum that we mark with a yellow star. We checked numerically that at the position of the yellow star where the gradient field vanishes the conditions on the second derivatives that define a maximum are verified. We note that at the position of the peak of the overdensity field the gradient field $\{\mathcal{R}_x, \mathcal{R}_y\}$ does not vanish but we find that its magnitude is of order $\mathcal{O}(1)$ (in units of σ_1) as we argued in eq. (C.0.32). Furthermore, we checked that the local maximum lies closer to the peak of $-\nabla^2\mathcal{R}/\sigma_2$ for increasing higher values of the latter.

This numerical result corroborates the validity of the analytical argument in eq. (C.0.32), and we conclude, therefore, that eq. (C.0.22) is the right distribution to consider: we count the peaks of δ by looking at the maxima of \mathcal{R} with large curvature.

Next, we ask if there exists some relation between the curvature of a local maximum of \mathcal{R} and the value of \mathcal{R} at the maximum. We can use the probability density distribution $\bar{n}_{\max}(\mathcal{R}, s)$ defined in eq. (C.0.22) to generate numerically, in position space, a sample of maxima by extracting randomly the value of \mathcal{R} and curvature $2s = -\nabla^2\mathcal{R}$. We can then use eq. (5.2.5) to extract from the distribution of s the distribution of the overdensity field (of course, with \mathcal{R} instead of h since we are considering here the gaussian case). The outcome of this exercise is shown in fig. 10, fig. 11 and fig. 12 (see captions for details).

Let us consider the case in which we take $\nu = 0.1$. We remind that this choice corresponds to a very narrow power spectrum. We have $\gamma \simeq 0.98$. As noticed before, in this case we expect a strong correlation between \mathcal{R} and s . This means that regions with large \mathcal{R}/σ_0 are likely to be also regions with large $2s/\sigma_2$ (and, consequently, regions where the overdensity field peaks). This is evident in fig. 10, fig. 11 and fig. 12 (left panel). In particular, in fig. 11 we see that maxima with large values of \mathcal{R} (left panel) maps precisely regions where the overdensity field δ peaks (right panel). As stated before, this is a consequence of the fact that \mathcal{R} and s (hence δ) are highly correlated. Furthermore, in the left panel of fig. 12 the symmetry of the randomly generated points under the exchange $\mathcal{R}/\sigma_0 \leftrightarrow 2s/\sigma_2$ is evident.

It is instructive to consider what happens if we take a different value of ν . Consider, for instance, the case with $\nu = 0.7$. We have $\gamma \simeq 0.37$, and \mathcal{R} and s are now much less correlated compared to the case with $\nu = 0.1$. This is shown in the right panel of fig. 12 (see caption for details). For $\nu = 0.7$, spiky maxima (that is maxima with large curvature) are seldom characterized also by a large value of \mathcal{R} . This means that if we aim at deriving a generic formula for the number density of spiky maxima we can not restrict eq. (C.0.21) to special values of \mathcal{R} .

Let us summarize our findings so far. We have that the number density of local maxima of \mathcal{R} with large curvature gives the number density of regions where the overdensity field peaks. Physically, we are only interested in local maxima with large curvature irrespectively on their value of \mathcal{R} . Since there is no special relation—for generic values of ν (hence γ)—between s and \mathcal{R} , eq. (C.0.21) must be integrated over the entire range of variability of \mathcal{R} .

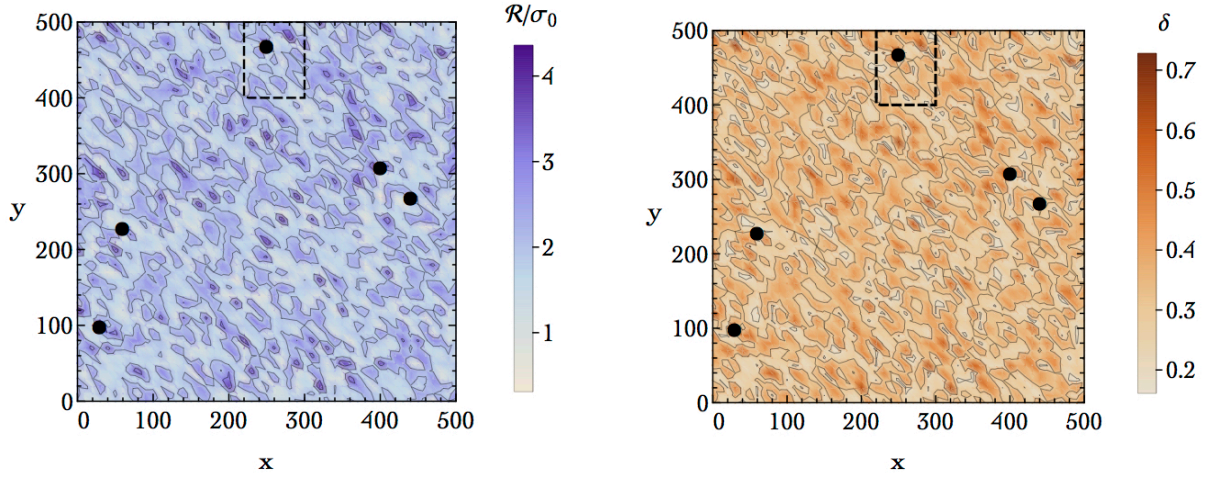


Figure 10: Numerical simulation of maxima of \mathcal{R} in two spatial dimensions. At each point (x, y) in space (discretized in steps $\Delta x = 10$ and $\Delta y = 10$), we extract randomly from the density distribution $\bar{n}_{\max}(\mathcal{R}, s)$ (defined in eq. (C.0.22)) the value of \mathcal{R} and $s = -\nabla^2 \mathcal{R}/2$. The former are shown in the left panel. We remark that, by construction, all point generated by means of $\bar{n}_{\max}(\mathcal{R}, s)$ are maxima of \mathcal{R} . As far as the values of s are concerned, we plot on the right panel the corresponding values of $\delta = (8/9)(1/aH)^2 s$. We use the power spectrum in eq. (C.0.24), and we set $\nu = 0.1$, $k_* = 1.5 \times 10^{14} \text{ Mpc}^{-1}$ and $A_g = 2.5 \times 10^{-3}$. Furthermore, we take $(k_*/aH)^2 \simeq 0.36$ as suggested by numerical simulations (see appendix F of [2]). For illustrative purposes, we set the threshold $\delta_c = 0.675$ (which is significantly smaller compared to the value expected from numerical simulation of gravitational collapse into black holes that is $\delta_c \simeq 1.19$, see appendix F of [2]; we use a smaller value of δ_c otherwise events over the threshold would be too rare to be simulated in our simplified numerical analysis). Points in the simulation with $\delta > \delta_c$ are marked with a black dot.

If we consider the case in which s_{\min} does not depend on \mathcal{R} , we can integrate eq. (C.0.21) analytically. We find the number density

$$\mathcal{N}_{\max}(s_{\min}) \equiv \int_{-\infty}^{\infty} d\mathcal{R} \int_{s_{\min}}^{\infty} ds \bar{n}_{\max}(\mathcal{R}, s) = \frac{\sigma_2^2}{2\sqrt{2}\pi^{3/2}\sigma_1^2} \left[\frac{s_{\min}}{\sigma_2} \exp\left(-\frac{2s_{\min}^2}{\sigma_2^2}\right) + \frac{1}{2}\sqrt{\frac{\pi}{6}} \text{Erfc}\left(\frac{\sqrt{6}s_{\min}}{\sigma_2}\right) \right]. \quad (\text{C.0.33})$$

We can define the dimensionful quantity $R_* \equiv \sqrt{d}\sigma_1/\sigma_2$, where d is the number of spatial dimensions. From eq. (C.0.25) we find

$$R_* = \frac{\sqrt{2}\sigma_1}{\sigma_2} = \frac{\sqrt{2}}{k_*} e^{-3\nu^2}. \quad (\text{C.0.34})$$

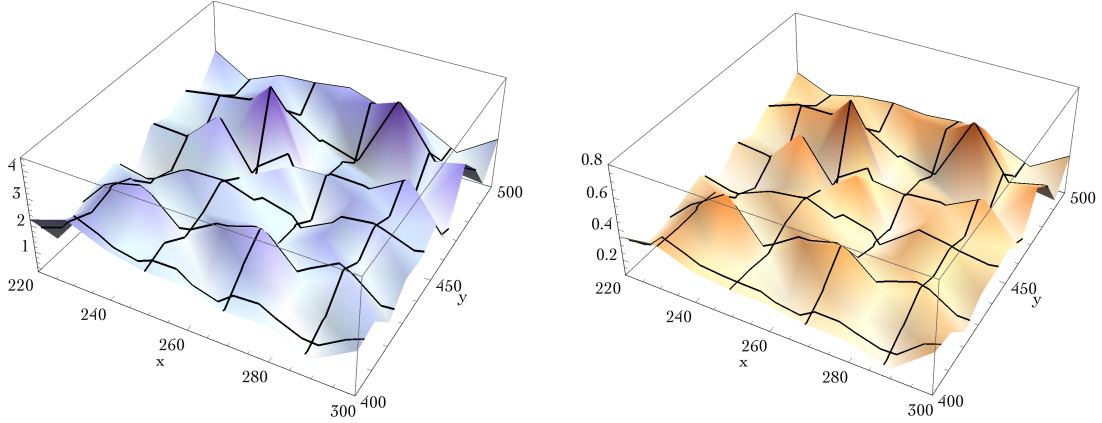


Figure 11: Same as in fig. 10 but zoomed in the region delimited by dashed lines and displayed in the form of a three-dimensional density plot. We see that spiky maxima with large values of \mathcal{R} (left panel) coincide with peaks of δ (right panel).

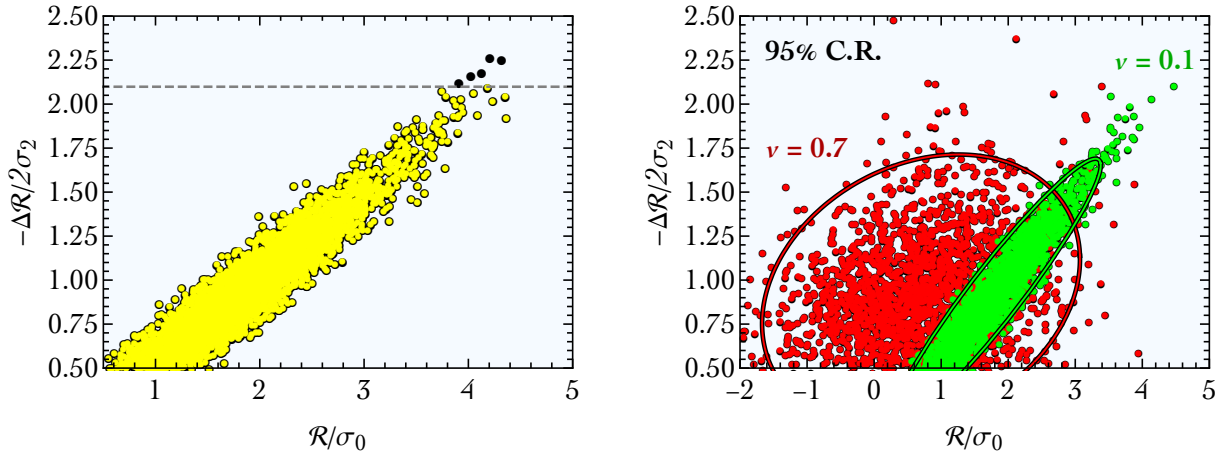


Figure 12: Left panel. Simulated points in figures. 10, 11 shown in the plane $\{\mathcal{R}/\sigma_0, -\nabla^2 \mathcal{R}/2\sigma_2\}$. The horizontal dashed line corresponds to the threshold value δ_c (see caption of fig. 10). Points above threshold collapse into black holes (marked with black dots here and in figures. 10, 11). This simulation corresponds to $\nu = 0.1$, and we see that \mathcal{R}/σ_0 and $-\nabla^2 \mathcal{R}/2\sigma_2$ are strongly correlated. Right panel. Comparison between two numerical simulations with $\nu = 0.1$ (green) and $\nu = 0.7$ (red). The two ellipses represent the 95% confidence regions.

In this simplified two-dimensional set-up, we can estimate the mass fraction of black holes by means of the dimensionless quantity (for more details, see section D.2)

$$\mathcal{R}_*^2 \mathcal{N}_{\max}(s_{\min}) = \frac{1}{\sqrt{2}\pi^{3/2}} \left[\frac{s_{\min}}{\sigma_2} \exp\left(-\frac{2s_{\min}^2}{\sigma_2^2}\right) + \frac{1}{2} \sqrt{\frac{\pi}{6}} \operatorname{Erfc}\left(\frac{\sqrt{6}s_{\min}}{\sigma_2}\right) \right] \approx \frac{1}{\sqrt{2}\pi^{3/2}} \left(\frac{s_{\min}}{\sigma_2}\right) \exp\left(-\frac{2s_{\min}^2}{\sigma_2^2}\right), \quad (\text{C.o.35})$$

where the last approximation is valid if $s_{\min}/\sigma_2 \gtrsim 1$. The mass fraction is controlled by an exponential decaying function with argument

$$\frac{s_{\min}}{\sigma_2} = \frac{9}{8} \frac{(aH)^2}{\sigma_2} \delta_c = \frac{9e^{-4v^2}}{8A_g^{1/2}} \left(\frac{aH}{k_*} \right)^2 \delta_c. \quad (\text{C.0.36})$$

The value of s_{\min}/σ_2 , which is crucial for the determination of the correct order-of-magnitude of the mass fraction, depends on the properties of the power spectrum via the factor $e^{-4v^2}/A_g^{1/2}k_*^2$ and the details of the gravitational collapse that leads to black hole formation via the factor $(aH)^2\delta_c$. The comoving horizon length $1/aH$ depends on time. The computation of the threshold for black hole production introduces the time t_m that is defined by the time when the curvature perturbations cross the horizon and become causally connected. This is the time at which eq. (C.0.36) has to be computed.³ The time t_m defines implicitly, by means of the condition $a(t_m)H(t_m)r_m = 1$, the length scale r_m . This length scale enters in the numerical evaluation of eq. (C.0.36), and one typically gets $(a_m H_m/k_*)^2 \delta_c = \mathcal{O}(1)$. A precise numerical evaluation of this factor is beyond the scope of this thesis but it is discussed in appendix F of [2].

It is important to check the validity of eq. (C.0.35) against the standard result. In ref. [48], the number density of peaks of the overdensity field is controlled by the exponential function $\exp(-\delta_c^2/2\sigma_\delta^2)$ where σ_δ^2 refers to the variance of the overdensity field. By means of eq. (5.2.5) (linearized, and with \mathcal{R} instead of h), one finds $\sigma_\delta^2 = (16/81)(1/aH)^4 \sigma_2^2$. Consequently, $\exp(-\delta_c^2/2\sigma_\delta^2)$ matches precisely the exponential function in eq. (C.0.35). This is another indication that computing the number density of peaks of the overdensity field via the number density of maxima of \mathcal{R} that are spiky enough leads to sensible results; importantly, this is in spite of the fact that we derived eq. (C.0.35) in two spatial dimensions.

After this long and detailed discussion about the gaussian case, we are ready to move to the more interesting situation in which local non-gaussianities are present. Actually, we are already in the position to make an interesting comment. Suppose that we compute the analogue of eq. (C.0.22) with local non-gaussianities with of course now h and $-\nabla^2 h$ instead of \mathcal{R} and $-\nabla^2 \mathcal{R}$. It is crucial to answer the same question that we asked in the gaussian case: is the number density of maxima of h with large curvature $-\nabla^2 h$ a good proxy for the number density of peaks of the overdensity field? The same analytical argument discussed in eqs. (C.0.26-C.0.32) can be repeated with h and $-\nabla^2 h$ instead of \mathcal{R} and $-\nabla^2 \mathcal{R}$. The estimate of the eigenvalues $\lambda_{i=1,2}$ in eq. (C.0.30) remains the same. In eq. (C.0.32), the only difference is that local non-gaussianities alter the entries of the covariance matrix that we used to estimate the magnitude of the gradient field. However, we anticipate that

³ More precisely, the process of black hole formation involves three different times. First of all, the number density of peaks that eventually form black holes has to be calculated at some initial time when perturbations are still super-horizon. All the analysis done so far is based on this time (even though we do not specify it explicitly) since we are considering comoving curvature perturbations which are constant (see appendix B). Second, we have the time t_m when the perturbations re-enter the horizon and become causally connected. Finally, we have the time t_f at which black holes form. In general $t_f \neq t_m$, and from simulations of gravitational collapse in numerical relativity we have $(t_f/t_m)^{1/2} \simeq 3$ [52]; eq. (5.2.6) is usually evaluated at time t_m while the factor $(t_f/t_m)^{1/2} \simeq 3$ can be included in the computation of the black hole abundance (see, e.g., discussion in ref. [76]).

we find (see eq. (E.0.76)) $\langle h_x h_x \rangle = \langle h_y h_y \rangle = \sigma_1^2(1 + 4\alpha^2 \sigma_0^2)/2$ and $\langle h_x h_y \rangle = 0$; we conclude that the non-gaussian correction in this case is negligible since we have $\alpha^2 \sigma_0^2 = \alpha^2 A_g \ll 1$. Remember indeed that the size of σ_0^2 is controlled by the amplitude of the power spectrum which is $\sigma_0^2 = A_g \ll 1$. This is particularly clear for the simple choice of $\mathcal{P}_{\mathcal{R}}$ in eq. (C.0.24) but remains true in general.

We conclude that the same argument discussed in eqs. (C.0.26-C.0.32) is valid also in the presence of local non-gaussianities. In appendix D and appendix E we will, therefore, move to compute the number density of maxima of h with curvature above the threshold for black hole production that is needed to generalize eq. (C.0.35) to the case $\alpha \neq 0$. We consider two different approaches.

- * In appendix D we come back to the formulation of the problem in three spatial dimensions. We will derive an expression analogue to eq. (C.0.35) but valid in the case $\alpha \neq 0$ and three spatial dimensions. We dub the result of appendix D “exact” because no approximations will be used throughout the computation (apart from the linearization in eq. (5.2.5)).
- * In appendix E we follow a different route. We will consider an expansion in cumulants around the gaussian probability density distribution. To make this approach more transparent from the analytic point of view, we will work again in two spatial dimensions.

D.1 NUMBER DENSITY OF PEAKS

In appendix C we have shown that the number density of peaks of the overdensity field can be approximated with good accuracy with the number density of maxima of the comoving density perturbation which are spiky enough, i.e. with a Laplacian smaller than a threshold. The analysis has been performed assuming two spatial dimensions, to have a better control of the analytic expressions, and for ease of visualization of our simulations. Nevertheless, the same conclusion is also valid in three dimensions, which is the case of physical interest that we are going to consider in this section. We shall now use these results to compute the number density of peaks of the overdensity field in presence of local non-gaussianities. Our starting point is the analogous of eq. (D.2.6) for the non-gaussian random field $h(\vec{x})$. Furthermore, as explained above, we are interested into maxima of h which are spiky enough. Explicitly, we have

$$n_{\text{pk}}(h) dh d^3x = dh d^3x \int_{\text{spiky max}} d^3h_i d^6h_{ij} P_{\text{NG}}(h, h_i, h_{ij}) \delta^{(3)}(h_i) |\det(h_{ij})|, \quad (\text{D.1.1})$$

where $P_{\text{NG}}(h, h_i, h_{ij})$ is the joint probability distribution function of the non-gaussian field h , the field gradient h_i and the second derivatives h_{ij} . The Dirac delta $\delta^{(3)}(h_i)$ enforces the condition that the point is stationary. We will show in a moment how to restrict the integration volume to the field configurations which represent spiky maxima of h . The comoving number density of peaks is obtained integrating over all the heights of the peaks

$$\mathcal{N}_{\text{pk}} = \int_{h_{\text{min}}}^{\infty} dh n_{\text{pk}}(h) = \int_{\text{spiky max}} dh d^3h_i d^6h_{ij} P_{\text{NG}}(h, h_i, h_{ij}) \delta^{(3)}(h_i) |\det(h_{ij})|. \quad (\text{D.1.2})$$

Notice that for $\alpha > 0$, which is the case relevant for the PBH production (see appendix B), and from the relation $h(\vec{x}) = \mathcal{R}(\vec{x}) + \alpha(\mathcal{R}(\vec{x})^2 - \sigma_0^2)$, one realizes that $h(\vec{x})$ attains a minimum $h_{\text{min}} = -(1 + 4\alpha^2\sigma_0^2)/4\alpha$ for $\mathcal{R} = -1/2\alpha$. To proceed, it turns out to be useful to consider the gaussian variables \mathcal{R} , \mathcal{R}_i and \mathcal{R}_{ij} instead of the non-gaussian fields h , h_i and h_{ij} . The reason is that the joint probability distribution function of the former variables, that we denote with $P(\mathcal{R}, \mathcal{R}_i, \mathcal{R}_{ij})$, is known and it has a simple analytic expression, see appendix C for the explicit formula in the case of two dimensions. Using the conservation of the probability in a differential volume $P_{\text{NG}}(h, h_i, h_{ij}) dh d^3h_i d^6h_{ij} = P(\mathcal{R}, \mathcal{R}_i, \mathcal{R}_{ij}) d\mathcal{R} d^3\mathcal{R}_i d^6\mathcal{R}_{ij}$, we can perform a change of variable and write

$$\mathcal{N}_{\text{pk}} = \int_{\text{spiky max}} d\mathcal{R} d^3\mathcal{R}_i d^6\mathcal{R}_{ij} P(\mathcal{R}, \mathcal{R}_i, \mathcal{R}_{ij}) \delta^{(3)}[h_i(\mathcal{R}, \mathcal{R}_i, \alpha)] |\det[h_{ij}(\mathcal{R}, \mathcal{R}_i, \mathcal{R}_{ij}, \alpha)]|. \quad (\text{D.1.3})$$

where the field gradient and the second derivatives of the non gaussian variables are written in terms of the gaussian fields as

$$h_i(\mathcal{R}, \mathcal{R}_i, \alpha) = \mathcal{R}_i(1 + 2\alpha\mathcal{R}), \quad h_{ij}(\mathcal{R}, \mathcal{R}_i, \mathcal{R}_{ij}, \alpha) = \mathcal{R}_{ij}(1 + 2\alpha\mathcal{R}) + 2\alpha\mathcal{R}_i\mathcal{R}_j. \quad (\text{D.1.4})$$

As noticed in sec. 5.2, stationary points of \mathcal{R} are also stationary points of h . Moreover, from the expressions above, one can see that also the configuration $(1 + 2\alpha\mathcal{R}) = 0$ is a stationary point of h . However, as mentioned above, it is a minimum of h (for $\alpha > 0$), therefore we need to focus only on the configurations with $\mathcal{R}_i = 0$. This means that one can write eq. (D.1.3) as

$$\begin{aligned} \mathcal{N}_{\text{pk}} &= \int_{\text{spiky max}} d\mathcal{R} d^6\mathcal{R}_{ij} \mathcal{P}(\mathcal{R}, \mathcal{R}_i = 0, \mathcal{R}_{ij}) \left| \det(h_{ij}(\mathcal{R}, \mathcal{R}_i = 0, \mathcal{R}_{ij}, \alpha)) \right| \frac{1}{|1 + 2\alpha\mathcal{R}|^3} \\ &= \int_{\text{spiky max}} d\mathcal{R} d^6\mathcal{R}_{ij} \mathcal{P}(\mathcal{R}, \mathcal{R}_i = 0, \mathcal{R}_{ij}) \left| \det(\mathcal{R}_{ij}) \right|. \end{aligned} \quad (\text{D.1.5})$$

In the equation above all the information about the non-gaussianities is confined in spiky max , i.e. in the condition to impose on the integration volume in order to restrict on maxima of h spiky enough. Let us see how these constraints can be implemented explicitly. The Hessian matrix, for $\mathcal{R}_i = 0$, is

$$h_{ij} = \mathcal{R}_{ij} (1 + 2\alpha\mathcal{R}). \quad (\text{D.1.6})$$

We should, therefore, select maxima (minima) of \mathcal{R} for positive (negative) values of $(1 + 2\alpha\mathcal{R})$. The calculation can be simplified aligning the coordinate axes along the eigenvectors of the matrix $-\mathcal{R}_{ij}$. The corresponding eigenvalues are denoted as λ_i with $i = 1, 2, 3$ (the same strategy has been adopted in appendix C in the case of two spatial dimensions). The three eigenvectors, and the three Euler angles defining their orientation, can be used to parametrize the six independent random fields of \mathcal{R}_{ij} . Let us also define the following variables

$$\bar{v} = \mathcal{R}/\sigma_0, \quad \begin{cases} \sigma_2 x &= -\nabla^2 \mathcal{R} = \lambda_1 + \lambda_2 + \lambda_3 \\ \sigma_2 y &= (\lambda_1 - \lambda_3)/2 \\ \sigma_2 z &= (\lambda_1 - 2\lambda_2 + \lambda_3)/2 \end{cases} \quad (\text{D.1.7})$$

Changing variables and integrating over the Euler angles, from eq. (D.1.5) one obtains [48]

$$\mathcal{N}_{\text{pk}} = \int_{\text{spiky max}} \bar{n}_{\text{pk}}(\bar{v}, x, y, z) d\bar{v} dx dy dz \quad \text{with} \quad \bar{n}_{\text{pk}}(\bar{v}, x, y, z) = A e^{-Q} |F(x, y, z)|, \quad (\text{D.1.8})$$

and

$$A \equiv \sqrt{\frac{5}{3}} \frac{\sigma_2^3}{\sigma_1^3} \frac{25}{16\pi^2 \sqrt{1-\gamma^2}}, \quad (\text{D.1.9})$$

$$Q \equiv \frac{\bar{v}^2}{2} + \frac{(x - x_*)^2}{2(1-\gamma^2)} + \frac{5}{2} (3y^2 + z^2), \quad (\text{D.1.10})$$

$$F(x, y, z) \equiv y (y^2 - z^2) \left[(x+z)^2 - 9y^2 \right] (x-2z), \quad (\text{D.1.11})$$

$$x_* \equiv \gamma \bar{v}. \quad (\text{D.1.12})$$

We can divide the integration on \bar{v} in two parts.

- $1 + 2\alpha\mathcal{R} > 0$.

This implies that maxima of \mathcal{R} are also maxima of h , and that we are considering $\bar{v} > -1/2\sigma_0\alpha$.

One can choose an ordering for the eigenvalues of the matrix $-\mathcal{R}_{ij}$: $\lambda_1 \geq \lambda_2 \geq \lambda_3$. Therefore, we can select maxima of \mathcal{R} requiring that $\lambda_3 > 0$. Under these conditions, and using eqs. (D.1.7), the domain of integration for the variables y and z reads:

$$\int_0^{x/4} dy \int_{-y}^y dz + \int_{x/4}^{x/2} dy \int_{3y-x}^y dz. \quad (\text{D.1.13})$$

Then, working within the linear approximation in eq. (5.2.5), eq. (5.2.6) implies that only spiky maxima should be selected

$$x > \frac{9(a_m H_m)^2}{4\sigma_2} \frac{\delta_c}{1 + 2\alpha\sigma_0 \bar{v}} \equiv x_\delta(\bar{v}). \quad (\text{D.1.14})$$

In the equation above, the horizon scale $1/aH$ has been evaluated at the time t_m when the curvature perturbations cross the horizon. Having specified the appropriate domain of integration for all the variables, we can now integrate eq. (D.1.8) and multiply by a factor 6 to take into account all the possible orderings of the eigenvalues λ_i . We find

$$\mathcal{N}_{\text{pk}}^{(I)} = \int_{-\frac{1}{2\alpha\sigma_0}}^{\infty} d\bar{v} \int_{x_\delta(\bar{v})}^{\infty} dx \bar{n}_{\text{pk}}(\bar{v}, x), \quad (\text{D.1.15})$$

where

$$\bar{n}_{\text{pk}}(\bar{v}, x) = \frac{e^{-\bar{v}^2/2}}{(2\pi)^2 R_*^3} f(x) \frac{e^{-\frac{(x-x_*)^2}{2(1-\gamma^2)}}}{\sqrt{2\pi(1-\gamma^2)}}, \quad (\text{D.1.16})$$

$$f(x) = \frac{x^3 - 3x}{2} \left[\text{Erf} \left(\sqrt{\frac{5}{2}} x \right) + \text{Erf} \left(\sqrt{\frac{5}{2}} \frac{x}{2} \right) \right] + \sqrt{\frac{2}{5\pi}} \left[\left(\frac{31x^2}{4} + \frac{8}{5} \right) e^{-\frac{5}{8}x^2} + \left(\frac{x^2}{2} - \frac{8}{5} \right) e^{-\frac{5}{2}x^2} \right], \quad (\text{D.1.17})$$

and we remind that $R_* \equiv \sqrt{3}\sigma_1/\sigma_2$.

- $1 + 2\alpha\mathcal{R} < 0$.

In this case minima of \mathcal{R} are maxima of h . Proceeding analogously as before, we have:

$$\mathcal{N}_{\text{pk}}^{(II)} = \int_{-\infty}^{-\frac{1}{2\alpha\sigma_0}} d\bar{v} \int_{-\infty}^{x_\delta(\bar{v})} dx \bar{n}_{\text{pk}}(\bar{v}, x). \quad (\text{D.1.18})$$

The comoving number density of peaks of the overdensity field is approximated as the sum of the two terms above: $\mathcal{N}_{\text{pk}} = \mathcal{N}_{\text{pk}}^{(I)} + \mathcal{N}_{\text{pk}}^{(II)}$. One can interpret these two contributions along the lines exposed in section 5.2. The term $\mathcal{N}_{\text{pk}}^{(II)}$ counts then minima of \mathcal{R} which are maxima of h . Instead $\mathcal{N}_{\text{pk}}^{(I)}$ corresponds to maxima of \mathcal{R} , and the restriction in the integration range of \bar{v} (the lower limit) is designed to subtract those maxima of \mathcal{R} which are minima of h . Obviously, the gaussian result is recovered for $\alpha \rightarrow 0$. In this limit we can compare with the standard expression in ref. [48]. Numerically, and for the power spectra under consideration, we found that the two calculations agree within a factor $\simeq 2$. As already mentioned in section C for the case of two spatial dimensions, this confirms that peaks of the overdensity field are well approximated by peaks of the comoving density perturbation which are spiky enough. In section D.2 we will discuss how to translate \mathcal{N}_{pk} into the primordial black hole abundance in eq. (6.1.2).

D.2 FROM THE NUMBER DENSITY TO THE ABUNDANCE

The PBH abundance at the time t_f of their formation is defined by

$$\beta = \frac{1}{\rho_b(t_f)} \int_{\nu_c}^{\infty} d\nu \rho_{\text{PBH}}(\nu), \quad (\text{D.2.1})$$

and it simply corresponds to the ratio between the mass density in PBHs and the background energy density at formation time, $\rho_b(t_f) = 3H_f^2/8\pi$. In eq. (D.2.1) we use $\nu \equiv \delta/\sigma_\delta = 2s/\sigma_2$. The parameter ν controls the height of the overdensity peak that collapses into a PBH, and the integration in eq. (D.2.1) tells us that only peaks above the threshold contribute to the PBH abundance (while perturbations with $\nu < \nu_c$ disperse into the expanding Universe). The mass density of PBHs takes the form

$$\rho_{\text{PBH}}(\nu) = M_{\text{PBH}}(\nu) n_{\text{max}}^{\text{phys}}(\nu), \quad (\text{D.2.2})$$

where $M_{\text{PBH}}(\nu)$ is the PBH mass (usually calculated at horizon crossing time t_m) and $n_{\text{max}}^{\text{phys}}(\nu)$ is the number density of peaks of height ν in the physical space at formation time. The latter is related to the comoving number density of peaks $n_{\text{max}}(\nu)$ by the scaling (in three spatial dimensions) $n_{\text{max}}^{\text{phys}}(\nu) = n_{\text{max}}(\nu)/a_f^3$. We consider for the moment the realistic case of three spatial dimensions. The PBH mass $M_{\text{PBH}}(\nu)$ is proportional to the horizon mass at horizon-crossing time, $M_H(t_m)$, according to the relation [51]

$$M_{\text{PBH}}(\nu) = \mathcal{K} M_H(t_m) \left(\frac{\bar{\sigma}_0 a^2 H^2}{a_m^2 H_m^2} \right)^{\tilde{\gamma}} (\nu - \nu_c)^{\tilde{\gamma}}. \quad (\text{D.2.3})$$

In this equation the horizon mass at horizon-crossing time is given by the equation $M_H(t_m) = 1/2H_m$ while the factor $(\nu - \nu_c)^\gamma$ is the scaling law for critical collapse (extracted from numerical simulation, and with $\tilde{\gamma} \simeq 0.36$ in the case of radiation [77]) while $\mathcal{K} = \mathcal{O}(1)$. In our notation, $\nu = 2s/\sigma_2$ and $\nu_c = 2s_{\text{min}}/\sigma_2$. Notice that in eq. (D.2.3) we introduce, following ref. [51], the spectral moments referred to the density perturbation

$$\bar{\sigma}_j^2 = \frac{16}{81} \frac{1}{(aH)^4} \int \frac{dk}{k} \mathcal{P}_{\mathcal{R}}(k) k^{2j+4}. \quad (\text{D.2.4})$$

All in all, eq. (D.2.1) translates into

$$\beta = \frac{4\pi}{3} \mathcal{K} \left(\frac{\bar{\sigma}_0 a^2 H^2}{a_m^2 H_m^2} \right)^{\tilde{\gamma}} \left(\frac{1}{a_m H_m} \right)^3 \frac{a_f}{a_m} \int_{\nu_c}^{\infty} d\nu (\nu - \nu_c)^{\tilde{\gamma}} n_{\text{max}}(\nu). \quad (\text{D.2.5})$$

We need to specify the peak number density and integrate. Let us consider first the gaussian case, in which we have [48]¹

$$n_{\text{max}}(\nu) = \frac{1}{4\pi^2} \left(\frac{\gamma}{R_*} \right)^3 \nu^3 \exp(-\nu^2/2), \quad \text{with} \quad \gamma \equiv \frac{\bar{\sigma}_1^2}{\bar{\sigma}_0 \bar{\sigma}_2}, \quad R_* \equiv \frac{\sqrt{3} \bar{\sigma}_1}{\bar{\sigma}_2}. \quad (\text{D.2.6})$$

¹ Notice that R_* is now defined in terms of the spectral moments $\bar{\sigma}_j$, differently from what done in appendix C where we have an analogous expression in terms of σ_j .

We, therefore, have

$$\beta = \frac{\mathcal{K}}{3\pi} \left(\frac{\bar{\sigma}_0 a^2 H^2}{a_m^2 H_m^2} \right)^{\tilde{\gamma}} \left(\frac{a_f}{a_m} \right) \left(\frac{\gamma r_m}{R_*} \right)^3 v_c^{4+\tilde{\gamma}} \int_1^\infty dx (x-1)^{\tilde{\gamma}} x^3 e^{-x^2 v_c^2/2}. \quad (\text{D.2.7})$$

Ref. [51] computed the above integral by means of a saddle point approximation. We, instead, note that it admits the following exact expression in terms of generalized hypergeometric functions

$$\int_1^\infty dx (x-1)^{\tilde{\gamma}} x^3 e^{-x^2 v_c^2/2} = \frac{2^{\tilde{\gamma}/2}}{v_c^{\tilde{\gamma}+4}} \left\{ 2\tilde{\gamma} \left(2 + \frac{\tilde{\gamma}}{2} \right) {}_2F_2 \left[\left\{ \frac{1}{2}(1-\tilde{\gamma}), -\frac{\tilde{\gamma}}{2} \right\}, \left\{ \frac{1}{2}, -1 - \frac{\tilde{\gamma}}{2} \right\}, -\frac{v_c^2}{2} \right] \right. \\ \left. - \sqrt{2} v_c \tilde{\gamma} \left(\frac{3+\tilde{\gamma}}{2} \right) {}_2F_2 \left[\left\{ \frac{1}{2}(1-\tilde{\gamma}), 1 - \frac{\tilde{\gamma}}{2} \right\}, \left\{ \frac{3}{2}, -\frac{1}{2} \left(1 - \frac{\tilde{\gamma}}{2} \right) \right\}, -\frac{v_c^2}{2} \right] \right\}. \quad (\text{D.2.8})$$

This result, in turn, allows us to extract the simple approximation

$$\int_1^\infty dx (x-1)^{\tilde{\gamma}} x^3 e^{-x^2 v_c^2/2} \approx e^{-v_c^2/2} v_c^{-2(1+\tilde{\gamma})} \Gamma(1+\tilde{\gamma}). \quad (\text{D.2.9})$$

which is valid for $v_c/\tilde{\gamma} \gg 1$. We checked numerically that this approximation works exquisitely well (at the % level for $v_c = 10$ with increasing precision for larger thresholds). We find

$$\beta \approx \underbrace{\left[\frac{\mathcal{K}}{3\pi} \left(\frac{\bar{\sigma}_0 a^2 H^2}{a_m^2 H_m^2 v_c} \right)^{\tilde{\gamma}} \left(\frac{a_f}{a_m} \right) \left(\frac{\gamma r_m}{R_*} \right)^3 \Gamma(1+\tilde{\gamma}) \right]}_{\sim O(1)} v_c^2 e^{-v_c^2/2} \quad (\text{D.2.10})$$

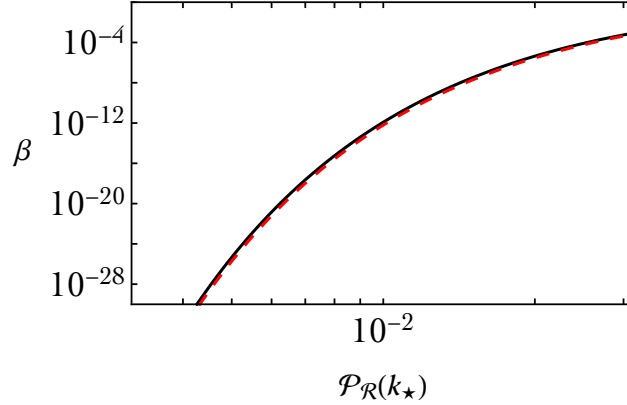


Figure 13: Abundance β computed with (black solid line) and without (red dashed line) the pre-factor in the square brackets in eq. 6.2.8.

The numerical value of β is controlled by the exponential function $e^{-v_c^2/2}$ while the pre-factor inside the square brackets in eq. (D.2.10) is a dimensionless $O(1)$ number whose exact value only plays a sub-leading role in the determination of β . To corroborate this statement, in the figure 13 we compare (as function of the peak amplitude of the power spectrum) the abundance β computed

with and without the pre-factor in the square brackets, and we show that the two computations almost coincide.

The computation in eq. (D.2.10) shows that in order to estimate the value of β in a pragmatic way we can just integrate the comoving number density of maxima of the overdensity field and make it dimensionless

$$\beta \approx 4\pi^2 R_*^3 \int_{\nu_c}^{\infty} d\nu n_{\max}(\nu). \quad (\text{D.2.11})$$

Eq. (D.2.11) gives a perfect approximation of eq. (D.2.10).

In presence of local non-gaussianities the abundance can be obtained following the same logic that leads to eq. (D.2.5), but computing the number density of peaks as explained in sec. D, namely identifying this quantity with the number density of spiky maxima of the comoving density perturbations, the sum of eq. (D.1.15) and eq. (D.1.18). We obtain

$$\beta = \frac{4\pi}{3} \mathcal{K} \left(\frac{\bar{\sigma}_0 a^2 H^2}{a_m^2 H_m^2} \right)^{\tilde{\gamma}} \left(\frac{1}{a_m H_m} \right)^3 \frac{a_f}{a_m} \times \left[\int_{-\frac{1}{2\alpha\sigma_0}}^{\infty} d\tilde{\nu} \int_{x_\delta(\tilde{\nu})}^{\infty} dx [\tilde{\nu}(\tilde{\nu}, x) - \nu_c]^{\tilde{\gamma}} \bar{n}_{\max}(\tilde{\nu}, x) + \int_{-\infty}^{\frac{1}{2\alpha\sigma_0}} d\tilde{\nu} \int_{-\infty}^{x_\delta(\tilde{\nu})} dx [\tilde{\nu}(\tilde{\nu}, x) - \nu_c]^{\tilde{\gamma}} \bar{n}_{\max}(\tilde{\nu}, x) \right], \quad (\text{D.2.12})$$

where $\bar{n}_{\max}(\tilde{\nu}, x)$ is defined in eqs. (D.1.16, D.1.17). Notice that $\tilde{\nu} = \mathcal{R}/\sigma_0$, while in eq. (D.2.3) we have $\nu = \delta/\sigma_\delta$. In the expression above we have written the latter quantity as $\nu = \tilde{\nu}(\tilde{\nu}, x) = x(1 + 2\alpha\sigma_0\tilde{\nu})$. Once again, we find that the abundance is well approximated by a simpler expression, obtained by taking the number density of peaks, $\mathcal{N}_{\text{pk}}^{(I)} + \mathcal{N}_{\text{pk}}^{(II)}$ (eqs. (D.1.15, D.1.18)), and making it dimensionless²

$$\beta \approx \pi^2 R_*^3 \left[\mathcal{N}_{\text{pk}}^{(I)} + \mathcal{N}_{\text{pk}}^{(II)} \right]. \quad (\text{D.2.13})$$

This equation reproduces eq. (6.1.2).

Having looked at the exact definition of β , let us now consider our simplified two-dimensional model. We follow the rationale that led to eq. (D.2.11). The number density of maxima above threshold of the overdensity field is given by $\mathcal{N}_{\max}(s_{\min})$ (that is, for instance, eq. (C.0.33) in the gaussian case) and, in two spatial dimensions, to make it dimensionless we need to multiply it times R_*^2

$$\beta \approx R_*^2 \mathcal{N}_{\max}(s_{\min}). \quad (\text{D.2.14})$$

² In eqs. (D.2.13, D.2.14) R_* is defined as in section C, i.e. $R_* \equiv \sqrt{d} \sigma_1/\sigma_2$.

PEAK THEORY WITH LOCAL NON-GAUSSIANITIES: A PERTURBATIVE APPROACH IN 2D

The idea is to derive the joint probability density distribution for the variables h , h_x , h_y , h_{xx} , h_{xy} , h_{yy} (considering again, for simplicity, the two-dimensional case). Once we get this probability density distribution, we set $h_x = h_y = 0$ and we integrate over h_{xx} , h_{xy} and h_{yy} in the domain defining maxima. This strategy was simple to implement in the case of the gaussian variable \mathcal{R} because the joint probability density distribution was a multivariate normal distribution. The non-gaussian case is more complicated.

In order to tackle the problem, we shall use the approach based on the characteristic function. In full generality, for a set of N correlated random variables ξ_i the characteristic function is the Fourier transform of their joint probability density distribution

$$\begin{aligned} \chi(\lambda_1, \dots, \lambda_N) &\equiv \int d\xi_1 \dots d\xi_N P(\xi_1, \dots, \xi_N) \exp [i(\xi_1 \lambda_1 + \dots + \xi_N \lambda_N)] = \\ &= \int d\xi_1 \dots d\xi_N P(\xi_1, \dots, \xi_N) \left[1 + i(\xi_1 \lambda_1 + \dots + \xi_N \lambda_N) + \frac{i^2}{2!} (\xi_1 \lambda_1 + \dots + \xi_N \lambda_N)^2 + \dots \right] = \\ &= 1 + i \sum_j \langle \xi_j \rangle \lambda_j + \frac{i^2}{2!} \sum_{j_1, j_2} \langle \xi_{j_1} \xi_{j_2} \rangle \lambda_{j_1} \lambda_{j_2} + \frac{i^3}{3!} \sum_{j_1, j_2, j_3} \langle \xi_{j_1} \xi_{j_2} \xi_{j_3} \rangle \lambda_{j_1} \lambda_{j_2} \lambda_{j_3} + \dots \end{aligned} \quad (\text{E.O.1})$$

where, after a Taylor expansion, we introduced the moments of the joint distribution by means of the integrals

$$\langle \xi_{j_1} \dots \xi_{j_k} \rangle = \int d\xi_1 \dots d\xi_N P(\xi_1, \dots, \xi_N) \xi_{j_1} \dots \xi_{j_k}. \quad (\text{E.O.2})$$

If we take the natural log of the characteristic function and Taylor expand, we define the cumulants

$$\log \chi(\lambda_1, \dots, \lambda_N) \equiv i \sum_j C_1(\xi_j) \lambda_j + \frac{i^2}{2!} \sum_{j_1, j_2} C_2(\xi_{j_1}, \xi_{j_2}) \lambda_{j_1} \lambda_{j_2} + \dots \quad (\text{E.O.3})$$

The relation between moments and cumulants follows from the comparison of the two Taylor expansions. We find the well-known relations

$$C_1(\xi_j) = \langle \xi_j \rangle, \quad (\text{E.O.4})$$

$$C_2(\xi_{j_1}, \xi_{j_2}) = \langle \xi_{j_1} \xi_{j_2} \rangle - \langle \xi_{j_1} \rangle \langle \xi_{j_2} \rangle, \quad (\text{E.O.5})$$

$$C_3(\xi_{j_1}, \xi_{j_2}, \xi_{j_3}) = \langle \xi_{j_1} \xi_{j_2} \xi_{j_3} \rangle - \langle \xi_{j_1} \rangle \langle \xi_{j_2} \xi_{j_3} \rangle - \langle \xi_{j_2} \rangle \langle \xi_{j_1} \xi_{j_3} \rangle - \langle \xi_{j_3} \rangle \langle \xi_{j_1} \xi_{j_2} \rangle + 2 \langle \xi_{j_1} \rangle \langle \xi_{j_2} \rangle \langle \xi_{j_3} \rangle, \quad (\text{E.O.6})$$

$$C_4(\xi_{j_1}, \xi_{j_2}, \xi_{j_3}, \xi_{j_4}) = \dots \quad (\text{E.O.7})$$

and so on. Working with cumulants instead of moments is more efficient. This is particularly true in the gaussian case. For a set of correlated gaussian variables, all cumulants of order higher than two vanish. In the gaussian case, eq. (E.0.3) gives

$$\chi(\lambda_1, \dots, \lambda_N) = \exp \left[i \sum_j \langle \xi_j \rangle \lambda_j - \frac{1}{2} \sum_{j_1, j_2} C_2(\xi_{j_1}, \xi_{j_2}) \lambda_{j_1} \lambda_{j_2} \right], \quad (\text{E.0.8})$$

and the inverse Fourier transform that gives the probability density distribution reads

$$P(\xi_1, \dots, \xi_N) = \int \frac{d\lambda_1}{(2\pi)} \dots \frac{d\lambda_N}{(2\pi)} \exp \left[i \sum_j (\langle \xi_j \rangle - \xi_j) \lambda_j - \frac{1}{2} \sum_{j_1, j_2} C_2(\xi_{j_1}, \xi_{j_2}) \lambda_{j_1} \lambda_{j_2} \right]. \quad (\text{E.0.9})$$

If we complete the square inside the integrand and compute the resulting multivariate gaussian integral, we find precisely eq. (C.0.6) where the second-order cumulants reconstruct the covariance matrix elements in eq. (C.0.7). This was precisely the strategy that we followed in the previous appendix: we computed the elements of the covariance matrix (that are the second-order cumulants) and we (implicitly) performed an inverse Fourier transform to get back the probability density distribution.

In the non-gaussian case, we can try to apply the same logic. First, we compute the cumulants; second, we reconstruct the probability density distribution by means of an inverse Fourier transform.

The computation of the cumulants require some mathematical tricks that we shall explain in the following. In full generality, we need to compute the n^{th} -order cumulant $C_n(\partial_j h, \dots, \partial_l h)$ where each $\partial_j h$ represents a certain number of spatial derivatives (zero, one or two) acting on h . Remember also that the random field h (and its derivatives) is computed at a specific spatial position (say, \bar{x}) that will be later identified with a stationary point. We can write

$$\begin{aligned} C_n(\partial_j h, \dots, \partial_l h) &= C_n[\partial_j h(\bar{x}), \dots, \partial_l h(\bar{x})] = \\ &= C_n[\partial_j h(\bar{x}_1), \dots, \partial_l h(\bar{x}_n)] \Big|_{\bar{x}_1 = \dots = \bar{x}_n = \bar{x}} = \partial_{j_1} \dots \partial_{l_n} C_n[h(\bar{x}_1), \dots, h(\bar{x}_n)] \Big|_{\bar{x}_1 = \dots = \bar{x}_n = \bar{x}}. \end{aligned} \quad (\text{E.0.10})$$

In the first step of eq. (E.0.10) we consider each $\partial_{j_k} h$ to act at a different point \bar{x}_k , and later we set all points equal again (we already used a similar trick in eq. (C.0.12)). The advantage of this step is that since now each derivative acts at a different spatial point, we can bring them outside the cumulant (as done in the last step of eq. (E.0.10)). It is a very simple exercise to check explicitly (for instance, by computing second-order cumulants of a gaussian variable with its derivatives) that this procedure is completely legitimate. Using our notation $h(\bar{x}_n) = h_n$, the problem reduces to the computation of $C_n(h_1, \dots, h_n)$ where now the random fields are evaluated at different spatial points. After computing $C_n(h_1, \dots, h_n)$, we will take the spatial derivatives and finally set all points equal according to the prescription in eq. (E.0.10).

To compute $C_n(h_1, \dots, h_n)$, we consider the relation $h = \mathcal{R} + \alpha \mathcal{R}^2$. We write in general $h = \mathcal{R} + f_{\text{NL}}(\mathcal{R})$ where $f_{\text{NL}}(\mathcal{R})$ can be a generic non-linear function controlled by the parameter α . Let us consider the term $\alpha \mathcal{R}^2$ as a perturbation and expand in α . We have

$$C_n(h_1, \dots, h_n) = C_n(\mathcal{R}_1, \dots, \mathcal{R}_n) + C_n[f_{\text{NL}}(\mathcal{R}_1), \dots, \mathcal{R}_n] + \dots + C_n[\mathcal{R}_1, \dots, f_{\text{NL}}(\mathcal{R}_n)] \quad (\text{E.o.11})$$

$$+ \{C_n[f_{\text{NL}}(\mathcal{R}_1), f_{\text{NL}}(\mathcal{R}_2), \dots, \mathcal{R}_n] + \dots\} + \mathcal{O}(\alpha^3). \quad (\text{E.o.12})$$

This deconstruction makes clear the fact that we can compute the cumulants $C_n(h_1, \dots, h_n)$ based on the cumulants computed for the gaussian random field \mathcal{R} .

The problem is now the computation of $C_n[f_{\text{NL}}(\mathcal{R}_1), \dots, \mathcal{R}_n]$ where we remind that $\mathcal{R}_n = \mathcal{R}(\bar{x}_n)$.

In order to compute $C_n[f_{\text{NL}}(\mathcal{R}_1), \dots, \mathcal{R}_n]$, we need to work out an intermediate result. First, remember the definition of random field that we gave at the beginning of appendix C: The scalar random field $\mathcal{R}(\bar{x})$ is a set of random variables, one for each point \bar{x} in space, equipped with a joint probability density distribution $p(\mathcal{R}_1, \dots, \mathcal{R}_n)$. When the random field is gaussian, $p(\mathcal{R}_1, \dots, \mathcal{R}_n)$ is a multivariate Gaussian distribution and we can write

$$p(\mathcal{R}_1, \dots, \mathcal{R}_n) = \frac{1}{(2\pi)^{n/2} \sqrt{\det \sigma}} \exp \left[-\frac{1}{2} \sum_{ij} (\sigma^{-1})_{ij} \mathcal{R}_i \mathcal{R}_j \right], \quad (\text{E.o.13})$$

where $\sigma_{ij} = \langle \mathcal{R}_i \mathcal{R}_j \rangle$ (as before, we consider zero-mean random field).

Consider now a new set of random variables $\{\mathcal{Y}_1, \dots, \mathcal{Y}_n\}$ related to the previous one via the transformations $\mathcal{Y}_1 = g_1(\mathcal{R}_1, \dots, \mathcal{R}_n), \dots, \mathcal{Y}_n = g_n(\mathcal{R}_1, \dots, \mathcal{R}_n)$ with inverse $\mathcal{R}_1 = g_1^{-1}(\mathcal{Y}_1, \dots, \mathcal{Y}_n), \dots, \mathcal{R}_n = g_n^{-1}(\mathcal{Y}_1, \dots, \mathcal{Y}_n)$. The joint probability density distribution for the transformed variables is given by

$$p_{\mathcal{Y}}(\mathcal{Y}_1, \dots, \mathcal{Y}_n) = p[g_1^{-1}(\mathcal{Y}_1, \dots, \mathcal{Y}_n), \dots, g_n^{-1}(\mathcal{Y}_1, \dots, \mathcal{Y}_n)] |\det J(\mathcal{Y}_1, \dots, \mathcal{Y}_n)|, \quad (\text{E.o.14})$$

where the Jacobian matrix is

$$J(\mathcal{Y}_1, \dots, \mathcal{Y}_n) \equiv \begin{pmatrix} \frac{\partial \mathcal{R}_1}{\partial \mathcal{Y}_1} & \dots & \frac{\partial \mathcal{R}_1}{\partial \mathcal{Y}_n} \\ \vdots & \ddots & \vdots \\ \frac{\partial \mathcal{R}_n}{\partial \mathcal{Y}_1} & \dots & \frac{\partial \mathcal{R}_n}{\partial \mathcal{Y}_n} \end{pmatrix}, \quad \text{with} \quad \frac{\partial \mathcal{R}_j}{\partial \mathcal{Y}_k} = \frac{\partial}{\partial \mathcal{Y}_k} [g_j^{-1}(\mathcal{Y}_1, \dots, \mathcal{Y}_n)]. \quad (\text{E.o.15})$$

Eq. (E.o.14) is known as Jacobi's multivariate theorem.

We note that in eq. (E.o.14) we can use the relation $|\det J(\mathcal{Y}_1, \dots, \mathcal{Y}_n)| = 1/|\det J(\mathcal{R}_1, \dots, \mathcal{R}_n)|$ where $J(\mathcal{R}_1, \dots, \mathcal{R}_n)$ is the Jacobian matrix of the inverse transformation with elements $\partial \mathcal{Y}_j / \partial \mathcal{R}_k = \partial g_j(\mathcal{R}_1, \dots, \mathcal{R}_n) / \partial \mathcal{R}_k$. This implies that we can rewrite

$$p_{\mathcal{Y}}(\mathcal{Y}_1, \dots, \mathcal{Y}_n) = \int d\mathcal{R}_1 \dots d\mathcal{R}_n p(\mathcal{R}_1, \dots, \mathcal{R}_n) \delta[\mathcal{Y}_1 - g_1(\mathcal{R}_1, \dots, \mathcal{R}_n)] \dots \delta[\mathcal{Y}_n - g_n(\mathcal{R}_1, \dots, \mathcal{R}_n)], \quad (\text{E.o.16})$$

and eq. (E.0.14) follows from eq. (E.0.16) if one applies the transformation property of the multi-dimensional delta function

$$\begin{aligned} & \delta[\mathcal{Y}_1 - g_1(\mathcal{R}_1, \dots, \mathcal{R}_n)] \dots \delta[\mathcal{Y}_n - g_n(\mathcal{R}_1, \dots, \mathcal{R}_n)] = \\ & = \frac{\delta[\mathcal{R}_1 - g_1^{-1}(\mathcal{Y}_1, \dots, \mathcal{Y}_n)] \dots \delta[\mathcal{R}_n - g_n^{-1}(\mathcal{Y}_1, \dots, \mathcal{Y}_n)]}{|\det J(\mathcal{R}_1, \dots, \mathcal{R}_n)|}, \end{aligned} \quad (\text{E.0.17})$$

and integrates over \mathcal{R}_i . Eq. (E.0.16) is a very useful formula. Consider the characteristic function of $p_{\mathcal{Y}}(\mathcal{Y}_1, \dots, \mathcal{Y}_n)$ defined by the Fourier transform

$$\chi_{\mathcal{Y}}(\lambda_1, \dots, \lambda_n) = \int d\mathcal{Y}_1 \dots d\mathcal{Y}_n p_{\mathcal{Y}}(\mathcal{Y}_1, \dots, \mathcal{Y}_n) \exp[i(\mathcal{Y}_1 \lambda_1 + \dots + \mathcal{Y}_n \lambda_n)]. \quad (\text{E.0.18})$$

Using eq. (E.0.16) and integrating over \mathcal{Y}_i thanks to the delta functions, we find

$$\chi_{\mathcal{Y}}(\lambda_1, \dots, \lambda_n) = \int d\mathcal{R}_1 \dots d\mathcal{R}_n e^{i[g_1(\mathcal{R}_1, \dots, \mathcal{R}_n)\lambda_1 + \dots + g_n(\mathcal{R}_1, \dots, \mathcal{R}_n)\lambda_n]} p(\mathcal{R}_1, \dots, \mathcal{R}_n). \quad (\text{E.0.19})$$

From the definition of cumulants with respect to the characteristic function $\chi_{\mathcal{Y}}(\lambda_1, \dots, \lambda_n)$, we finally find (see eq. (E.0.3))

$$\begin{aligned} C_n(\mathcal{Y}_1, \dots, \mathcal{Y}_n) &= (-i)^n \frac{\partial}{\partial \lambda_1} \dots \frac{\partial}{\partial \lambda_n} \log \chi_{\mathcal{Y}}(\lambda_1, \dots, \lambda_n) \Big|_{\lambda_1 = \dots = \lambda_n = 0} \\ &= (-i)^n \frac{\partial}{\partial \lambda_1} \dots \frac{\partial}{\partial \lambda_n} \log \int d\mathcal{R}_1 \dots d\mathcal{R}_n e^{i[g_1(\mathcal{R}_1, \dots, \mathcal{R}_n)\lambda_1 + \dots + g_n(\mathcal{R}_1, \dots, \mathcal{R}_n)\lambda_n]} p(\mathcal{R}_1, \dots, \mathcal{R}_n) \Big|_{\lambda_1 = \dots = \lambda_n = 0}. \end{aligned} \quad (\text{E.0.20})$$

This is a generic formula that can be applied to our case.

Consider the linear order in α . From eq. (E.0.20), the cumulant $C_n[f_{\text{NL}}(\mathcal{R}_1), \dots, \mathcal{R}_n]$ is given by

$$\begin{aligned} C_n[f_{\text{NL}}(\mathcal{R}_1), \dots, \mathcal{R}_n] &= \\ &= (-i)^n \frac{\partial}{\partial \lambda_1} \dots \frac{\partial}{\partial \lambda_n} \log \int d\mathcal{R}_1 \dots d\mathcal{R}_n e^{i[f_{\text{NL}}(\mathcal{R}_1)\lambda_1 + \mathcal{R}_2 \lambda_2 + \dots + \mathcal{R}_n \lambda_n]} p(\mathcal{R}_1, \dots, \mathcal{R}_n) \Big|_{\lambda_1 = \dots = \lambda_n = 0}. \end{aligned} \quad (\text{E.0.21})$$

A similar formula is applicable to all remaining first-order terms in eq. (E.0.11). Similarly, at order $\mathcal{O}(\alpha^2)$ one needs to compute, for instance, cumulants like

$$\begin{aligned} C_n[f_{\text{NL}}(\mathcal{R}_1), f_{\text{NL}}(\mathcal{R}_2), \dots, \mathcal{R}_n] &= \\ &= (-i)^n \frac{\partial}{\partial \lambda_1} \dots \frac{\partial}{\partial \lambda_n} \log \int d\mathcal{R}_1 \dots d\mathcal{R}_n e^{i[f_{\text{NL}}(\mathcal{R}_1)\lambda_1 + f_{\text{NL}}(\mathcal{R}_2)\lambda_2 + \dots + \mathcal{R}_n \lambda_n]} p(\mathcal{R}_1, \dots, \mathcal{R}_n) \Big|_{\lambda_1 = \dots = \lambda_n = 0}. \end{aligned} \quad (\text{E.0.22})$$

All we need to do is computing the integral and taking derivatives with respect to λ_i . The computation of the integrals is simplified by the fact that the variables \mathcal{R}_i are gaussian with joint distribution given by eq. (E.0.13).

Before proceeding, an important remark is in order. For the sake of simplicity, we derived eq. (E.0.14) assuming that the functions $\mathcal{Y}_{i=1, \dots, n} = g_{i=1, \dots, n}(\mathcal{R}_1, \dots, \mathcal{R}_n)$ define one-to-one mappings. In this

case, there exist unique inverse functions so that $\mathcal{R}_{i=1,\dots,n} = g_{i=1,\dots,n}^{-1}(\mathcal{Y}_1, \dots, \mathcal{Y}_n)$. The case we are interested in, however, is not exactly of this form. If we solve $h = \mathcal{R} + \alpha \mathcal{R}^2$ for \mathcal{R} , we indeed find $\mathcal{R} = (-1 \pm \sqrt{1 + 4\alpha h})/2\alpha$ which has two roots.

However, this is not an insurmountable problem since Jacobi's multivariate theorem in eq. (E.0.14) can be generalized to the case in which the system $\mathcal{Y}_{i=1,\dots,n} = g_{i=1,\dots,n}(\mathcal{R}_1, \dots, \mathcal{R}_n)$ admits at most a countable number of roots. Let us indicate these $q = 1, \dots, Q$ roots in the form $\mathcal{R}_{q,i=1,\dots,n} = g_{q,i=1,\dots,n}^{-1}(\mathcal{Y}_1, \dots, \mathcal{Y}_n)$. Eq. (E.0.14) becomes

$$p_{\mathcal{Y}}(\mathcal{Y}_1, \dots, \mathcal{Y}_n) = \sum_{q=1}^Q p[g_{q,1}^{-1}(\mathcal{Y}_1, \dots, \mathcal{Y}_n), \dots, g_{q,n}^{-1}(\mathcal{Y}_1, \dots, \mathcal{Y}_n)] |\det J_q(\mathcal{Y}_1, \dots, \mathcal{Y}_n)|, \quad (\text{E.0.23})$$

where now $J_q(\mathcal{Y}_1, \dots, \mathcal{Y}_n)$ is the Jacobian corresponding to the q^{th} root

$$J_q(\mathcal{Y}_1, \dots, \mathcal{Y}_n) \equiv \begin{pmatrix} \frac{\partial \mathcal{R}_{q,1}}{\partial \mathcal{Y}_1} & \dots & \frac{\partial \mathcal{R}_{q,1}}{\partial \mathcal{Y}_n} \\ \vdots & \ddots & \vdots \\ \frac{\partial \mathcal{R}_{q,n}}{\partial \mathcal{Y}_1} & \dots & \frac{\partial \mathcal{R}_{q,n}}{\partial \mathcal{Y}_n} \end{pmatrix}, \quad \text{with} \quad \frac{\partial \mathcal{R}_{q,j}}{\partial \mathcal{Y}_k} = \frac{\partial}{\partial \mathcal{Y}_k} [g_{q,j}^{-1}(\mathcal{Y}_1, \dots, \mathcal{Y}_n)]. \quad (\text{E.0.24})$$

The multi-dimensional delta-function identity in eq. (E.0.17) changes accordingly, and the final result in eq. (E.0.20) remains unaltered.

After this digression, we are ready to compute the integral in eq. (E.0.20). Instead of looking for a generic expression, let us consider specific cases organized for increasing level of difficulty.

- The simplest possibility is to truncate the analysis at the linear order in α , eq. (E.0.21). Consider the integral in eq. (E.0.21) which we rewrite as

$$\mathcal{I}(\lambda_1, \dots, \lambda_n) \equiv \int d\mathcal{R}_1 e^{i f_{\text{NL}}(\mathcal{R}_1) \lambda_1} \underbrace{\left[\int d\mathcal{R}_2 \dots d\mathcal{R}_n e^{i[\mathcal{R}_2 \lambda_2 + \dots + \mathcal{R}_n \lambda_n]} p(\mathcal{R}_1, \dots, \mathcal{R}_n) \right]}_{\equiv \mathcal{I}'(\mathcal{R}_1, \lambda_2, \dots, \lambda_n)}. \quad (\text{E.0.25})$$

The key observation is that the integral inside the square brackets would precisely match the definition of the characteristic function $\chi(\lambda_1, \dots, \lambda_n)$ of $p(\mathcal{R}_1, \dots, \mathcal{R}_n)$ if it were completed by an additional integration over \mathcal{R}_1 (see the definition in the first line of eq. (E.0.1)). In such case, we could simply use (see eq. (E.0.8))

$$\int d\mathcal{R}_1 e^{i\lambda_1 \mathcal{R}_1} \mathcal{I}'(\mathcal{R}_1, \lambda_2, \dots, \lambda_n) = \chi(\lambda_1, \dots, \lambda_n) = \exp \left[-\frac{1}{2} \sum_{ij} \sigma_{ij} \lambda_i \lambda_j \right], \quad (\text{E.0.26})$$

since $\{\mathcal{R}_1, \dots, \mathcal{R}_n\}$ are gaussian. However, the fact that integration over \mathcal{R}_1 is missing implies that the integral $\mathcal{I}'(\mathcal{R}_1, \lambda_2, \dots, \lambda_n)$ is actually equal to the inverse Fourier transform of $\chi(\lambda_1, \dots, \lambda_n)$ with respect to λ_1 . In formulas, eq. (E.0.25) becomes

$$\begin{aligned} \mathcal{I}(\lambda_1, \dots, \lambda_n) &= \int d\mathcal{R}_1 e^{i f_{\text{NL}}(\mathcal{R}_1) \lambda_1} \int \frac{d\lambda_1}{(2\pi)} e^{-i\lambda_1 \mathcal{R}_1} \exp\left[-\frac{1}{2} \sum_{ij} \sigma_{ij} \lambda_i \lambda_j\right] = \\ &= \int d\mathcal{R}_1 e^{i f_{\text{NL}}(\mathcal{R}_1) \lambda_1} \exp\left[-\frac{1}{2} \sum_{ij \geq 2} \sigma_{ij} \lambda_i \lambda_j\right] \int \frac{d\lambda_1}{(2\pi)} \exp\left[-\frac{1}{2} \sigma_{11} \lambda_1^2 - \left(i\mathcal{R}_1 + \sum_{j \geq 2} \sigma_{1j} \lambda_j\right) \lambda_1\right] = \\ &= \int d\mathcal{R}_1 e^{i f_{\text{NL}}(\mathcal{R}_1) \lambda_1} \frac{1}{\sqrt{2\pi\sigma_{11}}} \exp\left[-\frac{1}{2} \sum_{ij \geq 2} \sigma_{ij} \lambda_i \lambda_j + \frac{1}{2\sigma_{11}} \left(i\mathcal{R}_1 + \sum_{j \geq 2} \sigma_{1j} \lambda_j\right)^2\right], \end{aligned} \quad (\text{E.0.27})$$

where we just reorganized terms before integrating over λ_1 in the last step. If we take the natural log, we find

$$\log[\mathcal{I}(\lambda_1, \dots, \lambda_n)] = -\frac{1}{2} \sum_{ij \geq 2} \sigma_{ij} \lambda_i \lambda_j + \log \int d\mathcal{R}_1 e^{i f_{\text{NL}}(\mathcal{R}_1) \lambda_1} \frac{1}{\sqrt{2\pi\sigma_{11}}} \exp\left[\frac{1}{2\sigma_{11}} \left(i\mathcal{R}_1 + \sum_{j \geq 2} \sigma_{1j} \lambda_j\right)^2\right]. \quad (\text{E.0.28})$$

According to eq. (E.0.21), we now need to compute derivatives with respect to $\lambda_{i=1, \dots, n}$ and finally set $\lambda_{i=1, \dots, n} = 0$. We find

$$C_n[f_{\text{NL}}(\mathcal{R}_1), \dots, \mathcal{R}_n] = \frac{1}{\sqrt{2\pi\sigma_{11}}} \left(\prod_{k=2}^n \sigma_{1k} \right) \int d\mathcal{R}_1 f_{\text{NL}}(\mathcal{R}_1) g_n(\mathcal{R}_1^{n-1}) e^{-\mathcal{R}_1^2/2\sigma_{11}}, \quad (\text{E.0.29})$$

where $g_n(\mathcal{R}_1^{n-1})$ is a polynomial of order \mathcal{R}_1^{n-1} whose explicit expression is given by¹

$$g_n(\mathcal{R}_1^{n-1}) = (-1)^{n-1} e^{\mathcal{R}_1^2/2\sigma_{11}} \frac{d^{n-1}}{d\mathcal{R}_1^{n-1}} e^{-\mathcal{R}_1^2/2\sigma_{11}}. \quad (\text{E.0.31})$$

This result implies that we can just integrate by parts $n-1$ times in eq. (E.0.29). We find

$$C_n[f_{\text{NL}}(\mathcal{R}_1), \dots, \mathcal{R}_n] = \left(\prod_{k=2}^n \sigma_{1k} \right) \underbrace{\frac{1}{\sqrt{2\pi\sigma_{11}}} \int d\mathcal{R}_1 f_{\text{NL}}^{(n-1)}(\mathcal{R}_1) e^{-\mathcal{R}_1^2/2\sigma_{11}}}_{= \langle f_{\text{NL}}^{(n-1)}(\mathcal{R}_1) \rangle}. \quad (\text{E.0.32})$$

The leftover integral is nothing but the expectation value of $f_{\text{NL}}^{(n-1)}(\mathcal{R}_1)$. All in all, we find (remember that $\sigma_{ij} = \langle \mathcal{R}_i \mathcal{R}_j \rangle$)

$$C_n[f_{\text{NL}}(\mathcal{R}_1), \dots, \mathcal{R}_n] = \langle f_{\text{NL}}^{(n-1)}(\mathcal{R}_1) \rangle \langle \mathcal{R}_1 \mathcal{R}_2 \rangle \dots \langle \mathcal{R}_1 \mathcal{R}_n \rangle \quad (\text{E.0.33})$$

¹ We can notice that the g_n polynomials are nothing but the Hermite polynomials, except for a pre-factor. In particular:

$$g_n(\mathcal{R}_1^{n-1}) = \frac{1}{(2\sigma_{11})^{n/2}} H_{n-1}\left(\frac{\mathcal{R}_1}{\sqrt{2\sigma_{11}}}\right) \quad (\text{E.0.30})$$

◦ At order $\mathcal{O}(\alpha^2)$, consider eq. (E.0.22) and the integral

$$\mathcal{J}(\lambda_1, \dots, \lambda_n) \equiv \int d\mathcal{R}_1 d\mathcal{R}_2 e^{i f_{\text{NL}}(\mathcal{R}_1)\lambda_1 + i f_{\text{NL}}(\mathcal{R}_2)\lambda_2} \left[\int d\mathcal{R}_3 \dots d\mathcal{R}_n e^{i[\mathcal{R}_3\lambda_3 + \dots + \mathcal{R}_n\lambda_n]} p(\mathcal{R}_1, \dots, \mathcal{R}_n) \right]. \quad (\text{E.0.34})$$

The computation goes as before with the only difference that now we need to consider the inverse Fourier transform of the characteristic function with respect to both λ_1 and λ_2 . For the natural log of $\mathcal{J}(\lambda_1, \dots, \lambda_n)$ we find

$$\begin{aligned} \log[\mathcal{J}(\lambda_1, \dots, \lambda_n)] &= -\frac{1}{2} \sum_{i,j \geq 3} \sigma_{ij} \lambda_i \lambda_j + \\ &+ \log \int d\mathcal{R}_1 d\mathcal{R}_2 \frac{e^{i f_{\text{NL}}(\mathcal{R}_1)\lambda_1 + i f_{\text{NL}}(\mathcal{R}_2)\lambda_2}}{2\pi \sqrt{\sigma_{11}\sigma_{22} - \sigma_{12}^2}} \exp \left[\frac{1}{2(\sigma_{11}\sigma_{22} - \sigma_{12}^2)} \left(A_1^2 \sigma_{22} + A_2^2 \sigma_{11} - 2A_1 A_2 \sigma_{12} \right) \right], \end{aligned} \quad (\text{E.0.35})$$

where $A_1 \equiv i\mathcal{R}_1 + \sum_{j \geq 3} \sigma_{1j} \lambda_j$ and $A_2 \equiv i\mathcal{R}_2 + \sum_{j \geq 3} \sigma_{2j} \lambda_j$. This equation is the analogue of eq. (E.0.28) at order $\mathcal{O}(\alpha^2)$. As before, we need to compute derivatives with respect to $\lambda_{i=1, \dots, n}$ and finally set $\lambda_{i=1, \dots, n} = 0$. Let us consider first the derivatives with respect to λ_1 and λ_2 . We find

$$\begin{aligned} (-i)^2 \frac{\partial}{\partial \lambda_2} \frac{\partial}{\partial \lambda_1} \log[\mathcal{J}(\lambda_1, \dots, \lambda_n)] \Big|_{\lambda_1 = \lambda_2 = 0} &= \\ \frac{1}{2\pi \sqrt{\sigma_{11}\sigma_{22} - \sigma_{12}^2}} \int d\mathcal{R}_1 d\mathcal{R}_2 f_{\text{NL}}(\mathcal{R}_1) f_{\text{NL}}(\mathcal{R}_2) \exp \left[\frac{1}{2(\sigma_{11}\sigma_{22} - \sigma_{12}^2)} \left(A_1^2 \sigma_{22} + A_2^2 \sigma_{11} - 2A_1 A_2 \sigma_{12} \right) \right] & \\ \underbrace{\hspace{10em}}_{2\pi \sqrt{\det \tilde{\sigma}}} & \underbrace{\hspace{10em}}_{=(1/2) \sum_{i,j=1}^2 (\tilde{\sigma}^{-1})_{ij} A_i A_j} \\ - \left[\frac{1}{\sqrt{2\pi\sigma_{11}}} \int d\mathcal{R}_1 f_{\text{NL}}(\mathcal{R}_1) e^{A_1^2/2\sigma_{11}} \right] \left[\frac{1}{\sqrt{2\pi\sigma_{22}}} \int d\mathcal{R}_2 f_{\text{NL}}(\mathcal{R}_2) e^{A_2^2/2\sigma_{22}} \right], & \end{aligned} \quad (\text{E.0.36})$$

where $\tilde{\sigma}$ is the two-by-two sub-matrix of σ formed by the first two rows and columns. Before proceeding, let us consider a simple example. If we are interested to the computation of the second-order cumulant, these two derivatives are the only ones that we need to take. Furthermore, in this case we have $A_{j=1,2} = i\mathcal{R}_{j=1,2}$. We find the simple result

$$C_2[f_{\text{NL}}(\mathcal{R}_1), f_{\text{NL}}(\mathcal{R}_2)] = \langle f_{\text{NL}}(\mathcal{R}_1) f_{\text{NL}}(\mathcal{R}_2) \rangle - \langle f_{\text{NL}}(\mathcal{R}_1) \rangle \langle f_{\text{NL}}(\mathcal{R}_2) \rangle \quad (\text{E.0.37})$$

where the expectation values $\langle f_{\text{NL}}(\mathcal{R}_1) \rangle$ and $\langle f_{\text{NL}}(\mathcal{R}_2) \rangle$ are defined as in eq. (E.0.32) while $\langle f_{\text{NL}}(\mathcal{R}_1) f_{\text{NL}}(\mathcal{R}_2) \rangle$ is computed by means of the joint probability distribution of \mathcal{R}_1 and \mathcal{R}_2 ; in formulas, we have

$$\langle f_{\text{NL}}(\mathcal{R}_1) f_{\text{NL}}(\mathcal{R}_2) \rangle = \frac{1}{2\pi \sqrt{\det \tilde{\sigma}}} \int d\mathcal{R}_1 d\mathcal{R}_2 f_{\text{NL}}(\mathcal{R}_1) f_{\text{NL}}(\mathcal{R}_2) \exp \left[-\frac{1}{2} \sum_{i,j=1}^2 (\tilde{\sigma}^{-1})_{ij} \mathcal{R}_i \mathcal{R}_j \right]. \quad (\text{E.0.38})$$

For $n \geq 3$, we need to compute in eq. (E.0.36) derivatives with respect to $\lambda_{i=3, \dots, n}$ and finally set $\lambda_{i=3, \dots, n} = 0$. These derivatives act on the exponential functions in the integrands of the two terms on the right-hand side of eq. (E.0.36). Let us start from the second term; if we compute the λ -derivatives on the exponential function, we find the following result

$$\begin{aligned}
& (-i)^{n-2} \frac{\partial}{\partial \lambda_n} \dots \frac{\partial}{\partial \lambda_3} \left(e^{\Lambda_1^2/2\sigma_{11}} e^{\Lambda_2^2/2\sigma_{22}} \right) \Big|_{\lambda_3 = \dots = \lambda_n = 0} = & \text{(E.0.39)} \\
& (-1)^{n-2} \left(\prod_{k=3}^n \sigma_{1k} \right) \left(\frac{d^{n-2}}{d\mathcal{R}_1^{n-2}} e^{-\mathcal{R}_1^2/2\sigma_{11}} \right) e^{-\mathcal{R}_2^2/2\sigma_{22}} + (-1)^{n-2} \left(\prod_{k=3}^n \sigma_{2k} \right) \left(\frac{d^{n-2}}{d\mathcal{R}_2^{n-2}} e^{-\mathcal{R}_2^2/2\sigma_{22}} \right) e^{-\mathcal{R}_1^2/2\sigma_{11}} \\
& + (-1)^{n-2} \left[\sum_{a,b>0}^{a+b=n-2} \left(\prod_{k=3+b}^n \sigma_{1k} \right) \left(\prod_{j=3}^{n-a} \sigma_{2j} \right) \left(\frac{d^a}{d\mathcal{R}_1^a} e^{-\mathcal{R}_1^2/2\sigma_{11}} \right) \left(\frac{d^b}{d\mathcal{R}_2^b} e^{-\mathcal{R}_2^2/2\sigma_{22}} \right) + \text{perms of } (3, \dots, n) \right].
\end{aligned}$$

To fully understand the content of this equation, few comments are in order. Inside the square brackets, the sum $\sum_{a,b}$ runs over all possible combinations of $a > 0$ and $b > 0$ such that $a + b = n - 2$. For instance, if we take $n = 4$ we have only $\{a = 1, b = 1\}$ while for $n = 5$ we have two combinations, namely $\{a = 1, b = 2\}$ and $\{a = 2, b = 1\}$ (notice that if $n = 3$, there are no combinations that are allowed, and the term in the square brackets does not contribute to the third-order cumulant). Furthermore, after computing the sum over a and b , a further sum over all permutations of the indices $(3, \dots, n)$ that give distinct results is required. Let us clarify this point with an explicit example. Consider $n = 4$. The sum over $\{a = 1, b = 1\}$ gives $(e^{-\mathcal{R}_1^2/2\sigma_{11}} e^{-\mathcal{R}_2^2/2\sigma_{22}} \mathcal{R}_1 \mathcal{R}_2 / \sigma_{11} \sigma_{22}) \sigma_{14} \sigma_{23}$; we now need include the term with $(3, 4)$ exchanged so that the final result is $(e^{-\mathcal{R}_1^2/2\sigma_{11}} e^{-\mathcal{R}_2^2/2\sigma_{22}} \mathcal{R}_1 \mathcal{R}_2 / \sigma_{11} \sigma_{22}) (\sigma_{14} \sigma_{23} + \sigma_{13} \sigma_{24})$. Only permutations that give distinct results need to be included. For instance, take for $n = 5$ the term proportional to $\sigma_{14} \sigma_{15} \sigma_{23}$; in this case, the sum over permutations of $(3, 4, 5)$ gives only three distinct terms, $\sigma_{14} \sigma_{15} \sigma_{23} \rightarrow \sigma_{14} \sigma_{15} \sigma_{23} + \sigma_{13} \sigma_{15} \sigma_{24} + \sigma_{14} \sigma_{13} \sigma_{25}$ (instead of six—that is the number of permutations of three objects—since the remaining three do not give distinct results).

As far as the first term on the right-hand side of eq. (E.0.36) is concerned, we find

$$\begin{aligned}
& (-i)^{n-2} \frac{\partial}{\partial \lambda_n} \dots \frac{\partial}{\partial \lambda_3} \left[e^{\frac{\Lambda_1^2 \sigma_{22} + \Lambda_2^2 \sigma_{11} - 2\Lambda_1 \Lambda_2 \sigma_{12}}{2(\sigma_{11} \sigma_{22} - \sigma_{12}^2)}} \right] \Big|_{\lambda_3 = \dots = \lambda_n = 0} = & \text{(E.0.40)} \\
& (-1)^{n-2} \left(\prod_{k=3}^n \sigma_{1k} \right) \left[\frac{d^{n-2}}{d\mathcal{R}_1^{n-2}} e^{-\frac{\mathcal{R}_1^2 \sigma_{22} + \mathcal{R}_2^2 \sigma_{11} - 2\mathcal{R}_1 \mathcal{R}_2 \sigma_{12}}{2(\sigma_{11} \sigma_{22} - \sigma_{12}^2)}} \right] + (-1)^{n-2} \left(\prod_{k=3}^n \sigma_{2k} \right) \left[\frac{d^{n-2}}{d\mathcal{R}_2^{n-2}} e^{-\frac{\mathcal{R}_1^2 \sigma_{22} + \mathcal{R}_2^2 \sigma_{11} - 2\mathcal{R}_1 \mathcal{R}_2 \sigma_{12}}{2(\sigma_{11} \sigma_{22} - \sigma_{12}^2)}} \right] \\
& + (-1)^{n-2} \left\{ \sum_{a,b>0}^{a+b=n-2} \left(\prod_{k=3+b}^n \sigma_{1k} \right) \left(\prod_{j=3}^{n-a} \sigma_{2j} \right) \left[\frac{\partial^{n-2}}{\partial \mathcal{R}_1^a \partial \mathcal{R}_2^b} e^{-\frac{\mathcal{R}_1^2 \sigma_{22} + \mathcal{R}_2^2 \sigma_{11} - 2\mathcal{R}_1 \mathcal{R}_2 \sigma_{12}}{2(\sigma_{11} \sigma_{22} - \sigma_{12}^2)}} \right] + \text{perms of } (3, \dots, n) \right\},
\end{aligned}$$

where the sum $\sum_{a,b}$ and the subsequent one over different permutations have the same meaning explained before.

Eqs. (E.0.39, E.0.40) allow to compute the integrals in eq. (E.0.36) by means of $n - 2$ integration by parts. We find the final result (for $n \geq 3$)

$$\begin{aligned}
C_n[f_{\text{NL}}(\mathcal{R}_1), f_{\text{NL}}(\mathcal{R}_2), \dots, \mathcal{R}_n] = & \quad (\text{E.0.41}) \\
& \left[\langle f_{\text{NL}}^{(n-2)}(\mathcal{R}_1) f_{\text{NL}}(\mathcal{R}_2) \rangle - \langle f_{\text{NL}}^{(n-2)}(\mathcal{R}_1) \rangle \langle f_{\text{NL}}(\mathcal{R}_2) \rangle \right] \langle \mathcal{R}_1 \mathcal{R}_3 \rangle \dots \langle \mathcal{R}_1 \mathcal{R}_n \rangle + \\
& \left[\langle f_{\text{NL}}(\mathcal{R}_1) f_{\text{NL}}^{(n-2)}(\mathcal{R}_2) \rangle - \langle f_{\text{NL}}(\mathcal{R}_1) \rangle \langle f_{\text{NL}}^{(n-2)}(\mathcal{R}_2) \rangle \right] \langle \mathcal{R}_2 \mathcal{R}_3 \rangle \dots \langle \mathcal{R}_2 \mathcal{R}_n \rangle + \\
& \left\{ \sum_{a,b>0}^{a+b=n-2} \left[\langle f_{\text{NL}}^{(a)}(\mathcal{R}_1) f_{\text{NL}}^{(b)}(\mathcal{R}_2) \rangle - \langle f_{\text{NL}}^{(a)}(\mathcal{R}_1) \rangle \langle f_{\text{NL}}^{(b)}(\mathcal{R}_2) \rangle \right] \prod_{k=3+b}^n \langle \mathcal{R}_1 \mathcal{R}_k \rangle \prod_{j=3}^{n-a} \langle \mathcal{R}_2 \mathcal{R}_j \rangle + \right. \\
& \left. + \text{perms of } (3, \dots, n) \right\}
\end{aligned}$$

which generalizes eq. (E.0.33) at order $\mathcal{O}(\alpha^2)$. We remark that eqs. (E.0.33, E.0.41) are completely generic and do not depend on the functional form of $f_{\text{NL}}(\mathcal{R})$.

- One can in principle continue the computation and include higher-order α -corrections to the cumulants. Needless to say, the corresponding expressions quickly become quite unwieldy (even though the computation remains conceptually simple). One possible strategy is to include only $\mathcal{O}(\alpha)$ corrections, and check that $\mathcal{O}(\alpha^2)$ terms remain sub-leading. In order for this criterium to be satisfactory, one should correctly identify the expansion parameter. As we shall see, in the case with no derivatives involved in eq. (E.0.10) the latter turns out to be $\alpha^2 \sigma_0^2$.
- We can conclude this part with few checks of eqs. (E.0.33, E.0.41). For simplicity, let us consider the case in which there are no derivatives in eq. (E.0.10).

$n = 2$

We compute $C_2(h_1, h_2)$. At order $\mathcal{O}(\alpha)$, we have

$$C_2(h_1, h_2) = C_2(\mathcal{R}_1, \mathcal{R}_2) + C_2[f_{\text{NL}}(\mathcal{R}_1), \mathcal{R}_2] + C_2[\mathcal{R}_1, f_{\text{NL}}(\mathcal{R}_2)] \quad (\text{E.0.42})$$

$$= \langle \mathcal{R}_1 \mathcal{R}_2 \rangle + \langle f_{\text{NL}}^{(1)}(\mathcal{R}_1) \rangle \langle \mathcal{R}_1 \mathcal{R}_2 \rangle + \langle f_{\text{NL}}^{(1)}(\mathcal{R}_2) \rangle \langle \mathcal{R}_1 \mathcal{R}_2 \rangle, \quad (\text{E.0.43})$$

where we use eq. (E.0.5) to rewrite the first term (which is the gaussian one) and eq. (E.0.33) to rewrite the last two ones. Since we have $f_{\text{NL}}(\mathcal{R}) = \alpha \mathcal{R}^2$, we have $\langle f_{\text{NL}}^{(1)}(\mathcal{R}_{i=1,2}) \rangle = 0$ since we are considering zero-mean random fields. This means that there are no corrections at order $\mathcal{O}(\alpha)$. We now move to consider corrections at order $\mathcal{O}(\alpha^2)$. We use eq. (E.0.37). At order $\mathcal{O}(\alpha^2)$, we have

$$C_2(h_1, h_2) = \langle \mathcal{R}_1 \mathcal{R}_2 \rangle + \langle f_{\text{NL}}(\mathcal{R}_1) f_{\text{NL}}(\mathcal{R}_2) \rangle - \langle f_{\text{NL}}(\mathcal{R}_1) \rangle \langle f_{\text{NL}}(\mathcal{R}_2) \rangle = \quad (\text{E.0.44})$$

$$= \langle \mathcal{R}_1 \mathcal{R}_2 \rangle + \alpha^2 \langle \mathcal{R}_1^2 \mathcal{R}_2^2 \rangle - \alpha^2 \langle \mathcal{R}_1^2 \rangle \langle \mathcal{R}_2^2 \rangle. \quad (\text{E.0.45})$$

We now set the two points equal (since we are not considering derivatives of cumulants, there is no need of considering different spatial point). We have $\langle \mathcal{R}^2 \rangle = \sigma_0^2$ and $\langle \mathcal{R}^4 \rangle = 3\sigma_0^4$. In conclusion, we find

$$C_2(h, h) = \sigma_0^2 (1 + 2\alpha^2 \sigma_0^2). \quad (\text{E.0.46})$$

This is an exact result since corrections of order $\mathcal{O}(\alpha^3)$ enter only at higher-orders. As a rule of thumb, for a cumulant C_n of order n , only corrections up to order $\mathcal{O}(\alpha^n)$ are possible. Eq. (E.0.46) shows that the correct expansion parameter is $\alpha^2 \sigma_0^2$. In realistic models of inflation we expect $\alpha = \mathcal{O}(1)$ while we have $\sigma_0^2 = A_g$ for the specific power spectrum in eq. (C.0.24). Since one typically has $A_g = \mathcal{O}(10^{-3})$, we expect $\alpha^2 \sigma_0^2 \ll 1$. Let us also notice that in applications of cosmological interest it is customary to use $f_{\text{NL}}(\mathcal{R}) = \alpha(\mathcal{R}^2 - \langle \mathcal{R}^2 \rangle)$ since in this way one has a zero-mean non-gaussian field h , $\langle h \rangle = 0$. It is simple to see that the constant shift in $f_{\text{NL}}(\mathcal{R})$ that is implied by this particular choice does not affect the computation of cumulants of order equal or higher than two. However, it does change the first order cumulant since $C_1(h) = \langle h \rangle$ (see eq. (E.0.4)). The choice $f_{\text{NL}}(\mathcal{R}) = \alpha(\mathcal{R}^2 - \langle \mathcal{R}^2 \rangle)$, therefore, leads to $C_1(h) = 0$.

$n = 3$

Consider now $C_3(h_1, h_2, h_3)$. This cumulant vanishes in the gaussian limit. At order $\mathcal{O}(\alpha)$, we use eq. (E.0.33) and compute

$$C_3(h_1, h_2, h_3) = C_3[f_{\text{NL}}(\mathcal{R}_1), \mathcal{R}_2, \mathcal{R}_3] + C_3[\mathcal{R}_1, f_{\text{NL}}(\mathcal{R}_2), \mathcal{R}_3] + C_3[\mathcal{R}_1, \mathcal{R}_2, f_{\text{NL}}(\mathcal{R}_3)] \quad (\text{E.0.47})$$

$$= 2\alpha (\langle \mathcal{R}_1 \mathcal{R}_2 \rangle \langle \mathcal{R}_1 \mathcal{R}_3 \rangle + \langle \mathcal{R}_2 \mathcal{R}_1 \rangle \langle \mathcal{R}_2 \mathcal{R}_3 \rangle + \langle \mathcal{R}_3 \mathcal{R}_1 \rangle \langle \mathcal{R}_3 \mathcal{R}_2 \rangle). \quad (\text{E.0.48})$$

If we set all points equal, we find

$$C_3(h, h, h) = 6\alpha\sigma_0^4. \quad (\text{E.0.49})$$

We now move to consider the possible presence of a correction at order $\mathcal{O}(\alpha^2)$ that can be computed by means of eq. (E.0.41). As already noticed, for $n = 3$ the sum $\sum_{a,b}$ does not contribute to the final result. We are left with the two terms

$$\left[\langle f_{\text{NL}}^{(1)}(\mathcal{R}_1) f_{\text{NL}}(\mathcal{R}_2) \rangle - \langle f_{\text{NL}}^{(1)}(\mathcal{R}_1) \rangle \langle f_{\text{NL}}(\mathcal{R}_2) \rangle \right] \langle \mathcal{R}_1 \mathcal{R}_3 \rangle + \quad (\text{E.0.50})$$

$$+ \left[\langle f_{\text{NL}}(\mathcal{R}_1) f_{\text{NL}}^{(1)}(\mathcal{R}_2) \rangle - \langle f_{\text{NL}}(\mathcal{R}_1) \rangle \langle f_{\text{NL}}^{(1)}(\mathcal{R}_2) \rangle \right] \langle \mathcal{R}_2 \mathcal{R}_3 \rangle. \quad (\text{E.0.51})$$

If we set the three points equal and consider explicitly $f_{\text{NL}}(\mathcal{R}) = \alpha\mathcal{R}^2$, we find that eq. (E.0.50) reduces to $4\alpha^2 \langle \mathcal{R}^3 \rangle \sigma_0^2$ which is zero because $\langle \mathcal{R}^3 \rangle = 0$. Eq. (E.0.49), however, is not an exact result since for $n = 3$ corrections of order $\mathcal{O}(\alpha^3)$ are possible. Mimicking eq. (E.0.46), we expect

$$C_3(h, h, h) = 6\alpha\sigma_0^4 [1 + \mathcal{O}(\alpha^2 \sigma_0^2)]. \quad (\text{E.0.52})$$

The correction of order $\mathcal{O}(\alpha^3)$ can not be computed by means of eq. (E.0.41) but it is expected to be sub-leading since we work under the assumption that $\alpha^2 \sigma_0^2 \ll 1$.

$n = 4$

Consider the fourth-order cumulant $C_4(h_1, h_2, h_3, h_4)$. If we limit the analysis to quadratic non-gaussianities as in $f_{\text{NL}}(\mathcal{R}) = \alpha\mathcal{R}^2$, it is clear that there are no corrections of order $\mathcal{O}(\alpha)$ since $f_{\text{NL}}^{(3)}(\mathcal{R}) = 0$. The first non-trivial correction arises at order $\mathcal{O}(\alpha^2)$

$$C_4(h_1, h_2, h_3, h_4) = C_4[f_{\text{NL}}(\mathcal{R}_1), f_{\text{NL}}(\mathcal{R}_2), \mathcal{R}_3, \mathcal{R}_4] + 5 \text{ combinations}. \quad (\text{E.0.53})$$

If we take eq. (E.0.41) it is simple to see that the first two terms on the right-hand side give vanishing contribution. In the last line, we have one contribution corresponding to $a = b = 1$ that gives two terms since one has to sum $3 \leftrightarrow 4$ exchange. We have

$$C_4[f_{\text{NL}}(\mathcal{R}_1), f_{\text{NL}}(\mathcal{R}_2), \mathcal{R}_3, \mathcal{R}_4] = \quad (\text{E.0.54})$$

$$= \left[\langle f_{\text{NL}}^{(1)}(\mathcal{R}_1) f_{\text{NL}}^{(1)}(\mathcal{R}_2) \rangle - \langle f_{\text{NL}}^{(1)}(\mathcal{R}_1) \rangle \langle f_{\text{NL}}^{(1)}(\mathcal{R}_2) \rangle \right] (\langle \mathcal{R}_1 \mathcal{R}_4 \rangle \langle \mathcal{R}_2 \mathcal{R}_3 \rangle + 3 \leftrightarrow 4) =$$

$$= 4\alpha^2 \langle \mathcal{R}_1 \mathcal{R}_2 \rangle (\langle \mathcal{R}_1 \mathcal{R}_4 \rangle \langle \mathcal{R}_2 \mathcal{R}_3 \rangle + \langle \mathcal{R}_1 \mathcal{R}_3 \rangle \langle \mathcal{R}_2 \mathcal{R}_4 \rangle). \quad (\text{E.0.55})$$

If we set all points equal and multiply by six because of eq. (E.0.53), we find

$$C_4(h, h, h, h) = 48\alpha^2 \sigma_0^6 [1 + \mathcal{O}(\alpha^2 \sigma_0^2)], \quad (\text{E.0.56})$$

where we introduced again a sub-leading correction of order $\mathcal{O}(\alpha^4)$.

We can check the validity of eqs. (E.0.46, E.0.52, E.0.56) explicitly. The reason is that if we limit the analysis—as done here—to random variables *without derivatives*, the computation of the cumulants of h admits an exact analytical solution. We can indeed extract the probability density distribution of the random variable h —at a given spatial point, that is what we need in order to compare with eqs. (E.0.46, E.0.52, E.0.56)—by means of the Jacobi's multivariate theorem in eq. (E.0.23) using the fact that \mathcal{R} is a gaussian variable with zero mean and variance σ_0^2 . We find

$$p(h) = \frac{e^{-\mathcal{R}_+^2/2\sigma_0^2} + e^{-\mathcal{R}_-^2/2\sigma_0^2}}{\sqrt{2\pi}\sigma_0\sqrt{1+4\alpha h}}, \quad \text{where } \mathcal{R}_\pm = \frac{-1 \pm \sqrt{1+4\alpha h}}{2\alpha}, \quad (\text{E.0.57})$$

with $h \in [-1/4\alpha, \infty)$. By means of the Faà di Bruno's formula, we find the generic n^{th} -order cumulant²

$$C_n(h, \dots, h) = 2^{n-3} \sigma_0^2 (\alpha \sigma_0^2)^{n-2} (n + 4\alpha^2 \sigma_0^2) (n-1)!, \quad (\text{E.0.58})$$

One can check that eqs. (E.0.46, E.0.52, E.0.56) are correctly reproduced in the appropriate limits.

- Since in the case with no derivatives the probability density distribution can be obtained analytically (see eq. (E.0.57)), it is instructive to do the following exercise. First of all, let us rewrite eq. (E.0.57) for the case with $f_{\text{NL}}(\mathcal{R}) = \alpha(\mathcal{R}^2 - \langle \mathcal{R}^2 \rangle)$ with $\langle \mathcal{R}^2 \rangle = \sigma_0^2$. We find

$$p(h) = \frac{e^{-\mathcal{R}_+^2/2\sigma_0^2} + e^{-\mathcal{R}_-^2/2\sigma_0^2}}{\sqrt{2\pi}\sigma_0\sqrt{1+4\alpha(h+\alpha\sigma_0^2)}}, \quad \text{where } \mathcal{R}_\pm = \frac{-1 \pm \sqrt{1+4\alpha(h+\alpha\sigma_0^2)}}{2\alpha}. \quad (\text{E.0.59})$$

² From the probability density distribution we compute the moments $\mu_n = \int_{-1/4\alpha}^{\infty} dh h^n p(h)$. The explicit expression for the n^{th} cumulant in terms of the first n moments can be obtained by using Faà di Bruno's formula for higher derivatives of composite functions; explicitly, for $n \geq 2$, we have $C_n = \sum_{k=1}^n (-1)^{k-1} (k-1)! B_{n,k}(0, \mu_2, \dots, \mu_{n-k+1})$, where $B_{n,k}$ are the incomplete Bell polynomials.

In this case we have $C_1(h) = 0$ while $C_n(h, \dots, h) \equiv C_n(h)$ are still given by eq. (E.o.58). We can compute analytically the characteristic function $\log \chi(\lambda) = \sum_{n=2}^{\infty} (i^n/n!) C_n(h) \lambda^n$. We find

$$\chi(\lambda) = \exp \left[-\frac{\lambda^2 \sigma_0^2}{2(1 - 2i\alpha\lambda\sigma_0^2)} - i\alpha\lambda\sigma_0^2 \right] \frac{1}{\sqrt{1 - 2i\alpha\lambda\sigma_0^2}}, \quad (\text{E.o.60})$$

and one can check for consistency that $p(h)$ in eq. (E.o.59) is given by the inverse Fourier transform

$$p(h) = \frac{1}{2\pi} \int_{-\infty}^{\infty} d\lambda \chi(\lambda) e^{-ih\lambda}. \quad (\text{E.o.61})$$

Once we know $p(h)$, we can compute the integral $\bar{p}(h_c) \equiv \int_{h_c}^{\infty} dh p(h)$, which is the probability to find h above the threshold h_c . We find

$$\bar{p}_{\text{NG}}(h_c) = \frac{1}{2} \left[2 - \text{Erf} \left(\frac{1 + \sqrt{1 + 4h_c\alpha + 4\alpha^2\sigma_0^2}}{2\sqrt{2}\alpha\sigma_0} \right) - \text{Erf} \left(\frac{-1 + \sqrt{1 + 4h_c\alpha + 4\alpha^2\sigma_0^2}}{2\sqrt{2}\alpha\sigma_0} \right) \right], \quad (\text{E.o.62})$$

with $\text{Erf}(x)$ the error function. This simple case, therefore, can be solved exactly. This means that we can use it as a playground to test the following approximation. Let us organize the sum over cumulants in a power-series expansion in α . We have

$$\sum_{n=2}^{\infty} \frac{i^n}{n!} C_n(h) \lambda^n = -\frac{\sigma_0^2 \lambda^2}{2} - i\alpha\lambda^3 \sigma_0^4 + \alpha^2 \sigma_0^4 (-\lambda^2 + 2\lambda^4 \sigma_0^2) + \mathcal{O}(\alpha^3), \quad (\text{E.o.63})$$

where the first term on the right-hand side corresponds to the quadratic cumulant that reproduces the gaussian limit. We can truncate eq. (E.o.63) at some order in α , compute the corresponding $\bar{p}(h_c)$ and compare with eq. (E.o.62). At order α^0 , we find the gaussian result

$$\bar{p}_{\text{G}}(h_c) = \frac{1}{2} \text{Erf} \left(\frac{h_c}{\sqrt{2}\sigma_0} \right) \approx \frac{1}{\sqrt{2\pi}v_c} \exp \left(-\frac{v_c^2}{2} \right), \quad (\text{E.o.64})$$

where we define $v_c \equiv h_c/\sigma_0$, and the last approximation corresponds to $v_c \gg 1$ which is the limit that is relevant for our analysis. Consider now the order $\mathcal{O}(\alpha)$. Let us write eq. (E.o.62) at order $\mathcal{O}(\alpha)$ as $\bar{p}_{\alpha}(h_c) = \int_{h_c}^{\infty} dh p_{\alpha}(h)$ with

$$\begin{aligned} p_{\alpha}(h) &= \frac{1}{2\pi} \int_{-\infty}^{\infty} d\lambda \exp \left[-\frac{\sigma_0^2 \lambda^2}{2} - i(\alpha\sigma_0)\lambda^3 \sigma_0^3 \right] e^{-ih\lambda} = \\ &= \frac{1}{2\pi} \int_{-\infty}^{\infty} d\lambda e^{-\sigma_0^2 \lambda^2/2} \left[\sum_{m=0}^{\infty} \frac{(-i\alpha\sigma_0^4)^m}{m!} \right] \underbrace{\lambda^{3m} e^{-ih\lambda}}_{i^{3m} \frac{\partial^{3m} e^{-ih\lambda}}{\partial h^{3m}}} = \\ &= \sum_{m=0}^{\infty} \frac{(-i\alpha\sigma_0^4)^m}{m!} i^{3m} \frac{\partial^{3m}}{\partial h^{3m}} \underbrace{\frac{1}{2\pi} \int_{-\infty}^{\infty} d\lambda e^{-\sigma_0^2 \lambda^2/2} e^{-ih\lambda}}_{\text{gaussian integral } \frac{1}{\sqrt{2\pi}\sigma_0} e^{-h^2/2\sigma_0^2}} \equiv \sum_{m=0}^{\infty} p_{\alpha}^{(m)}(h). \end{aligned} \quad (\text{E.o.65})$$

In practice, we can approximate $\bar{p}_\alpha(h_c)$ as a sum of terms, $\bar{p}_\alpha(h_c) = \sum_{m=0}^{\infty} \bar{p}_\alpha^{(m)}(h_c)$ each one of them defined by means of eq. (E.o.65), that is $\bar{p}_\alpha^{(m)}(h_c) = \int_{h_c}^{\infty} dh p_\alpha^{(m)}(h)$. A similar decomposition can be defined at higher orders in α . At order $\mathcal{O}(\alpha)$, we find

$$\bar{p}_\alpha^{(1)}(h_c) = \frac{1}{\sqrt{2\pi v_c}} \exp\left(-\frac{v_c^2}{2}\right) (\alpha\sigma_0) v_c^3 \left(1 - \frac{1}{v_c^2}\right), \quad (\text{E.o.66})$$

$$\bar{p}_\alpha^{(2)}(h_c) = \frac{1}{\sqrt{2\pi v_c}} \exp\left(-\frac{v_c^2}{2}\right) (\alpha\sigma_0)^2 \frac{v_c^6}{2} \left(1 - \frac{10}{v_c^2} + \frac{15}{v_c^4}\right), \quad (\text{E.o.67})$$

$$\bar{p}_\alpha^{(3)}(h_c) = \frac{1}{\sqrt{2\pi v_c}} \exp\left(-\frac{v_c^2}{2}\right) (\alpha\sigma_0)^3 \frac{v_c^9}{6} \left(1 - \frac{28}{v_c^2} + \frac{210}{v_c^4} - \frac{420}{v_c^6} + \frac{105}{v_c^8}\right) \quad (\text{E.o.68})$$

$$\bar{p}_\alpha^{(4)}(h_c) = \dots$$

Since $v_c \gg 1$, we are tempted to approximate (by neglecting all sub-leading terms in each of the round brackets)

$$\bar{p}_\alpha^{(m)}(h_c) = \frac{1}{\sqrt{2\pi v_c}} \exp\left(-\frac{v_c^2}{2}\right) \frac{(\alpha\sigma_0 v_c^3)^m}{m!} \implies \bar{p}_\alpha(h_c) = \frac{1}{\sqrt{2\pi v_c}} \exp\left(-\frac{v_c^2}{2} + \alpha\sigma_0 v_c^3\right). \quad (\text{E.o.69})$$

We are now in the position to compare *i*) the gaussian result in eq. (E.o.64), *ii*) the exact non-gaussian result in eq. (E.o.62), *iii*) the order $\mathcal{O}(\alpha)$ approximation $\bar{p}_\alpha(h_c) = \sum_{m=0}^{\infty} \bar{p}_\alpha^{(m)}(h_c)$ obtained by truncating the series for increasing values of m and *iv*) the order $\mathcal{O}(\alpha)$ approximation resummed as in eq. (E.o.69). This comparison is shown in the left panel of fig. 14.

We can now consider the order $\mathcal{O}(\alpha^2)$. We find

$$\bar{p}_{\alpha^2}^{(1)}(h_c) = \frac{1}{\sqrt{2\pi v_c}} \exp\left(-\frac{v_c^2}{2}\right) (\alpha\sigma_0) \left[v_c^3 \left(1 - \frac{1}{v_c^2}\right) + 2v_c^4 \alpha\sigma_0 \left(1 - \frac{5}{2v_c^2}\right) \right], \quad (\text{E.o.70})$$

$$\begin{aligned} \bar{p}_{\alpha^2}^{(2)}(h_c) = & \frac{1}{\sqrt{2\pi v_c}} \exp\left(-\frac{v_c^2}{2}\right) (\alpha\sigma_0)^2 \times \\ & \left[\frac{v_c^6}{2} \left(1 - \frac{10}{v_c^2} + \frac{15}{v_c^4}\right) + 2\alpha\sigma_0 v_c^7 \left(1 - \frac{29}{2v_c^2} + \frac{42}{v_c^4} - \frac{27}{2v_c^6}\right) + 2(\alpha\sigma_0)^2 v_c^8 \left(1 - \frac{20}{v_c^2} + \frac{381}{4v_c^4} - \frac{363}{4v_c^6}\right) \right], \end{aligned} \quad (\text{E.o.71})$$

$$\bar{p}_{\alpha^2}^{(3)}(h_c) = \dots$$

We are again tempted to consider the limit $v_c \gg 1$ in which we keep only the leading term inside the round brackets, meaning that we write

$$\bar{p}_{\alpha^2}^{(1)}(h_c) = \frac{1}{\sqrt{2\pi v_c}} \exp\left(-\frac{v_c^2}{2}\right) (\alpha\sigma_0) (v_c^3 + 2v_c^4 \alpha\sigma_0), \quad (\text{E.o.72})$$

$$\bar{p}_{\alpha^2}^{(2)}(h_c) = \frac{1}{\sqrt{2\pi v_c}} \exp\left(-\frac{v_c^2}{2}\right) (\alpha\sigma_0)^2 \left[\frac{v_c^6}{2} + 2\alpha\sigma_0 v_c^7 + 2(\alpha\sigma_0)^2 v_c^8 \right], \quad (\text{E.o.73})$$

$$\bar{p}_{\alpha^2}^{(3)}(h_c) = \dots$$

In this case, we find that the series $\bar{p}_{\alpha^2}(h_c) = \sum_{m=0}^{\infty} \bar{p}_{\alpha^2}^{(m)}(h_c)$ can be resummed, and we get the neat expression

$$\bar{p}_{\alpha^2}(h_c) = \frac{1}{\sqrt{2\pi v_c}} \exp\left[-\frac{v_c^2}{2} + \alpha\sigma_0 v_c^3(1 + 2\alpha\sigma_0 v_c)\right]. \quad (\text{E.o.74})$$

We can do the same comparison we did before, and compare *i*) the gaussian result in eq. (E.o.64), *ii*) the exact non-gaussian result in eq. (E.o.62), *iii*) the order $\mathcal{O}(\alpha^2)$ approximation $\bar{p}_{\alpha^2}(h_c) = \sum_{m=0}^{\infty} \bar{p}_{\alpha^2}^{(m)}(h_c)$ obtained by truncating the series at increasing values of m and *iv*) the order $\mathcal{O}(\alpha^2)$ approximation resummed as in eq. (E.o.74). This comparison is shown in the right panel of fig. 14.

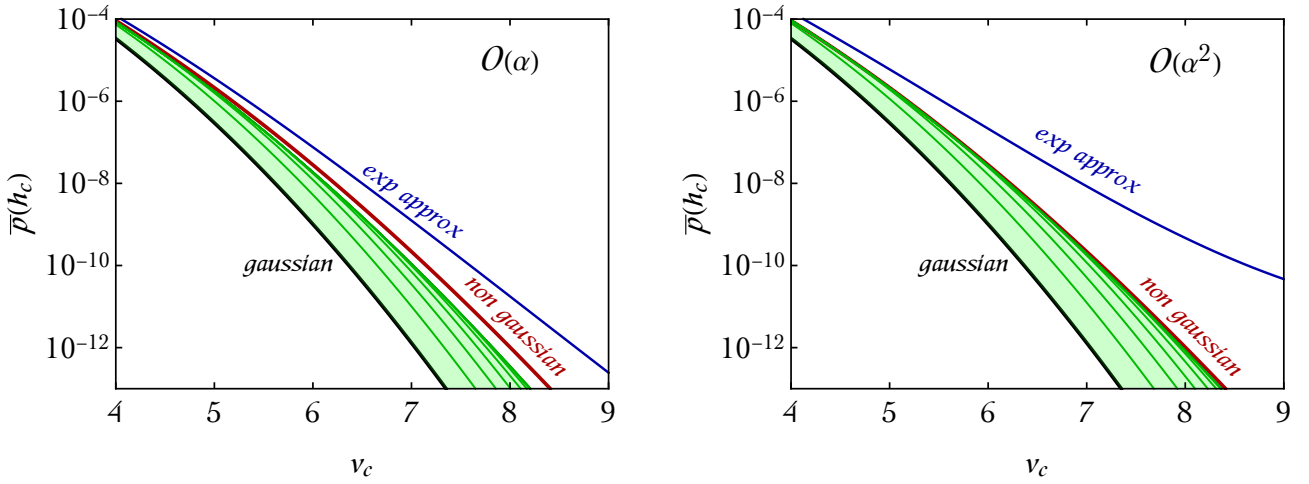


Figure 14: Left panel. We compare at order $\mathcal{O}(\alpha)$ the exact non-gaussian expression for $\bar{p}(h_c)$ (defined below eq. (E.o.61)) given in eq. (E.o.62) with: *i*) its gaussian limit (eq. (E.o.64)), *ii*) its power-series expansion $\bar{p}_{\alpha}(h_c) = \sum_{m=0}^{\infty} \bar{p}_{\alpha}^{(m)}(h_c)$ for increasing values of m (green region) and *iii*) the resummed expression (labelled “exp approx”) given in eq. (E.o.69). For illustration, we take $\sigma_0 = 0.1$ and $\alpha = 0.2$. Right panel. Same as in the left panel but at order $\mathcal{O}(\alpha^2)$.

The simplified setup studied in this exercise is conceptually different compared to the actual problem we are facing (since we are only considering here the non-gaussian random field h without any information about its derivatives) but, as we shall discuss later, we will use an approximation scheme very similar to the one adopted above. It is, therefore, instructive to draw some conclusions (this is particularly important in light of the fact that in the case without derivatives we know the exact form of the probability density distribution). Consider first the $\mathcal{O}(\alpha)$ approximation illustrated in the left panel of fig. 14. The sum $\bar{p}_{\alpha}(h_c) = \sum_{m=0}^{\infty} \bar{p}_{\alpha}^{(m)}(h_c)$ (truncated at some finite m ; in the plot we show the cases with $m \leq 9$) already gives a good—even though not optimal—approximation of $\bar{p}_{\text{NG}}(h_c)$. On the contrary, the resummed expression in eq. (E.o.69), more simple to handle, tends to overestimate the true

result. Consider now the $\mathcal{O}(\alpha^2)$ approximation illustrated in the right panel of fig. 14. The sum $\bar{p}_{\alpha^2}(h_c) = \sum_{m=0}^{\infty} \bar{p}_{\alpha^2}^{(m)}(h_c)$ (truncated at some finite m ; in the plot we show the cases with $m \leq 9$) gives an excellent approximation of $\bar{p}_{\text{NG}}(h_c)$. On the contrary, it is evident that the resummed expression in eq. (E.0.74) quickly diverges from the true result and can not be trusted.

The reason why the exponential approximation deviates from the exact result can be identified already at order $\mathcal{O}(\alpha)$. Consider (in units of $\bar{p}_G(h_c)$) the first term in eq. (E.0.66) that we kept in our expansion, that is $(\alpha\sigma_0)v_c^3$, and compare it with one of the terms that we neglected in eq. (E.0.68), for instance the fourth in the round brackets $-70(\alpha\sigma_0)^3v_c^3$. These two terms have the same power of v_c but the latter is parametrically suppressed by $(\alpha\sigma_0)^2$. It is true that we expect $(\alpha\sigma_0)^2 \sim 10^{-2} \ll 1$ but we also have an extra numerical factor -70 that partially compensate the suppression. On similar ground, neglecting the term $-(14/3)(\alpha\sigma_0)^3v_c^7$ in eq. (E.0.68) compared to the terms that we kept in eq. (E.0.66) and eq. (E.0.67) seems not justifiable.

We conclude that the exponential approximations in eq. (E.0.69) and eq. (E.0.74) can not be considered as acceptably good proxies for the exact result since they may overestimate it by many orders of magnitude. However, in order to have a good approximation of the exact result it is more proper to decompose $\bar{p}_{\alpha}(h_c) = \sum_{m=0}^{\infty} \bar{p}_{\alpha}^{(m)}(h_c)$ (or even better at order $\mathcal{O}(\alpha^2)$) and sum over m up to some finite value according to the desired accuracy.

After this digression, we are finally ready to compute the non-gaussian cumulants for the random variables h, h_i, h_{ij} . For simplicity, we start again from the two-dimensional case, and we have six random variables $\{h, h_x, h_y, h_{xx}, h_{xy}, h_{yy}\}$. We consider the non-gaussian function $f_{\text{NL}}(\mathcal{R}) = \alpha(\mathcal{R}^2 - \langle \mathcal{R}^2 \rangle)$ since in this case we have $C_1(h) = \langle h \rangle = 0$. Furthermore, in order to fully exploit the properties of homogeneity and isotropy (see discussion below eq. (C.0.9)), it is useful to change basis to the complex conjugated random variables $\{h, h_z, h_{z^*}, h_{zz}, h_{zz^*}, h_{z^*z^*}\}$.³

All first-order cumulants vanish. This is true for $C_1(h) = \langle h \rangle = 0$ as discussed before. As far as the other first-order cumulants are concerned, we have for instance $C_1(h_z) = \langle h_z \rangle = \partial_z \langle h \rangle = 0$ which vanishes (even without imposing $C_1(h) = 0$) because $\langle h \rangle$ does not depend, as a consequence of homogeneity, on the specific spatial point at which it is computed. Similarly, we have C_1 also for the remaining random variables.

³ The following relations turn out to be useful. For a generic function $f(x, y) : \mathbb{R}^2 \rightarrow \mathbb{R}$ we have $f_z = (f_x - if_y)/2$, $f_{z^*} = (f_x + if_y)/2$ and

$$f_{zz^*} = \frac{1}{4}(f_{xx} + f_{yy}), \quad f_{zz} = \frac{1}{4}(f_{xx} - f_{yy} - 2if_{xy}), \quad f_{z^*z^*} = \frac{1}{4}(f_{xx} - f_{yy} + 2if_{xy}). \quad (\text{E.0.75})$$

The stationary point condition $f_x = f_y = 0$ becomes $f_z = 0$ (hence $f_{z^*} = 0$). The condition $f_{xx}f_{yy} - f_{xy}^2 > 0$ that separates extrema from saddle points becomes $f_{zz^*}^2 > f_{zz}f_{z^*z^*} = |f_{zz}|^2$ that is $f_{zz^*} < -|f_{zz}| \vee f_{zz^*} > |f_{zz}|$ (equivalently, $|f_{zz^*}| > |f_{zz}|$). Notice that f_{zz^*} is real. Maxima correspond to the condition $f_{zz^*} < 0$ while minima are identified by $f_{zz^*} > 0$.

As far as the second-order cumulants are concerned, we find the following non-zero entries

$$\begin{array}{c}
 \begin{array}{cccccc}
 & \mathbf{h} & \mathbf{h}_z & \mathbf{h}_{z^*} & \mathbf{h}_{zz} & \mathbf{h}_{zz^*} & \mathbf{h}_{z^*z^*} \\
 \mathbf{h} & C_2(\mathbf{h}, \mathbf{h}) & 0 & 0 & 0 & C_2(\mathbf{h}, \mathbf{h}_{zz^*}) & 0 \\
 \mathbf{h}_z & 0 & 0 & C_2(\mathbf{h}_z, \mathbf{h}_{z^*}) & 0 & 0 & 0 \\
 \mathbf{h}_{z^*} & 0 & C_2(\mathbf{h}_z, \mathbf{h}_{z^*}) & 0 & 0 & 0 & 0 \\
 \mathbf{h}_{zz} & 0 & 0 & 0 & 0 & 0 & C_2(\mathbf{h}_{zz}, \mathbf{h}_{z^*z^*}) \\
 \mathbf{h}_{zz^*} & C_2(\mathbf{h}, \mathbf{h}_{zz^*}) & 0 & 0 & 0 & C_2(\mathbf{h}_{zz^*}, \mathbf{h}_{zz^*}) & 0 \\
 \mathbf{h}_{z^*z^*} & 0 & 0 & 0 & C_2(\mathbf{h}_{zz}, \mathbf{h}_{z^*z^*}) & 0 & 0
 \end{array} \\
 \end{array} \Bigg) , \tag{E.o.76}$$

with

$$C_2(\mathbf{h}, \mathbf{h}) = \sigma_0^2(1 + 2\alpha^2\sigma_0^2), \tag{E.o.77}$$

$$C_2(\mathbf{h}_z, \mathbf{h}_{z^*}) = \frac{\sigma_1^2}{4}(1 + 4\alpha^2\sigma_0^2), \tag{E.o.78}$$

$$C_2(\mathbf{h}, \mathbf{h}_{zz^*}) = -\frac{\sigma_1^2}{4}(1 + 4\alpha^2\sigma_0^2), \tag{E.o.79}$$

$$C_2(\mathbf{h}_{zz}, \mathbf{h}_{z^*z^*}) = C_2(\mathbf{h}_{zz^*}, \mathbf{h}_{zz^*}) = \frac{\sigma_2^2}{16} \left[1 + 4\alpha^2 \left(\frac{2\sigma_1^4}{\sigma_2^2} + \sigma_0^2 \right) \right]. \tag{E.o.80}$$

At order $\mathcal{O}(\alpha)$, all non-gaussian corrections vanish. We already computed $C_2(\mathbf{h}, \mathbf{h})$ in eq. (E.o.46). It is instructive to consider explicitly few more cases. The relevant equations are eq. (E.o.10), eq. (E.o.33), eq. (E.o.37) and eq. (E.o.41).

Consider for instance the computation of $C_2(\mathbf{h}_z, \mathbf{h}_{z^*})$. We have

$$C_2(\mathbf{h}_z, \mathbf{h}_{z^*}) \stackrel{\text{eq. (E.o.10)}}{=} \partial_{z_1} \partial_{z_2^*} C_2(\mathbf{h}_1, \mathbf{h}_2) \Big|_{\bar{x}_1 = \bar{x}_2} \tag{E.o.81}$$

$$\begin{aligned}
 &= \partial_{z_1} \partial_{z_2^*} \{ C_2(\mathcal{R}_1, \mathcal{R}_2) + C_2[f_{\text{NL}}(\mathcal{R}_1), \mathcal{R}_2] + C_2[\mathcal{R}_1, f_{\text{NL}}(\mathcal{R}_2)] + C_2[f_{\text{NL}}(\mathcal{R}_1), f_{\text{NL}}(\mathcal{R}_2)] \} \Big|_{\bar{x}_1 = \bar{x}_2} \\
 &= \partial_{z_1} \partial_{z_2^*} \left[\underbrace{\langle \mathcal{R}_1 \mathcal{R}_2 \rangle + \langle f_{\text{NL}}^{(1)}(\mathcal{R}_1) \rangle \langle \mathcal{R}_1 \mathcal{R}_2 \rangle + \langle f_{\text{NL}}^{(1)}(\mathcal{R}_2) \rangle \langle \mathcal{R}_1 \mathcal{R}_2 \rangle}_{\mathcal{O}(\alpha), \text{ eq. (E.o.33)}} + \underbrace{\langle f_{\text{NL}}(\mathcal{R}_1) f_{\text{NL}}(\mathcal{R}_2) \rangle - \langle f_{\text{NL}}(\mathcal{R}_1) \rangle \langle f_{\text{NL}}(\mathcal{R}_2) \rangle}_{\mathcal{O}(\alpha^2), \text{ eq. (E.o.37)}} \right] \Big|_{\bar{x}_1 = \bar{x}_2}
 \end{aligned}$$

$$= \langle \mathcal{R}_z \mathcal{R}_{z^*} \rangle + 2 \langle f_{\text{NL}}^{(1)}(\mathcal{R}) \rangle \langle \mathcal{R}_z \mathcal{R}_{z^*} \rangle + \alpha^2 \partial_{z_1} \partial_{z_2^*} \langle \mathcal{R}_1^2 \mathcal{R}_2^2 \rangle \Big|_{\bar{x}_1 = \bar{x}_2} \tag{E.o.82}$$

$$= \langle \mathcal{R}_z \mathcal{R}_{z^*} \rangle + 4\alpha^2 \langle \mathcal{R}^2 \mathcal{R}_z \mathcal{R}_{z^*} \rangle. \tag{E.o.83}$$

Eq. (E.o.82) follows from the fact that the expectation values $\langle f_{\text{NL}}(\mathcal{R}) \rangle$ and $\langle f_{\text{NL}}^{(1)}(\mathcal{R}) \rangle$ do not depend, because of homogeneity, on the specific spatial point at which they are evaluated and, therefore, their spatial derivatives vanish. Eq. (E.o.83) follows from the fact that $\langle f_{\text{NL}}^{(1)}(\mathcal{R}) \rangle = 2\alpha \langle \mathcal{R} \rangle = 0$; at order $\mathcal{O}(\alpha^2)$, we moved the derivatives inside the statistical average and set $\bar{x}_1 = \bar{x}_2$. In eq. (E.o.83) we

have $\langle \mathcal{R}_z \mathcal{R}_{z^*} \rangle = (\langle \mathcal{R}_x \mathcal{R}_x \rangle + \langle \mathcal{R}_y \mathcal{R}_y \rangle)/4 = \sigma_1^2/4$ and $\langle \mathcal{R}^2 \mathcal{R}_z \mathcal{R}_{z^*} \rangle = \langle \mathcal{R}^2 (\mathcal{R}_x^2 + \mathcal{R}_y^2) \rangle/4$. This statistical average can be computed by means of the multivariate normal distribution in eq. (C.0.13)

$$\begin{aligned} \langle \mathcal{R}^2 (\mathcal{R}_x^2 + \mathcal{R}_y^2) \rangle &= \int d\mathcal{R} d\mathcal{R}_x d\mathcal{R}_y d\mathcal{R}_{xx} d\mathcal{R}_{xy} d\mathcal{R}_{yy} \mathcal{R}^2 (\mathcal{R}_x^2 + \mathcal{R}_y^2) P(\mathcal{R}_x) P(\mathcal{R}_y) P(\mathcal{R}_{xy}) P(\mathcal{R}, \mathcal{R}_{xx}, \mathcal{R}_{yy}) \\ &= \underbrace{\int d\mathcal{R}_x d\mathcal{R}_y (\mathcal{R}_x^2 + \mathcal{R}_y^2) P(\mathcal{R}_x) P(\mathcal{R}_y)}_{=\sigma_1^2} \underbrace{\int d\mathcal{R}_{xy} P(\mathcal{R}_{xy})}_{=1} \underbrace{\int d\mathcal{R} \mathcal{R}^2 \int d\mathcal{R}_{xx} d\mathcal{R}_{yy} P(\mathcal{R}, \mathcal{R}_{xx}, \mathcal{R}_{yy})}_{=\frac{1}{\sqrt{2\pi\sigma_0^2}} \exp(-\mathcal{R}^2/2\sigma_0^2)}, \end{aligned} \quad (\text{E.o.84})$$

and, from the explicit computation of the integrals, we get $\langle \mathcal{R}^2 (\mathcal{R}_x^2 + \mathcal{R}_y^2) \rangle = \sigma_0^2 \sigma_1^2$. All in all, we find $C_2(h_z, h_{z^*}) = \sigma_1^2 (1 + 4\alpha^2 \sigma_0^2)/4$. All the remaining non-zero entries in eq. (E.0.76) can be derived in the same way.

In eq. (E.0.76) the zero entries vanish as a consequence of isotropy. We can introduce again the parameter $\kappa \equiv (\#z^* \text{ derivatives in } C_2) - (\#z \text{ derivatives in } C_2)$ and set to zero all cumulants with $\kappa \neq 0$ since not invariant under spatial rotations. The reasoning that we followed in the gaussian case for the computations of the two-point correlators (see discussion below eq. (C.0.9)) applies also in the case of generic n^{th} -order cumulants. This is because cumulants are functions of moments (see eqs. (E.0.4-E.0.7)). Furthermore, the relation between $C_2(h_z, h_{z^*})$ and $C_2(h, h_{zz^*})$ can be understood as a consequence of homogeneity.

We now move to consider the third-order cumulants. Based on isotropy, we expect only a handful of non-zero cumulants (that are those with $\kappa = 0$) that we list in table 2.

We already computed $C_3(h, h, h) = 6\alpha\sigma_0^4$ in eq. (E.0.52). As far as the remaining cumulants are concerned, we find

$$C_3(h, h_z, h_{z^*}) = \alpha\sigma_0^2\sigma_1^2, \quad (\text{E.o.85})$$

$$C_3(h, h, h_{zz^*}) = -2\alpha\sigma_0^2\sigma_1^2, \quad (\text{E.o.86})$$

$$C_3(h, h_{zz^*}, h_{zz^*}) = \frac{\alpha}{8} (3\sigma_1^4 + 2\sigma_0^2\sigma_2^2), \quad (\text{E.o.87})$$

$$C_3(h, h_{zz}, h_{z^*z^*}) = \frac{\alpha}{4} \sigma_0^2 \sigma_2^2, \quad (\text{E.o.88})$$

$$C_3(h_z, h_{z^*}, h_{zz^*}) = -\frac{\alpha}{8} \sigma_1^4, \quad (\text{E.o.89})$$

$$C_3(h_z, h_z, h_{z^*z^*}) = C_3(h_{z^*}, h_{z^*}, h_{zz}) = \frac{\alpha}{4} \sigma_1^4, \quad (\text{E.o.90})$$

$$C_3(h_{zz^*}, h_{zz^*}, h_{zz^*}) = -\frac{3\alpha}{16} \sigma_1^2 \sigma_2^2, \quad (\text{E.o.91})$$

$$C_3(h_{zz}, h_{z^*z^*}, h_{zz^*}) = -\frac{\alpha}{16} \sigma_1^2 \sigma_2^2. \quad (\text{E.o.92})$$

No derivatives	2 derivatives	4 derivatives	6 derivatives
$C_3(\mathbf{h}, \mathbf{h}, \mathbf{h})$ ×1	$C_3(\mathbf{h}, \mathbf{h}, \mathbf{h}_{zz^*})$ ×3	$C_3(\mathbf{h}, \mathbf{h}_{zz^*}, \mathbf{h}_{zz^*})$ ×3	$C_3(\mathbf{h}_{zz^*}, \mathbf{h}_{zz^*}, \mathbf{h}_{zz^*})$ ×1
	$C_3(\mathbf{h}, \mathbf{h}_z, \mathbf{h}_{z^*})$ ×6	$C_3(\mathbf{h}_z, \mathbf{h}_{z^*}, \mathbf{h}_{zz^*})$ ×6	$C_3(\mathbf{h}_{zz}, \mathbf{h}_{z^*z^*}, \mathbf{h}_{zz^*})$ ×6
		$C_3(\mathbf{h}, \mathbf{h}_{zz}, \mathbf{h}_{z^*z^*})$ ×6	
		$C_3(\mathbf{h}_z, \mathbf{h}_z, \mathbf{h}_{z^*z^*})$ ×3	
		$C_3(\mathbf{h}_{z^*}, \mathbf{h}_{z^*}, \mathbf{h}_{zz})$ ×3	

Table 2: Third-order cumulants for the random variables $\{\mathbf{h}, \mathbf{h}_z, \mathbf{h}_{z^*}, \mathbf{h}_{zz}, \mathbf{h}_{zz^*}, \mathbf{h}_{z^*z^*}\}$ that are non-zero based on isotropy. For these cumulants, we have $\kappa \equiv (\#z^* \text{ derivatives in } C_3) - (\#z \text{ derivatives in } C_3) = 0$. We gather together in each column cumulants with the same number of spatial derivatives (cumulants without derivatives in the first column, with two derivatives in the second, four in the third and so on). For each entry, the tiny numbers in the second row indicate the multiplicity of the corresponding cumulant due to distinct permutations of its arguments.

We find that corrections at order $\mathcal{O}(\alpha^2)$ vanish for all third-order cumulants listed before⁴. However, as already discussed in the case of eq. (E.0.52), eqs. (E.0.85-E.0.92) are not exact because we expect the presence of $\mathcal{O}(\alpha^3)$ corrections we did not include. It is simple to check that properties of homogeneity are respected by the explicit expressions in eqs. (E.0.85-E.0.92). For instance, from $\partial_{z^*} C_3(\mathbf{h}_z, \mathbf{h}_z, \mathbf{h}_{z^*}) = 0$ we find $2C_3(\mathbf{h}_z, \mathbf{h}_{z^*}, \mathbf{h}_{zz^*}) = -C_3(\mathbf{h}_z, \mathbf{h}_z, \mathbf{h}_{z^*z^*})$ that is indeed verified by eq. (E.0.89) and eq. (E.0.90). Similarly, from $\partial_{z^*} C_3(\mathbf{h}, \mathbf{h}, \mathbf{h}_z) = 0$ we have $C_3(\mathbf{h}, \mathbf{h}, \mathbf{h}_{zz^*}) = -2C_3(\mathbf{h}, \mathbf{h}_z, \mathbf{h}_{z^*})$ that is indeed verified by eq. (E.0.85) and eq. (E.0.86).

After computing the cumulants at the desired order in α , we are finally ready to take the last step in our computation. From the cumulants, we will reconstruct the characteristic function and, via an inverse Fourier transform, the probability density distribution. Few technical remarks are in order

⁴ This happens because the $\mathcal{O}(\alpha^2)$ contribute to $C_3(\mathbf{h}_1, \mathbf{h}_2, \mathbf{h}_3)$ is:

$$\Delta C_3(\mathbf{h}_1, \mathbf{h}_2, \mathbf{h}_3) = 2\alpha^2 \left[\langle \mathcal{R}_1 \mathcal{R}_2 \rangle \langle \mathcal{R}_3^2 (\mathcal{R}_1 + \mathcal{R}_2) \rangle + \langle \mathcal{R}_2 \mathcal{R}_3 \rangle \langle \mathcal{R}_1^2 (\mathcal{R}_2 + \mathcal{R}_3) \rangle + \langle \mathcal{R}_3 \mathcal{R}_1 \rangle \langle \mathcal{R}_2^2 (\mathcal{R}_3 + \mathcal{R}_1) \rangle \right]$$

Thus, when we derive and then we set $\bar{x}_1 = \bar{x}_2 = \bar{x}_3$, following the prescription (E.0.10) and we return to the $\{x, y\}$ basis, we see that all the terms have the form $\langle \xi_{j_1}, \xi_{j_2}, \xi_{j_3} \rangle$, where $\xi_{j_k} \in \{\mathcal{R}, \mathcal{R}_x, \mathcal{R}_y, \mathcal{R}_{xx}, \mathcal{R}_{xy}, \mathcal{R}_{yy}\}$. These are third order moments of a gaussian multivariate distribution, which are vanishing.

because it is crucial to properly identify the variables participating to the Fourier transforms. The inverse Fourier transform of the first line in eq. (E.0.1) is given by

$$P(\xi_1, \dots, \xi_N) = \int \frac{d\lambda_1}{(2\pi)} \dots \frac{d\lambda_N}{(2\pi)} \chi(\lambda_1, \dots, \lambda_N) \exp[-i(\xi_1 \lambda_1 + \dots + \xi_N \lambda_N)]. \quad (\text{E.o.93})$$

Both eq. (E.0.1) and eq. (E.0.93) are valid for real variables. The simplest identification, therefore, would be $\{\xi_{i=1, \dots, 6}\} = \{h, h_x, h_y, h_{xx}, h_{xy}, h_{yy}\}$. However, we found more efficient to work with $\{h, h_z, h_{z^*}, h_{zz}, h_{zz^*}, h_{z^*z^*}\}$ since properties like isotropy become more transparent. Among these variables, h and h_{zz^*} are real while h_z and h_{zz} are complex (with conjugated variables given by h_{z^*} and $h_{z^*z^*}$, respectively). In this case a suitable choice of real variables, therefore, is $\{\xi_{i=1, \dots, 6}\} = \{h, \text{Re}h_z, \text{Im}h_z, \text{Re}h_{zz}, h_{zz^*}, \text{Im}h_{zz}\}$ with the obvious relations

$$\text{Re}h_z = (h_z + h_{z^*})/2, \quad \text{Im}h_z = -i(h_z - h_{z^*})/2, \quad \text{Re}h_{zz} = (h_{zz} + h_{z^*z^*})/2, \quad \text{Im}h_{zz} = -i(h_{zz} - h_{z^*z^*})/2. \quad (\text{E.o.94})$$

Consequently, we introduce their Fourier counterparts $\{\lambda_{i=1, \dots, 6}\} \equiv \{\lambda, \lambda_{\text{Re}h_z}, \lambda_{\text{Im}h_z}, \lambda_{\text{Re}h_{zz}}, \lambda_{z z^*}, \lambda_{\text{Im}h_{zz}}\}$ such that the characteristic function in eq. (E.0.1) is given by the integral

$$\int dh d\text{Re}h_z d\text{Im}h_z d\text{Re}h_{zz} dh_{z z^*} d\text{Im}h_{zz} \quad (\text{E.o.95})$$

$$P(h, h_z, h_{z^*}, h_{zz}, h_{z z^*}, h_{z^*z^*}) \exp[i(h\lambda + \text{Re}h_z \lambda_{\text{Re}h_z} + \text{Im}h_z \lambda_{\text{Im}h_z} + \dots)].$$

Consider, for instance, the two terms $\text{Re}h_z \lambda_{\text{Re}h_z} + \text{Im}h_z \lambda_{\text{Im}h_z}$ in the argument of the exponential. By means of eqs. (E.0.94) we can simply rewrite $\text{Re}h_z \lambda_{\text{Re}h_z} + \text{Im}h_z \lambda_{\text{Im}h_z} = h_z \lambda_z^* + h_{z^*} \lambda_z$ if we define $\lambda_z \equiv (\lambda_{\text{Re}h_z} + i\lambda_{\text{Im}h_z})/2$. Notice that in this case we have $\lambda_{\text{Re}h_z} = 2\text{Re}\lambda_z$ and $\lambda_{\text{Im}h_z} = 2\text{Im}\lambda_z$. We can, therefore, use λ_z as the complex Fourier variable associated to h_{z^*} (and, correspondingly, its conjugated λ_z^* associated to h_z). Similarly, we introduce $\lambda_{zz} \equiv (\lambda_{\text{Re}h_{zz}} + i\lambda_{\text{Im}h_{zz}})/2$, and the exponential function in eq. (E.0.95) reads $\exp\{i[h\lambda + h_{z z^*} \lambda_{z z^*} + (h_z \lambda_z^* + h_{z z^*} \lambda_z + \text{c.c.})]\}$. We are now in the position to consider explicitly the inverse Fourier transform of eq. (E.0.95). As integration variables, instead of $\lambda_{\text{Re}h_z}, \lambda_{\text{Im}h_z}, \lambda_{\text{Re}h_{zz}}, \lambda_{\text{Im}h_{zz}}$ we use λ_z and λ_{zz} introduced before by means of the relations $\lambda_{\text{Re}h_z} = 2\text{Re}\lambda_z, \lambda_{\text{Im}h_z} = 2\text{Im}\lambda_z, \lambda_{\text{Re}h_{zz}} = 2\text{Re}\lambda_{zz}$ and $\lambda_{\text{Im}h_{zz}} = 2\text{Im}\lambda_{zz}$. We have

$$P(h, h_z, h_{z^*}, h_{zz}, h_{z z^*}, h_{z^*z^*}) = \int \frac{d\lambda}{(2\pi)} \frac{d\text{Re}\lambda_z}{\pi} \frac{d\text{Im}\lambda_z}{\pi} \frac{d\lambda_{z z^*}}{(2\pi)} \frac{d\text{Re}\lambda_{zz}}{\pi} \frac{d\text{Im}\lambda_{zz}}{\pi} \quad (\text{E.o.96})$$

$$\chi(\lambda, \lambda_z, \lambda_{zz}, \lambda_{z z^*}) \exp\{-i[h\lambda + h_{z z^*} \lambda_{z z^*} + (h_z \lambda_z^* + h_{z z^*} \lambda_z + \text{c.c.})]\},$$

with of course $\lambda_z = \text{Re}\lambda_z + i\text{Im}\lambda_z$ and $\lambda_{zz} = \text{Re}\lambda_{zz} + i\text{Im}\lambda_{zz}$. The natural log of the characteristic function $\log \chi(\lambda, \lambda_z, \lambda_{zz}, \lambda_{z z^*})$ is written, according to eq. (E.0.3), as a series expansion in terms of the cumulants with respect to the Fourier variables $\{\lambda, \lambda_z, \lambda_{zz}, \lambda_{z z^*}\}$ (remember that λ_z and λ_{zz} are

complex variables while λ and λ_{zz^*} are real). The first non-gaussian correction arises at order $\mathcal{O}(\alpha)$ and reads

$$\begin{aligned} \log \chi(\lambda, \lambda_z, \lambda_{zz}, \lambda_{zz^*}) = & \tag{E.o.97} \\ & -\frac{1}{2}C_2(h, h)\lambda^2 - C_2(h_z, h_{z^*})|\lambda_z|^2 - C_2(h, h_{zz^*})\lambda\lambda_{zz^*} - C_2(h_{zz}, h_{z^*z^*})|\lambda_{zz}|^2 - \frac{1}{2}C_2(h_{zz^*}, h_{zz^*})\lambda_{zz^*}^2 \\ & -\frac{i}{6}C_3(h, h, h)\lambda^3 - \frac{i}{2}C_3(h, h, h_{zz^*})\lambda^2\lambda_{zz^*} - iC_3(h, h_z, h_{z^*})\lambda|\lambda_z|^2 - \frac{i}{2}C_3(h, h_{zz^*}, h_{zz^*})\lambda\lambda_{zz^*}^2 \\ & - iC_3(h, h_{zz}, h_{z^*z^*})\lambda|\lambda_{zz}|^2 - iC_3(h_z, h_{z^*}, h_{zz^*})|\lambda_z|^2\lambda_{zz^*} - \frac{i}{2}C_3(h_z, h_z, h_{z^*z^*})(\lambda_z^*)^2\lambda_{zz} \\ & -\frac{i}{2}C_3(h_{z^*}, h_{z^*}, h_{zz})\lambda_z^2\lambda_{zz}^* - \frac{i}{6}C_3(h_{zz^*}, h_{zz^*}, h_{zz^*})\lambda_{zz^*}^3 - iC_3(h_{zz}, h_{z^*z^*}, h_{zz^*})|\lambda_{zz}|^2\lambda_{zz^*}, \end{aligned}$$

where the second-order cumulants given in eq. (E.o.76) are taken at order $\mathcal{O}(\alpha)$ and, therefore, coincide with their gaussian limit. Notice that each term in the series expansion enters with a coefficient that counts its multiplicity (explicitly written in table 2). This follows from the fact that in the last line in eq. (E.o.1) there are different terms that give the same contribution. The integration in eq. (E.o.96) gives the probability density distribution $P(h, h_z, h_{z^*}, h_{zz}, h_{zz^*}, h_{z^*z^*})$. After computing $P(h, h_z, h_{z^*}, h_{zz}, h_{zz^*}, h_{z^*z^*})$, it is also possible to reconstruct $P(h, h_x, h_y, h_{xx}, h_{xy}, h_{yy})$ by means of the Jacobi's multivariate theorem in eq. (E.o.14) using the transformation in eq. (E.o.75).

It is possible to check this procedure in the gaussian limit $\alpha \rightarrow 0$. In the gaussian limit only the second-order cumulants survive (with $\alpha \rightarrow 0$ taken in the corresponding expressions given in eq. (E.o.76)). The inverse Fourier transform in eq. (E.o.96) can be computed analytically in the gaussian limit, and one gets $P(\mathcal{R}, \mathcal{R}_z, \mathcal{R}_{z^*}, \mathcal{R}_{zz}, \mathcal{R}_{zz^*}, \mathcal{R}_{z^*z^*})$ where we used \mathcal{R} instead of h since $\alpha \rightarrow 0$. The determinant of the Jacobian matrix is $|\det J(\mathcal{R}, \mathcal{R}_x, \mathcal{R}_y, \mathcal{R}_{xx}, \mathcal{R}_{xy}, \mathcal{R}_{yy})| = 1/64$, and Jacobi's multivariate theorem gives precisely eq. (C.o.13). This is a non-trivial check that our procedure is technically correct.

In the presence of local non-gaussianities, the computation of eq. (E.o.96) is much more complicated because $\chi(\lambda, \lambda_z, \lambda_{zz}, \lambda_{zz^*})$ in eq. (E.o.97) is an exponential function whose argument is a polynomial of cubic order. A possible solution strategy is the following. Let us write eq. (E.o.96) in the schematic form (we use for illustration a generic set of variables $\{\lambda_{i=1, \dots, N}\}$ that in the actual computation must be replaced with $\{\lambda, \lambda_z, \lambda_{zz}, \lambda_{zz^*}\}$)

$$\chi(\lambda_i) = \exp[p_2(\lambda_i) + p_3(\lambda_i)] = \exp[p_2(\lambda_i)] \exp[p_3(\lambda_i)] = \exp[p_2(\lambda_i)] \sum_{m=0}^{\infty} \frac{1}{m!} p_3(\lambda_i)^m, \tag{E.o.98}$$

where $p_2(\lambda_i)$ is the quadratic polynomial in $\{\lambda_i\}$ that corresponds to the gaussian limit $\alpha \rightarrow 0$ while $p_3(\lambda_i)$ is the cubic polynomial that contains $\mathcal{O}(\alpha)$ deviations. At a given order m in the series expansion defined by eq. (E.o.98), the inverse Fourier integral in eq. (E.o.96) can be computed analytically. This is because we can make use of the following identity (the sum over k is understood)

$$\begin{aligned} & \int d\lambda_1 \dots \lambda_N (\lambda_i^n \dots \lambda_j^m) \exp[p_2(\lambda_i)] \exp(-i\lambda_k h_k) = \\ & = (i)^n \dots (i)^m \frac{\partial^n}{\partial h_i^n} \dots \frac{\partial^m}{\partial h_j^m} \int d\lambda_1 \dots \lambda_N \exp[p_2(\lambda_i)] \exp(-i\lambda_k h_k), \end{aligned} \tag{E.o.99}$$

where the last integral is nothing but the gaussian integral that can be easily computed. We go along with this strategy, that we summarize for ease of reading in the following.

- i) For fixed m , we compute the probability density distribution in eq. (E.0.96) performing the inverse Fourier transform by means of the trick in eq. (E.0.98) and eq. (E.0.99).
- ii) We transform $P(h, h_z, h_{z^*}, h_{zz}, h_{zz^*}, h_{z^*z^*})$ into $P(h, h_x, h_y, h_{xx}, h_{xy}, h_{yy})$ by means of Jacobi's multivariate theorem (as illustrated before for the gaussian case).
- iii) We set $h_x = h_y = 0$, and compute the number density of local maxima $n_{\max}(h)$ according to the general definition in eq. (C.0.5) (with of course h instead of \mathcal{R} , and working in two spatial dimensions).
- iv) We use the same change of variables proposed in eq. (C.0.17) (with again h instead of \mathcal{R}), and we integrate over θ, r, h and s in the domain defining maxima, as discussed in the gaussian case; similarly, we implement the same lower bound of integration over s given by the threshold condition for black hole formation in eq. (C.0.36). Notice that in the following we will set the lower limit of integration over h to be $h_{\min} = -\infty$ despite the fact that we have $h_{\min} = -(1 + 4\alpha^2\sigma_0^2)/4\alpha$ for $h = \mathcal{R} + \alpha(\mathcal{R}^2 - \sigma_0^2)$ and $\mathcal{R} \in (-\infty, +\infty)$. Approximating h_{\min} with its gaussian value allows to obtain close analytical formulas. We shall justify the validity of this approximation at the end of this section.
- v) Finally, we define the mass fraction of black holes as in eq. (C.0.35).

We now illustrate the result of this procedure. Needless to say, the term with $m = 0$ reproduces the gaussian result in eq. (C.0.35). The first correction is given by the term with $m = 1$. Let us introduce for the sake of simplicity the notation $\beta = \beta_G + \sum_{m=1}^{\infty} \beta_{\text{NG}}^{(\alpha, m)}$ with β_G given by eq. (C.0.35). We find

$$\beta_{\text{NG}}^{(\alpha, 1)} = \left(\frac{\alpha\sigma_1^2}{\sigma_2} \right) \frac{2\sqrt{2}}{\pi^{3/2}} e^{-6s_{\min}^2/\sigma_2^2} \left[\frac{s_{\min}^2}{\sigma_2^2} + e^{4s_{\min}^2/\sigma_2^2} \left(-\frac{s_{\min}^2}{\sigma_2^2} + 4\frac{s_{\min}^4}{\sigma_2^4} \right) \right]. \quad (\text{E.0.100})$$

For $m = 2$, we find

$$\beta_{\text{NG}}^{(\alpha, 2)} = \left(\frac{\alpha\sigma_1^2}{\sigma_2} \right)^2 \frac{e^{-6s_{\min}^2/\sigma_2^2}}{3\pi^{3/2}} \left\{ 2\sqrt{3}\pi e^{6s_{\min}^2/\sigma_2^2} \text{Erfc} \left(\frac{\sqrt{6}s_{\min}}{\sigma_2} \right) + 3\sqrt{2} \frac{s_{\min}}{\sigma_2} \left[7 - 40\frac{s_{\min}^2}{\sigma_2^2} + 48\frac{s_{\min}^4}{\sigma_2^4} \right. \right. \\ \left. \left. + e^{4s_{\min}^2/\sigma_2^2} \left(-3 + 68\frac{s_{\min}^2}{\sigma_2^2} - 176\frac{s_{\min}^4}{\sigma_2^4} + 64\frac{s_{\min}^6}{\sigma_2^6} \right) \right] \right\}. \quad (\text{E.0.101})$$

For increasing values of m the corresponding expressions of $\beta_{\text{NG}}^{(m)}$ become more lengthy and less transparent, and we do not report them explicitly. On the contrary, we make use of the same expansion introduced in eq. (C.0.35) for $s_{\min}/\sigma_2 \gtrsim 1$. Interestingly, in this limit we find that the generic term $\beta_{\text{NG}}^{(\alpha, m)}$ can be written as

$$\beta_{\text{NG}}^{(\alpha, m)} \approx \left[\left(\frac{s_{\min}^3}{\sigma_2^3} \right) \frac{\alpha\sigma_1^2}{\sigma_2} \right]^m \frac{2^{4m-1/2}}{\pi^{3/2} m!} \left(\frac{s_{\min}}{\sigma_2} \right) e^{-2s_{\min}^2/\sigma_2^2}, \quad (\text{E.0.102})$$

and the sum $\sum_{m=1}^{\infty} \beta_{\text{NG}}^{(\alpha, m)}$ admits the following analytical form

$$\sum_{m=1}^{\infty} \beta_{\text{NG}}^{(\alpha, m)} \approx \frac{1}{\sqrt{2\pi}^{3/2}} \left(\frac{s_{\text{min}}}{\sigma_2} \right) e^{-2s_{\text{min}}^2/\sigma_2^2} \left\{ -1 + \exp \left[16 \left(\frac{s_{\text{min}}^3}{\sigma_2^3} \right) \frac{\alpha \sigma_1^2}{\sigma_2} \right] \right\}. \quad (\text{E.o.103})$$

The sum $\beta = \beta_{\text{G}} + \sum_{m=1}^{\infty} \beta_{\text{NG}}^{(\alpha, m)}$ gives

$$\beta \approx \frac{1}{\sqrt{2\pi}^{3/2}} \left(\frac{s_{\text{min}}}{\sigma_2} \right) \exp \left[-\frac{2s_{\text{min}}^2}{\sigma_2^2} + 16 \left(\frac{s_{\text{min}}^3}{\sigma_2^3} \right) \frac{\alpha \sigma_1^2}{\sigma_2} \right]. \quad (\text{E.o.104})$$

Notice that the structure of this equation is analogue to the one that we found in eq. (E.o.69).

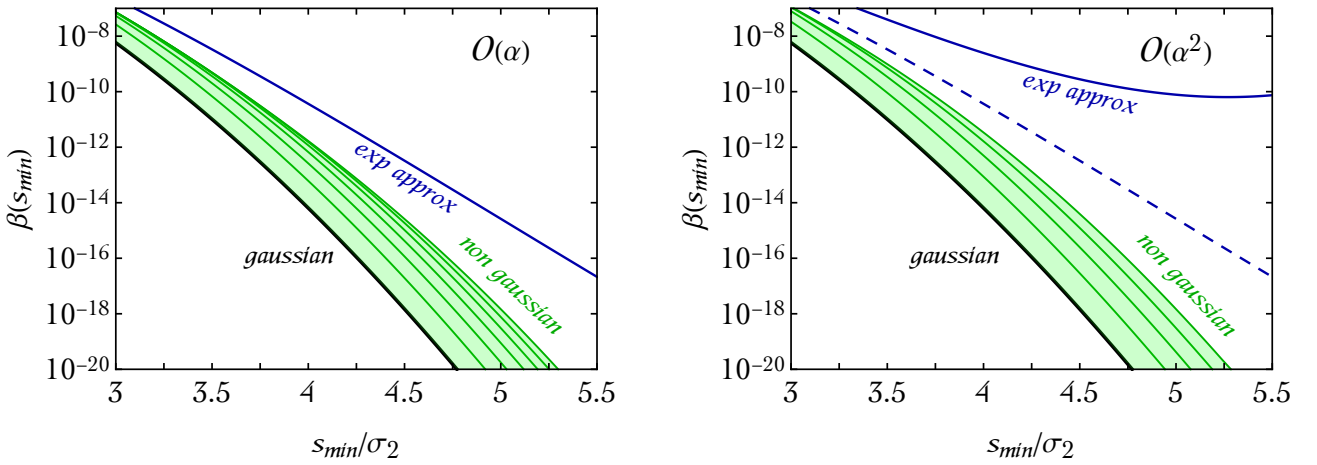


Figure 15: Left panel. We compare the gaussian approximation for β given in eq. (C.o.35) with i) its power-series expansion $\beta = \beta_{\text{G}} + \sum_{m=1}^{\infty} \beta_{\text{NG}}^{(\alpha, m)}$ computed at order $\mathcal{O}(\alpha)$ for increasing values of m (green region, with the thin solid green lines that label the case $m = 1, \dots, 6$) and ii) the resummed expression (labelled “exp approx”) given in eq. (E.o.104). Right panel. Same as in the left panel but at order $\mathcal{O}(\alpha^2)$ and up to $m = 4$. In both panels we consider the log-normal model for the power spectrum, and we use the benchmark values $\nu = 0.6$ and $\mathcal{P}_{\mathcal{R}}(k_*) = 5 \times 10^{-3}$. We take $\alpha = 0.2$.

Before proceeding, let us come back to the issue of the lower limit of integration over h . As anticipated, from the very same definition $h = \mathcal{R} + \alpha(\mathcal{R}^2 - \sigma_0^2)$ it follows that $h > h_{\text{min}} = -(1 + \alpha^2 \sigma_0^2)/4\alpha$. To be precise, therefore, this lower limit of integration should be implemented when computing the non-gaussian contributions $\beta_{\text{NG}}^{(\alpha, m)}$. However, implementing the gaussian lower limit of integration $h_{\text{min}} = -\infty$ does not change qualitatively our results, and the reason is the following. When computing β , we only focus on maxima with large curvature $-\nabla^2 h/\sigma_2$ since they correspond to peak of the overdensity field. The value of $-\nabla^2 h/\sigma_2$ is positively correlated with the value of h/σ_0 , and the amount of correlation is controlled by the parameter γ . This fact was illustrated in appendix C in the gaussian case, and it remains valid also in the presence of non-gaussianities (for the values of α that are relevant for our analysis). When $\gamma \rightarrow 1$, the correlation is maximal and

regions with large $-\nabla^2 h/\sigma_2$ are also regions with positive $h/\sigma_0 \gtrsim 1$. This means that regions where h takes negative values are completely irrelevant for our purposes. In the cases that are relevant for our analysis, we typically have $\gamma \sim 0.6$; we checked numerically (using for simplicity the log-normal power spectrum, and integrating numerically over s) that the value of $\beta_{\text{NG}}^{(\alpha, m)}$ computed with the proper lower bound of integration over h remain equal to those obtained with the gaussian limit $h_{\text{min}} \rightarrow -\infty$. In order to see some deviation, one should consider the opposite limit $\gamma \rightarrow 0$. In this limit $-\nabla^2 h/\sigma_2$ and h/σ_0 are only weakly correlated and it is therefore possible to find regions with large $-\nabla^2 h/\sigma_2$ in which h takes negative values. In such situation, of course, implementing the correct lower limit of integration over h becomes important. However, cases with $\gamma \rightarrow 0$ fall outside the class of models we are considering in this paper.

We compare in the left panel of fig. 15 the series $\beta = \beta_G + \sum_{m=1}^{m_{\text{max}}} \beta_{\text{NG}}^{(\alpha, m)}$, truncated at some finite m_{max} , with the resummed expression in eq. (E.0.104). We show the cases $m_{\text{max}} = 1, \dots, 6$ and we use the log-normal power spectrum in eq. (C.0.24) to compute the spectral parameters. The situation is very similar to what already discussed in fig. 14, and we can exploit the knowledge that we gained from that case to argue the following conclusions. The series $\beta = \beta_G + \sum_{m=1}^{m_{\text{max}}} \beta_{\text{NG}}^{(\alpha, m)}$ shows a convergence towards the order $\mathcal{O}(\alpha)$ approximation (that is, we recall, the approximation in which we only include the leading part of the third-order cumulants) of the exact non-gaussian result while the exponential approximation overestimates the abundance.

We move to consider corrections at order $\mathcal{O}(\alpha^2)$. We already computed in eqs. (E.0.77-E.0.80) the second-order cumulants at order $\mathcal{O}(\alpha^2)$. In addition, we need to compute the fourth-order cumulants at order $\mathcal{O}(\alpha^2)$. We computed in eq. (E.0.56) the simplest one without derivatives, $C_4(h, h, h, h) = 48\alpha^2 \sigma_0^6$. The remaining non-zero cumulants are summarized in table 3. We find the following explicit expressions

$$C_4(h, h, h, h_{zz^*}) = -18\alpha^2 \sigma_0^4 \sigma_1^2, \quad (\text{E.0.105})$$

$$C_4(h, h, h_z, h_{z^*}) = 6\alpha^2 \sigma_0^4 \sigma_1^2, \quad (\text{E.0.106})$$

$$C_4(h, h, h_{zz}, h_{z^*z^*}) = \frac{3\alpha^2}{2} \sigma_0^4 \sigma_2^2, \quad (\text{E.0.107})$$

$$C_4(h, h, h_{zz^*}, h_{zz^*}) = \frac{\alpha^2}{2} \sigma_0^2 (10\sigma_1^4 + 3\sigma_0^2 \sigma_2^2), \quad (\text{E.0.108})$$

$$C_4(h, h_z, h_{z^*}, h_{zz^*}) = -\frac{3\alpha^2}{2} \sigma_0^2 \sigma_1^4, \quad (\text{E.0.109})$$

$$C_4(h, h_z, h_z, h_{z^*z^*}) = C_4(h, h_{z^*}, h_{z^*}, h_{zz}) = \alpha^2 \sigma_0^2 \sigma_1^4, \quad (\text{E.0.110})$$

$$C_4(h_z, h_z, h_{z^*}, h_{z^*}) = 2\alpha^2 \sigma_0^2 \sigma_1^4, \quad (\text{E.0.111})$$

$$C_4(h_z, h_{z^*}, h_{zz^*}, h_{zz^*}) = \frac{\alpha^2}{4} \sigma_1^2 (\sigma_1^4 + \sigma_0^2 \sigma_2^2), \quad (\text{E.0.112})$$

$$C_4(h_z, h_z, h_{z^*z^*}, h_{zz^*}) = C_4(h_{z^*}, h_{z^*}, h_{zz}, h_{zz^*}) = 0, \quad (\text{E.0.113})$$

$$(\text{E.0.114})$$

No derivatives	2 derivatives	4 derivatives	6 derivatives	8 derivatives
$C_4(h, h, h, h)$ ×1	$C_4(h, h, h, h_{zz^*})$ ×4	$C_4(h, h, h_{zz}, h_{z^*z^*})$ ×12	$C_4(h_z, h_{z^*}, h_{zz^*}, h_{zz^*})$ ×12	$C_4(h_{zz}, h_{zz}, h_{z^*z^*}, h_{z^*z^*})$ ×6
	$C_4(h, h, h_z, h_{z^*})$ ×12	$C_4(h, h, h_{zz^*}, h_{zz^*})$ ×6	$C_4(h_z, h_z, h_{z^*z^*}, h_{zz^*})$ ×12	$C_4(h_{zz^*}, h_{zz^*}, h_{zz^*}, h_{zz^*})$ ×1
		$C_4(h, h_z, h_{z^*}, h_{zz^*})$ ×24	$C_4(h_{z^*}, h_{z^*}, h_{zz}, h_{zz^*})$ ×12	$C_4(h_{zz}, h_{z^*z^*}, h_{zz^*}, h_{zz^*})$ ×12
		$C_4(h, h_z, h_z, h_{z^*z^*})$ ×12	$C_4(h, h_{zz^*}, h_{zz^*}, h_{zz^*})$ ×4	
		$C_4(h, h_{z^*}, h_{z^*}, h_{zz})$ ×12	$C_4(h, h_{zz}, h_{z^*z^*}, h_{zz^*})$ ×24	
		$C_4(h_z, h_z, h_{z^*}, h_{z^*})$ ×6	$C_4(h_z, h_{z^*}, h_{zz}, h_{z^*z^*})$ ×24	

Table 3: Fourth-order cumulants for the random variables $\{h, h_z, h_{z^*}, h_{zz}, h_{zz^*}, h_{z^*z^*}\}$ that are non-zero based on isotropy. For these cumulants, we have $\kappa \equiv (\#z^* \text{ derivatives in } C_4) - (\#z \text{ derivatives in } C_4) = 0$. As in table 2, we gather together in each column cumulants with the same number of spatial derivatives (cumulants without derivatives in the first column, with two derivatives in the second, four in the third and so on). For each entry, the tiny numbers in the second row indicate the multiplicity of the corresponding cumulant due to distinct permutations of its arguments.

$$C_4(h, h_{zz^*}, h_{zz^*}, h_{zz^*}) = -\frac{3\alpha^2}{4} \sigma_1^2 (\sigma_1^4 + 2\sigma_0^2 \sigma_2^2), \quad (\text{E.o.115})$$

$$C_4(h, h_{zz}, h_{z^*z^*}, h_{zz^*}) = -\frac{\alpha^2}{2} \sigma_0^2 \sigma_1^2 \sigma_2^2, \quad (\text{E.o.116})$$

$$C_4(h_z, h_{z^*}, h_{zz}, h_{z^*z^*}) = \frac{\alpha^2}{4} \sigma_1^2 (\sigma_1^4 + \sigma_0^2 \sigma_2^2), \quad (\text{E.o.117})$$

$$C_4(h_{zz}, h_{zz}, h_{z^*z^*}, h_{z^*z^*}) = \frac{\alpha^2}{8} \sigma_0^2 \sigma_2^4, \quad (\text{E.o.118})$$

$$C_4(h_{zz^*}, h_{zz^*}, h_{zz^*}, h_{zz^*}) = \frac{3\alpha^2}{16} \sigma_2^2 (3\sigma_1^4 + \sigma_0^2 \sigma_2^2), \quad (\text{E.o.119})$$

$$C_4(h_{zz}, h_{z^*z^*}, h_{zz^*}, h_{zz^*}) = \frac{\alpha^2}{32} \sigma_2^2 (3\sigma_1^4 + 2\sigma_0^2 \sigma_2^2), \quad (\text{E.o.120})$$

that we derive as before using eq. (E.o.10) and eq. (E.o.41). Conceptually, the rest of the computation follows again points *i-v*) discussed below eq. (E.o.99). At the technical level, instead of eq. (E.o.98) we now have

$$\chi(\lambda_i) = \exp[p_2(\lambda_i) + p_4(\lambda_i)] = \exp[p_2(\lambda_i)] \exp[p_4(\lambda_i)] = \exp[p_2(\lambda_i)] \sum_{m=0}^{\infty} \frac{1}{m!} p_4(\lambda_i)^m, \quad (\text{E.o.121})$$

where $p_4(\lambda_i)$ is the quartic polynomial that contains $\mathcal{O}(\alpha)$ and $\mathcal{O}(\alpha^2)$ deviations. The computation of the abundance follows the same prescription discussed before, and we introduce the series

expansion $\beta = \beta_G + \sum_{m=1}^{m_{\max}} \beta_{\text{NG}}^{(\alpha^2, m)}$ with β_G given by eq. (C.0.35) and $\beta_{\text{NG}}^{(\alpha^2, m)}$ which corresponds to the series in eq. (E.0.121) truncated at some $m > 0$. For instance, we find (with $\bar{s}_{\min} \equiv s_{\min}/\sigma_2$ and $\gamma = \sigma_1^2/\sigma_2\sigma_0$)

$$\begin{aligned} \beta_{\text{NG}}^{(\alpha^2, 1)} &= \\ &= \frac{\sqrt{2}\alpha\sigma_0\bar{s}_{\min}}{\pi^{3/2}} e^{-2\bar{s}_{\min}^2} \left[\alpha(2 + \gamma^2)\sigma_0 - 2\gamma\bar{s}_{\min} - 4\alpha(5 + 8\gamma^2)\sigma_0\bar{s}_{\min}^2 + 8\gamma\bar{s}_{\min}^3 + 16\alpha(1 + 3\gamma^2)\sigma_0\bar{s}_{\min}^4 \right] + \mathcal{O}(e^{-6\bar{s}_{\min}^2}). \end{aligned} \quad (\text{E.0.122})$$

The exact analytic expressions for $\beta_{\text{NG}}^{(\alpha^2, m)}$ are quite lengthy and we do not report them here explicitly. The sum $\sum_{m=1}^{\infty} \beta_{\text{NG}}^{(\alpha^2, m)}$ admits an analytical expression only if we retain, in each one of the $\beta_{\text{NG}}^{(\alpha^2, m)}$, the highest power of \bar{s}_{\min} in the polynomial that multiplies the leading exponential suppression. We find

$$\beta \approx \frac{1}{\sqrt{2}\pi^{3/2}} \left(\frac{s_{\min}}{\sigma_2} \right) \exp \left\{ -\frac{2s_{\min}^2}{\sigma_2^2} + 16 \left(\frac{s_{\min}^3}{\sigma_2^3} \right) \frac{\alpha\sigma_1^2}{\sigma_2} + 32 \left(\frac{s_{\min}^4}{\sigma_2^4} \right) \alpha^2 \left[3 \left(\frac{\sigma_1^2}{\sigma_2} \right)^2 + \sigma_0^2 \right] \right\}. \quad (\text{E.0.123})$$

The structure of this expression is analogue to eq. (E.0.74). As shown in fig. 15, the exponential approximation contained in eqs. (E.0.104) and (E.0.123) gets worse for increasing s_{\min}/σ_2 and diverges from the actual result, overestimating the abundance. The failure of the exponential approximation is analogue to the one discussed in section 6.2 in the context of threshold statistics.

TOWARDS AN EXACT COMPUTATION

The generic n -th order cumulant can be exactly computed if we specify the explicit form of the non-gaussianity. In our case $f_{\text{NL}}(\mathcal{R}) = \alpha(\mathcal{R}^2 - \langle \mathcal{R}^2 \rangle)$.

The translation only affects the first-order cumulant:

$$C_1[\mathcal{R} + \alpha(\mathcal{R}^2 - \langle \mathcal{R}^2 \rangle)] = C_1(\mathcal{R} + \alpha\mathcal{R}^2) - \alpha\langle \mathcal{R}^2 \rangle, \quad (\text{F.0.1})$$

$$C_n[\mathcal{R}_1 + \alpha(\mathcal{R}_1^2 - \langle \mathcal{R}^2 \rangle), \dots, \mathcal{R}_n + \alpha(\mathcal{R}_n^2 - \langle \mathcal{R}^2 \rangle)] = C_n(\mathcal{R}_1 + \alpha\mathcal{R}_1^2, \dots, \mathcal{R}_n + \alpha\mathcal{R}_n^2), \quad \forall n > 1. \quad (\text{F.0.2})$$

Therefore we can set, without loss of generality, $f_{\text{NL}}(\mathcal{R}) = \alpha\mathcal{R}^2$ in the computation of the cumulants of order higher than one. The quadratic form of the non-linearity allows us to use the Gaussian integral extended to the complex plane thanks to analytic continuation.

We know that, in general $C_n(h_1, \dots, h_n)$ is sum of a series of contributes of different orders of which the last one must be $\mathcal{O}(\alpha^n)$ and it is represented by $C_n(\alpha\mathcal{R}_1^2, \dots, \alpha\mathcal{R}_n^2)$.

F.1 CANCELLATION OF THE CONTRIBUTES UP TO $\mathcal{O}(\alpha^{n-2})$

As a first step, we want to prove that $C_n(\alpha\mathcal{R}_1^2, \dots, \alpha\mathcal{R}_k^2, \mathcal{R}_{k+1}, \dots, \mathcal{R}_n) = 0$ for $k < n - 2$. This implies that $C_n(h_1, \dots, h_n)$ starts at order $\mathcal{O}(\alpha^{n-2})$. Using eq. (E.0.20):

$$C_n(\alpha\mathcal{R}_1^2, \dots, \alpha\mathcal{R}_k^2, \mathcal{R}_{k+1}, \dots, \mathcal{R}_n) = \quad (\text{F.1.1})$$

$$= (-i)^n \frac{\partial}{\partial \lambda_1} \dots \frac{\partial}{\partial \lambda_n} \log \int d\mathcal{R}_1 \dots d\mathcal{R}_n e^{i \sum_{i=1}^k \alpha \mathcal{R}_i^2 \lambda_i + i \sum_{i=k+1}^n \mathcal{R}_i \lambda_i} p(\mathcal{R}_1, \dots, \mathcal{R}_n) \Big|_{\lambda_1 = \dots = \lambda_n = 0} = \quad (\text{F.1.2})$$

$$= (-i)^n \frac{\partial}{\partial \lambda_1} \dots \frac{\partial}{\partial \lambda_n} \log \int d\mathcal{R}_1 \dots d\mathcal{R}_k e^{i \sum_{i=1}^k \alpha \mathcal{R}_i^2 \lambda_i} \underbrace{\left[\int d\mathcal{R}_{k+1} \dots d\mathcal{R}_n e^{i \sum_{i=k+1}^n \mathcal{R}_i \lambda_i} p(\mathcal{R}_1, \dots, \mathcal{R}_n) \right]}_{\equiv \mathcal{I}'(\mathcal{R}_1, \dots, \mathcal{R}_k, \lambda_{k+1}, \dots, \lambda_n)} \Big|_{\lambda=0}. \quad (\text{F.1.3})$$

We know that

$$\int d\mathcal{R}_1 \dots d\mathcal{R}_k e^{i \sum_{i=1}^k \mathcal{R}_i \lambda_i} \mathcal{I}'(\mathcal{R}_1, \dots, \mathcal{R}_k, \lambda_{k+1}, \dots, \lambda_n) = \chi(\lambda_1, \dots, \lambda_n) = e^{-\frac{1}{2} \sum_{i,j=1}^n \sigma_{ij} \lambda_i \lambda_j}, \quad (\text{F.1.4})$$

and so

$$\begin{aligned} \mathcal{I}'(\mathcal{R}_1, \dots, \mathcal{R}_k, \lambda_{k+1}, \dots, \lambda_n) &= \quad (\text{F.1.5}) \\ &= \int \frac{d\lambda_1}{2\pi} \dots \frac{d\lambda_k}{2\pi} \exp \left[-i \sum_{i=1}^k \lambda_i \mathcal{R}_i - \frac{1}{2} \left(\sum_{i,j=1}^k \sigma_{ij} \lambda_i \lambda_j + 2 \sum_{i=1}^k \sum_{j=k+1}^n \sigma_{ij} \lambda_i \lambda_j + \sum_{i,j=k+1}^n \sigma_{ij} \lambda_i \lambda_j \right) \right]. \end{aligned}$$

Let us use the matrix notation, defining the following objects:

$$\vec{\lambda} \equiv (\lambda_1, \dots, \lambda_k)^T = (\lambda_i)_{i=1}^k, \quad \vec{\mathcal{R}} \equiv (\mathcal{R}_1, \dots, \mathcal{R}_k)^T = (\mathcal{R}_i)_{i=1}^k, \quad (\text{F.1.6})$$

$$\hat{\sigma} \equiv (\sigma_{ij})_{i,j=1}^k, \quad \vec{\sigma}_j \equiv (\sigma_{1j}, \dots, \sigma_{kj})^T = (\sigma_{ij})_{i=1}^k \text{ with } j \in \{k+1, \dots, n\}. \quad (\text{F.1.7})$$

In this way

$$\begin{aligned} \mathcal{I}'(\vec{\mathcal{R}}, \lambda_{k+1}, \dots, \lambda_n) &= e^{-\frac{1}{2} \sum_{i,j=k+1}^n \sigma_{ij} \lambda_i \lambda_j} \int \frac{d^k \lambda}{(2\pi)^k} e^{-\frac{1}{2} \vec{\lambda}^T \hat{\sigma} \vec{\lambda} + \vec{\lambda} \cdot (-i\vec{\mathcal{R}} - \sum_{j=k+1}^n \lambda_j \vec{\sigma}_j)} = \\ &= \frac{1}{\sqrt{(2\pi)^k \det \hat{\sigma}}} \exp \left[\frac{1}{2} \left(i\vec{\mathcal{R}} + \sum_{j=k+1}^n \lambda_j \vec{\sigma}_j \right)^T \hat{\sigma}^{-1} \left(i\vec{\mathcal{R}} + \sum_{l=k+1}^n \lambda_l \vec{\sigma}_l \right) - \frac{1}{2} \sum_{i,j=k+1}^n \sigma_{ij} \lambda_i \lambda_j \right]. \end{aligned} \quad (\text{F.1.8})$$

Now, let us consider the integral

$$\mathcal{I}(\lambda_1, \dots, \lambda_n) = \int d\mathcal{R}_1 \dots d\mathcal{R}_k e^{i \sum_{i=1}^k \alpha \mathcal{R}_i^2 \lambda_i} \mathcal{I}'(\vec{\mathcal{R}}, \lambda_{k+1}, \dots, \lambda_n); \quad (\text{F.1.9})$$

we can write

$$\sum_{i=1}^k \alpha \mathcal{R}_i^2 \lambda_i = \sum_{i,j=1}^k \alpha \mathcal{R}_i \lambda_i \delta_{ij} \mathcal{R}_j = \alpha \vec{\mathcal{R}}^T \Lambda \vec{\mathcal{R}}, \quad (\text{F.1.10})$$

where we defined the diagonal matrix $\Lambda = \text{diag}(\lambda_1, \dots, \lambda_k)$. In this way, we have

$$\begin{aligned} \mathcal{I}(\lambda_1, \dots, \lambda_n) &= \frac{1}{\sqrt{(2\pi)^k \det \hat{\sigma}}} \int d^k \mathcal{R} \exp \left[i\alpha \vec{\mathcal{R}}^T \Lambda \vec{\mathcal{R}} + \frac{1}{2} \left(i\vec{\mathcal{R}} + \sum_{j=k+1}^n \lambda_j \vec{\sigma}_j \right)^T \hat{\sigma}^{-1} \left(i\vec{\mathcal{R}} + \sum_{l=k+1}^n \lambda_l \vec{\sigma}_l \right) - \frac{1}{2} \sum_{i,j=k+1}^n \sigma_{ij} \lambda_i \lambda_j \right] \\ & \quad (\text{F.1.11}) \end{aligned}$$

$$= \frac{1}{\sqrt{(2\pi)^k \det \hat{\sigma}}} e^{\frac{1}{2} \left(\sum_{j=k+1}^n \lambda_j \vec{\sigma}_j \hat{\sigma}^{-1} \sum_{l=k+1}^n \lambda_l \vec{\sigma}_l - \sum_{i,j=k+1}^n \sigma_{ij} \lambda_i \lambda_j \right)} \int d^k \mathcal{R} e^{-\frac{1}{2} \vec{\mathcal{R}}^T (\hat{\sigma}^{-1} - 2i\alpha\Lambda) \vec{\mathcal{R}} + i\vec{\mathcal{R}}^T \hat{\sigma}^{-1} \sum_{j=k+1}^n \lambda_j \vec{\sigma}_j} \quad (\text{F.1.12})$$

$$= \frac{1}{\sqrt{\det(\mathbb{1} - 2i\alpha\hat{\sigma}\Lambda)}} \exp \left\{ -\frac{1}{2} \sum_{j=k+1}^n \lambda_j \vec{\sigma}_j^T \hat{\sigma}^{-1} \left[(\mathbb{1} - 2i\alpha\hat{\sigma}\Lambda)^{-1} - \mathbb{1} \right] \sum_{l=k+1}^n \lambda_l \vec{\sigma}_l - \frac{1}{2} \sum_{i,j=k+1}^n \sigma_{ij} \lambda_i \lambda_j \right\}, \quad (\text{F.1.13})$$

where we used that $\det(\hat{\sigma}^{-1} - 2i\alpha\Lambda) = \det \hat{\sigma}^{-1} \det(\mathbb{1} - 2i\alpha\hat{\sigma}\Lambda)$ and $\hat{\sigma}^T = \hat{\sigma}$. Using the following property of the determinant of a matrix:

$$\det(\mathbb{1} - 2i\alpha\hat{\sigma}\Lambda) = \exp[\text{tr} \log(\mathbb{1} - 2i\alpha\hat{\sigma}\Lambda)] = \exp \left[-\text{tr} \sum_{m=1}^{\infty} \frac{1}{m} (2i\alpha\hat{\sigma}\Lambda)^m \right], \quad (\text{F.1.14})$$

and also the geometric series

$$[(\mathbb{1} - 2i\alpha\hat{\sigma}\Lambda)^{-1} - \mathbb{1}] = \sum_{m=1}^{\infty} (2i\alpha\hat{\sigma}\Lambda)^m, \quad (\text{F.1.15})$$

we find

$$\mathcal{I}(\lambda_1, \dots, \lambda_n) = \exp \left[\frac{1}{2} \text{tr} \sum_{m=1}^{\infty} \frac{1}{m} (2i\alpha \hat{\sigma} \Lambda)^m - \frac{1}{2} \sum_{j=k+1}^n \lambda_j \bar{\sigma}_j^T \hat{\sigma}^{-1} \sum_{m=1}^{\infty} (2i\alpha \hat{\sigma} \Lambda)^m \sum_{l=k+1}^n \lambda_l \bar{\sigma}_l - \frac{1}{2} \sum_{i,j=k+1}^n \sigma_{ij} \lambda_i \lambda_j \right].$$

Thus, the cumulant is

$$\begin{aligned} C_n(\alpha \mathcal{R}_1^2, \dots, \alpha \mathcal{R}_k^2, \mathcal{R}_{k+1}, \dots, \mathcal{R}_n) &= (-i)^n \frac{\partial}{\partial \lambda_1} \dots \frac{\partial}{\partial \lambda_n} \log \mathcal{I}(\lambda_1, \dots, \lambda_n) \Big|_{\lambda=0} = \quad (\text{F.1.16}) \\ &= (-i)^n \frac{\partial}{\partial \lambda_1} \dots \frac{\partial}{\partial \lambda_n} \left[\frac{1}{2} \text{tr} \sum_{m=1}^{\infty} \frac{1}{m} (2i\alpha \hat{\sigma} \Lambda)^m - \frac{1}{2} \sum_{j=k+1}^n \lambda_j \bar{\sigma}_j^T \hat{\sigma}^{-1} \sum_{m=1}^{\infty} (2i\alpha \hat{\sigma} \Lambda)^m \sum_{l=k+1}^n \lambda_l \bar{\sigma}_l - \frac{1}{2} \sum_{i,j=k+1}^n \sigma_{ij} \lambda_i \lambda_j \right] \Big|_{\lambda=0}. \end{aligned}$$

A term is non zero only if it contains all the λ_i 's. For $k < n$ the first term vanishes because it does not contain the λ_i with $i > k$. Instead the last term is always vanishing for $n > 2$, because the number of derivatives is higher than the number of λ_i 's present. So, until now

$$C_n(\alpha \mathcal{R}_1^2, \dots, \alpha \mathcal{R}_k^2, \mathcal{R}_{k+1}, \dots, \mathcal{R}_n) = (-i)^n \frac{\partial}{\partial \lambda_1} \dots \frac{\partial}{\partial \lambda_n} \left[-\frac{1}{2} \sum_{j=k+1}^n \lambda_j \bar{\sigma}_j^T \hat{\sigma}^{-1} \sum_{m=1}^{\infty} (2i\alpha \hat{\sigma} \Lambda)^m \sum_{l=k+1}^n \lambda_l \bar{\sigma}_l \right] \Big|_{\lambda=0}. \quad (\text{F.1.17})$$

Now, let us make the derivative with respect to λ_n

$$\begin{aligned} C_n(\alpha \mathcal{R}_1^2, \dots, \alpha \mathcal{R}_k^2, \mathcal{R}_{k+1}, \dots, \mathcal{R}_n) &= \\ &= (-i)^n \frac{\partial}{\partial \lambda_1} \dots \frac{\partial}{\partial \lambda_{n-1}} \quad (\text{F.1.18}) \\ &\left[-\frac{1}{2} \sum_{j=k+1}^n \delta_{jn} \bar{\sigma}_j^T \hat{\sigma}^{-1} \sum_{m=1}^{\infty} (2i\alpha \hat{\sigma} \Lambda)^m \sum_{l=k+1}^n \lambda_l \bar{\sigma}_l - \frac{1}{2} \sum_{j=k+1}^n \lambda_j \bar{\sigma}_j^T \hat{\sigma}^{-1} \sum_{m=1}^{\infty} (2i\alpha \hat{\sigma} \Lambda)^m \sum_{l=k+1}^n \delta_{ln} \bar{\sigma}_l \right] \Big|_{\lambda=0}. \end{aligned}$$

The two terms can be summed up, since $\hat{\sigma}^{-1} (\hat{\sigma} \Lambda)^{m+1} = \Lambda (\hat{\sigma} \Lambda)^m$ and this matrix is symmetric:

$$[\Lambda (\hat{\sigma} \Lambda)^m]^T = [(\hat{\sigma} \Lambda)^m]^T \Lambda^T = [(\hat{\sigma} \Lambda)^m]^T \Lambda = [(\hat{\sigma} \Lambda)^T]^m \Lambda = (\Lambda^T \hat{\sigma}^T)^m \Lambda = (\Lambda \hat{\sigma})^m \Lambda = \Lambda (\hat{\sigma} \Lambda)^m; \quad (\text{F.1.19})$$

so, deriving with respect to λ_{n-1}

$$\begin{aligned} C_n(\alpha \mathcal{R}_1^2, \dots, \alpha \mathcal{R}_k^2, \mathcal{R}_{k+1}, \dots, \mathcal{R}_n) &= (-i)^n \frac{\partial}{\partial \lambda_1} \dots \frac{\partial}{\partial \lambda_{n-1}} \left[-\bar{\sigma}_n^T \Lambda \sum_{m=1}^{\infty} (2i\alpha \hat{\sigma} \Lambda)^{m-1} \sum_{l=k+1}^n \lambda_l \bar{\sigma}_l \right] \Big|_{\lambda=0} \\ &= (-i)^n \frac{\partial}{\partial \lambda_1} \dots \frac{\partial}{\partial \lambda_{n-2}} \left[-\bar{\sigma}_n^T \Lambda \sum_{m=1}^{\infty} (2i\alpha \hat{\sigma} \Lambda)^{m-1} \bar{\sigma}_{n-1} \right] \Big|_{\lambda=0}. \quad (\text{F.1.20}) \end{aligned}$$

It is clear that, if $k < n - 2$ there are still the derivatives $\frac{\partial}{\partial \lambda_{k+1}} \dots \frac{\partial}{\partial \lambda_{n-2}}$ to apply, but no $\lambda_{k+1}, \dots, \lambda_{n-2}$ to meet. Therefore:

$$C_n(\alpha \mathcal{R}_1^2, \dots, \alpha \mathcal{R}_k^2, \mathcal{R}_{k+1}, \dots, \mathcal{R}_n) = 0, \quad \forall k < n - 2 \quad (\text{F.1.21})$$

Now let us move to compute the only three orders left.

F.2 COMPUTATION OF THE $\mathcal{O}(\alpha^{n-2})$

For the leading part of the cumulant, it is enough to set $k = n - 2$ in the eq. (F.1.20) (let us consider the case $n > 2$, so we can get rid of the last term that we canceled in eq. F.1.16):

$$C_n(\alpha\mathcal{R}_1^2, \dots, \alpha\mathcal{R}_{n-2}^2, \mathcal{R}_{n-1}, \mathcal{R}_n) = (-i)^n \frac{\partial}{\partial\lambda_1} \dots \frac{\partial}{\partial\lambda_{n-2}} \left[-\tilde{\sigma}_n^T \Lambda \sum_{m=1}^{\infty} (2i\alpha\hat{\sigma}\Lambda)^{m-1} \tilde{\sigma}_{n-1} \right] \Big|_{\lambda=0}, \quad (\text{F.2.1})$$

where now $\Lambda = \text{diag}(\lambda_1, \dots, \lambda_{n-2})$.

The first observation we can do is that only the $\mathcal{O}(\alpha^{n-2})$ matters in the sum over m . In fact, for $m < n - 2$ the derivatives are too much and they annihilate the term. Instead, for $m > n - 2$ the derivatives are not enough and when we put $\lambda = 0$ the term vanishes.

$$C_n(\alpha\mathcal{R}_1^2, \dots, \alpha\mathcal{R}_{n-2}^2, \mathcal{R}_{n-1}, \mathcal{R}_n) = (2\alpha)^{n-2} \frac{\partial}{\partial\lambda_1} \dots \frac{\partial}{\partial\lambda_{n-2}} \left[\tilde{\sigma}_{n-1}^T \Lambda (\hat{\sigma}\Lambda)^{n-3} \tilde{\sigma}_n \right] \Big|_{\lambda=0}. \quad (\text{F.2.2})$$

Now we can see that:

$$\tilde{\sigma}_{n-1}^T [\Lambda (\hat{\sigma}\Lambda)^{n-3}] \tilde{\sigma}_n = \sum_{i,j=1}^{n-2} \sigma_{n-1,i} \left(\sum_{i_1, \dots, i_{n-4}=1}^{n-2} \lambda_{i_1} \sigma_{i_1 i_2} \lambda_{i_2} \sigma_{i_2 i_3} \dots \lambda_{i_{n-4}} \sigma_{i_{n-4} j} \lambda_j \right) \sigma_{jn}. \quad (\text{F.2.3})$$

Of course, because of the presence of the derivatives, in the sum, only the terms with all the $\{\lambda_i\}_{i=1}^{n-2}$ different matters, i.e. we only keep the permutations of $\{1, 2, \dots, n-2\}$. So, putting all together

$$\begin{aligned} C_n[\alpha\mathcal{R}_1^2, \dots, \alpha\mathcal{R}_{n-2}^2, \mathcal{R}_{n-1}, \mathcal{R}_n] &= \\ &= (2\alpha)^{n-2} \frac{\partial}{\partial\lambda_1} \dots \frac{\partial}{\partial\lambda_{n-2}} \sum_{i_1, \dots, i_{n-2}=1}^{n-2} \lambda_{i_1} \dots \lambda_{i_{n-2}} \sigma_{n-1, i_1} \sigma_{i_1 i_2} \dots \sigma_{i_{n-3} i_{n-2}} \sigma_{i_{n-2} n} \Big|_{\lambda=0} = \\ &= (2\alpha)^{n-2} \sum_{\substack{\{i_1, \dots, i_{n-2}\} = \\ = \text{perms}\{1, \dots, n-2\}}} \sigma_{n-1, i_1} \sigma_{i_1 i_2} \dots \sigma_{i_{n-3} i_{n-2}} \sigma_{i_{n-2} n}. \end{aligned} \quad (\text{F.2.4})$$

So, the formula for the $\mathcal{O}(\alpha^{n-2})$ contribution to the n -th order cumulant is:

$$\begin{aligned} C_n(\alpha\mathcal{R}_1^2, \dots, \alpha\mathcal{R}_{n-2}^2, \mathcal{R}_{n-1}, \mathcal{R}_n) &= \\ &= (2\alpha)^{n-2} \sum_{\substack{\{i_1, \dots, i_{n-2}\} = \\ = \text{perms}\{1, \dots, n-2\}}} \langle \mathcal{R}_{n-1} \mathcal{R}_{i_1} \rangle \langle \mathcal{R}_{i_1} \mathcal{R}_{i_2} \rangle \dots \langle \mathcal{R}_{i_{n-3}} \mathcal{R}_{i_{n-2}} \rangle \langle \mathcal{R}_{i_{n-2}} \mathcal{R}_n \rangle \end{aligned} \quad (\text{F.2.5})$$

For example, we can check this formula for $n = 4$

$$\begin{aligned} C_4(\alpha\mathcal{R}_1^2, \alpha\mathcal{R}_2^2, \mathcal{R}_3, \mathcal{R}_4) &= (2\alpha)^2 \sum_{\{i,j\}=\text{perms}\{1,2\}} \langle \mathcal{R}_3 \mathcal{R}_i \rangle \langle \mathcal{R}_i \mathcal{R}_j \rangle \langle \mathcal{R}_j \mathcal{R}_4 \rangle \\ &= 4\alpha^2 (\langle \mathcal{R}_3 \mathcal{R}_1 \rangle \langle \mathcal{R}_1 \mathcal{R}_2 \rangle \langle \mathcal{R}_2 \mathcal{R}_4 \rangle + \langle \mathcal{R}_3 \mathcal{R}_2 \rangle \langle \mathcal{R}_2 \mathcal{R}_1 \rangle \langle \mathcal{R}_1 \mathcal{R}_4 \rangle) = \\ &= 4\alpha^2 \langle \mathcal{R}_1 \mathcal{R}_2 \rangle (\langle \mathcal{R}_3 \mathcal{R}_1 \rangle \langle \mathcal{R}_2 \mathcal{R}_4 \rangle + \langle \mathcal{R}_3 \mathcal{R}_2 \rangle \langle \mathcal{R}_1 \mathcal{R}_4 \rangle), \end{aligned} \quad (\text{F.2.6})$$

that precisely matches the result obtained in eq. (E.0.55).

F.3 COMPUTATION OF THE $\mathcal{O}(\alpha^{n-1})$

For $k = n - 1$ we have:

$$\mathcal{I}(\lambda_1, \dots, \lambda_n) = \frac{1}{\sqrt{\det(\mathbb{1} - 2i\alpha\hat{\sigma}\Lambda)}} \exp \left\{ -\frac{1}{2} \lambda_n^2 \bar{\sigma}_n^T \hat{\sigma}^{-1} [(\mathbb{1} - 2i\alpha\hat{\sigma}\Lambda)^{-1} - \mathbb{1}] \bar{\sigma}_n - \frac{1}{2} \sigma_{nn} \lambda_n^2 \right\}, \quad (\text{F.3.1})$$

and so:

$$C_n(\alpha\mathcal{R}_1^2, \dots, \alpha\mathcal{R}_{n-1}^2, \mathcal{R}_n) = (-i)^n \frac{\partial}{\partial \lambda_1} \dots \frac{\partial}{\partial \lambda_n} \log \mathcal{I}(\lambda_1, \dots, \lambda_n) \Big|_{\lambda=0} = \quad (\text{F.3.2})$$

$$= (-i)^n \frac{\partial}{\partial \lambda_1} \dots \frac{\partial}{\partial \lambda_n} \left[\frac{1}{2} \text{tr} \sum_{m=1}^{\infty} \frac{1}{m} (2i\alpha\hat{\sigma}\Lambda)^m - \frac{1}{2} \lambda_n^2 \bar{\sigma}_n^T \hat{\sigma}^{-1} \sum_{m=1}^{\infty} (2i\alpha\hat{\sigma}\Lambda)^m \bar{\sigma}_n - \frac{1}{2} \sigma_{nn} \lambda_n^2 \right] \Big|_{\lambda=0} = \quad (\text{F.3.3})$$

$$= (-i)^n \frac{\partial}{\partial \lambda_1} \dots \frac{\partial}{\partial \lambda_{n-1}} \left[-\lambda_n \left(\bar{\sigma}_n^T \hat{\sigma}^{-1} \sum_{m=1}^{\infty} (2i\alpha\hat{\sigma}\Lambda)^m \bar{\sigma}_n + \sigma_{nn} \right) \right] \Big|_{\lambda=0}. \quad (\text{F.3.4})$$

In the last step, everything vanishes since it remains a λ_n with no more derivatives with respect to it and in the end we must set $\lambda = 0$, so there is no $\mathcal{O}(\alpha^{n-1})$ contribution:

$$C_n(\alpha\mathcal{R}_1^2, \dots, \alpha\mathcal{R}_{n-1}^2, \mathcal{R}_n) = 0 \quad (\text{F.3.5})$$

 F.4 COMPUTATION OF THE $\mathcal{O}(\alpha^n)$

Now we have $\Lambda = \text{diag}(\lambda_1, \dots, \lambda_n)$ and the trace part is the only term left, so:

$$\mathcal{I}(\lambda_1, \dots, \lambda_n) = \frac{1}{\sqrt{(2\pi)^n \det \sigma}} \int d^n \mathcal{R} e^{-\frac{1}{2} \bar{\mathcal{R}}^T (\sigma^{-1} - 2i\alpha\Lambda) \bar{\mathcal{R}}} = \exp \left[-\frac{1}{2} \text{tr} \log (\mathbb{1} - 2i\alpha\sigma\Lambda) \right], \quad (\text{F.4.1})$$

where now $\sigma = (\sigma_{ij})_{i,j=1}^n$ and $\Lambda = \text{diag}(\lambda_1, \dots, \lambda_n)$. With the usual steps, knowing that only the $\mathcal{O}(\alpha^n)$ matters:

$$C_n(\alpha\mathcal{R}_1^2, \dots, \alpha\mathcal{R}_n^2) = (-i)^n \frac{\partial}{\partial \lambda_1} \dots \frac{\partial}{\partial \lambda_n} \left[\frac{1}{2} \text{tr} \sum_{m=0}^{\infty} \frac{1}{m} (2i\alpha\sigma\Lambda)^m \right] \Big|_{\lambda=0} = \frac{2^{n-1} \alpha^n}{n} \frac{\partial}{\partial \lambda_1} \dots \frac{\partial}{\partial \lambda_n} \text{tr}(\sigma\Lambda)^n \Big|_{\lambda=0}. \quad (\text{F.4.2})$$

The trace is:

$$\text{tr}(\sigma\Lambda)^n = \sum_{i_1, \dots, i_n=1}^n \lambda_{i_1} \lambda_{i_2} \dots \lambda_{i_n} \sigma_{i_n i_1} \sigma_{i_1 i_2} \dots \sigma_{i_{n-1} i_n}, \quad (\text{F.4.3})$$

and after the derivation only the permutations of $\{1, 2, \dots, n\}$ survive, so:

$$C_n(\alpha\mathcal{R}_1^2, \dots, \alpha\mathcal{R}_n^2) = \frac{2^{n-1} \alpha^n}{n} \sum_{\substack{\{i_1, \dots, i_n\} = \\ = \text{perms}\{1, \dots, n\}}} \langle \mathcal{R}_{i_n} \mathcal{R}_{i_1} \rangle \dots \langle \mathcal{R}_{i_{n-1}} \mathcal{R}_{i_n} \rangle \quad (\text{F.4.4})$$

F.5 COMPUTATION OF THE GENERIC CUMULANT

Now that we have all the ingredients, we can compute the generic n -th order cumulant up to all orders. First of all, let us focus on the $\mathcal{O}(\alpha^{n-2})$ contribute:

$$C_n^{\mathcal{O}(\alpha^{n-2})}(h_1, \dots, h_n) = (2\alpha)^{n-2} \sum_{\{i,j\} \in A} \sum_{\substack{\{i_1, \dots, i_{n-2}\} = \\ = \text{perms}\{1, \dots, n\} \setminus \{i,j\}}} \langle \mathcal{R}_i \mathcal{R}_{i_1} \rangle \langle \mathcal{R}_{i_1} \mathcal{R}_{i_2} \rangle \dots \langle \mathcal{R}_{i_{n-2}} \mathcal{R}_j \rangle \quad (\text{F.5.1})$$

where A is the set in which all the non-ordered couples of numbers between $\{1, \dots, n\}$ are contained. E.g. for $n = 4$, $A = \{\{1,2\}, \{1,3\}, \{1,4\}, \{2,3\}, \{2,4\}, \{3,4\}\}$. From combinatorics we know that the permutations of $n - 2$ different objects are $(n - 2)!$, while the cardinality of A is the number of ways in which we can take 2 objects among n different objects without taking care of their order, which is $\binom{n}{2} = \frac{n(n-1)}{2}$. So, putting these 2 together, the total sum is composed of $\frac{n!}{2}$ elements. If we compute also the exchanged couples, we double the sum, having $n!$ elements, that is the cardinality of $\text{perms}\{1, \dots, n\}$. So we can put the two sums together dividing by 2:

$$C_n^{\mathcal{O}(\alpha^{n-2})}(h_1, \dots, h_n) = 2^{n-3} \alpha^{n-2} \sum_{\substack{\{i_1, \dots, i_n\} = \\ = \text{perms}\{1, \dots, n\}}} \langle \mathcal{R}_{i_1} \mathcal{R}_{i_2} \rangle \langle \mathcal{R}_{i_2} \mathcal{R}_{i_3} \rangle \dots \langle \mathcal{R}_{i_{n-1}} \mathcal{R}_{i_n} \rangle \quad (\text{F.5.2})$$

Now, let us add also the $\mathcal{O}(\alpha^n)$ contribution, that we can write as

$$C_n(\alpha \mathcal{R}_1^2, \dots, \alpha \mathcal{R}_n^2) = \frac{2^{n-1} \alpha^n}{n} \sum_{\substack{\{i_1, \dots, i_n\} = \\ = \text{perms}\{1, \dots, n\}}} \langle \mathcal{R}_{i_1} \mathcal{R}_{i_2} \rangle \dots \langle \mathcal{R}_{i_n} \mathcal{R}_{i_1} \rangle \quad (\text{F.5.3})$$

And so, summing the two

$$C_n(h_1, \dots, h_n) = 2^{n-3} \alpha^{n-2} \sum_{\substack{\{i_1, \dots, i_n\} = \\ = \text{perms}\{1, \dots, n\}}} \langle \mathcal{R}_{i_1} \mathcal{R}_{i_2} \rangle \dots \langle \mathcal{R}_{i_{n-1}} \mathcal{R}_{i_n} \rangle \left(1 + \frac{4\alpha^2}{n} \langle \mathcal{R}_{i_1} \mathcal{R}_{i_n} \rangle \right) \quad (\text{F.5.4})$$

And we can easily see that, putting $\vec{x}_1 = \dots = \vec{x}_n$:

$$C_n(h, \dots, h) = 2^{n-3} \alpha^{n-2} n! \langle \mathcal{R}^2 \rangle^{n-1} \left(1 + \frac{4\alpha^2}{n} \langle \mathcal{R}^2 \rangle^2 \right) = 2^{n-3} (n-1)! \sigma_0^2 (\alpha \sigma_0^2)^{n-2} (n + 4\alpha^2 \sigma_0^2), \quad (\text{F.5.5})$$

and this result exactly reproduces the formula given in eq. (E.0.58).

BIBLIOGRAPHY

- [1] Mehrdad Mirbabayi and Flavio Ricciardi. “Probing de Sitter from the horizon.” In: *JHEP* 04 (2023), p. 053. DOI: [10.1007/JHEP04\(2023\)053](https://doi.org/10.1007/JHEP04(2023)053). arXiv: [2211.11672](https://arxiv.org/abs/2211.11672) [hep-th].
- [2] Flavio Ricciardi, Marco Taoso, and Alfredo Urbano. “Solving peak theory in the presence of local non-gaussianities.” In: *JCAP* 08 (2021), p. 060. DOI: [10.1088/1475-7516/2021/08/060](https://doi.org/10.1088/1475-7516/2021/08/060). arXiv: [2102.04084](https://arxiv.org/abs/2102.04084) [astro-ph.CO].
- [3] R. A. Konoplya and A. Zhidenko. “Quasinormal modes of black holes: From astrophysics to string theory.” In: *Rev. Mod. Phys.* 83 (2011), pp. 793–836. DOI: [10.1103/RevModPhys.83.793](https://doi.org/10.1103/RevModPhys.83.793). arXiv: [1102.4014](https://arxiv.org/abs/1102.4014) [gr-qc].
- [4] Patrick R. Brady, Chris M. Chambers, William G. Laarakkers, and Eric Poisson. “Radiative falloff in Schwarzschild-de Sitter space-time.” In: *Phys. Rev. D* 60 (1999), p. 064003. DOI: [10.1103/PhysRevD.60.064003](https://doi.org/10.1103/PhysRevD.60.064003). arXiv: [gr-qc/9902010](https://arxiv.org/abs/gr-qc/9902010).
- [5] Mehrdad Mirbabayi. “Markovian dynamics in de Sitter.” In: *JCAP* 09 (2021), p. 038. DOI: [10.1088/1475-7516/2021/09/038](https://doi.org/10.1088/1475-7516/2021/09/038). arXiv: [2010.06604](https://arxiv.org/abs/2010.06604) [hep-th].
- [6] E. S. C. Ching, P. T. Leung, W. M. Suen, and K. Young. “Wave propagation in gravitational systems: Late time behavior.” In: *Phys. Rev. D* 52 (1995), pp. 2118–2132. DOI: [10.1103/PhysRevD.52.2118](https://doi.org/10.1103/PhysRevD.52.2118). arXiv: [gr-qc/9507035](https://arxiv.org/abs/gr-qc/9507035).
- [7] Jacques Bros. “Complexified de Sitter space: Analytic causal kernels and Kallen-Lehmann type representation.” In: *Nucl. Phys. B Proc. Suppl.* 18 (1991), pp. 22–28. DOI: [10.1016/0920-5632\(91\)90119-Y](https://doi.org/10.1016/0920-5632(91)90119-Y).
- [8] Matthijs Hogervorst, João Penedones, and Kamran Salehi Vaziri. “Towards the non-perturbative cosmological bootstrap.” In: *JHEP* 02 (2023), p. 162. DOI: [10.1007/JHEP02\(2023\)162](https://doi.org/10.1007/JHEP02(2023)162). arXiv: [2107.13871](https://arxiv.org/abs/2107.13871) [hep-th].
- [9] Lorenzo Di Pietro, Victor Gorbenko, and Shota Komatsu. “Analyticity and unitarity for cosmological correlators.” In: *JHEP* 03 (2022), p. 023. DOI: [10.1007/JHEP03\(2022\)023](https://doi.org/10.1007/JHEP03(2022)023). arXiv: [2108.01695](https://arxiv.org/abs/2108.01695) [hep-th].
- [10] Allan Adams, Nima Arkani-Hamed, Sergei Dubovsky, Alberto Nicolis, and Riccardo Rattazzi. “Causality, analyticity and an IR obstruction to UV completion.” In: *JHEP* 10 (2006), p. 014. DOI: [10.1088/1126-6708/2006/10/014](https://doi.org/10.1088/1126-6708/2006/10/014). arXiv: [hep-th/0602178](https://arxiv.org/abs/hep-th/0602178).
- [11] Dionysios Anninos, Frederik Denef, Y. T. Albert Law, and Zimo Sun. “Quantum de Sitter horizon entropy from quasicanonical bulk, edge, sphere and topological string partition functions.” In: *JHEP* 01 (2022), p. 088. DOI: [10.1007/JHEP01\(2022\)088](https://doi.org/10.1007/JHEP01(2022)088). arXiv: [2009.12464](https://arxiv.org/abs/2009.12464) [hep-th].

- [12] Emil Albrychiewicz and Yasha Neiman. “Scattering in the static patch of de Sitter space.” In: *Phys. Rev. D* 103.6 (2021), p. 065014. DOI: [10.1103/PhysRevD.103.065014](https://doi.org/10.1103/PhysRevD.103.065014). arXiv: [2012.13584](https://arxiv.org/abs/2012.13584) [[hep-th](#)].
- [13] Y. T. Albert Law and Klaas Parmentier. “Black hole scattering and partition functions.” In: *JHEP* 10 (2022), p. 039. DOI: [10.1007/JHEP10\(2022\)039](https://doi.org/10.1007/JHEP10(2022)039). arXiv: [2207.07024](https://arxiv.org/abs/2207.07024) [[hep-th](#)].
- [14] Marcus Spradlin, Andrew Strominger, and Anastasia Volovich. “Les Houches lectures on de Sitter space.” In: *Les Houches Summer School: Session 76: Euro Summer School on Unity of Fundamental Physics: Gravity, Gauge Theory and Strings*. Oct. 2001, pp. 423–453. arXiv: [hep-th/0110007](https://arxiv.org/abs/hep-th/0110007).
- [15] Alexei A. Starobinsky. “STOCHASTIC DE SITTER (INFLATIONARY) STAGE IN THE EARLY UNIVERSE.” In: *Lect. Notes Phys.* 246 (1986), pp. 107–126. DOI: [10.1007/3-540-16452-9_6](https://doi.org/10.1007/3-540-16452-9_6).
- [16] Alexei A. Starobinsky and Junichi Yokoyama. “Equilibrium state of a selfinteracting scalar field in the De Sitter background.” In: *Phys. Rev. D* 50 (1994), pp. 6357–6368. DOI: [10.1103/PhysRevD.50.6357](https://doi.org/10.1103/PhysRevD.50.6357). arXiv: [astro-ph/9407016](https://arxiv.org/abs/astro-ph/9407016).
- [17] Victor Gorbenko and Leonardo Senatore. “ $\lambda\phi^4$ in dS.” In: (Oct. 2019). arXiv: [1911.00022](https://arxiv.org/abs/1911.00022) [[hep-th](#)].
- [18] Timothy Cohen, Daniel Green, Akhil Premkumar, and Alexander Ridgway. “Stochastic Inflation at NNLO.” In: *JHEP* 09 (2021), p. 159. DOI: [10.1007/JHEP09\(2021\)159](https://doi.org/10.1007/JHEP09(2021)159). arXiv: [2106.09728](https://arxiv.org/abs/2106.09728) [[hep-th](#)].
- [19] George Panagopoulos and Eva Silverstein. “Primordial Black Holes from non-Gaussian tails.” In: (June 2019). arXiv: [1906.02827](https://arxiv.org/abs/1906.02827) [[hep-th](#)].
- [20] Rafael A. Porto. “The effective field theorist’s approach to gravitational dynamics.” In: *Phys. Rept.* 633 (2016), pp. 1–104. DOI: [10.1016/j.physrep.2016.04.003](https://doi.org/10.1016/j.physrep.2016.04.003). arXiv: [1601.04914](https://arxiv.org/abs/1601.04914) [[hep-th](#)].
- [21] Solomon Endlich, Alberto Nicolis, Rafael A. Porto, and Junpu Wang. “Dissipation in the effective field theory for hydrodynamics: First order effects.” In: *Phys. Rev. D* 88 (2013), p. 105001. DOI: [10.1103/PhysRevD.88.105001](https://doi.org/10.1103/PhysRevD.88.105001). arXiv: [1211.6461](https://arxiv.org/abs/1211.6461) [[hep-th](#)].
- [22] Hong Liu and Paolo Glorioso. “Lectures on non-equilibrium effective field theories and fluctuating hydrodynamics.” In: *PoS TASI2017* (2018), p. 008. DOI: [10.22323/1.305.0008](https://doi.org/10.22323/1.305.0008). arXiv: [1805.09331](https://arxiv.org/abs/1805.09331) [[hep-th](#)].
- [23] Henri Epstein. “Remarks on quantum field theory on de Sitter and anti-de Sitter space-times,” in: *Pramana - J Phys* 78 (2012), pp. 853–864. DOI: [10.1007/s12043-012-0312-7](https://doi.org/10.1007/s12043-012-0312-7).
- [24] Harry Goodhew, Sadra Jazayeri, and Enrico Pajer. “The Cosmological Optical Theorem.” In: *JCAP* 04 (2021), p. 021. DOI: [10.1088/1475-7516/2021/04/021](https://doi.org/10.1088/1475-7516/2021/04/021). arXiv: [2009.02898](https://arxiv.org/abs/2009.02898) [[hep-th](#)].
- [25] Stephen Hawking. “Gravitationally collapsed objects of very low mass.” In: *Mon. Not. Roy. Astron. Soc.* 152 (1971), p. 75. DOI: [10.1093/mnras/152.1.75](https://doi.org/10.1093/mnras/152.1.75).

- [26] Bernard J. Carr and S. W. Hawking. “Black holes in the early Universe.” In: *Mon. Not. Roy. Astron. Soc.* 168 (1974), pp. 399–415. DOI: [10.1093/mnras/168.2.399](https://doi.org/10.1093/mnras/168.2.399).
- [27] B. J. Carr, Kazunori Kohri, Yuuiti Sendouda, and Jun’ichi Yokoyama. “New cosmological constraints on primordial black holes.” In: *Phys. Rev. D* 81 (2010), p. 104019. DOI: [10.1103/PhysRevD.81.104019](https://doi.org/10.1103/PhysRevD.81.104019). arXiv: [0912.5297](https://arxiv.org/abs/0912.5297) [[astro-ph.CO](https://arxiv.org/archive/astro-ph)].
- [28] Hiroko Niikura et al. “Microlensing constraints on primordial black holes with Subaru/HSC Andromeda observations.” In: *Nature Astron.* 3.6 (2019), pp. 524–534. DOI: [10.1038/s41550-019-0723-1](https://doi.org/10.1038/s41550-019-0723-1). arXiv: [1701.02151](https://arxiv.org/abs/1701.02151) [[astro-ph.CO](https://arxiv.org/archive/astro-ph)].
- [29] Andrey Katz, Joachim Kopp, Sergey Sibiryakov, and Wei Xue. “Femtolensing by Dark Matter Revisited.” In: *JCAP* 12 (2018), p. 005. DOI: [10.1088/1475-7516/2018/12/005](https://doi.org/10.1088/1475-7516/2018/12/005). arXiv: [1807.11495](https://arxiv.org/abs/1807.11495) [[astro-ph.CO](https://arxiv.org/archive/astro-ph)].
- [30] Tomohiro Harada, Chul-Moon Yoo, Kazunori Kohri, Ken-ichi Nakao, and Sanjay Jhingan. “Primordial black hole formation in the matter-dominated phase of the Universe.” In: *Astrophys. J.* 833.1 (2016), p. 61. DOI: [10.3847/1538-4357/833/1/61](https://doi.org/10.3847/1538-4357/833/1/61). arXiv: [1609.01588](https://arxiv.org/abs/1609.01588) [[astro-ph.CO](https://arxiv.org/archive/astro-ph)].
- [31] A. Vilenkin. “Cosmological Density Fluctuations Produced by Vacuum Strings.” In: *Phys. Rev. Lett.* 46 (1981). [Erratum: *Phys.Rev.Lett.* 46, 1496 (1981)], pp. 1169–1172. DOI: [10.1103/PhysRevLett.46.1496](https://doi.org/10.1103/PhysRevLett.46.1496).
- [32] S. W. Hawking. “Gravitational radiation from collapsing cosmic string loops.” In: *Phys. Lett. B* 246 (1990), pp. 36–38. DOI: [10.1016/0370-2693\(90\)91304-T](https://doi.org/10.1016/0370-2693(90)91304-T).
- [33] Joaquim Fort and Tanmay Vachaspati. “Do global string loops collapse to form black holes?” In: *Phys. Lett. B* 311 (1993), pp. 41–46. DOI: [10.1016/0370-2693\(93\)90530-U](https://doi.org/10.1016/0370-2693(93)90530-U). arXiv: [hep-th/9305081](https://arxiv.org/abs/hep-th/9305081).
- [34] Heling Deng, Jaume Garriga, and Alexander Vilenkin. “Primordial black hole and wormhole formation by domain walls.” In: *JCAP* 04 (2017), p. 050. DOI: [10.1088/1475-7516/2017/04/050](https://doi.org/10.1088/1475-7516/2017/04/050). arXiv: [1612.03753](https://arxiv.org/abs/1612.03753) [[gr-qc](https://arxiv.org/archive/gr-qc)].
- [35] Alexei A. Starobinsky. “Spectrum of adiabatic perturbations in the universe when there are singularities in the inflation potential.” In: *JETP Lett.* 55 (1992), pp. 489–494.
- [36] P. Ivanov, P. Naselsky, and I. Novikov. “Inflation and primordial black holes as dark matter.” In: *Phys. Rev. D* 50 (1994), pp. 7173–7178. DOI: [10.1103/PhysRevD.50.7173](https://doi.org/10.1103/PhysRevD.50.7173).
- [37] Ryo Saito, Jun’ichi Yokoyama, and Ryo Nagata. “Single-field inflation, anomalous enhancement of superhorizon fluctuations, and non-Gaussianity in primordial black hole formation.” In: *JCAP* 06 (2008), p. 024. DOI: [10.1088/1475-7516/2008/06/024](https://doi.org/10.1088/1475-7516/2008/06/024). arXiv: [0804.3470](https://arxiv.org/abs/0804.3470) [[astro-ph](https://arxiv.org/archive/astro-ph)].
- [38] Samuel M. Leach and Andrew R. Liddle. “Inflationary perturbations near horizon crossing.” In: *Phys. Rev. D* 63 (2001), p. 043508. DOI: [10.1103/PhysRevD.63.043508](https://doi.org/10.1103/PhysRevD.63.043508). arXiv: [astro-ph/0010082](https://arxiv.org/abs/astro-ph/0010082).

- [39] Samuel M Leach, Misao Sasaki, David Wands, and Andrew R Liddle. “Enhancement of super-horizon scale inflationary curvature perturbations.” In: *Phys. Rev. D* 64 (2001), p. 023512. DOI: [10.1103/PhysRevD.64.023512](https://doi.org/10.1103/PhysRevD.64.023512). arXiv: [astro-ph/0101406](https://arxiv.org/abs/astro-ph/0101406).
- [40] N. C. Tsamis and Richard P. Woodard. “Improved estimates of cosmological perturbations.” In: *Phys. Rev. D* 69 (2004), p. 084005. DOI: [10.1103/PhysRevD.69.084005](https://doi.org/10.1103/PhysRevD.69.084005). arXiv: [astro-ph/0307463](https://arxiv.org/abs/astro-ph/0307463).
- [41] William H. Kinney. “Horizon crossing and inflation with large η .” In: *Phys. Rev. D* 72 (2005), p. 023515. DOI: [10.1103/PhysRevD.72.023515](https://doi.org/10.1103/PhysRevD.72.023515). arXiv: [gr-qc/0503017](https://arxiv.org/abs/gr-qc/0503017).
- [42] William H. Kinney. “A Hamilton-Jacobi approach to nonslow roll inflation.” In: *Phys. Rev. D* 56 (1997), pp. 2002–2009. DOI: [10.1103/PhysRevD.56.2002](https://doi.org/10.1103/PhysRevD.56.2002). arXiv: [hep-ph/9702427](https://arxiv.org/abs/hep-ph/9702427).
- [43] Yi-Fu Cai, Xi Tong, Dong-Gang Wang, and Sheng-Feng Yan. “Primordial Black Holes from Sound Speed Resonance during Inflation.” In: *Phys. Rev. Lett.* 121.8 (2018), p. 081306. DOI: [10.1103/PhysRevLett.121.081306](https://doi.org/10.1103/PhysRevLett.121.081306). arXiv: [1805.03639](https://arxiv.org/abs/1805.03639) [[astro-ph](https://arxiv.org/abs/astro-ph).C0].
- [44] Eric Cotner, Alexander Kusenko, and Volodymyr Takhistov. “Primordial Black Holes from Inflaton Fragmentation into Oscillons.” In: *Phys. Rev. D* 98.8 (2018), p. 083513. DOI: [10.1103/PhysRevD.98.083513](https://doi.org/10.1103/PhysRevD.98.083513). arXiv: [1801.03321](https://arxiv.org/abs/1801.03321) [[astro-ph](https://arxiv.org/abs/astro-ph).C0].
- [45] Vicente Atal and Cristiano Germani. “The role of non-gaussianities in Primordial Black Hole formation.” In: *Phys. Dark Univ.* 24 (2019), p. 100275. DOI: [10.1016/j.dark.2019.100275](https://doi.org/10.1016/j.dark.2019.100275). arXiv: [1811.07857](https://arxiv.org/abs/1811.07857) [[astro-ph](https://arxiv.org/abs/astro-ph).C0].
- [46] Marco Taoso and Alfredo Urbano. “Non-gaussianities for primordial black hole formation.” In: *JCAP* 08 (2021), p. 016. DOI: [10.1088/1475-7516/2021/08/016](https://doi.org/10.1088/1475-7516/2021/08/016). arXiv: [2102.03610](https://arxiv.org/abs/2102.03610) [[astro-ph](https://arxiv.org/abs/astro-ph).C0].
- [47] G. Franciolini, A. Kehagias, S. Matarrese, and A. Riotto. “Primordial Black Holes from Inflation and non-Gaussianity.” In: *JCAP* 03 (2018), p. 016. DOI: [10.1088/1475-7516/2018/03/016](https://doi.org/10.1088/1475-7516/2018/03/016). arXiv: [1801.09415](https://arxiv.org/abs/1801.09415) [[astro-ph](https://arxiv.org/abs/astro-ph).C0].
- [48] James M. Bardeen, J. R. Bond, Nick Kaiser, and A. S. Szalay. “The Statistics of Peaks of Gaussian Random Fields.” In: *Astrophys. J.* 304 (1986), pp. 15–61. DOI: [10.1086/164143](https://doi.org/10.1086/164143).
- [49] Chul-Moon Yoo, Jinn-Ouk Gong, and Shuichiro Yokoyama. “Abundance of primordial black holes with local non-Gaussianity in peak theory.” In: *JCAP* 09 (2019), p. 033. DOI: [10.1088/1475-7516/2019/09/033](https://doi.org/10.1088/1475-7516/2019/09/033). arXiv: [1906.06790](https://arxiv.org/abs/1906.06790) [[astro-ph](https://arxiv.org/abs/astro-ph).C0].
- [50] Tomohiro Harada, Chul-Moon Yoo, Tomohiro Nakama, and Yasutaka Koga. “Cosmological long-wavelength solutions and primordial black hole formation.” In: *Phys. Rev. D* 91.8 (2015), p. 084057. DOI: [10.1103/PhysRevD.91.084057](https://doi.org/10.1103/PhysRevD.91.084057). arXiv: [1503.03934](https://arxiv.org/abs/1503.03934) [[gr-qc](https://arxiv.org/abs/gr-qc)].
- [51] Cristiano Germani and Ilia Musco. “Abundance of Primordial Black Holes Depends on the Shape of the Inflationary Power Spectrum.” In: *Phys. Rev. Lett.* 122.14 (2019), p. 141302. DOI: [10.1103/PhysRevLett.122.141302](https://doi.org/10.1103/PhysRevLett.122.141302). arXiv: [1805.04087](https://arxiv.org/abs/1805.04087) [[astro-ph](https://arxiv.org/abs/astro-ph).C0].

- [52] Ilia Musco. “Threshold for primordial black holes: Dependence on the shape of the cosmological perturbations.” In: *Phys. Rev. D* 100.12 (2019), p. 123524. DOI: [10.1103/PhysRevD.100.123524](https://doi.org/10.1103/PhysRevD.100.123524). arXiv: [1809.02127](https://arxiv.org/abs/1809.02127) [gr-qc].
- [53] V. De Luca, G. Franciolini, A. Kehagias, M. Peloso, A. Riotto, and C. Ünal. “The Ineludible non-Gaussianity of the Primordial Black Hole Abundance.” In: *JCAP* 07 (2019), p. 048. DOI: [10.1088/1475-7516/2019/07/048](https://doi.org/10.1088/1475-7516/2019/07/048). arXiv: [1904.00970](https://arxiv.org/abs/1904.00970) [astro-ph.CO].
- [54] Misao Sasaki, Teruaki Suyama, Takahiro Tanaka, and Shuichiro Yokoyama. “Primordial black holes—perspectives in gravitational wave astronomy.” In: *Class. Quant. Grav.* 35.6 (2018), p. 063001. DOI: [10.1088/1361-6382/aaa7b4](https://doi.org/10.1088/1361-6382/aaa7b4). arXiv: [1801.05235](https://arxiv.org/abs/1801.05235) [astro-ph.CO].
- [55] Guillermo Ballesteros, Julián Rey, Marco Taoso, and Alfredo Urbano. “Primordial black holes as dark matter and gravitational waves from single-field polynomial inflation.” In: *JCAP* 07 (2020), p. 025. DOI: [10.1088/1475-7516/2020/07/025](https://doi.org/10.1088/1475-7516/2020/07/025). arXiv: [2001.08220](https://arxiv.org/abs/2001.08220) [astro-ph.CO].
- [56] Guillermo Ballesteros and Marco Taoso. “Primordial black hole dark matter from single field inflation.” In: *Phys. Rev. D* 97.2 (2018), p. 023501. DOI: [10.1103/PhysRevD.97.023501](https://doi.org/10.1103/PhysRevD.97.023501). arXiv: [1709.05565](https://arxiv.org/abs/1709.05565) [hep-ph].
- [57] Ioannis Dalianis, Alex Kehagias, and George Tringas. “Primordial black holes from α -attractors.” In: *JCAP* 01 (2019), p. 037. DOI: [10.1088/1475-7516/2019/01/037](https://doi.org/10.1088/1475-7516/2019/01/037). arXiv: [1805.09483](https://arxiv.org/abs/1805.09483) [astro-ph.CO].
- [58] Christian T. Byrnes, Philippa S. Cole, and Subodh P. Patil. “Steepest growth of the power spectrum and primordial black holes.” In: *JCAP* 06 (2019), p. 028. DOI: [10.1088/1475-7516/2019/06/028](https://doi.org/10.1088/1475-7516/2019/06/028). arXiv: [1811.11158](https://arxiv.org/abs/1811.11158) [astro-ph.CO].
- [59] Ogan Özsoy and Gianmassimo Tasinato. “On the slope of the curvature power spectrum in non-attractor inflation.” In: *JCAP* 04 (2020), p. 048. DOI: [10.1088/1475-7516/2020/04/048](https://doi.org/10.1088/1475-7516/2020/04/048). arXiv: [1912.01061](https://arxiv.org/abs/1912.01061) [astro-ph.CO].
- [60] Jacopo Fumagalli, Sébastien Renaux-Petel, John W. Ronayne, and Lukas T. Witkowski. “Turning in the landscape: A new mechanism for generating primordial black holes.” In: *Phys. Lett. B* 841 (2023), p. 137921. DOI: [10.1016/j.physletb.2023.137921](https://doi.org/10.1016/j.physletb.2023.137921). arXiv: [2004.08369](https://arxiv.org/abs/2004.08369) [hep-th].
- [61] Ilia Musco, Valerio De Luca, Gabriele Franciolini, and Antonio Riotto. “Threshold for primordial black holes. II. A simple analytic prescription.” In: *Phys. Rev. D* 103.6 (2021), p. 063538. DOI: [10.1103/PhysRevD.103.063538](https://doi.org/10.1103/PhysRevD.103.063538). arXiv: [2011.03014](https://arxiv.org/abs/2011.03014) [astro-ph.CO].
- [62] Ogan Özsoy, Susha Parameswaran, Gianmassimo Tasinato, and Ivonne Zavala. “Mechanisms for Primordial Black Hole Production in String Theory.” In: *JCAP* 07 (2018), p. 005. DOI: [10.1088/1475-7516/2018/07/005](https://doi.org/10.1088/1475-7516/2018/07/005). arXiv: [1803.07626](https://arxiv.org/abs/1803.07626) [hep-th].
- [63] Michele Cicoli, Victor A. Diaz, and Francisco G. Pedro. “Primordial Black Holes from String Inflation.” In: *JCAP* 06 (2018), p. 034. DOI: [10.1088/1475-7516/2018/06/034](https://doi.org/10.1088/1475-7516/2018/06/034). arXiv: [1803.02837](https://arxiv.org/abs/1803.02837) [hep-th].

- [64] Harald Cramér. *Mathematical Methods of Statistics (PMS-9)*. Princeton University Press, 1999. ISBN: 9780691005478. URL: <http://www.jstor.org/stable/j.ctt1bpm9r4> (visited on 07/19/2023).
- [65] Louis Comtet. *Advanced Combinatorics*. D. Reidel publishing company, 1974, p. 134.
- [66] James Alexander Shohat and Jacob David Tamarkin. *The problem of moments*. Vol. 1. Mathematical Surveys and Monographs, 1943.
- [67] Alex Kamenev. “Field Theory of Non-Equilibrium Systems.” In: *Field Theory of Non-Equilibrium Systems*, by Alex Kamenev, Cambridge, UK: Cambridge University Press, 2011 (Sept. 2011). DOI: [10.1017/CB09781139003667](https://doi.org/10.1017/CB09781139003667).
- [68] Antonio Riotto. “Inflation and the theory of cosmological perturbations.” In: *ICTP Lect. Notes Ser. 14* (2003). Ed. by G. Dvali, Abdel Perez-Lorenzana, G. Senjanovic, G. Thompson, and F. Vissani, pp. 317–413. arXiv: [hep-ph/0210162](https://arxiv.org/abs/hep-ph/0210162).
- [69] Claus Kiefer and David Polarski. “Emergence of classicality for primordial fluctuations: Concepts and analogies.” In: *Annalen Phys.* 7 (1998), pp. 137–158. DOI: [10.1002/andp.2090070302](https://doi.org/10.1002/andp.2090070302). arXiv: [gr-qc/9805014](https://arxiv.org/abs/gr-qc/9805014).
- [70] Juan Martin Maldacena. “Non-Gaussian features of primordial fluctuations in single field inflationary models.” In: *JHEP* 05 (2003), p. 013. DOI: [10.1088/1126-6708/2003/05/013](https://doi.org/10.1088/1126-6708/2003/05/013). arXiv: [astro-ph/0210603](https://arxiv.org/abs/astro-ph/0210603).
- [71] Guillermo Ballesteros, Julián Rey, Marco Taoso, and Alfredo Urbano. “Stochastic inflationary dynamics beyond slow-roll and consequences for primordial black hole formation.” In: *JCAP* 08 (2020), p. 043. DOI: [10.1088/1475-7516/2020/08/043](https://doi.org/10.1088/1475-7516/2020/08/043). arXiv: [2006.14597](https://arxiv.org/abs/2006.14597) [[astro-ph](https://arxiv.org/abs/astro-ph).CO].
- [72] Noriyuki Kogo and Eiichiro Komatsu. “Angular trispectrum of cmb temperature anisotropy from primordial non-gaussianity with the full radiation transfer function.” In: *Phys. Rev. D* 73 (2006), p. 083007. DOI: [10.1103/PhysRevD.73.083007](https://doi.org/10.1103/PhysRevD.73.083007). arXiv: [astro-ph/0602099](https://arxiv.org/abs/astro-ph/0602099).
- [73] Sam Young and Christian T. Byrnes. “Primordial black holes in non-Gaussian regimes.” In: *JCAP* 08 (2013), p. 052. DOI: [10.1088/1475-7516/2013/08/052](https://doi.org/10.1088/1475-7516/2013/08/052). arXiv: [1307.4995](https://arxiv.org/abs/1307.4995) [[astro-ph](https://arxiv.org/abs/astro-ph).CO].
- [74] Vicente Atal, Jaume Garriga, and Airam Marcos-Caballero. “Primordial black hole formation with non-Gaussian curvature perturbations.” In: *JCAP* 09 (2019), p. 073. DOI: [10.1088/1475-7516/2019/09/073](https://doi.org/10.1088/1475-7516/2019/09/073). arXiv: [1905.13202](https://arxiv.org/abs/1905.13202) [[astro-ph](https://arxiv.org/abs/astro-ph).CO].
- [75] Giacomo Ferrante, Gabriele Franciolini, Antonio Iovino Junior., and Alfredo Urbano. “Primordial non-Gaussianity up to all orders: Theoretical aspects and implications for primordial black hole models.” In: *Phys. Rev. D* 107.4 (2023), p. 043520. DOI: [10.1103/PhysRevD.107.043520](https://doi.org/10.1103/PhysRevD.107.043520). arXiv: [2211.01728](https://arxiv.org/abs/2211.01728) [[astro-ph](https://arxiv.org/abs/astro-ph).CO].
- [76] Alba Kalaja, Nicola Bellomo, Nicola Bartolo, Daniele Bertacca, Sabino Matarrese, Ilia Musco, Alvise Raccanelli, and Licia Verde. “From Primordial Black Holes Abundance to Primordial Curvature Power Spectrum (and back).” In: *JCAP* 10 (2019), p. 031. DOI: [10.1088/1475-7516/2019/10/031](https://doi.org/10.1088/1475-7516/2019/10/031). arXiv: [1908.03596](https://arxiv.org/abs/1908.03596) [[astro-ph](https://arxiv.org/abs/astro-ph).CO].

- [77] David W. Neilsen and Matthew W. Choptuik. "Critical phenomena in perfect fluids." In: *Class. Quant. Grav.* 17 (2000), pp. 761–782. doi: [10.1088/0264-9381/17/4/303](https://doi.org/10.1088/0264-9381/17/4/303). arXiv: [gr-qc/9812053](https://arxiv.org/abs/gr-qc/9812053).